SYNTHESES AND STRUCTURAL STUDIES OF METAL COMPLEXES OF SULFA DRUGS

A thesis submitted to the Cardiff University

By

G. M. Golzar Hossain

in candidature of the degree of

Doctor of Philosophy

August 2005

Department of Chemistry

Cardiff University

ProQuest LLC
789 East Eisenhower Parkway
P.O. Box 1346
Ann Arbor, MI 48106-1346

DEDICATED TO

Afroza and Asif

ACKNOWLEDGEMENTS

This work would not have been completed without the encouragement and patience of my supervisors Professor Peter G. Edwards and Dr. Angelo J. Amoroso, to whom, I will always be grateful. I am also grateful to Dr. K. M. A. Malik for collecting crystal data and valuable advice.

I want to express my gratitude to Dr. Ian A. Fallis and Dr. S. Aldridge for their helpful discussion.

Many thanks go to Dr. Murphy and Dr. Farley for EPR data and discussion.

Thanks go to all the technical staffs- Rob Jenkins, Alan, Robin, Ricky, Sham, John Bowly and Gary for helping me to work smoothly.

Special thanks go to everyone in the Department of Chemistry, Cardiff University, specially Caroline, Ozra, Steve, Graham, Dave, Miles, Claire, Rob, Willium, Deborah, Lisa, Amal, Chris, Andrea and Mark for making the work enjoyable.

Finally, I would like thank my wife Afroza and lovely son Asif for their support and inspiration throughout the research works.

ABSTRACT

This thesis presents the results of the synthesis of metal complexes of sulfa drugs (sulfadiazine, sulfamerazine, sulfamethazine, sulfathiazole and sulfadimethoxine) with secondary ligands, which were subjected to X-ray crystallographic studies. The aim of this work was to synthesise metal complexes of sulfa drugs with secondary nitrogen donor ligands e.g. ammonia, pyridine (py), ethylenediamine (en), diethylenetriamine (dien), 2,2′-bipyridine, 1,10-phenanthroline, 4,4′-dimethyl-2,2′-bipyridine, *N,N′*(3-aminopropyl)-bis-(ethylenediamine) (apen) and oxygen donor ligands such as, water and dimethylformamide (DMF) and to investigate the different modes of coordination of the sulfa drugs molecules to the metal ions in the presence of nitrogen/oxygen donor ligands.

Chapter 1, details an introduction into the fundamental concepts, procedures and equipment involved in data collection, solution and refinement of single crystal structures.

In Chapter 2, a review of the literature on the metal complexes of sulfa drugs along with the main aims of this work is presented.

In Chapter 3, the general experimental procedure and synthetic methods have been described for the metal complexes of sulfa drugs whose results and discussion are described in chapter 4.

In chapter 4, the crystal structure of sulfadiazine, a new polymorph of sulfamerazine and the syntheses of the metal complexes of sulfadiazine, sulfamerazine and sulfamethazine, their analytical and spectral data along with the X-ray structure determination of the complexes are presented. The complexes studied in this chapter are: A) Cobalt complex $\{[Co(smz)_2(H_2O)].DMF\}_n$ (**3**); B) Nickel complexes $[Ni(en)_3(sdz)_2].H_2O$ (**4**) and $[Ni(smr)_2(py)_2].4py$ (**5**); C) copper complexes $[Cu(en)_2(sdz)_2]$ (**6**), $[Cu(dien)_2(sdz)_2]$ (**7**), $[Cu(en)_2(H_2O)_2][smr)_2]$ (**8**), $[Cu(en)_2(H_2O)_2][smr)_2].H_2O$ (**9**), $[Cu_2(smr)_4].2DMF$ (**10**), $[Cu_2(smr)_4].2DMSO$ (**11**), $[Cu(smz)_2(apen)].3H_2O.CH_3OH$ (**12**) and $\{[Cu(smz)_2.NH_3].2H_2O\}_n$ (**13**); D) Zinc complexes $[Zn(smz)_2(NH_3)_2]$ (**14**) and $[Zn(smz)_2(py)_2].2py$ (**15**), E) Cadmium complexes $[Cd(dien)_2(sdz)_2].DMF$ (**16**),

$[Cd(dien)(smr)_2].H_2O$ (**17**), $[Cd(sdz)_2(bpy)]$ (**18**), $[Cd(sdz)_2(phen)]$ (**19**), $[Cd(sdz)_2(dmbpy)].2DMF$ (**20**), $[Cd(smr)_2(phen)]$ (**21**), $\{[Cd(smz)_2(H_2O)].DMF\}_n$ (**22**), $\{[Cd(smz)_2(H_2O)].2H_2O\}_n$ (**23**) and $[Cd(smz)_2(en)].2DMF$ (**24**); and F) Mercury complexes $[Hg(sdz)_2(DMF)_2]$ (**25**), $[Hg(smr)_2]$ (**26**) $[Hg(smr)_2(bpy)]$ (**27**) and $[Hg(smz)_2(DMF)_2]$ (**28**).

The structural results for the complexes are discussed and compared with other related complexes. In this context, the different types of coordination geometries, important parameters within the coordination sphere, the various modes of coordination of the sulfa drugs in the anionic form, dimeric polymeric complexes, the role of hydrogen bonds in the formation of the "cation-anion pair" and the packing diagram have been discussed.

In Chapter 5, we have described the syntheses and characterisation of the complexes of sulfathiazole, their analytical and spectral data along with the X-ray structure determination of these complexes are presented. The complexes studied are: $[(H_2stz)_2][NO_3].H_2O$ (**29**), $[CoCl_4][(H_2stz)_2].CH_3COOH$ (**30**) and $[Cu(en)_2(H_2O)_2][stz)_2].2H_2O$ (**31**). In all the complexes the sulfathiazole molecules act as ionic species. The structural results for the complexes are discussed and compared with other related complexes. In this context, the role of hydrogen bonds in the formation of the "cation-anion pair" and the packing diagram has been discussed.

Chapter 6 describes the structure of sulfadimethoxine and synthesis and characterisation of a zinc complex of sulfadimethoxine $[Zn(sdm)_2(NH_3)_2].2H_2O$ (**33**) by analytical and spectral data along with the X-ray structure determination. The structural results of the complex are discussed and compared with other related complexes. The packing diagram of the complex with the hydrogen bonds is discussed in this chapter.

ABBREVIATIONS

Å	ångström (1Å = 10^{-10} cm)
λ	wavelength
V	cell volume
a, *b*, *c*	cell axes
α, β, γ	cell angles
d	interplanar spacing
F_{hkl}	structure factor
f_j	scattering factor
hkl	general indices
(°)	degree centigrade (Celcius)
cm	centimeter
cm^{-1}	wave number
g	grams
ml	milliliter
mmol	millimolar
tsd	triple sulfa drugs
Hsdz	sulfadiazine
Hsmr	sulfamerazine
Hsmz	sulfamethazine
Hstz	sulfathiazole
Hsdm	sulfadimethoxine
py	pyridine
DMF	dimethylformamide
DMSO	dimethylsulfoxide

en	ethylenediamine
bpy	2,2′-bipyridine
phen	1,10-phenanthroline
dmbpy	4,4′-dimethyl-2,2′-bipyridine
dien	diethylenetriamine
apen	*N*,*N*′(3-aminopropyl)-bis(ethylenediamine)
IR	infrared
EPR	Electron Paramagnetic Resonance
c. w.	continuous wave
NMR	nuclear magnetic resonance
s	singlet
d	doublet
t	triplet
PABA	*p*-aminobenzoic acid
UTI	urinary tract infection

CONTENTS

Chapter 1

X-RAY CRYSTALLOGRAPHY

X-RAY CRYSTALLOGRAPHY

1.1 HISTORICAL BACKGROUND

X-ray crystallography[1–5] is an experimental technique that exploits the fact that X-rays are diffracted by crystals. X-rays have the appropriate wavelength (in the Å range, ~10^{-8} cm) to be scattered by the electron cloud of an atom of comparable size. Based on the diffraction pattern obtained from X-ray scattering off the periodic assembly of molecules or atoms in the crystal, the electron density can be reconstructed. Additional phase information must be extracted either from the diffraction data or from supplementing diffraction experiments to complete the reconstruction (the phase problem in crystallography). A model is then progressively built into the experimental electron density, refined against the data and the result is a quite accurate molecular structure.

The knowledge of accurate molecular structures is a prerequisite for rational drug design and for structure based functional studies to aid the development of effective therapeutic agents and drugs. Crystallography can reliably provide the answer to many structure related questions, from global folds to atomic details of bonding.

The region of the electromagnetic spectrum for X-rays is between ultra-violet and gamma radiation, with wavelengths 0.1–100 Å. X-rays with these wavelengths are produced when fast moving electrons are suddenly decelerated and their kinetic energy of motion is converted directly or indirectly into a quantum of radiation. To generate X-rays, electrons are accelerated by an electric field and directed against metal target, which slows them rapidly by multiple collisions. The minimum wavelength of this white radiation is determined by the accelerating voltage. X-rays are produced when the cathode is a hot filament that releases electrons which are accelerated by a high voltage applied between cathode and anode toward the anode, called the target and the electron beam strikes its surface. The energy of some electrons striking the target is used to eject electrons from the inner shells of target atoms, if the energy is sufficient. Subsequently electrons from higher energy shells fall into these vacancies and X-ray photons are emitted. This leads to an

atomic line spectrum called the characteristic spectrum. When the electrons bombard the target reach certain critical energies (threshold potentials) which are capable of knocking electrons out of their atomic orbitals, in particular, at energies of about 10,000 eV (for elements with atomic number *ca.* 30).

The crystal is a repeating array of closely packed atoms, molecules or ions in three dimensions. Some solids can be crystals, usually have flat surfaces or faces that make definite angles with one another. The orderly stacks of particles that produce these faces also cause the solids to have highly regular shapes. Quartz and diamond are the examples of crystalline solids.

The shapes of crystal depend on its growing, and these may be sheet like, needle like, plate like or twin like. In general the growth should be very slow so that a regular arrangement of molecules or ions, leading to a well-formed crystal, may be obtained.

To choosing a crystal for collecting X-ray data, two main requirements must be met:
a) It must possess uniform internal structure and
b) It must be of proper size and shape.

To fulfil the first requirement, a crystal must be pure at the molecular, ionic, or atomic level and a single in the usual sense, it should not be twinned or composed of microscopic subcrystals. It should not be grossly fractured, bent, or otherwise physically distorted. For X-ray work, specimens with dimensions 0.2–0.4mm on an edge are usually appropriate.

In 1895, X-rays were discovered by Wilhelm Rontgen. It was still unknown upto 1912 whether X-rays consisted of particles or they were electromagnetic waves. In order for the wave hypothesis to be correct, the wavelength would have had to be of the order of 1Å (10^{-8} cm). It was not believed possible to use a grating to measure such short wavelengths, due to the fact that all previous experiments had involved wavelengths of the same order of magnitude as the grating spacing.

There was still no direct evidence for the structure of crystals and in 1912 came the great turning point in crystallography and the German Physicist Max Laue suggested that crystals

might serve as diffraction gratings for X-rays. Friedrick and Knipping carried out an experiment to test Laue's suggestion and irradiated a crystal of $CuSO_4.5H_2O$ with X-rays. The detection of diffraction confirmed Laue's suggestions and launched the science of X-ray crystallography.

1.2 BRAGG'S EQUATION

Following the discovery by Friedrick, Knipping and Laue, W. H. Bragg and his son, W. L. Bragg developed and used X-ray diffraction techniques to determine crystal structures. The first crystal structure for sodium chloride was published in 1913 by W. L. Bragg. The excited electrons become themselves "secondary" scatterers of the same kind of X-radiation. This is called *coherent scattering.*

Bragg showed that the coherent scattering of X-rays by crystals is mathematically equivalent to the reflection of light from parallel planes. If an incident X-ray beam makes an angle θ with such a set of planes, the reflected beam makes an angle θ with the planes. The planes are known as the *hkl* set of planes where *h*, *k* and *l* are the number of parts into which *a*, *b* and *c* axes of the unit cell are divided respectively.

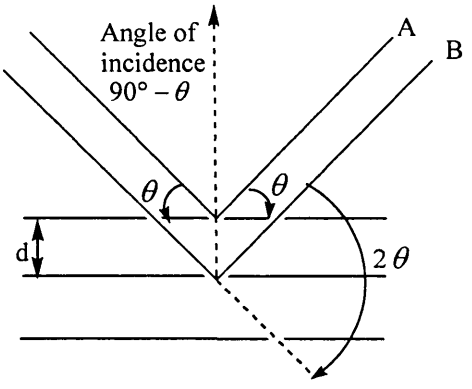

Figure 1.1

X-rays of wavelength λ impinge on the crystal at an angle of incidence θ_{hkl}. The path length of an X-ray which strikes the top layer of atoms (A) in a crystal is shorter than that of an X-ray which strikes the second layer (B). This is shown in Figure 1.1.

If two emitted waves are to be in phase and reinforce each other, their path lengths must differ by a number of wavelengths. This difference is $n\lambda$ where n is a whole number and λ

is the wavelength of the radiation used. Bragg showed that the angle (θ_{hkl}) of reflection of X-rays could be related to the distance (d_{hkl}-the perpendicular spacing of the *hkl* set of planes) between the two layers of atoms and is as follows;

$$2d_{hkl}\sin\theta_{hkl} = n\lambda \qquad (1)$$

If equation (1) is rearranged, the spacing between the planes can be calculated as shown in equation (2);

$$d_{hkl} = \lambda/2\sin\theta_{hkl} \qquad (2)$$

1.3 RECIPROCAL LATTICE

The concept of the reciprocal lattice was used by P. P. Ewald and extended by Laue (1913) to describe the relationship between crystal structure and diffraction spectrum. For every real lattice it is possible to construct a reciprocal lattice.

The advantages of using reciprocal distances may be appreciated by considering Bragg's Law in the form

$$\sin\theta_{hkl} = n\lambda/2d_{hkl} \qquad (3)$$

From equation (3), it can be seen that $\sin\theta$ is inversely proportional to d.

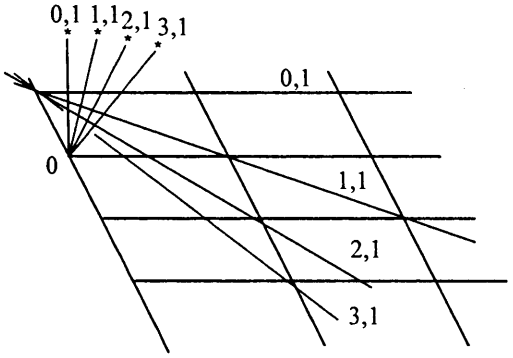

Figure 1.2

To construct a reciprocal lattice, any point of the real lattice is taken as an origin, from which lines are drawn perpendicular to all sets of real lattice planes. Reciprocal lattice points arise on these lines at distances (d_{hkl}) inversely proportional to the spacing of the real planes, and also fall on sets of parallel planes. The indices of the reciprocal lattice point, *hkl*, are the same as the indices of the planes in the real lattice that the point represents.

The interplanar spacing in the real lattice, and not the distance between lattice points, is the parameter which gives the distance between lattice points in the reciprocal space. The axes

and angles of the unit cell in the real lattice are labelled a, b, c and α, β, γ respectively. However in the reciprocal lattice they are labelled a^*, b^*, c^* and α^*, β^*, γ^*. A two dimensional reciprocal lattice can be seen in Figure 1.2.

The most important property of the reciprocal lattice is that it allows a simple visualisation of Bragg's Law. If a crystal is positioned in a beam of X-rays of wavelength λ and a^*c^* section of the reciprocal lattice is considered, it can be assumed that the crystal is oriented so that the X-ray beam is parallel to a^*c^* plane. A line XO can be drawn, as shown in Figure 1.3, in the direction of the beam which passes through the reciprocal lattice origin O. A circle of radius $1/\lambda$ with its centre C on XO can be considered, so that O falls on its circumference. If we now consider a point (P) on the circle, the angle OPB is inscribed in a semicircle and is at a right angle (Equation 4).

$$\sin OBP = \sin\theta = \frac{OP}{OB} = \frac{OP}{2/\lambda} = \left(\frac{OP}{2}\right)\lambda \qquad (4)$$

P is a reciprocal lattice point and therefore the length of OP is equal to $1/d_{hkl}$. Equation (4) can be rewritten to give equation (5).

$$\sin\theta = \frac{1.\lambda}{2d_{hkl}} \qquad \text{Therefore, } \frac{1}{\lambda} = 2d_{hkl}\sin\theta \qquad (5)$$

This can be regarded as Bragg's Law with $n = 1$

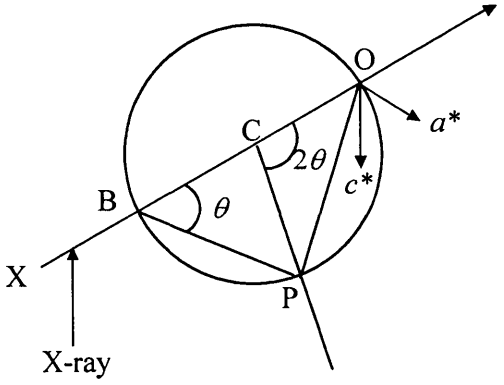

Figure 1.3

Bragg's Law is satisfied when a reciprocal lattice point coincides with the circle and reflection occurs.

1.4 Crystal Lattice

A crystal contains atoms arranged in a repetitive three dimensional pattern. If each repeat unit of this pattern is taken as a point then a three dimensional point lattice is created. Each crystal consists of a basic building block that repeats over and over again in all directions. The building block which repeats in a perfectly regular array is known as the Unit Cell.

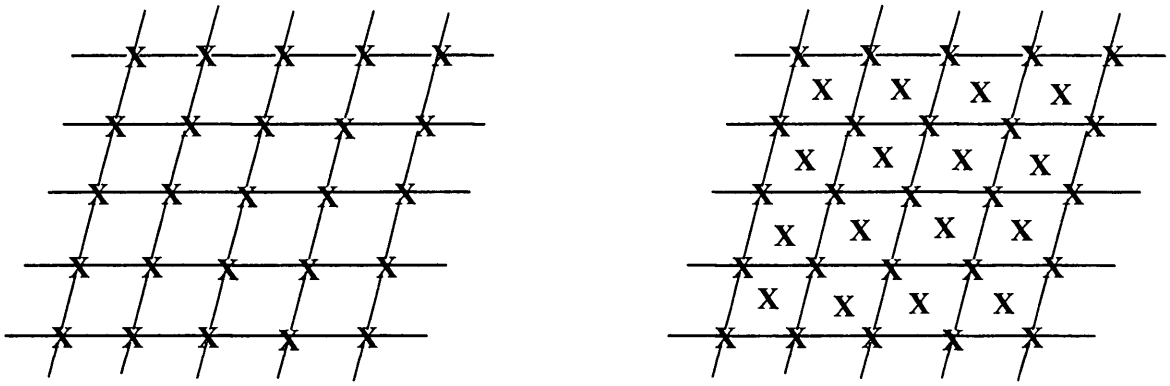

Primitive (P) *Centred* (C)

Figure 1.4: Primitive and centred cells

There are infinite numbers of possibilities for unit cells. It is possible to have lattice points inside a unit cell. When this occurs there is more than one lattice point per unit cell and the cell is *centred.* On the other hand, a unit cell with lattice points only on the corners is called *primitive.* This is explained in Figure 1.4.

There are seven crystal systems used to classify crystal structure depending on the symmetry present. In addition there are thirty-two type crystal classes or point group, so that there are differing degrees of symmetry of crystal belonging to the same system, and in three dimensions there are fourteen distinctive space lattices known as Bravais lattices, consisting of 7 primitive and 7 non-primitive lattices.

Table 1.1 shows the seven crystal systems, their respective parameters and the Laue symmetry (i.e. diffraction symmetry). In general, the unit cell is characterized by six parameters, three axial lengths and three interaxial angles. The lengths of the unit cell edges are designated by a, b, c and the interaxial angles by α, β, γ. The α is between b and c, β is between a and c, while γ is between a and b. The crystal classes may be divided into seven main systems, each characterized by the possesion of a certain minimum of symmetry elements, and referable to certain characteristic axis.

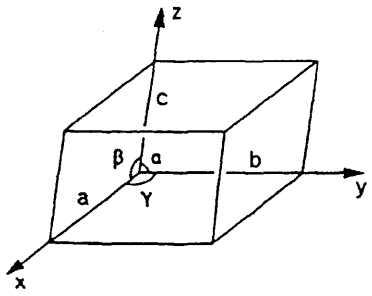

Figure 1.5

It is conventional to label the edges of the unit cell *a, b, c* and the angles between them α, β, γ with the angle α between *b* and *c*, β that between *a* and *c* and γ that between *a* and *b*. It is conventional to choose a unit cell that is the simplest, with the axial (repeat) lengths as short as possible and interaxial angles as near to 90° as possible. Lattice planes are defined as sheets of lattice points and are expressed by indices *h, k, l* where *a/h, b/k* and *c/l* are proportional to the intercepts made on the *a, b* and *c* unit cell axes respectively, and are synonymous with Miller indices used by morphological crystallographers. Since the crystal (and therefore lattice) structure is infinite, for a given lattice plan definition, *hkl*, there will be an infinite stack of parallel planes with a constant interplanar spacing d_{hkl}.

Table 1.1: Crystal systems with parameters, Laue symmetry and Lattice type

Crystal Systems	Symmetry Restrictions	Parameters	Laue Symmetry	Lattice Type
Triclinic	Rotational Symmetry is absent	$a \neq b \neq c$; $\alpha \neq \beta \neq \gamma$	$\bar{1}$	P
Monoclinic	2–Fold Rotation axis and a mirror plane perpendicular to it	$a \neq b \neq c$; $\alpha = \gamma = 90°$; $\beta \neq 90°$	$2/m$	P, C*
Orthorhombic	3, 2–Fold rotation axes parallel to the three axes and 3 mirror planes perpendicular to them	$a \neq b \neq c$; $\alpha = \beta = \gamma = 90°$	mmm	P, C*, I, F
Tetragonal	4–Fold Rotation axis parallel to the *c* axis	$a = b \neq c$; $\alpha = \beta = \gamma = 90°$	$4/m$, $4/mmm$	P, I
Trigonal	3–Fold Rotation axis parallel to the *c* axis	$a = b \neq c$; $\alpha = \beta = 90°$; $\gamma = 120°$	$\bar{3}$, $\bar{3}m$	†P, R
Hexagonal	6–Fold Rotation axis parallel to the *c* axis	$a = b \neq c$; $\alpha = \beta = 90°$; $\gamma = 120°$	$6/m$, $6/mmm$	†P
Cubic	4, 3–Fold rotation axes	$a = b = c$; $\alpha = \beta = \gamma = 90°$	$m\bar{3}$, $m\bar{3}m$ m	P, F, I

*C ⇒ in monoclinic can alternatively be A or I.

⇒ in orthorhombic it can be replaced by A or B.

† ⇒ Trigonal P and Hexagonal P have the same shape, but different symmetry

1.4.1 CRYSTAL SYSTEMS

There are seven crystal systems depending on the unit cells. Table 1.1 shows that each crystal system has associated with its specific minimum symmetry restrictions. There are seven three-dimensional coordinate systems that are useful in describing crystals and are the basis for their classification. The systems are:

(1) Triclinic: Possessing no symmetry at all, or at the most, an inversion centre. In the first case opposite faces will have different properties, in the second, the same properties. Referable to 3 unequal axes, not at right angles.

(2) Monoclinic: Possessing a single 2-fold axes, or a single reflection plane. Referable to 3 unequal axes, not at right angles to the other two.

(3) Orthorhombic: Having two symmetry planes at right angles, or three 2-fold axes at right angles to one another. The existence of two such axes demands the existence of a third. Referable to 3 unequal axes at right angles.

(4) Trigonal: Having a single 3-fold axes. Referable to 3 unequal axes equally inclined to the 3-fold axes.

(5) Tetragonal: Having a single 4-fold axes, simple or alternating. Referable to 3 axes at right angles, two of them are equal.

(6) Hexagonal: Having a single 6-fold axes, simple or alternating. Referable to 2 equal axes inclined at 120^{o} and a third unequal axis at right angles to them.

(7) Cubic or regular: Having four 3-fold axes, corresponding in direction to the diagonals of a cube. Referable to 3 equal axes at right angles to one another.

1.4.2 Unit Cell

It is usual to select out from a regular array of molecules or ions in a crystal, one small unit, called the unit cell. This unit cell repeats in a regular manner in each direction. The lengths of the sides of this unit cell and the angles between these sides are all that is needed definite. There are four different types of three-dimensional unit cell

1. The primitive unit cell (symbol P) contains one lattice point.

2. The body-centred unit cell (symbol I) has a lattice point at each corner and also one at the centre of the cell.
3. The face-centred unit cell (symbol F) has a lattice point at each corner and one in the centre of each face.
4. The face-centred unit cell (symbol A, B or C) has a lattice point at each corner, and one in the centres of one pair of opposite faces.

There are seven primitive lattices and seven centred lattices and when combined they constitute the fourteen Bravais Lattices which are represented by lattice symbols and are shown in Table 1.2.

Table 1.2: Relation between the Lattice Symbol and the Lattice Points.

Lattice Symbol	No. of lattice points per unit cell	Lattice Points
P (Primitive)	1	All corners
I (Inner)	2	At corners and at centre of cell
A (Centred on two faces)	2	At corners and at centre of A face
B (centred on two faces)	2	At corners and at centre of B face
C (Centred on two faces)	2	At corners and at centre of C face
F (Centred on all faces)	4	At corners and all face centres
R (Rhombohedral)	3	At corners

1.4.3 Miller Indices

If any crystal plane is taken which has intercepts on the three crystal axes a, b, c, then any other plane in the crystal is then described by a/h, b/k and c/l. Here h, k and l are small whole numbers or zero and are known as the indices of the plane.

If a plane intercepts all three axes a, b and c, then the unit cell will have three indices hkl and if only two axes are cut parallel to the third, then depending on which axis a, b or c is cut dictates the indices $0kl$, $h0l$ or $hk0$ respectively. The indices $00l$, $0k0$ and $h00$ occur if only one axis is cut and is parallel to the axes a and b, a and c or b and c respectively.

1.5 SYSTEMATIC ABSENCES

Preliminary stages of a crystal structure analysis is carried out with an inspection of the systematic absences. An absence is observed when the reflections are too weak to be measured. The presence of systematic absences can be used to help determine the space group of the crystal.

Two examples are given here and others are given later on in the chapter.
(1) If $h00$ is absent for h odd, then this indicates a 2_1 axis parallel to the a axis.
(2) If $0k0$ is absent for k odd, then this indicates a 2_1 axis parallel to the b axis.

1.6 Symmetry Elements

The symmetry element is a geometrical property, such as a point, a line or a plane with respect to which the symmetry operation is performed. There are two types of symmetry elements, point symmetry and translational symmetry.

1.6.1 Point Symmetry

It is an operation which when repeated returns the object to its original position. Reflections, rotations and inversions are the three main types of point group symmetry.

Firstly a rotational axis can occur at an angle of $360°/n$ and this corresponds to n-fold rotations. Only 2, 3, 4 and 6 fold rotational axes are possible in crystals. Secondly an inversion centre is a point through which an object can be moved in a straight line, so that it finishes up at an equal distance from the inversion centre as it did originally. Thirdly a reflection operation is the reflection of an object through a plane.

1.6.2 Translational Symmetry

Two such elements used are the screw axis and the glide plane. A screw axis combines rotation about an axis with translation in the direction of the axis. A three fold screw axis would be represented as 3_1, meaning a rotation about a 3-fold axis and a translation by 1/3 of the unit cell. A glide plane combines reflections across a plane with translations parallel to the plane. If a glide plane is parallel to the a-axis, the symbol for the glide plane is simply "a" and for the operation is reflection in the plane and translation by $a/2$.

Table 1.3 indicates three important features. The disappearance of reflections along an axial line in the reciprocal lattice can be explained by the presence of screw axes. *Glide* planes affect reflections in the corresponding reciprocal lattice planes and centring causes systematic absences throughout reciprocal space.

Table 1.3

Symmetry Element	Affected reflections	Conditions for Systematic Absences
2–fold screw axis (2_1) parallel to the *a*-axis	*h*00	$h = 2n + 1$ = odd
2–fold screw axis (2_1) parallel to the *b*-axis	0*k*0	$k = 2n + 1$
2–fold screw axis (2_1) parallel to the *c*-axis	00*l*	$l = 2n + 1$
n-glide plane perpendicular to the *a*-axis	0*kl*	$k + l = 2n + 1$
n-glide plane perpendicular to the *b*-axis	*h*0*l*	$h + l = 2n + 1$
n-glide plane perpendicular to the *c*-axis	*hk*0	$h + k = 2n + 1$
a-glide plane perpendicular to the *b*-axis	*h*0*l*	$h = 2n + 1$
a-glide plane perpendicular to the *c*-axis	*hk*0	$h = 2n + 1$
b-glide plane perpendicular to the *a*-axis	0*kl*	$k = 2n + 1$
b-glide plane perpendicular to the *c*-axis	*hk*0	$k = 2n + 1$
c-glide plane perpendicular to the *a*-axis	0*kl*	$l = 2n + 1$
c-glide plane perpendicular to the *b*-axis	*h*0*l*	$l = 2n + 1$

The atomic scattering factor, f_j, is a measure of the amplitude of the wavelet caused by the scattering of the j^{th} atom.

1.6.3 SPACE GROUPS

A space group can be thought of as a group of symmetry operations consistent with an infinitely extended, regularly repeating pattern. In 1890 Federov and Schoenflies independently derived the 230^6 possible space groups that correspond to the 32 point groups combined with the 14 Bravais lattices. A group whose elements include both point symmetry elements and the translations of a crystal is called a "space group"

The space group symbol will always consist of a capital letter donating the centring followed by a generalisation of the Hermann-Mauguin point group symbol to allow for *glide* planes and screw axes. An example of some space groups are $P2_1/c$, $P\bar{1}$ and $P2_12_12_1$.

1.7 STRUCTURE DETERMINATION

It has already been shown that if a beam of X-rays is directed at a crystal consisting of a regular array of atoms, a pattern of reflections can be recorded.

1.7.1 Atomic Scattering Factor

Every electron in an atom is responsible for scattering and each wavelet has an amplitude. The amplitude caused therefore by a cell of the crystal, can be written as the sum of the unit amplitudes of the wavelets. Each atom has a specific number of electrons associated with it in space and it is useful to know the general distribution of the electrons with respect to the centre of the atom.

The scattering power of an atom, f, is expressed in terms of the scattering power of a single electron. The maximum scattering by an atom is equal to its atomic number (Z). This is observed at $\sin\theta/\lambda = 0$. If all the electrons in an atom were concentrated at one point, there would be no destructive interference between the wavelets and also there wouldn't be any variation in f with $\sin\theta/\lambda$. When the electrons are distributed, as in actual atoms, destructive interference occurs and the larger the volume of the atom then the greater the fall-off in f with $\sin\theta/\lambda$.

1.7.2 Structure Factor

The diffraction from one atom cannot be considered alone. The whole of the crystal causes diffraction and therefore all the atomic scatterings have to be accounted. This is represented as the Structure Factor F_{hkl} which describes the amplitude and the phase of the X-rays scattered by a unit cell for a particular reflection, *hkl*.

The Structure Factor depends upon;

(1) The atomic scattering factors

(2) Arrangements of the scattering materials (including thermal motion)

(3) The direction of scattering

The intensity of the scattered radiation from the plane, *hkl*, is proportional to the square of the amplitude.

$$I_{(hkl)} \propto \left| F_{(hkl)} \right|^2 \qquad (6)$$

The structure factor, $F_{(hkl)}$, can be represented by the following equation:

$$F_{(hkl)} = \sum_{j=1}^{N} f_j \exp 2\pi i(hx_j + ky_j + lz_j) \quad (7)$$

Here $F_{(hkl)}$ = Structure factor for *hkl* reflection

f_j = Scattering factor for the j^{th} atom

x, y, z = Positions of the j^{th} atom in the unit cell

i = $\sqrt{-1}$

Also it can be described as

$$F_{(hkl)} = \left|F_{(hkl)}\right| e^{i\alpha(hkl)} \quad (8)$$

$$F_{(hkl)} = A_{(hkl)} + iB_{(hkl)} \quad (9)$$

With $|F_{(hkl)}|$ = the amplitude of the scattered wave

α or $\alpha_{(hkl)}$ = its phase relative to the origin of the unit cell

Figure 1.6 shows the phase difference between two waves.

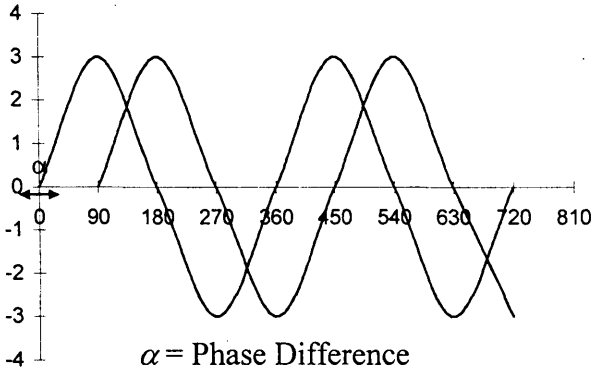

Figure 1.6

The components of the wave A and B, in its vector representation, is related to the amplitude of the wave through equation (10) and also can be represented using an Argand diagram (Figure1.7).

$$\left|F_{(hkl)}\right| = (A^2 + B^2)^{1/2} \quad (10)$$

$$\text{and } \alpha = \tan^{-1}(B/A) \quad (11)$$

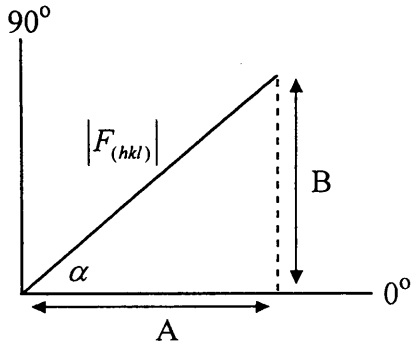

Figure 1.7 Argand Diagram

A and B are products of the individual atomic scattering factor amplitudes, f_j, and the cosines and sines of the phase angles of the waves scattered from the individual atoms. This is shown in equations (12) and (13).

$$A_{(hkl)} = \sum_{j=1}^{N} f_j \cos 2\pi i(hx_j + ky_j + lz_j) \qquad (12)$$

$$B_{(hkl)} = \sum_{j=1}^{N} f_j \cos 2\pi i(hx_j + ky_j + lz_j) \qquad (13)$$

1.7.3 Thermal motion

The description of atomic scattering factors has yet not taken into account of the thermal vibrations of an atom. When the temperature is raised the atomic vibrations are larger and as a result the size of the atom appears to have increased.

The volume occupied by the electrons producing the scattering of the X-rays has increased. The result is a more rapid fall-off of the scattering power than would be obtained for an atom at rest.

As a result, a reduction in the scattering factor would be observed as governed by equation (14).

$$e^{-B(\sin^2\theta)/\lambda^2} \qquad (14)$$

Where B is the temperature coefficient which is related to the mean square displacement of the atoms from their mean position by expression $B = 8\pi^2U^2$.

$I_{(hkl)} \propto F_{(hkl)}$ excludes geometric factors, absorption corrections and other minor effects. If these factors were considered then equation (15) would be true.

$$I_{(hkl)} = K\left|F_{(hkl)}\right|^2 (Lp)(Abs) \qquad (15)$$

Here (Lp) = an abbreviation for the geometric factors
(Abs) = an abbreviation for the absorption factors
and K = A Scale Factor .

For an explanation of Lp and Abs see 1.7.7 (page 20)

If an intensity, ($I_{(corr)}$), was corrected taking into account (Lp) and (Abs) it would equal

$$I_{(corr)} = I/(Abs).(Lp) \qquad (16)$$

$$I_{(corr)} = K\left|F_{(hkl)}\right|^2 \qquad (17)$$

$$I_{(corr)} = K\left|F_{(novib)}\right|^2 \exp(-2B_{iso}\sin^2\theta/\lambda^2) \qquad (18)$$

$F_{(novib)}$ is the value of F for a structure composed of no vibrating atoms.

The value of F may be reduced as a result of thermal vibrations so that if $F_{(novib)}$ is the value for the structure containing stationary atoms, the experimental values will correspond to

$$F_{(hkl)} = F_{(novib)} \exp(-2B_{iso}\sin^2\theta/\lambda^2) \qquad (19)$$

and $B_{(iso)}$ is the temperature factor.

1.7.4 THE LORENTZ FACTOR (L), POLARISATION FACTOR (p) AND ABSORPTION CORRECTIONS (Abs)

When X-rays are reflected by a plane in a crystal, a reduction in the intensity of the reflected beam occurs as a result of polarisation, scattering and absorption. The polarisation factor (p) is a measure of this polarisation. Equation (15) shows how the intensity is affected by L, p and Abs.

The Lorentz factor is an expression for the time a plane of a rotating crystal spends in the reflecting position. In terms of the reciprocal lattice or reflecting sphere concept, this is the length of time the lattice point is in contact with the sphere of reflection. This is obviously dependent on the distance of the reciprocal lattice point from the origin.

As stated previously, the intensity of the reflected rays decreases and if this is not corrected for then this results in systematic errors. The effect of this which can be attributed to absorption can be measured and corrected for using a program called SORTAV[12].

1.7.5 THERMAL ELLIPSOID

We have considered the vibrations as being isotropic, however, it would be more accurate if they were considered as anisotropic. The location of an atom in a molecule is determined by considering the average time which the atom spends in all the positions it occupies while the structure was being determined. The resultant structure is then often represented in terms of *thermal ellipsoids*, which are probability indicators of where the atoms are most likely to be found.

Six parameters can be used to describe an ellipsoid compared to a single parameter for a sphere. Three are used to define the lengths of the three mutually perpendicular axes and three to define the orientations of the ellipsoidal axes.

The ellipsoidal motion is accounted for in the structure factor equation by an anisotropic exponential factor with six anisotropic vibration parameters b_{1j} and shown in equation (20).

$$e^{-(b_{11}h^2+b_{22}k^2+b_{33}l^2+b_{12}hk+b_{23}kl+b_{31}hl)} \qquad (20)$$

The mean square vibrational amplitude in any direction, specified by the cosines, l, of the angles between the direction and the reciprocal axes, is given as;

$$\left|U^2\right| = U_{11}l_1^2 + U_{22}l_2^2 + U_{33}l_3^2 + 2U_{12}l_1l_2 + 2U_{23}l_{21}l_3 + 2U_{31}l_3l_1 \qquad (21)$$

If the ellipsoid takes the shape of a rugby ball, then the motion of the atom is mostly back and forth along the bond axis. If however it takes the shape of a curling-stone, then the motion is mostly wobbling about the bond axis. The less the thermal ellipsoid of the molecule, the smaller of its thermal motion.

The computer program used during this project to represent the thermal ellipsoids was SNOOPI[6].

1.7.6 Electron Density

X-rays are scattered by the electrons of the atom and therefore it is important to know something of the electron density at different positions within the unit cell. If a point in the

unit cell has co-ordinates x, y, z then the electron density, $\rho(x\ y\ z)$, per unit volume near the point is given by

$$\rho(x+p, y+q, z+r) = \rho(x\ y\ z) \tag{22}$$

In this equation p, q and r are any integers.

It is convenient to be able to express a function by means of a *Fourier Series*. This is the sum of the sine and cosine terms with appropriate coefficients. Fourier expansions are advantageous when the function is periodic and the electron density is one such function. Fractional co-ordinates x_n, y_n, z_n, are often used to give the precise location of an atom in a unit cell. A crystal is a periodic structure and can therefore be described by the periodic function, the *Fourier Series (or Synthesis).*

In three dimension the electron density at the point x_n, y_n, z_n is

$$\rho(x_n y_n z_n) = \left(\frac{1}{V}\right)\Sigma_h \Sigma_k \Sigma_l \left|F_{(hkl)}\right| \cos 2\pi(hx_n + ky_n + lz_n - \alpha_{(hkl)}) \tag{23}$$

Where $\rho(x_n, y_n, z_n)$ = the electron density at the points x_n, y_n, z_n.

$\left(\frac{1}{V}\right)$ = the volume of the unit cell

$\Sigma_h \Sigma_k \Sigma_l$ = the mean sum over h, k, l and $F_{(hkl)}$

$\left|F_{(hkl)}\right|$ = the structure amplitude

$\alpha_{(hkl)}$ = the phase angle of each Bragg reflection

1.7.7 PHASE PROBLEM

As stated previously in 1.7.2, $I_{hkl} \propto \left|F_{(hkl)}\right|^2$. However sets of values of $\left|F_{(hkl)}\right|^2$ do not lead to the determination of a crystal's structure. $\left|F_{(hkl)}\right|$ values are needed in equation (23) whereas, the intensities only give $\left|F_{(hkl)}\right|^2$.

If we know $|F_{(hkl)}|$ and α (of each *hkl*) we could calculate the electron densities at all values of x, y, z and plot the $\rho(x\ y\ z)$ values to give a three dimensional electron density map. However, structure factor amplitudes, $|F_{(hkl)}|$, and not phase angles, α, are obtainable from the experimental measurements.

The problem of getting estimates of the phase angles so that an image of the scattering matter can be calculated is called the *Phase Problem* and is the central one in X-ray crystallography.

The phase angle can be derived from values of A and B from statistical methods (trial structures) or by analytical methods. Once the phase angle has been determined, the structure factor amplitude can also be determined. The calculated, F_c, can then be compared with the observed amplitudes F_o. F_o has to be as close to F_c as possible in order to give a structure that best fits the calculated values.

1.7.8 SOLUTIONS TO THE PHASE PROBLEM

There are many methods which are commonly used to determine the relative phase angles of the Bragg reflections, *hkl*. The two main methods of solving the Phase Problem are:

(1) by Direct Methods and

(2) by Patterson Methods.

1.7.8.1 Direct Methods

Direct methods of structure determination, are based on two fundamental physical principles.

Firstly, the electron density in the unit cell cannot be negative at any point, and so the large majority of possible sets of values for the phases of various structure factors are not allowed. A random set of phases would give positive and negative regions in the electron density map with equal probability.

Secondly, the electron density in the cell is not randomly distributed, but is mainly concentrated in small areas which we identify as atoms.

A consequence of these two principles is that for certain sets of reflections having particular combinations of miller indices, there are theoretical probability relationships among their phases. The phases can be assigned to some reflections usually the most intense and then the positions of some or all of the heaviest atoms can be located.

When direct methods are used for phases determination, *"normalised structure factors"* are used. The structure factor $|F|$ is modified by the removal of the fall-off in the scattering factors, f, with increasing scattering angle, 2θ. In the normalisation factor, E, (equation 24) the sum is taken over all atoms in the unit cell at the value of sin θ/λ.

$$|E_{(hkl)}| = \frac{|F_{(hkl)}|}{\left[\varepsilon \sum_j f_j^2(hkl)\right]^{\frac{1}{2}}} \qquad (24)$$

where,

ε = an integer for improving the space group symmetry. The values of ε can be obtained from International Tables[5].

F = Structure Factor magnitude.

F_j = Atomic scattering factor of the j^{th} atom.

Thus showing that E is independent of sin θ/λ.

The E values give us information about the structure of the crystal. If the mean value of E is 0.798 then the structure is centrosymmetric. However, if E were 0.886 then this would indicate a noncentrosymmetric structure.

A noncentrosymmetric crystal structure has phase angles anywhere between 0° and 360°. A centrosymmetric structure on the other hand has phase angles of 0° or 180° which means $\cos\alpha = \pm 1$, $\sin\theta = 0$.

1.7.8.2 Patterson Synthesis

This is the "heavy atom" method of solving structures and is very useful for transition metal complexes, which often have one atom much heavier than the rest.

In 1934, A. L. Patterson discovered that a Fourier series using values of $|F_{(hkl)}|^2$ as coefficients instead of $F_{(hkl)}$ could produce useful information about the structure. If the

electron density at point x, y, z is taken and multiplied by the electron density at the point $x + u, y + v, z + w$ a product

$$\rho(x,y,z)\rho(x+u,y+v,z+w) \qquad (25)$$

is now formed. This is then multiplied by $d_x d_y d_z$ and integrated over the volume of the unit cell.

When the equation for the Fourier expansion is substituted for each electron density function we arrive at equation (26).

$$P_{(u,v,w)} = \frac{1}{V}\sum_{(hkl)}\left|F_{(hkl)}\right|^2 \cos 2\pi(hu+kv+lw) \qquad (26)$$

Where, $P_{(u,v,w)}$ = the electron density at u, v, w in the unit cell.

u, v, w = the vectors between the two atoms.

$u = x_1 - x_2$ $\qquad$ $v = y_1 - y_2$

$w = z_1 - z_2$ $\qquad$ V = volume of the unit cell

$F_{(hkl)}$ = is the structure factor of the *hkl* set of planes

Here Patterson used the squares of the structure amplitudes, $\left|F_{(hkl)}\right|^2$, as Fourier coefficients and these values were directly derivable from the primary experimental quantities. No phase information is required for this map because $\left|F_{(hkl)}\right|^2$ is independent of phase.

The peaks in the Patterson map occur at points whose distances from the origin correspond in magnitude and direction with distances between atoms in the crystal. This results from

$$P_{(u,v,w)} = V\iiint \rho(x,y,z)\rho(x+u,y+v,z+w)dxdydz \qquad (27)$$

The height [$P_{(u,v,w)}$] of each peak is also proportional to the product of the atomic numbers of the atom giving rise to it. The very high peaks correspond to the heavy atoms and therefore the peaks corresponding to the hydrogens are the ones appearing last in the map and are of low intensity.

One difficulty with the Patterson function is that there are so many interatomic vectors. If a unit cell contains N atoms there are N^2 vectors. There are N origin vectors and therefore there are (N^2-N) peaks other than the origin peak. Of these half are related to the other half by a centre of symmetry so there are (N^2 - N)/2 independent peaks. If N is 20, there are 190 independent Patterson peaks and the vector map will be very crowded. A further complication is that the atoms are not points, but they occupy a considerable volume.

1.7.9 STRUCTURE REFINEMENT

The aim of refinement is to obtain the best agreement between the observed (F_o) and the calculated structure factors (F_c). There is sufficient information for every atom within the unit cell to be located once the phase problem has been overcome. The most suitable sets of parameters are those which will produce the most accurate values of interatomic distances and bond angles. It is anticipated that the most suitable set will also give the best agreement between the calculated and observed structure factors.

The correctness of the structure is measured in terms of a discrepancy index, R, where

$$R = \frac{\sum |F_o - F_c|}{\sum |F_o|} \qquad (28)$$

Generally, if R has a value of 0.30 then this indicates that the correct structure is near. However, if R is 0.1 or less then F_o is close to F_c and the results are probably very reliable.

Once all the phases have been determined, a Fourier map can be calculated and the atomic positions are taken as the locations of the maxima of the electron density function (or Fourier Synthesis).

Alternatively, the least-squares process could be carried out. In 1806, Legendre introduced the idea of least-squares which is a statistical method of obtaining the best fit. This is done by minimising the sum of the square of the deviations between the exponential and the calculated parameters.

If the difference in the amplitudes of the observed and calculated structure factors $|F_o|-|F_c|$, be simply called $\Delta|F|$ and the standard deviations of the experimental values of $|F_o(hkl)|$ be $[w(hkl)]^{-1/2}$, then the best parameters for a structure are those corresponding to the minimum value of the quantity

$$Q = \Sigma\omega(hkl)\Delta|F_{(hkl)}| \tag{29}$$

The sum in this equation is taken over independent observations that is the unique diffraction maxima.

In equation (15) the scale factor (K) was introduced and this brings the observed structure factor, F_o, on to the same scale as the calculated structure factor, F_c. The relationship between K, F_o and F_c is given in equation (30).

$$K = \frac{\Sigma|F_c|}{\Sigma|F_o|} \tag{30}$$

1.8 Experimental Section

This section presents very briefly the most important aspects of the hardware, software and procedures used for X-ray data collection. CCD area detector diffractometer were used to collect the crystallographic data for the compounds presented in this work.

X-ray diffractometers basically comprise three principal parts. These are:

- *The X-ray source*: This consists of the target material, usually molybdenum or copper, housed to that it is at the focus of an 'electron gun'. Only about 0.1% of the power supplied to the source is converted to X-rays, thus there is a considerable amount of heat produced. There are generally two types of X-ray source in laboratory use, a 'sealed tube' source, where the target metal is fixed within a vacuum tube; and a rotating anode generator, where the anode is constantly allowing heat to dissipate more effectively thus more intense radiation can be generated. This requires constant pumping of the vacuum.

- *A goniometer*: This is a device to orientate the crystal into the desired positions for diffraction. The goniometer head has adjustments in the vertical and horizontal

directions to allow alignment of the crystal within the X-ray beam. There are two main types of goniometer in general use. The four-circle, where there are four arcs (χ, ϕ, θ and ω), which may be used to bring the crystal into the diffractometer position, and Kappa goniometer consisting of a Kappa block mounted at 50° to the Omega block, orienting the χ axis at 50° to the ω axis. This geometry allows the crystal to be oriented in all available in the four-circle goniometer, without the steric restriction of the χ circle.

- *A detector*: Detectors fall into two categories, single point counters and area detectors. Single point counters such as scintillation counters can measure only one diffraction at a time, thus giving long data collection times. Area detectors have the advantage of measuring several diffractions concurrently, thus speeding up data collection. There are several types of area detectors available, such as image plates, CCD and the FAST system.

1.8.1 Data collection using a CCD area detector

Data are collected using a Bruker-Nonius KappaCCD area detector diffractometer at the window of a Nonius FR590 X-ray generator (Mo). The assembly, as it stands in our laboratory, is shown below.

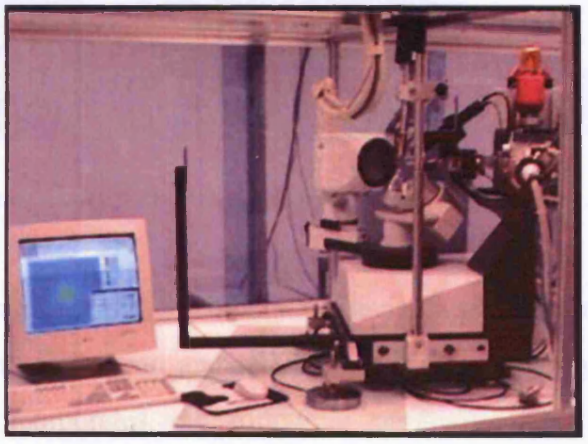

Figure 1.8: Bruker-Nonius Kappa CCD area detector diffractometer

The diffractometer has Kappa geometry, where the goniometer consists of three parts, each with its own rotation axis, intersecting with each other at a central point. The head is mounted on the phi (φ) axis, which sits on the Kappa block, which rotates around the

Kappa axis. The Kappa block is mounted on the omega block, this rotates about the omega (ω) axis. The Kappa axis forms an angle of approximately 50 degrees, the alpha angle, with the omega axis. The assembly is positioned on the theta axis, to which the detector is linked. The detector may be positioned a distance, dx, away from the crystal (where dx may be variable between 25 mm and 165 mm). The distance is selected so as to give optimum resolvability of reflections, coupled with efficient recording of the desired portions of the Ewald sphere.

The CCD detector consists of a phosphor faceplate behind a Beryllium window. When X-rays hit the faceplate the phosphor 'glows' and the light is transmitted down a tapered bundle of glass fibres, which are bonded to the CCD chip. The CCD chip is cooled to –60° by a step down Peltier cooling system. The chip is then read and a digital image produced. Images may now be stacked together in order to extract intensities from individual reflections.

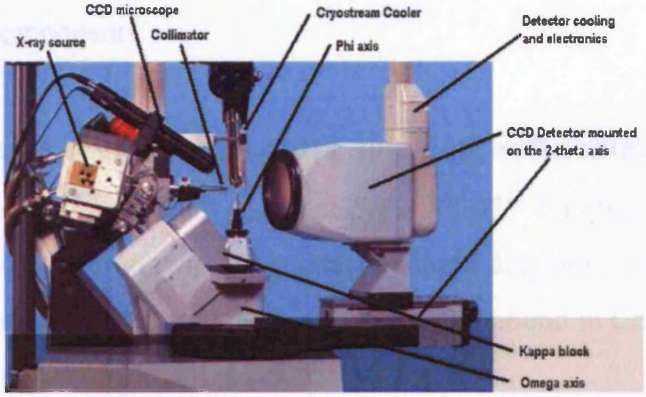

Figure 1.9: Position of Oxford cryostream in relation to the X-ray source and detector

Oxford Cryosystems cryostream low temperature device was used for data collection at 150 K[7]. The process of data collection and reduction are automated by the Nonius program COLLECT[8], which incorporates the following programs; DENZO[9], SCALEPACK[9], DirAx[10], maXus[11] and SORTAV[12].

After an initial "pre-scan" to check the crystal quality, an attempt is made to index the unit cell. This is usually done using a phi/chi experiment[13], which is combined with the program DirAx[11] but may also be performed using DENZO[9] in combination with a 10 degree ϕ scan.

Once the unit cell and orientation matrix have been obtained COLLECT[8] will calculate a data collection strategy to access all the reflections in the asymmetric unit. This is achieved via ϕ and ω scans and incorporates a Kappa offset to avoid excessive cooling of the head and icing of the crystal. In situations where the true crystal is not clear a 'triclinic' data set will be collected.

Once the data have been collected they are integrated using DENZO and passed through SCALEPACK. No scaling is actually carried out at this point but the cell is refined using all reflections. An empirical correction for absorption is applied using SORTAV from within the maXus suite of programs.

An alternative data reduction procedure may be used in the case of twins or other difficult non-standard crystals. This revolves around the phi/chi experiment, which enables the identification of twin lattices. The program evalCCD is then used to resolve the overlaps and integrate the reflections writing either an 'HKLF 4' file for the major component or an 'HKLF 5' for both components.

1.8.2 The programs used for structure solution, refinement and drawing

SHELXS-97[14] was used for structure solution: *SHELXL*-97[15] for structure refinement and *ORTEP*-3[16] for Windows for drawing of crystal structural diagrams. Absorption correction programs are cited when relevant with each individual compound in Chapters 4 – 6.

REFERENCES

1. G. H. Stout and L. H. Jensen; *X-ray Structure Determination; A Practical Guide*, McMillan, New York, 1968

2. J. P. Glusker and K. N. Trueblood; *Crystal Structure Analysis, A Primer*, 2nd Edition, Oxford University Press, 1985

3. D. E. Sands; *Introduction to Crystallography*, Benjamin Inc., New York, 1968

4. M. J. Buerger; *Crystal Structure Analysis*, J. Wiley and Sons, New York, 1960

5. *International Tables for X-ray crystallography*, Vol. II, J. S. Kasper and K. Lonsdale, Editors, D. Reidel Publishing Company, Dordrecht, Holland, 1969

6. M.F.C. Ladd and R.A. Palmer; "*Structure Determination by X-ray Crystallography*", 3rd Edition, Plenum Press, New York, 1960, 434

7. J. Cosier and A. M. Glazer; *J. Appl. Cryst.*, 1986, **19**, 105

8. R. Hooft; "*Collect: Data Collection Software*", Nonius B.V. 1998

9. Z. Otwinosnowski and W. Minor; "*Methods in Enzymology,* 1997, Vol. **276**, *Macromolecular Crystallography*, Part A, edited by C. W. Carter, Jr. and R. M. Sweet, Academic Press, New York, 1997, 307-326

10. A. J. M. Duisenberg; *J. Appl. Cryst.*, 1992, **25**, 92

11. S. Mackay, C. J. Gilmore, C. Edwards, M. Tremayne, N. Stewart and K. Shankland; *maXus, A computer program for the solution and refinement of crystal structures from diffraction data.*

12. (a) R. H. Blessing; *Acta Cryst.*, 1995, **A51**, 33 and (b) R. H. Blessing; *J. Appl. Cryst.*, 1997, **30**, 421

13. A. J. M. Duisenberg, R. W. W. Hooft, A. M. M. Schreurs and Kroon; *J. Appl. Cryst.*, 2000, **33**, 893

14. G. M. Sheldrick; *Acta Cryst.*, 1990, **A46**, 467

15. G. M. Sheldrick; *SHELXL-97 Program for Crystal structure determination*, University of Göttingen, Germany, 1997

16. L. J. Farrugia; *J. App. Cryst.*, 1997, **30**, 565

Chapter 2

METAL COMPLEXES OF SULFA DRUGS – A LITERATURE REVIEW

INTRODUCTION

A sulphonamide is any member of a class of chemical compounds, which contain the group —SO_2N—. The class includes several groups of drugs used in the treatment of bacterial infections, diabetes mellitus, oedema, hypertension and gout.[1]

Sulfonamides are analogues of *p*-aminobenzoic acid (PABA). The first sulphonamide of clinical importance was prontosil, an azo dye, which is metabolized *in vivo* to sulfanilamide. Many sulfonamides have been synthesised but they differ only slightly in their antimicrobial activity, but vary in their pharmacokinetic properties. The sulfonamides have been classified according to their rate of excretion as short-, medium- or intermediate-, long and ultra-long activity. The short-acting sulfonamides are excreted in the urine in high concentrations and have therefore been of particular use in the treatment of urinary-tract infections. Of the short-acting sulfonamides most commonly used sulfadiazine has low solubility in urine whereas sulfamerazine and sulfamethazine and their acetyl conjugates are very soluble.

The sulfonamides are synthetic bacteriostatic antibiotics with a wide spectrum against most gram-positive and many gram-negative organisms. However, many strains of an individual species may be resistant. Sulfonamides inhibit multiplication of bacteria by acting as competitive inhibitors of *p*-aminobenzoic acid in the folic acid metabolism cycle. Bacterial sensitivity is the same for the various sulfonamides, and resistance to one sulfonamide indicates resistance to all.

These drugs are extensively used in medicine and they were the first agents to be used for the treatment of bacterial infection for both human and animal disease. Use of sulfonamides today is limited to specific disease treatment in human medicine such as urinary tract infections. However, sulfonamides are more often encountered in animal medicine. The presence of certain residues in animal products presents a potential health hazard due to their allergic properties.[2] Also, some people exhibit hypersensivity to drug residues and/or low levels of drug residue may produce genetically altered bacteria that are resistant to existing drug therapy.[3] In addition, a study by the National centre for Toxicological Research indicated that sulfamethazine may be a thyroid carcinogen.[4]

2.1 History

Sulfonamides were first synthesised by Gelmo *et al.*[5] in 1908 while doing research into azo dyes. Directly following this work, Hoerlien *et al.*[6] discovered dyes containing the sulfanyl group that had affinity for proteins of silk and wool. This led to the discovery by Eisenberg in 1913, that chrysolidine, one of the azo dyes studied, had pronounced bactericidal action *in vitro*.

However, until 1932 the therapeutic properties of sulfonamides were not recognised. The German scientists Domagk *et al.*[7] found that prontosil had pronounced *in vivo* antibacterial activity. They observed that mice with streptococcal septicaemia could be cured with prontosil. Domagk also discovered that prontosil was rapidly reduced in the cell to sulphanilamide and that it was in fact the sulphanilamide and not the prontosil, which was the actual antibiotic.[8]

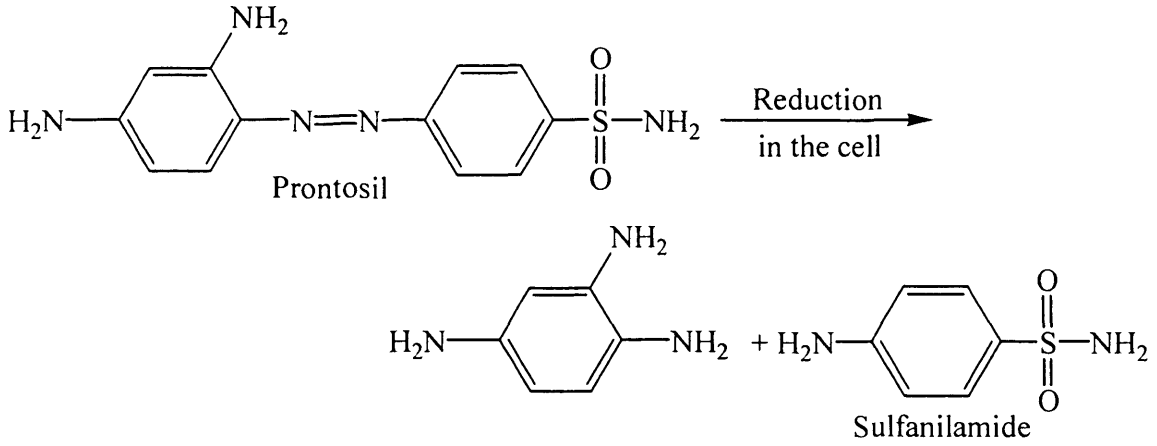

Figure 2.1: Sulfanilamide from prontosil

Many different sulfonamides were synthesised during the late 1930's. A great number of those were discovered to possess considerable antibacterial activity for a variety of streptococci and pneumonococci bacteria. Several sulfapyrimidines which were introduced in 1941[9] were found to possess considerable antibacterial activity as well as lower toxicity than previous sulfonamides. This advancement led to many new sulfonamides being synthesised. Today there are over 5000 sulfa drugs in existence but only 33 of those have been introduced for general medical use.

The use of sulphonamides as drugs dates back to the beginning of the twentieth century, when the discovery of the medicinal use of sulphonamides and their derivatives was a milestone in the history of chemotherapy. It represented the first investigation of synthetic organic molecules as potential drugs to fight infection carried in the bloodstream.

This new class of sulpha drugs was the only effective antibacterial drugs until penicillin became available in the early 1940's. Despite the benefits of the sulpha drugs, they proved ineffective against infections such as salmonella (the organism responsible for typhoid). Problems have resulted from the way in which they are metabolised in the human body, since toxic products are frequently obtained. This has ultimately led to the sulphonamides being superseded in many instances by penicillin. These drugs act by inhibiting the growth of the bacteria, rather than killing the organisms. The sulphonamides act as competitive enzyme inhibitors and block the biosynthesis of the vitamin folic acid in bacterial cells. The enzyme responsible for linking together the component parts of folic acid is inhibited and the consequences to the cell are disastrous.

The importance of sulphonamides within the pharmaceutical industry could even be seen from the database search when the compound 5-Acetamido-1, 3, 4-thiadiazole-2-sulphonamide was located. Acetazolamide, or Diamox as it is commonly known, is used in the treatment of many types of glaucoma (elevated pressure in the anterior chamber of the eye; the anterior chamber is the most forward section of the eye, behind the cornea). It is also used as a diuretic in some problems such as heart failure, or where fluid is retained in the body. This medication impedes the action of an enzyme, carbonic anhydrase throughout the body. In the eye, this leads to a decrease in production of fluid secreted in the anterior chamber of the eye, leading to a reduction in pressure. It acts in the kidney to increase the amount of bicarbonate excreted in the urine and thus increases salt and water elimination from the body. The way it works on the central nervous system is as yet not well understood.

2.2 Pharmacology

Most sulfonamides are readily absorbed orally. However, parenteral administration is difficult, since the soluble sulfonamide salts are highly alkaline and irritating to the tissues. The sulfonamides are widely distributed throughout all tissues. High levels are achieved in pleural, peritoneal, synovial, and ocular fluids. Although these drugs are no longer used to

treat meningitis, CSF levels are high in meningeal infections. Their antibacterial action is inhibited by pus.

The sulfonamides are metabolized mainly by the liver to acetylated forms and glucuronides, both of which are therapeutically inactive. Excretion is primarily renal by glomerular filtration with minimal tubular secretion or reabsorption. When these drugs are given in pregnancy, high levels are achieved in the fetus. Sulfonamides are loosely and reversibly bound in varying degrees to serum albumin. Since the bound sulfonamide is inactive and nondiffusible, the degree of binding can affect antibacterial effectiveness, distribution, and excretion.

The relative insolubility of most sulfonamides, especially their acetylated metabolites, may cause precipitation in the renal tubules. The more soluble analogues, such as sulfisoxazole and sulfamethoxazole, should generally be chosen, and the patient must be well hydrated. To avoid crystalluria and renal damage, fluid intake should be sufficient to produce a urinary output of 1200 to 1500 mL/day. Sulfonamides should not be used in renal insufficiency.

2.3 Mechanism of Action[10]

Certain microbes require *p*-aminobenzoic acid in order to synthesize dihydrofolic acid which is required to produce purines and ultimately nucleic acids. Sulfonamides, chemical analogues of PABA, are competitive inhibitors of dihydropteroate synthetase. Sulfonamides are therefore reversible inhibitors of folic acid synthesis and are bacterostatic not bacteriocidal

Spectrum of antibacterial activity and Resistance

Sulfonamides inhibit (bacteriostatic) gram-positive and gram-negative bacteria, Nocardia, Chlamydia trachomatis and some protozoa. Enteric bacteria such as *E. coli*, *Klebsiella*, *Salmonella*, *Shigella* and *Enterobacter* are also inhibited. Resistance to sulfonamides may develop when bacterial mutations result: (i) in PABA overproduction, (ii) in a folic acid synthesizing enzyme protein that has low affinity for sulfonamides and (iii) from a loss of cell permeability to sulfonamides.

2.4 Pharmacokinetics[10]

Sulfonamides can be classified in three groups: oral, absorbable oral, nonabsorbable topical and oral and absorbable oral agents may be further classified as short-, medium, or long acting sulfonamides. Sulfonamides are absorbed from the stomach and small intestine and widely distributed to tissues, including the CNS. Sulfonamides and inactivated metabolites are excreted by the kidney mainly through glomerular filtration.

2.5 Clinical Uses[10]

Sulfonamides are useful in treating urinary tract infections (UTI), but in general are rarely used as single agents. The fixed drug combination of trimethoprim-sulfamethoxazole (Bactrim) has supplanted many previous sulfonamide clinical uses. Examples are, sulfisoxazole (Gantrisin) and sulfamethoxazole (Gantanol) are used almost exclusive to treat UTI. In combination with phenazopyridine, a urinary tract anesthetic, sulfonamides are available as Azo Gantrisin and Azo Gantanol. Sulfadiazine in combination with pyrimethamine (Daraprim) (antiprotozoal agent, dihydrofolate reductase inhibitor) is first-line treatment for acute toxoplasmosis. Cefpodoxime (Vantin), a long-acting sulfonamide, is used in combination with pyrimethamine as a second-line option for treating malaria. Oral, non-absorbable drugs: Sulfasalazine (Azulfidine, salicylazosulfapyridine) is used in treating ulcerative colitis, enteritis and other inflammatory bowel disorders. The antiinflammatory action is due to the release of salicylate following splitting of sulfasalazine by intestinal bacteria. Topical Agents such as Bacterial conjunctivitis may be treated with sodium sulfacetamide opthalmic solution/ointment. Sodium sulfacetamide is an adjunctive drug in treating trachoma. Mafenide acetate is used in preventing infection in burn wounds.

2.6 Adverse reactions[10]

The most common such as fever, rash, exoliative dermatitis, photosensitivity, urticaria, nausea, vomiting, diarrhea, urinary tract problems may occur due to the precipitation of drug in urine. Sulfonamides may cause Stevens-Johnson syndrome (<1% frequency) and hemopoietic disturbances, including hemolytic or aplastic anemia, granulcytopenia, thrombocytopenia may also be caused by sufonamides.

2.7 Previous work on triple sulfa drugs (TSD)

Sulfadiazine, sulfamerazine and sulfamethazine are called together as triple sulfa drugs (TSD). The general formula is:

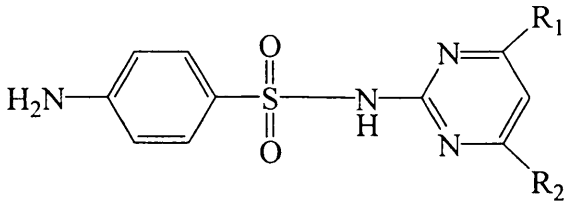

Sulfadiazine when R_1 and R_2 are hydrogen (H)

Sulfamerazine when R_1 is H and R_2 is methyl group (CH_3)

Sulfamethazine when R_1 and R_2 are methyl group (CH_3)

The presence of several potential donor sites, e.g. the sulfonamidic nitrogen, one amino nitrogen, two pyrimido nitrogen and two sulfonyl oxygen atoms make them versatile complexing agent with metal ions. The sulfonamide derivatives and their metal complexes possess antibacterial activity. A few metal complexes of the sulfonamides are still used in topical medicine as antiseptics, although it is known that interactions of heavy metal ions with biomolecules can yield potentially toxic effects.

Metal complexes of the triple sulfa drugs have gained a significant role in co-ordination chemistry. Yet the studies of metal complexes that have been reported are neither systematic nor exhaustive.

Replacement of the acidic hydrogen from the triple sulfa drug molecules produces a negative centre on the sulfonamidic nitrogen atom, which could then co-ordinate with a suitable metal(II) ion (Figure 2.2).

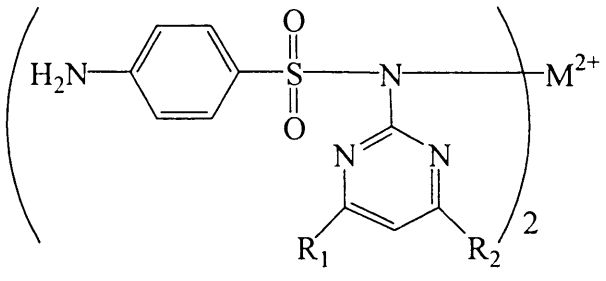

Figure 2.2

Some authors reported the preparation of several transition metal complexes of triple sulfa drugs in different mediums such as methanol, alcohol, acetone, DMSO etc. Cu(II), Zn(II), Cd(II) and Hg(II) complexes were prepared by mixing the methanolic solution of metal chloride or metal acetate and triple sulfa drugs in the molar ratio of 1:2. A precipitate was formed, stirred for six hours and the precipitate collected. Based on spectrophotometric investigations those workers suggested that Cu(II), Zn(II), Cd(II) and Hg(II) form 1:2 complexes, while Ag(I) form 1:1 complexes. The molecular compositions of the complexes were proposed on the basis of chemical analyses and spectrophotometric evidences.

It is to be noted that apart from the stereochemical interest of metal complexes of TSD, there are also interesting for their clinical use. For example, the silver and zinc complexes have already found application as topical drugs for burn healing.[11-17]

2.7.1 Sulfadiazine

The X-ray crystal structure of sulfadiazine (Figure 2.3) was initially reported for the first time by Shin *et al.*[11] in 1974.

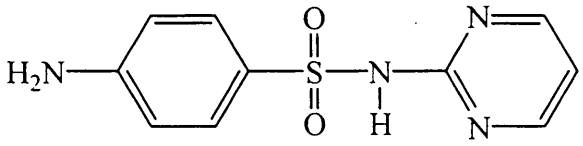

Figure 2.3: Sulfadiazine molecule

The crystal was grown by slow evaporation of sulfadiazine dissolved in a mixture of acetone and ethanol. It was found to be monoclinic space group $P2_1/c$ with a = 13.71(4), b = 5.84(3), c = 15.11(5)Å, β = 115.0(3)°, Z = 4 and R = 0.15 for 1517 reflections.

Sandmann *et al.*[12] prepared a series of silver complexes of sulfa drugs and characterised them by spectroscopic methods. It was concluded that in the silver sulfadiazine complex, the silver is ionically bound to the sulfonamidic nitrogen and the sulfonyl oxygen atoms are not coordinated to the silver ion and he suggested that the copper complex of sulfadiazine is coordinated through the sulfonyl oxygen atom. Fox[13] reported that the structure of silver sulfadiazine was analogous to the silver ammines. The metal complexes of sulfadiazine have gained a significant role in coordination chemistry.

The first crystal structure of stoichiometry Ag(sdz) was determined by Cook *et al.*[14] in 1975 and in 1976, the same crystal structure was also reported by Baenziger *et al.*[15] The crystal was found to have the monoclinic space group $P2_1/c$ with a = 6.173(2), b = 9.600(5), c = 20.30(2)Å, β = 96.22(8)°, Z = 4 and R = 0.102 for 1865 reflections. The structure of the silver sulfadiazinato complex reported by Baenziger *et al.*[15] is shown in Figure 2.4.

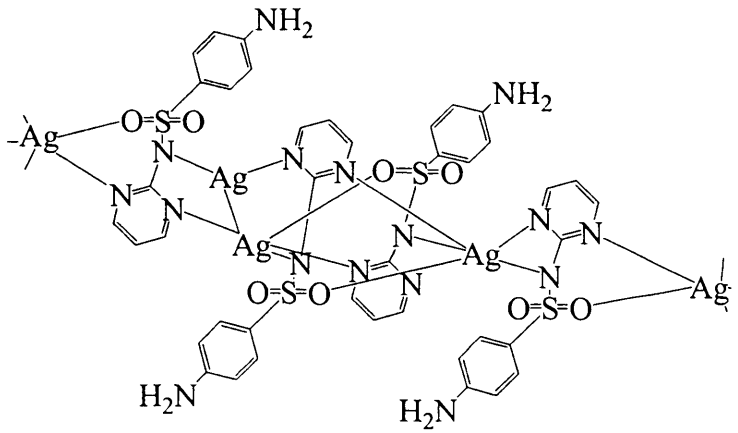

Figure 2.4: Polymeric silver complex of sulfadiazine

In the complex the nitrogen atoms of the pyrimidine ring coordinate to two different silver atoms to form a polymeric chain extending through the crystal. Each silver atom in the chain is also coordinated to one oxygen atom of sulfonyl group of the sulfadiazine molecule. A second identical chain (related by the centre of symmetry) is joined to the first chain by coordination of the silver atom from each chain to the sulfonamidic nitrogen atom of the sulfadiazine molecule in the opposite chain. In fact the silver atom in the complex is five coordinated, one is a metal-metal bond with one silver atom 2.916(1)Å away from the other silver atom in the complex. The Ag–N(imido), Ag–N(pyrimido), and Ag–O(sulfonyl) distances[15] are 2.277(6), 2.205(6), 2.459(6) and 2.571(6) Å respectively.

The crystal structure of the zinc complex $[Zn(sdz)_2]$ was determined by Yuan *et al.*[16] in 1983. It crystallises in the monoclinic space group $P2_1/n$ with a = 13.9463(3), b = 10.2008(2) and c = 17.5299(4)Å, β =113.252(1)°, Z = 4 and R = 0.0488 for 3453 reflections. The crystal structure of the complex is polymeric, with local environment of the zinc atom as shown in Figure 2.5.

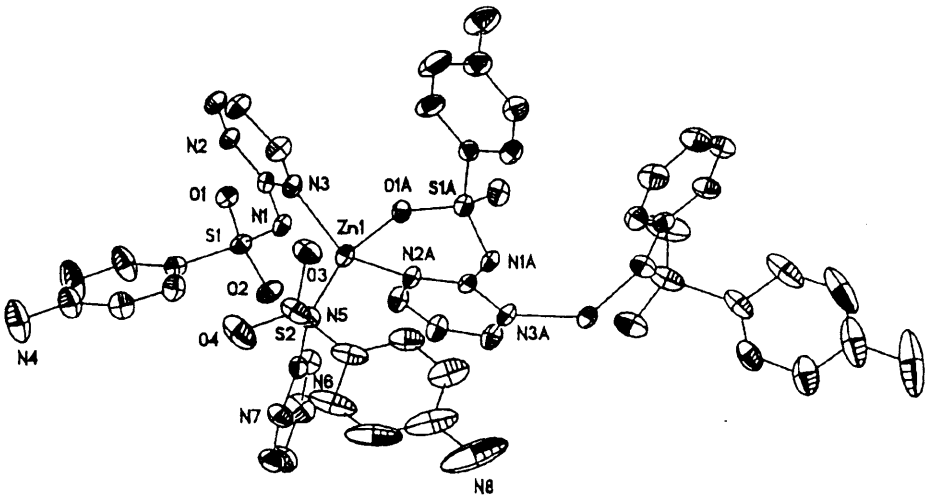

Figure 2.5

Part of the polymeric structure of $Zn(sdz)_2$ showing the coordination around Zn atom

In this complex the zinc atoms binds three sulfadiazine molecules in which one sulfadiazine acts as a monodentate ligand using imido nitrogen as the donor atom and the other two act as the tridentate bridging ligand. The zinc atom is four coordinated, one sulfonamidic nitrogen from one sulfadiazine and two pyrimido nitrogen atoms from two different sulfadiazine and one sulfonyl oxygen atom from sulfadiazine molecules.

Baenziger *et al.*[17] reported the crystal structure of the ammonia derivative of the zinc complex of sulfadiazine $[Zn(sdz)_2(NH_3)_2]$. It crystallises in the orthorhombic space group $Pn2_1a$, a = 13.894(1), b = 14.221(1), c = 12.608(1)Å, Z = 4 and R = 0.040 for 3485 independent reflections. The structure of the complex is as follows:

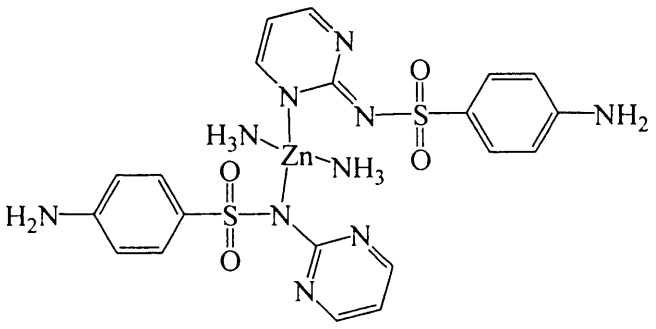

Figure 2.6

Zinc complex of sulfadiazine with two molecules of ammonia $[Zn(sdz)_2(NH_3)_2]$

It was suggested that the complex has a distorted tetrahedral arrangement with four Zn-N bonds, two from ammonia molecules with distances of 2.036(4) and 2.050(4)Å and two

from the sulfadiazine molecules. The sulfadiazine molecules are coordinated at different sites, one molecule uses its imido nitrogen atom [2.166(4)Å] and the other uses its pyrimido nitrogen atom [2.078(4)Å]. In addition, there are two Zn-N interactions at distances of 2.406 and 2.729Å with pyrimido nitrogen and sulfonamidic nitrogen atoms respectively. From this evidence it is concluded that the complex $[Zn(sdz)_2(NH_3)_2]$ may be described as five or six coordinate. The crystal structure of the same complex was also determined by Brown *et al.*[18] and confirms the earlier study.

The crystal structure of the analogous copper complex of sulfadiazine $[Cu(sdz)_2(NH_3)_2]$ was reported by Brown *et al.*[19] It crystallises in the orthorhombic with space group $Pn2_1a$ with a = 13.915(5), b = 14.356(5), c = 12.659(5)Å, Z = 4 and R = 0.045 for 1417 reflections. The structure of the complex is shown in Figure 2.7.

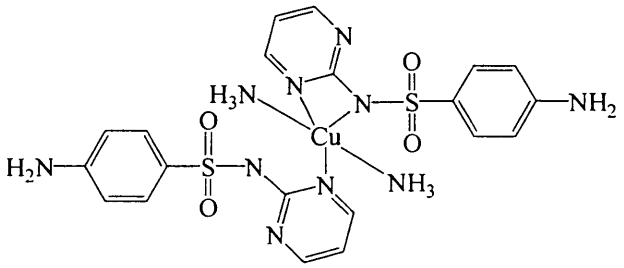

Figure 2.7

Copper complex of sulfadiazine with two molecules of ammonia $[Cu(sdz)_2(NH_3)_2]$

It was found that the complex the copper atom coordinates five nitrogen atoms in a distorted square pyramidal arrangement. The basal plane contains two nitrogen atoms from ammonia molecules and two nitrogen atoms from one sulfadiazine molecule. The other nitrogen from the second sulfadiazine molecule occupies the apex position. The Cu–N bond distances of 2.071(13), 2.479(18), 2.083(11) and 1.894(10)Å are in an irregular square with a mean N–Cu–N angles of 87.6(4)°. The Cu–N bond distance of 2.377(10)Å is at the apex position with an angle of 100.0(4)°. This compound is isostructural with the corresponding zinc complexes.[17,18]

In 1993 Menabue *et al.*[20] reported the cadmium complex of sulfadiazine $[Cd(sdz)_2].2H_2O$. The crystals are monoclinic, space group $C2/c$, a = 19.879(3), b = 8.730(3) and c = 16.538(3)Å, β = 122.15(2)°, Z = 4 and R = 0.034 for 2019 reflections. The structure of the complex is as follows:

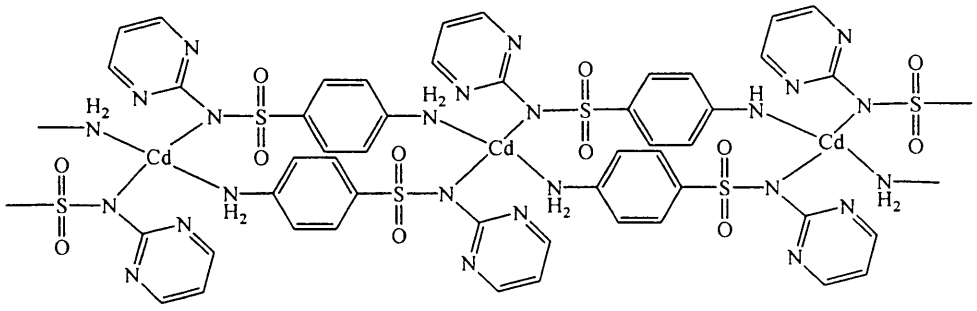

Figure 2.8: Cadmium complex of sulfadiazine

The cadmium atom in the complex lies on the two-fold axis and is four coordinated to two sulfonamidic nitrogen and two amino nitrogen from the symmetry related sulfadiazinato anions giving rise to the polymeric chain along the *b*-direction. In the complex the cadmium ion has a distorted tetrahedral geometry.

In 1997, Garcia-Raso *et al.*[21] reported the mercury complex of sulfadiazine with DMSO as a secondary ligand $[Hg(sdz)_2(DMSO)_2]$. The compound crystallises in the monoclinic space group $C2/c$ with a = 20.537(7), b = 8.653(3), c = 18.846(6)Å, β = 106.68(2)°, Z = 4 and R = 0.418 for 3551 reflections. The structure is shown in Figure 2.9.

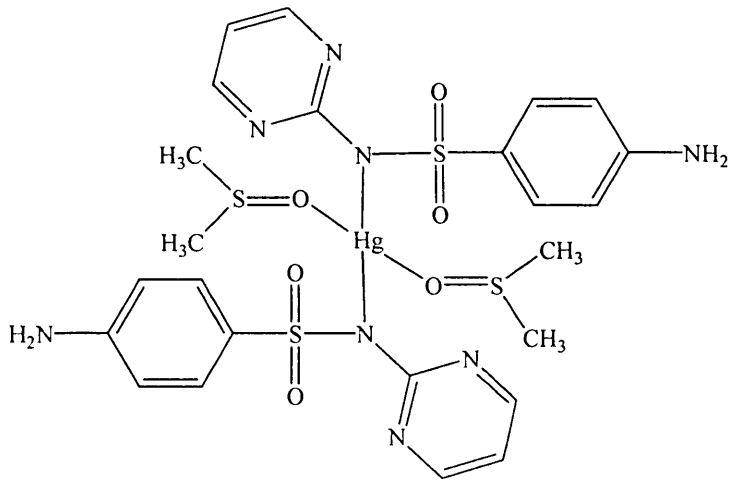

Figure 2.9: Mercury complex of sulfadiazine with two molecules of DMSO

The coordination geometry about the mercury atom is approximately linear with Hg–N distance 2.087(4)Å and N–Hg–N angle 175.0(2)°. Two DMSO molecules bound to the mercury atom with Hg–O distance 2.769(2)° result in a four fold coordination.

The metal complexes of sulfadiazine show different coordination geometries, *e.g.*, copper and zinc atoms in the complexes $[M(sdz)_2(NH_3)_2]$ are five coordinated but zinc atom in the complex $[Zn(sdz)_2]$ is four coordinate. The silver, cadmium and mercury atoms in the complexes of sulfadiazine have four coordination spheres

2.7.2 Sulfamerazine

In an early stage thermomicroscopic studies indicated the existence of two polymorphs of sulfamerazine.[22,23] This was subsequently confirmed by the crystal structure determination. In 1982, Acharya *et al.*[24] reported the crystal structure of one form of sulfamerazine. The crystal was orthorhombic with space group *Pbca*, a = 9.145(1), b = 11.704(1), and c = 22.884(2)Å, Z = 4 and R = 0.078 for 2082 reflections. The structure of the sulfamerazine molecule is as follows:

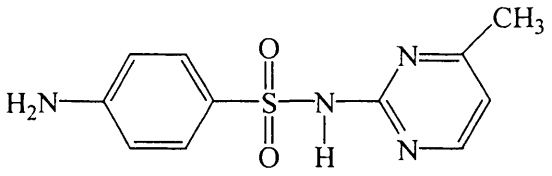

Figure 2.10: Sulfamerazine molecule

In 1992, Caira *et al.*[25] reported the polymorph of sulfamerazine which was orthorhombic with space group $Pna2_1$, a = 14.474(2), b = 21.953(2), c = 8.203(1)Å, Z = 8 and R = 0.047 for 1886 reflections. The structure was dimeric form where hydrogen atom of sulfonamidic nitrogen of one sulfamerazine molecule is hydrogen bonded with the pyrimido nitrogen atom of the second sulfamerazine molecule which is shown in Figure 2.11.

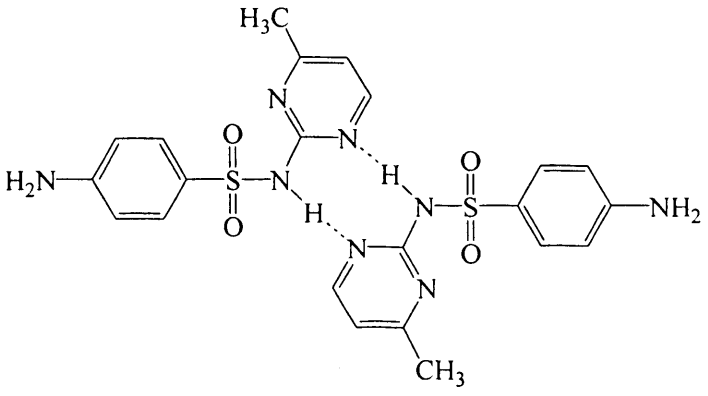

Figure 2.11: Structure of sulfamerazine as dimer

Caira *et al.*[25] suggested that the two polymorphs are dimer where pseudocentro-symmetric exists in their structure and centrosymmetric exists in the structure, reported by Acharya *et al.*,[24] formed via two N(imide)–H···N(pyrimido) hydrogen bonds.

This ligand has also capability of forming complexes with metal ions but there is no report of metal complexes of sulfamerazine in the literature.

2.7.3 Sulfamethazine

Basak *et al.*[26] reported the X-ray crystal structure of sulfamethazine in 1983. It was found that the molecule exists as dimer, which linked together in an infinite chain. The crystal of sulfamethazine was monoclinic with space group $P2_1/a$, a = 7.427(2), b = 18.986(11), c = 9.323(4)Å, β = 99.09(2)°, Z = 4 and R = 0.045 for 1766 reflections.

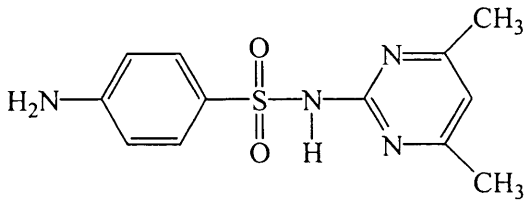

Figure 2.12: Sulfamethazine molecule

In 1984 Tiwari *et al.*[27] reported the same crystal structure of sulfamethazine with the same unit cell dimensions. The crystal structure is stabilised by network hydrogen bonds and van der Waal's forces. The amino nitrogen atom of one sulfamethazine participates in two unequal hydrogen bonds with pyrimido nitrogen atoms of other sulfamethazine molecule.

Recently some metal complexes of the sulfamethazine have been published. In 2000, Garcia-Raso *et al.*[28] reported the crystal structure of polymeric cadmium complex $[Cd(smz)_2(H_2O)].2H_2O$ in the monoclinic space group $P2_1/c$ with a = 13.357(2), b = 15.046(2), c = 15.369(1)Å, β = 97.60°, Z = 4 and R = 0.1125 for 9258 reflections.

The cadmium ion in the complex exhibits a highly distorted octahedral geometry, being coordinated to two sulfonamidic nitrogen and two pyrimido nitrogen atoms of two bidentate chelating sulfamethazine ligands generating four membered rings. The terminal amino nitrogen atom of a third sulfamethazine, which is bonded to the adjacent cadmium

ion and oxygen atom of a water molecule complete the coordination sphere. In the complex one of the sulfamethazine molecules presents two equivalent Cd–N bond distances.

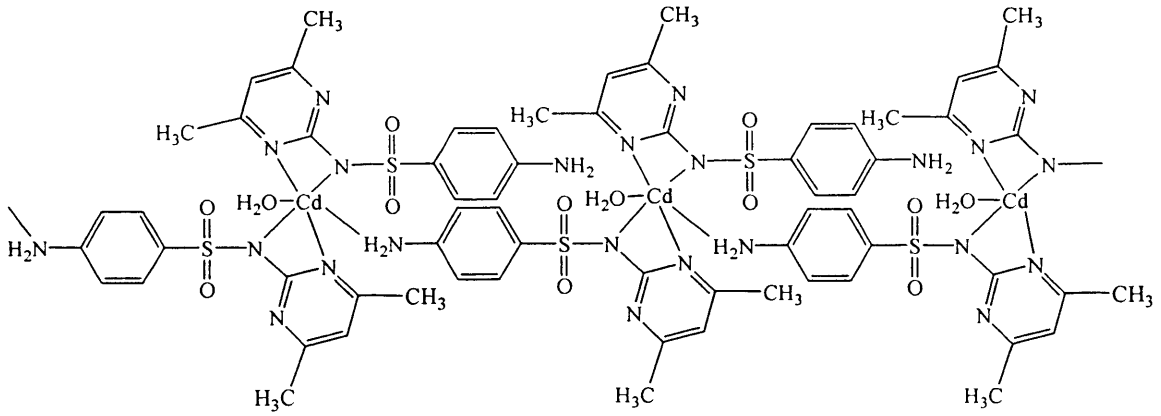

Figure 2.13: Polymeric cadmium complex of sulfamethazine

In 2001, Gutierrez *et al.*[29] reported another polymeric crystal structure of copper complex $\{[Cu(smz)_2].2H_2O\}_n$. The crystals are monoclinic, space group $P2_1/c$, a = 13.810(2), b = 14.577(2), c = 13.785(1)Å, β = 96.03(3)°, Z = 4 and R = 0.526 for 5772 reflections.

The copper ion is five coordinated and bound to five nitrogen atoms from three sulfamethazine molecules and two pyrimido nitrogen atoms of two sulfamethazine molecules one of which belongs to the adjacent copper atom. The copper ion exhibits a distorted square pyramidal geometry. The structure is shown in Figure 2.14

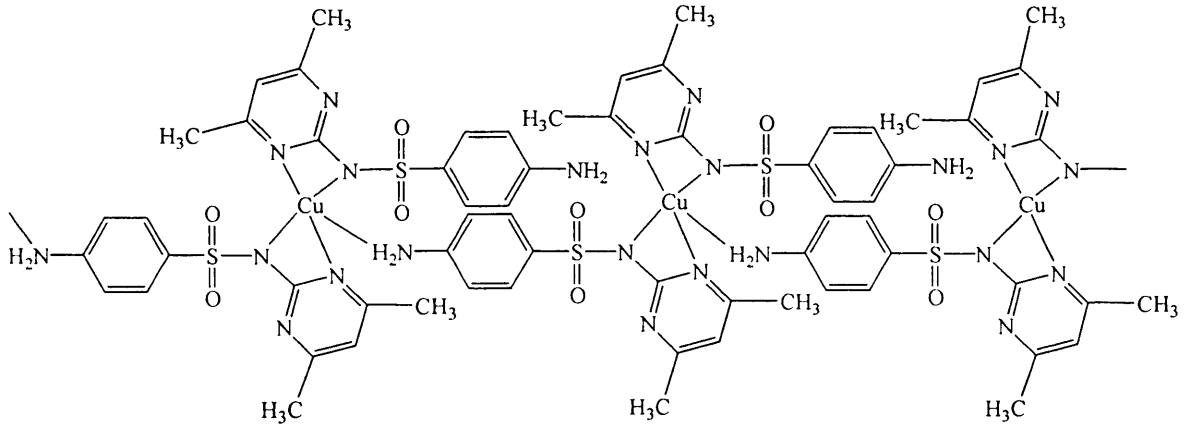

Figure 2.14: Polymeric copper complex of sulfamethazine

They[29] also reported the dimeric copper complex of sulfamethazine with two molecules of dimethylformamide $[Cu(CH_3COO)_2(smz)_2].2dmf$. The crystals are monoclinic space group with a = 8.9486(9), b = 15.0956(2) and c = 16.542(3)Å, β = 105.584°, Z = 2 and R = 0.0409 for 6508 reflections. The structure of the complex is shown in Figure 2.15.

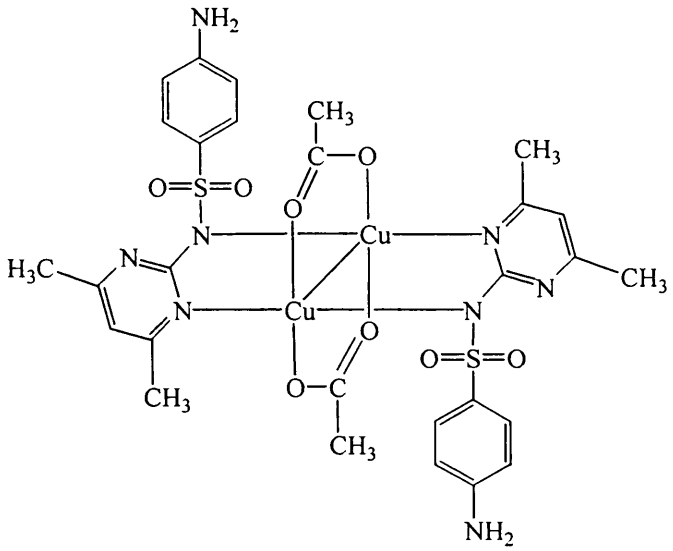

Figure 2.15: Dimeric copper complex of sulfamethazine with two acetate ions

The crystal consists of dinuclear units and two solvent molecules of dimethylformamide. In the complex the Cu-Cu distance is 2.5412(6)Å. The copper atom presents a nearly square planar geometry.

2.8 Aim of the work

The development of sulfonamides is one of the most fascinating and informative chapters in medicinal chemistry, highlighting the roles of skillful planning and providence in drug research. About 30 sulfonamides are now used in clinical practice. Of them three sulfonamides, sulfadiazine, sulfamerazine and sulfamethazine, also known as "triple sulfa drugs", were used as antibacterial agents since the 1940's.

Sulfonamides are one of the few groups of drugs whose mechanism of antimicrobial action is now known at the enzyme level. Their action is characterized by a competitive antagonism of certain essential factors vital to the metabolism of microorganism. Evidence of this antagonism started coming soon after the discovery of sulfonamides.

Many studies on the sulfonamide have been carried out in the past. Most of these focused on its antibacterial activity, but studies on the complexes of transition metals, particularly those playing important roles in the biological systems were very few and far between.

Interactions of sulfa drugs with different metal ions normally present in the body system are therefore quite important. Since transition metals, particularly Cu and Zn, play vital roles in life processes, some synthetic and structural studies of the sulfa drug complexes of these metals have been carried out. A general series of complexes with general formula $[M(tsd)_2(L)_x]$ [M = Co, Ni, Cu, Zn, Cd and Hg; where tsd = triple sulfa drugs and L = any secondary ligands containing two nitrogen donor atoms when $x = 1$ and one nitrogen atom when $x = 2$] have been prepared and structurally characterised.

Triple sulfa drugs have also been shown to react with heavy metals such as Ag, Cd and Hg, which may lead to the potential use of sulfa drugs as topical medicine for burn treatment. In all these cases, a maximum of two drug ions are directly bonded with the metal centre, other positions in the coordination sphere being filled up by the secondary ligands such as water, ammonia or other nitrogen containing donor species.

In some of these complexes, triple sulfa drug molecules are directly bonded with the metal ions. Previous work on this type of complexes has been rather fragmentary and without systematic approach. We have therefore endeavoured in the present work to examine the synthesis of such complexes in a systematic way and examine in details the important structural features to be discussed later.

The secondary ligands that have been used in this study, most of which contain nitrogen donor atoms, namely ammonia, pyridine (py), ethylenediamine (en), 2,2′-bipyridine (bpy), 1,10-phenanthroline (phen), 4,4′-dimethyl-2,2′-bipyridyl (dmbpy) and diethylenetriamine (dien), [(*N*,*N*′-bis(3-aminopropyl)-1,2-ethylenediamine (apen) and in some cases, water and dimethylformamide (DMF) are the secondary ligands which contains oxygen as donor atom. These species utilise their nitrogen atoms to bind with metals and can be monodentate (ammonia, water, py, DMF), bidentate (en, bpy, phen, dmbpy), tridentate (dien) or tetradentate (apen) depending on the number of nitrogen atoms available. The purpose of this study has been primarily to examine the behaviour of the secondary ligands in the presence of sulfonamides, the relative ease with which the compounds would be

formed and also to correlate their properties to gain greater insight into the bonding characteristics and structural chemistry.

The chemistry of metal complexes of sulfa drugs is important not only from the point of view of synthetic routes and structural varieties associated with such complexes, but also due to the fact that the coordination modes of sulfa drugs under different conditions and in different environments are particularly important. One of our aims in this work has been to explore the different coordination modes of sulfa drugs in different metal complexes.

It is well known that the neutral sulfa drug molecules contain hydrogen atom on its sulfonamidic nitrogen atom and act as weak acid. In solution, this acidic hydrogen can be easily removed from the triple sulfa drug molecules to produce a negative centre on the sulfonamidic nitrogen atom. Most of the resultant negative charge is located on the nitrogen atom, which could then act as a Lewis base (donor) and coordinate with a suitable Lewis acid (metal ion).

In many cases the sulfa drug molecules act as a bidentate ligand involving the formation of a chelate or even a bridge between two metal centres and in some cases act as a tridentate ligand. The later mode of coordination is rather rare, but there is at least one example where the sulfa drug ion acts as a chelating as well as a bridging ligand. This happens with the compound $Zn(sdz)_2$ as shown in Figure 2.8. The coordination chemistry of sulfa drug is thus quite versatile and definitely very interesting from a structural point of view. This has prompted us to undertake research in this field. Different possible coordination modes of the sulfa drug ion are illustrated later in this chapter.

These studies reveal that sulfonamides form metal complexes rather easily under ambient or nearly ambient conditions most of which are biologically essential and some are toxic. Whether these aspects could have any bearing with the living systems need to be fully explored. The structural studies carried out so far clearly establish sulfonamides as coordinating agents of considerable interest in that it can use any or all of its potential sites (N and O) for coordination with metals producing complexes. There are a few metal complexes of sulfonamides in the literatures, and we decided to carry out an in depth study on the topic. The sulfonyl oxygen atoms are particularly polar which enable them to interact with metal ions under suitable conditions. Owing to these properties the

sulfonamides would react with different metal ions in different ways, the course of which cannot be predicted during synthetic reactions. In view of the presence of multi-center coordinating positions in the sulfonamide molecules, the possibilities of coordination with metal ions or the formation of ionic species may follow several modes of reactions.

i) It can act as a monodentate ligand by forming bond either through sulfonamidic or pyrimidine nitrogen or sulfonyl oxygen atoms:

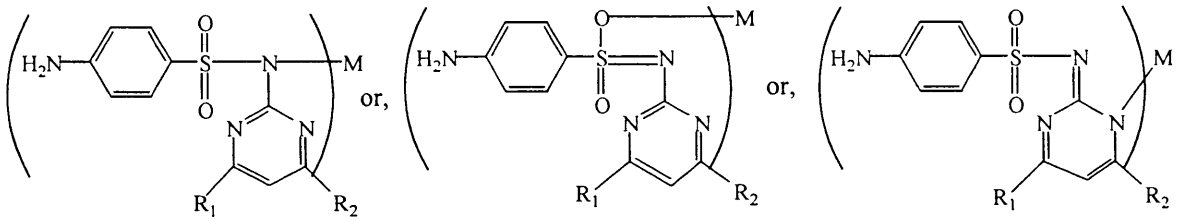

ii) It can behave as a bidentate ligand in the chelating mode:

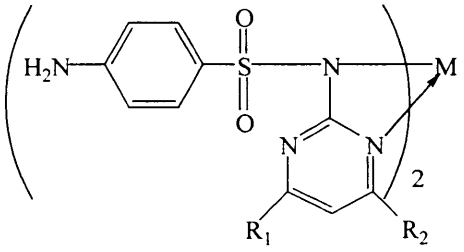

iii) It can involve more than two donor atoms in the formation of polymeric compounds:

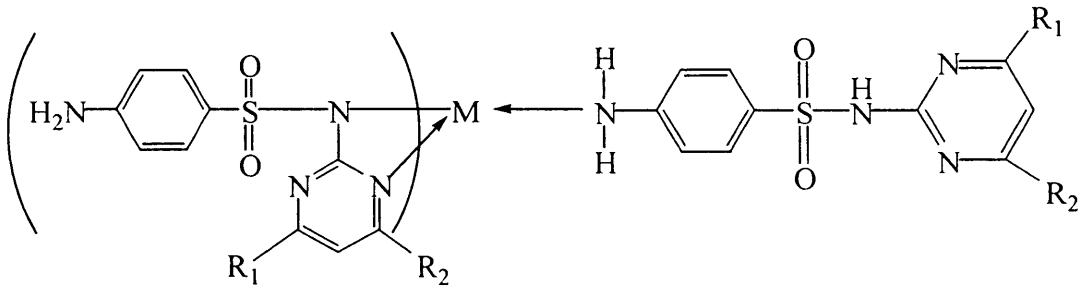

or,

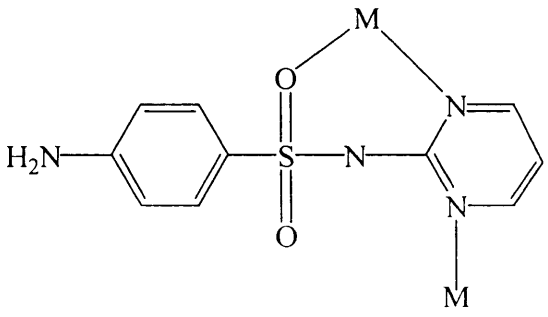

The presence of secondary ligand such as ammonia could produce a variety of metal complexes with interesting stereochemistry and properties.

It has been mentioned earlier that the deprotonation of neutral sulfa drug molecules leave the negative charge (–) on the sulfonamidic nitrogen atom and this is the main reason why the nitrogen site is preferred when bonding with metal ions. However, since the pyrimidine nitrogen and sulfonyl oxygen atoms are also found to be involved in bonding with the metal ions, it is very likely that the negative charge or a fraction of it is shifted away from the nitrogen atom along the ring bonds to the oxygen atoms. In addition to the synthetic and structural work, we carried out theoretical calculations to investigate the charge distribution in the sulfa drug ions and in the neutral sulfa drug, to find out if the above assumption is true.

Finally, the roles of weak intermolecular forces particularly the hydrogen bonds in the formation of packing diagram and determining the properties of materials are now well recognised, especially in organic chemistry. One of our particular aims in this work has been to investigate the nature of these interactions both within and between different complex "molecules" that we have studied by X-ray crystallography.

REFERENCES

1. L. A. Cates; "Sulfa Drugs in *Handbook of Chemotherapeutic Agents*, Vol. 1", M. Verderame ed., CRC Press, Boca Raton, 1986, 1

2. W. J. Blanchflower and D. A. Rice; *J. Assoc. Anal. Chem.*, 1988, **71**, 302

3. B. M. Kagan, "*Antimicrobial Therapy*", W.B. Saunders, Philadelphia, 1974

4. N. Littlefield; Technical Report, *National Center for Toxicological Research*, Jeffersons, A. R., 1988

5. P. H. Long and E. A. Bliss; "*The Clinical and Experimental Use of Sulfanilamide, Sulfapyridine, and Allied Compounds*", The Macmillan Co., New York, 1939

6. H. Hoerlein; *Proc. Roy. Soc. Med.*, 1935, **29**, 313

7. G. Domagk; *Deutsche Med. Wehnschr.*, 1935, **61**, 250

8. J. Trefouel, Mme. Trefouel, F. Nittie and D. Bovet; *C. R. Soc. Biol.*, 1935, **120**, 756

9. L. H. Sophian, D. L. Piper and G. H. Schneller, "*The Sulfapyrimidines*", A. Colish, New York, 1952

10. H. F. Chambers and E. Jawetz; "*Sulfonamides, Trimethoprim and Quinolones, in Basic and Clinical Pharmacology*", (Katzung, B.G., ed) Appleton-Lange, 1998, pp. 761-763

11. H. S. Shin, G. S. Ihn, H. S. Kim and C. H. Koo; *J. Korean Chem. Soc.*, 1974, **18**, 329

12. B. J. Sandmann, R. U. Nesbitt and R. H. Sandmann; *J. Pharm. Sci.*, 1974, **63**, 1948

13. C. L Fox, Jr., *U.S.P.* 1971, 1, 240, 545

14. D. S. Cook and M. F. Turner; *J. Chem. Soc. Perkin Trans.*, 1975, **2**, 1021

15. N. C. Baenziger and A. W. Struss; *Inorg. Chem.*, 1976, **15**, 1807

16. R. –X. Yuan, R. –G. Xiong, Z. –F. Chen, P. Zhang, H. –X. Ju, Z. Dai, Z. –J. Guo, H. –K. Fun and X. –Z. You; *J. Chem. Soc. Dalton Trans.*, 2001, 774

17. N. C. Baenziger; *Acta Cryst.*, 1983, **C39**, 1620

18. C. J. Brown, D. S. Cook and L. Sengier; *Acta Cryst.*, 1987, **C43**, 2332

19. C. J. Brown, D. S. Cook and L. Sengier; *Acta Cryst.*, 1985, **C41**, 718

20. L. Menabue and M. Saladini; *J. Inorg. Biochem.*, 1993, **49**, 201

21. A. Garcia-Raso, J. J. Fiol, G. Martorell, A. Lopez-Zafra and M. Quiros; *Polyhedron*, 1997, **16**, 613

22. M. Kuhnert-Brandstatter and S. Wunsch; *Mikrochim. Acta*, 1969, **6**, 1308

23. M. Kuhnert-Brandstatter; *Thermomicroscopy in the analysis of Pharmaceuticals*, Oxford: Pergamon Press, 1971, 34

24. K. R. Acharya, K.N. Kuchela and G. Kartha; *J. Cryst. Spect. Res.*, 1982, **12**, 369

25. M. R. Caira and R. Mohamed; *Acta Cryst.*, 1992, **B48**, 492

26. A. K. Basak, S. K. Mazumdar and S. Chaudhuri; *Acta Crsyt.*, 1983, **C39**, 492

27. R. K. Tiwari, M. Haridas and T. P. Sing; *Acta Cryst.*, 1984, **C40**, 655

28. A. Garcia-Raso, J. J. Fiol, S. Rigo, A. Lopez-Lopez, E. Molins, E. Espinosa, E. Borras, G. Alzuet, J. Borras and A. Castineiras; *Polyhedron*, 2000, **19**, 991

29. L. Gutierrez, G. Alzuet, J. Borras, A. Castineiras; A. Rodriguez-Fortea and E. Ruiz; *Inorg. Chem.*, 2001, **40**, 3089

Chapter 3

EXPERIMENTAL-PREPARATION OF METAL COMPLEXES OF TRIPLE SULFA DRUGS WITH SECONDARY LIGANDS

EXPERIMENTAL

3.1 Chemicals and their purifications

The Analar grade chemicals (SIGMA and BDH) were purchased and used as received and the solvents acetone, methanol, dimethylformamide and dimethylsulfoxide were also used as received throughout the experiments.

3.2 Physical measurements

3.2. 1 Elemental analysis

C, H and N were estimated microanalytically using a Perkin-Elmer 2400 CHN elemental analyzer.

3.2.2 IR studies

The IR spectra were recorded on a Nicolet 510 FTIR spectrometer, each compound was pressed into a KBr disk that was prepared in a sample holder by compressing a powdered sample with a ten-fold excess of KBr, which was preheated in an oven before use.

3.2.3 Electron Paramagnetic Resonance

ENDOR (Electron Nuclear Double resonance) spectroscopy is an EMR (Electron Magnetic Resonance) technique that is often described as EPR-Detected NMR. EPR and ENDOR spectra recorded on a Bruker ESP 300E series spectrometer fitted with a Bruker ESP 360 DICE ENDOR system and an Oxford Instruments liquid helium variable temperature system. X-band EPR and ENDOR spectra were recorded using a Bruker EN 801 ENDOR cavity operating at a modulation frequency of 12.5 kHz in both cases and the ENDOR spectra were obtained using an ENI A-300 RF power amplifier operating at an attenuation of 8 dB. Accurate g values were obtained at X-band using a Bruker ER 035 M NMR gaussmeter calibrated to the perylene radical cation in concentrated H_2SO_4, g = 2.002569. Q-band EPR and ENDOR spectra were obtained using a Bruker ER 5106 QTE ENDOR cavity operating at a modulation frequency of 100 kHz for the EPR experiments and 12.5

kHz for the ENDOR. The ENDOR spectra were recorded using an ENI ER 3200L RF power amplifier operating at a total attenuation of 13 dB.

3.2.4 ^{1}H NMR and ^{13}C NMR spectra

NMR spectra were recorded on a Bruker Avance AMX-400 spectrometer. ^{1}H and ^{13}C NMR spectra were obtained from a solution of the compounds in d_6-DMSO. The chemical shifts are expressed in ppm relative to internal TMS.

3.2.5 X-ray crystallography

The crystallographic measurements for the complexes were made at 150 K on a Bruker Nonius Kappa CCD area detector using graphite monochromatised Mo Kα radiation, λ = 0.71073 Å. The structures were solved by direct methods (SHELXS-97) and refined on F^2 by full-matrix least squares (SHELXL-97) using all unique data and parameters. The hydrogen atoms on the amino groups of sulfa drugs in the complexes and water molecules (where present) were located from the difference Fourier maps and refined freely.

3.3 Synthetic Procedure

The complexes were synthesized by the following simple reaction procedures: the sodium salt of sulfadiazine (Nasdz), sulfamerazine (Hsmr) and the sodium salt of sulfamethazine (Nasmz) were dissolved in 50 mL of hot methanol and the methanolic solution of the respective metal salts were added slowly with constant stirring on a hot plate, a precipitate was formed and the mixture was continued to stir for six hours. The precipitate was filtered and dried over silica gel. The complexes of transition metals were colored whereas those of zinc, cadmium and mercury were white powders.

Reaction scheme:

$$M^{2+} + 2(Na/Htsd) \longrightarrow M(tsd)_2 + 2Na^{+}/2H^{+}$$

[where M^{2+} is any divalent metal ion and Htsd any sulfa drugs]

The precipitate was used for further reaction with secondary ligands in DMF solution to obtain the single crystals for the complexes (**3**) to (**28**).

$$M(tsd)_2 + xL \longrightarrow M(tsd)_2(L)_x$$

Where L is any secondary ligand, bidentate when x = 1 and monodentate when x = 2.

All the complexes are stable in air and at room temperature. The complexes are insoluble in water, alcohol and most organic solvents but soluble in DMF and DMSO.

We used the following metal salts:

1) Cobalt chloride ($CoCl_2.6H_2O$) (Pink precipitate)

2) Nickel chloride ($NiCl_2.6H_2O$) (Light blue precipitate)

3) Copper chloride ($CuCl_2.6H_2O$) (Red precipitate)

4) Zinc chloride ($ZnCl_2.6H_2O$) (White precipitate)

5) Cadmium acetate [$(CH_3COO)_2Cd.6H_2O$] (White precipitate)

6) Mercury acetate [$(CH_3COO)_2Hg.6H_2O$] (White precipitate)

These precipitates were dissolved in DMF/DMSO and a secondary ligand was added, stirred for 30 minutes, filtered and the filtrate was left for crystallization.

3.4 Syntheses of the complexes

3.4.1 Preparation of the crystal of sulfadiazine (1)

Solid sulfadiazine (0.563 g, 1 mmol) was dissolved in a minimum amount of DMF and stirred for 30 minutes. It was filtered and left for crystallisation. After three days white block crystals were obtained. IR: (KBr disc), cm^{-1}, 3461(s), 3365(s), 3125(s), 2956(sh), 1625(vs), 1598, 1570, 1507(vs), 1465(sh), 1408, 1351, 1325(m),, 1306, 1259, 1155(vs), 1125(s), 1106, 1093(s), 1045, 1005(s), 945(vs), 881(vw), 796(vs), 746, 680(s), 656(m), 633(vs), 589, 535(vs). ^{1}H NMR (DMSO-d_6): δ 11.35s [1H, N(11)], 8.49d [1H, C(12/14), J = 11.7Hz], 6.59d [H, C(17/19), J = 8.7], 7.65d [1H, C(16/20), J = 8.6], 6.99t [1H, C(13), J = 4.8], 6.00s [2H (–NH_2)]. ^{13}C NMR (DMSO-d_6): δ 157.5 [C11], 158.6 [C12/14], 153.4 [C18], 130.3 [C16/C20], 125.1 [C15], 115.9 [C13], 112.6 [C17/C19].

3.4.2 Preparation of the new polymorph of sulfamerazine (2)

Solid sulfamerazine (0.265g; 1 mmol) was dissolved in DMF (20 mL) and stirred for 30 minutes, filtered and the clear solution of sulfamerazine was left for crystallization. White block crystals of sulfamerazine were obtained by slow evaporation of the solution at room temperature. IR: (KBr disc): ν cm^{-1}, 3468(m), 3370(s), 3238, 3120(s), 1630(vs), 1570(vs), 1505(sh), 1446(sh), 1408(vs), 1372, 1343(m), 1331(vs), 1304(vs), 1245(sh), 1153(vs), 1107(s), 1093(s), 1040(s), 973, 965(vs), 889(vw), 836, 798(vw), 748(vs), 717(sh), 681(s),

636(s), 616(vs), 579, 548(vs). ^{1}H NMR (DMSO-d_6): δ 11.20 [1H, N(11)], 8.37d [1H, C(14), J = 4.8], 7.69d [2H, C(16)/C(20), J = 8.2], 6.95d [2H, C(17)/C(19), J = 4.9], 6.62d [1H, C(13), J = 8.2], 6.07s [2H N(14)], 2.41s [3H (CH_3)]. ^{13}CNMR (DMSO-d_6): δ 168.0 [C11], 157.5 [C12], 156.8 [C14], 152.9 [C18], 130.1 [C15], 124.9 [C16/20], 114.7 [C17/19], 112.1 [C13], 23.3 [CH_3].

3.4.3 Preparation of the complex $\{[Co(smz)_2(H_2O)].DMF\}_n$ (3)

The DMF solution was filtered and left for crystallisation. Two weeks later, pink prismatic crystals were obtained. It was filtered and dried over silica gel. The compound is soluble in DMF and DMSO but insoluble in water and all other organic solvents. Anal. Found: C, 54.25, H, 3.40; N, 11.10%. Calc. for $C_{32}H_{30}CoN_{10}O_4S_2$: C, 54.20, H, 3.48; N, 11.15%. IR: (KBr disc), cm^{-1}, 3435(m), 3353(s), 3291(s), 2925, 2873, 1665(vs), 1598, 1581, 1561(vs), 1501(sh), 1434(vs), 1395, 1373, 1344(m), 1301(vs), 1251(vs), 1178(sh), 1144(vs), 1126(s), 1081, 999(s), 974(vs), 878(vw), 835, 794, 733(vs), 678(s), 636(s), 598, 557, 522(vs).

3.4.4 Preparation of the complex $[Ni(en)_3][sdz)_2].H_2O$ (4)

To the solution of nickel precipitate of sulfadiazine, ethylenediamine (en) (0.5 mL) was added, stirred for 30 minutes. The solution was filtered and left for crystallisation. A few days later, white block crystals were obtained. It was filtered and dried over silica gel. The compound is soluble in DMF and DMSO but insoluble in water and all other organic solvents. Anal. Found: C, 41.31, H, 5.90; N, 25.89%. Calc. for $C_{26}H_{44}NiN_{14}O_5S_2$: C, 41.29, H, 5.87; N, 25.94%. IR: (KBr disc), cm^{-1}, 3441(m), 3332(s), 3225(s), 1643(vs), 1596, 1581, 1552(vs), 1470(sh), 1448(sh), 1439(vs), 1414, 1348, 1313(m), 1298(vs), 1268(vs), 1181(sh), 1161(vs), 1134(s), 1102, 1091(s), 1083, 1061, 1011(s), 975(vs), 840(vw), 828, 811, 806, 763(vs), 681(s), 651(m), 644(s), 626(vs), 584, 558, 524(vs).

3.4.5 Preparation of the complex $[Ni(smr)_2(py)_2].4py$ (5)

To prepare this complex, the light blue powder nickel precipitate of sulfamerazine was dissolved in pyridine and stirred for 30 minutes. The solution was filtered and left for crystallisation. A week later, pink crystals were obtained. It was filtered and dried over silica gel. The compound is soluble in DMF and DMSO but insoluble in water and all other organic solvents. Anal. Found: C, 58.95, H, 4.90; N, 18.40. Calc. for $C_{52}H_{52}NiN_{14}O_4S_2$: C, 58.93, H, 4.94; N, 18.5%. IR: (KBr disc), cm^{-1}, 3438(m), 3349(s), 3223(s), 1632(vs), 1595(vs), 1551, 1516, 1501, 1434(sh), 1411(sh), 1351(vs), 1338(m), 1316, 1295(vs),

1266(vs), 1227(sh), 1177(vs), 1131(s), 1103, 1091, 1083(s), 1011(s), 1001, 973(vs), 866(vw), 852, 816, 801, 774(vw), 725(sh), 680(s), 645(m), 583(vs), 556(vs).

3.4.6 Preparation of the complex $[Cu(en)_2(sdz)_2]$ (6)

To the DMF solution of copper precipitate of sulfadiazine, ethylenediamine (en) (1 mL) was added, stirred for 30 minutes. Five days later, blue block crystals were filtered and dried over silica gel. The compound is soluble in DMF and DMSO but insoluble in water and all other organic solvents. Anal. Found: C, 38.14, H, 4.54; N, 22.21%. Calc. for $C_{24}H_{34}CuN_{12}O_4S_2$: C, 38.12, H, 4.53; N, 22.24%. IR: (KBr disc), cm^{-1}, 3439(m), 3341(s), 3229(s), 1641(vs), 1599, 1584, 1554(vs), 1469(sh), 1446(sh), 1439(vs), 1413, 1347, 1312(m), 1297(vs), 1267(vs), 1178(sh), 1158(vs), 1131(s), 1102, 1091(s), 1081, 1058, 1008(s), 977(vs), 840(vw), 763(vs), 678(s), 651(m), 643(s), 625(vs), 583, 556, 523(vs).

3.4.7 Preparation of the complex $[Cu(dien)(sdz)_2]$ (7)

With the same procedure but diethylenetriamine (dien) (1 mmol) was added in the solution and stirred for 30 minutes. After seven days, white block crystals were filtered and dried over silica gel. The compound is soluble in DMF and DMSO but insoluble in water and all other organic solvents. Anal. Found: C, 46.71, H, 5.75; N, 25.48%. Calc. for $C_{28}H_{44}CuN_{14}O_4S_2$: C, 46.73, H, 5.73; N, 25.51%. IR: (KBr disc), cm^{-1}, 3452(m), 3379(s), 3339(s), 3304(m), 3155(s), 1629(vs), 1598, 1578, 1537(vs), 1501(s), 1465(sh), 1417(vs), 1362, 1315, 1301(m), 1265(vs), 1240, 1221, 1173(sh), 1126(s), 1091(s), 1071, 1000(s), 968(vs), 835(vw), 809, 676(s), 661(m), 636(s), 574, 564, 528(vs).

3.4.8 Preparation of the complex $[Cu(en)_2(H_2O)_2][smr)_2]$ (8)

To the solution of DMSO, a few drops of ethylenediamine were added, stirred for 30 minutes. After seven days, blue prismatic crystals were obtained. It was filtered and dried over silica gel. The compound is soluble in DMF and DMSO but insoluble in water, alcohol and acetonitrile. Anal. Found: C, 41.84, H, 5.67; N, 22.52%. Calc. for $C_{26}H_{42}CuN_{12}O_6S_2$: C, 41.81; H, 5.67; N, 22.56%. IR: (KBr disc): cm^{-1}, 3523(m), 3387(s), 3331(s), 3174(s), 3275(s), 3174, 1662(vs), 1597(vs), 1576(vs), 1558(m), 1504(vs), 1458(sh), 1422(vs), 1400(m), 1365(s), 1317(m), 1294(sh), 1272(vs), 1228(m), 1178(m), 1122(sh), 1089(s), 1074(m), 1037(s), 1008(w), 994(m), 971(w), 898(s), 828(s), 810(s), 755(s), 719(vw), 680(w), 634(w), 625(vw), 591(vs).

3.4.9 Preparation of the complex $[Cu_2(en)_4(H_2O)_4][smr)_2].H_2O$ (9)

To the solution of DMF, a few drops of ethylenediamine were added, stirred for 30 minutes. After filtration it was left for crystallization. A week later, blue prismatic crystals were obtained. It was filtered and dried over silica gel. The compound is soluble in DMF and DMSO but insoluble in water, alcohol and acetonitrile. Anal. Found: C, 40.87, H, 5.75; N, 22.93%. Calc. for $C_{26}H_{44}CuN_{12}O_7S_2$: C, 40.83; H, 5.77; N, 21.99%. IR: (KBr disc): cm^{-1}, 3524(m), 3387(s), 3331(s), 3275(s), 3174(m), 1660(m), 1597(vs), 1576(vs), 1558(m), 1504(vs), 1454(sh), 1422(vs), 1394(m), 1363(s), 1318(m), 1294(sh), 1272(vs), 1228(m), 1178(m), 1122(sh), 1089(s), 1074(m), 1037(s), 1010(w), 996(m), 971(w), 898(s), 830(s), 807(s), 755(s), 719(vw), 680(w), 637(w), 621(vw), 592(vs), 555(vs).

3.4.10 Preparation of the complex $[Cu_2(smr)_4].2DMF$ (10)

The DMF solution of copper precipitate of sulfamerazine was left for crystallization. Ten days later, deep green plate like crystals were obtained. The compound is soluble in DMF and DMSO but insoluble in water, alcohol and acetonitrile. Anal. Found: C, 45.31, H, 4.40; N, 18.97%. Calc. for $C_{50}H_{58}CuN_{18}O_{16}S_4$: C, 45.26; H, 4.42; N, 19.02%. IR: (KBr disc): ν cm^{-1}, 3423(s), 3346(s), 3228(m), 1636(vs), 1597(vs), 1554(vs), 1502(vs), 1452(sh), 1413(vs), 1386(vs), 1319(sh), 1282(vs), 1205(m), 1177(m), 1131(sh), 1078(s), 1046(w), 971(w), 957(w), 872(w), 833, 811, 792(s), 779(vw), 716(vw), 682(s), 583(vs), 547(vs).

3.4.11 Preparation of the complex $[Cu_2(smr)_4].2DMSO$ (11)

The DMSO solution of the same precipitate was filtered and left for crystallization. Two weeks later, deep green block crystals were obtained. The compound is soluble in DMF and DMSO but insoluble in water, alcohol and acetonitrile. Anal. Found: C, 41.85, H, 4.60; N, 15.00%. Calc. for $C_{26}H_{34}CuN_8O_6S_4$: C, 41.89; H, 4.59; N, 15.06%. IR: (KBr disc): ν cm^{-1}, 3420(s), 3341(s), 3232(m), 1639(vs), 1596(vs), 1552(vs), 1501(vs), 1450(sh), 1414(vs), 1383(vs), 1317(sh), 1281(vs), 1204(m), 1178(m), 1130(sh), 1076(s), 1045(w), 974(w), 953(w), 876(w), 830, 810, 789(s), 779(vw), 712(vw), 677(s), 589(vs).

3.4.12 Preparation of the complex $[Cu(smz)_2(apen)].3H_2O.CH_3OH$ (12)

To the DMSO solution of copper precipitate of sulfamethazine, a few drops of *N,N'*(3-aminopropyl)-bis-ethylenediamine (apen) were added and stirred for 30 minutes, filtered and left for crystallization. After five days, blue prismatic crystals were obtained, filtered

and dried over silica gel. The compound is soluble in DMF and DMSO but insoluble in water, alcohol and acetonitrile. Anal. Found: C, 44.95, H, 6.75; N, 19.10%. Calc. for $C_{33}H_{60}CuN_{12}O_8S_2$: C, 44.97; H, 6.81; N, 19.08%. IR: (KBr disc): cm^{-1}, 3345(m), 3210(s), 2980(m), 1625(s), 1598(vs), 1570(vs), 1520(m), 1506(vs), 1483(sh), 1423(vs), 1388(m), 1350(s), 1315(m), 1294(sh), 1270(vs), 1214(m), 1182(m), 1120(sh), 1092(s), 1042(s), 1020(w), 982(m), 938(w), 905(s), 845(s), 812(s), 768(s), 692(w), 634(w), 625(vw).

3.4.13 Preparation of the complex $\{[Cu(smz)_2.NH_3].2H_2O\}_n$ (13)

The copper precipitate of sulfamethazine was dissolved in NH_3-H_2O (1:1) and stirred for 30 minutes. A week later, green prismatic crystals were obtained. The compound is soluble in water, DMF and DMSO. Anal. Found: C, 41.63, H, 4.65; N, 18.57. Calc. for $C_{24}H_{33}CuN_9O_6S_2$: C, 42.94, H, 4.96; N, 18.78. IR: (KBr disc), cm^{-1}, 3436(m), 3350(s), 3237(m), 1629(vs), 1597(vs), 1581(sh), 1560(m), 1501(s), 1434(m), 1397(m), 1373(m), 1322(m), 1300(m), 1250(m), 1210(s), 1184(vs), 1143(m), 1127(sh), 1081(sh), 999(sh), 975(vs), 881(s), 832(m), 791(vw), 735(sh), 677(s), 639(s), 600(vs), 557(vs).

3.4.14 Preparation of the complex $[Zn(smz)_2(NH_3)_2]$ (14)

The white zinc precipitate of sulfamethazine was dissolved in 1:1 NH_3:H_2O solution and stirred for 30 minutes. A week later, white block crystals were obtained. The compound is soluble in DMF and DMSO but insoluble in water, alcohol and acetonitrile. Anal. Found: C, 44.01; H, 4.95; N, 21.41%. Calc. for $C_{24}H_{32}ZnN_{10}O_4S_2$: C, 44.03; H, 4.89; N, 21.40%. IR: (KBr disc): cm^{-1}, 3544(m), 3365(s), 3272(s), 3150(m), 1640(m), 1599(vs), 1557(m), 1501(vs), 1434(sh), 1378(m), 1318(s), 1306(m), 1293(sh), 1244(vs), 1209(m), 1184(m), 1142(sh), 1117(s), 1081(m), 1050(s), 1010(w), 978(w), 885(s), 830(s), 794(s), 743(s), 677(w), 601(vs), 548(vs). ^{1}H NMR (DMSO-d_6): δ 7.58d [2H, C(16/20), J = 8.2 Hz], 6.42d [2H, C(17/19), J = 8.1], 6.33s [1H, C(13)], 5.50s [2H (–NH_2)], 2.49s [6H, CH_3], ^{13}C NMR (DMSO-d_6): δ 167.5 [C(11)], 162.3 [C(12/14)], 151.2 [C(18)], 130.3 [C(15)], 129.8 [C(16/20)], 111.9 [C(17/C19)], 110.3 [C(13)], 23.3 [CH_3].

3.4.15 Preparation of the complex $[Zn(smz)_2(py)_2].2py$ (15)

The same precipitate of the previous experiment was dissolved in a 1:10 C_5H_5N:H_2O solution and stirred for 30 minutes. Five days later, white prismatic crystals were obtained. The compound is soluble in DMF and DMSO but insoluble in water, alcohol and

acetonitrile. Anal. Found: C, 59.95, H, 5.25; N, 19.10%. Calc. for $C_{44}H_{46}ZnN_{12}O_4S_2$: C, 59.96; H, 5.22; N, 19.08%. IR: (KBr disc): cm^{-1}, 3464(m), 3387(s), 3174(m), 1629(m), 1593(vs), 1552(vs), 1501(vs), 1445(sh), 1416(vs), 1383(m), 1316(s), 1296(sh), 1260(vs), 1214(m), 1138(m), 1116(sh), 1081(s), 1009(w), 979(w), 835(s), 784(s), 676(w), 589(vs), 554(vs). ^{1}H NMR (DMSO-d_6): δ 8.68d [2H, C(1/5), J = 4.6 Hz], 7.85t [1H, C(3), J = 7.3 Hz], 7.57d [2H, C(16/20), J = 8.3 Hz], 7.45t [2H, C(2/4), J = 5.3 Hz], 6.43d [2H, C(17/19), J = 7.8], 6.32s [1H, C(13)], 5.56s [2H, (–NH_2)], 2.41s [6H, CH_3], ^{13}C NMR (DMSO-d_6): δ 166.9 [C(11)], 162.4 [C(12/14)], 151.2 [C(18)], 150.0 [C(1/5)], 136.4 [C(3)], 130.1 [C(15)], 129.2 [C(16/20)], 124.2 [C(2/4)], 111.7 [C(17/C19)], 110.5 [C(13)], 23.0 [CH_3].

3.4.16 Preparation of the complex [Cd(dien)(sdz)$_2$].DMF (16)

To the DMF solution, diethylenetriamine (dien) (1 mmol) was added, stirred for 30 minutes. After seven days white block crystals were obtained. Anal. Found: C, 41.21, H, 4.90; N, 21.36%. Calc. for $C_{27}H_{38}CdN_{12}O_5S_2$: C, 41.16, H, 4.87; N, 21.34%. IR: (KBr disc), cm^{-1}, 3436(m), 3350(s), 3246, 2925(w), 2878(w), 1665(vs), 1629(s), 1593, 1547(vs), 1501(sh), 1449(sh), 1409(vs), 1357, 1317(m), 1265(vs), 1244, 1178(sh), 1132(s), 1096(s), 1071, 1015(s), 979(vs), 841(vw), 800, 682(s), 579, 554. ^{1}H NMR (DMSO-d_6): δ 8.11d [2H, C(12/14), J = 4.7], 7.47d [2H, C(16/20), J = 8.2], 6.40t [1H, C(13), J = 4.5], 6.45d [2H, C(17/19), J = 8.3], 5.39s [2H, (–NH_2)], 2.89d [4H, C(2/3), J = 6.3], 2.73d [4H, C(1/4), J = 5.8]. ^{13}CNMR (DMSO-d_6): δ 164.5 [C(12/14)], 157.5 [C(11)], 150.3 [C18], 133.3 [C(16/20)], 128.8 [C(15)], 112.1 [C(13)], 109.7 [C(17/19)], 48.3 [C(2/3)], 31.1 [C(1/4)].

3.4.17 Preparation of the complex [Cd(dien)(smr)$_2$].H_2O (17)

To the DMF solution of cadmium precipitate of sulfamerazine, diethylenetriamine (dien) (1 mL) was added and stirred for 30 minutes. A week later, white block crystals were obtained. The compound is soluble in DMF and DMSO but insoluble in water and all other organic solvents. Anal. Found: C, 41.01, H, 4.90; N, 22.29%. Calc. for $C_{26}H_{37}CdN_{11}O_5S_2$: C, 41.07, H, 4.92; N, 20.26%. IR: (KBr disc), cm^{-1}, 3446(m), 3345(s), 3242(s), 2922, 2872, 1645(vs), 1597, 1581, 1553(vs), 1470(sh), 1445(sh), 1439(vs), 1412, 1361, 1314(m), 1294(vs), 1271(vs), 1181(sh), 1162(vs), 1132(s), 1101, 1093(s), 1085, 1061, 1007(s), 976(vs), 843(vw), 825, 811, 803, 762(vs), 684(s), 653(m), 642(s), 625(vs), 587, 559. ^{1}H NMR (DMSO-d_6): δ 8.24d [1H, C(14), J = 5.2], 7.76d [2H, C(16, 20), J = 8.4], 6.83d [2H, C(17, 19), J = 5.1], 6.53d[1H, C(13), J = 8.7], 5.89s [2H (–NH_2)], 2.88d [4H, C(2/3), J =

6.1], 2.79d [4H, C(1/4), J = 5.9], 2.37s [3H (CH_3)]. ^{13}CNMR (DMSO-d_6): δ 167.9 [C(11)], 162.5 [C(12)], 157.1 [C(14)], 151.0 [C(18)], 131.0 [C(15)], 129.5 [C(16/20)], 112.1 [C(17/19)], 110.1 [C(13)], 47.6 [C(2/3)], 38.8 [C(1/4)], 23.6 [CH_3].

3.4.18 Preparation of the complex [Cd(sdz)$_2$(bpy)] (18)

To the DMF solution of cadmium precipitate of sulfadiazine, 2,2'-bipyridine (bpy) (1 mmol) was added, stirred for 30 minutes. Two weeks later, white block crystals were obtained. Anal. Found: C, 46.91, H, 3.40; N, 18.29%. Calc. for $C_{32}H_{30}CdN_{10}O_4S_2$: C, 46.97, H, 3.42; N, 18.26%. IR: (KBr disc), cm^{-1}, 3409(m), 3334(s), 3226(s), 1645(vs), 1599, 1583, 1553(vs), 1471(sh), 1447(sh), 1438(vs), 1415, 1349, 1314(m), 1299(vs), 1269(vs), 1180(sh), 1160(vs), 1133(s), 1101, 1092(s), 1082, 1060, 1010(s), 978(vs), 841(vw), 829, 812, 805, 764(vs), 680(s), 652(m), 645(s), 627(vs), 585, 557, 525(vs), 411(w). ^{1}H NMR (DMSO-d_6): δ 9.14 [1H, C(1)], 8.63 [(1H, C(4)], 8.37d [2H, C(12/14), J = 4.7], 8.25 [1H, C(3)], 7.39d [2H, C(16/20), J = 6.7], 7.78 [1H, C(2)], 6.74t [1H, C(13), J = 4.8], 6.36d [2H, C(17/19), J = 8.4], 5.58s [2H, (–NH_2)]. ^{13}CNMR (DMSO-d_6): δ 162.9 [C(12/14)], 158.8 [C(11)], 153.4 [C18], 155.2 [C(5)], 149.2 [C(1)], 137.1 [C(4)], 129.1 [C(16/20)], 125.8 [C(15)], 124.9 [C(3)], 121.2 [C(2)], 112.2 [C(13)], 111.8 [C(17/19)].

3.4.19 Preparation of the complex [Cd(sdz)$_2$(phen)] (19)

To the DMF solution of the same precipitate of the previous experiment, 1,10-phenanthroline (1 mmol) was added, stirred for 30 minutes. A week later, white block crystals were obtained. The compound is soluble in DMF and DMSO but insoluble in water and all other organic solvents. Anal. Found: C, 48.55, H, 3.28; N, 17.74; Calc. for $C_{32}H_{30}CdN_{10}O_4S_2$: C, 48.58, H, 3.31; N, 17.70. IR: (KBr disc), cm^{-1}, 3431(m), 3339(s), 3227(s), 1638(vs), 1598(vs), 1553, 1515, 1503, 1438(sh), 1413(sh), 1351(vs), 1339(m), 1317, 1294(vs), 1265(vs), 1228(sh), 1178(vs), 1133(s), 1104, 1092, 1081(s), 1011(s), 1003, 978(vs), 868(vw), 850, 816, 804, 773(vw), 727(sh), 680(s), 645(m), 583(vs), 556(vs), 523(vw), 441(w), 420(w), 409. ^{1}H NMR (DMSO-d_6): δ 9.60 [1H, C(1)], 8.90 [(1H, C(2)], 8.43d [2H, C(12/14), J = 3.7], 8.25 [1H, C(3)], 7.29d [2H, C(16/20), J = 4.8], 8.18 [1H, C(6)], 6.76t [1H, C(13), J = 4.7, 4.6], 6.30d [2H, C(17/19), J = 7.8], 5.54s [2H, (–NH_2)]. ^{13}CNMR (DMSO-d_6): δ 162.7 [C(12/14)], 158.8 [C(11)], 152.8 [C18], 151.5 [C(5)], 150.8 [C(1)], 138.4 [C(4)], 129.1 [C(16/20)], 127.4 [C(6)], 124.9 [C(3)], 121.2 [C(2)], 112.2 [C(13)], 111.9 [C(17/19)].

3.4.20 Preparation of the complex [Cd(smr)$_2$(phen)] (20)

To the DMF solution of cadmium precipitate of sulfamerazine, 1,10-phenanthroline (1 mmol) was added, stirred for 30 minutes. A week later, white block crystals were obtained. The compound is soluble in DMF and DMSO but insoluble in water and all other organic solvents. Anal. Found: C, 49.85, H, 3.68; N, 17.14; Calc. for $C_{34}H_{30}CdN_{10}O_4S_2$: C, 49.82, H, 3.69; N, 17.10. IR: (KBr disc), cm^{-1}, 3438(m), 3345(s), 3236(s), 1631(vs), 1596(vs), 1583, 1551, 1511, 1503, 1433(sh), 1412(sh), 1360(vs), 1338(m), 1316, 1299(vs), 1268(vs), 1223(sh), 1179(vs), 1132(s), 1103, 1090, 1083(s), 1012(s), 1001, 978(vs), 861(vw), 852, 813, 807, 776(vw), 723(sh), 682(s), 645(m), 585(vs), 558(vs). ^{1}H NMR (DMSO-d_6): δ 9.26d [1H, C(1), J = 4.9], 8.69t [1H, C(2), J = 5.1], 8.30d [1H, C(14), J = 5.1], 8.15d [1H, C(3), J = 4.8], 8.03s [1H, C(6)], 7.72d [2H, C(16, 20), J = 8.2], 6.81d [2H, C(17, 19), J = 5.2], 6.51d[1H, C(13), J = 8.6], 5.87s [2H (–NH_2)], 2.36s [3H (CH_3)]. ^{13}CNMR (DMSO-d_6): δ 168.1 [C(11)], 163.4 [C(12)], 156.2 [C(14)], 151.5 [C(18)], 150.3 [C(5)], 148.8 [C(1)], 138.3 [C(4)], 130.5 [C(15)], 129.1 [C(16/20)], 127.3 [C(6)], 124.7 [C(3)], 121.6 [C(2)], 112.5 [C(17/19)], 110.3 [C(13)], 23.4 [CH_3].

3.4.21 Preparation of the complex [Cd(sdz)$_2$(dmbpy)].2DMF (21)

The white cadmium precipitate of sulfadiazine was dissolved in DMF and to this solution 4,4'-dimethyl-2,2'-bipyridine (1 mmol) was added and stirred for 30 minutes. The solution was filtered and left for crystallisation. A few days later, white block crystals were obtained, filtered and dried over silica gel. The compound is soluble in DMF and DMSO but insoluble in water and all other organic solvents. Anal. Found: C, 48.55, H, 3.28; N, 17.74; Calc. for $C_{32}H_{30}CdN_{10}O_4S_2$: C, 48.58, H, 3.31; N, 17.70. IR: (KBr disc), cm^{-1}, 3421(m), 3353(s), 3240(s), 1669(vs), 1600(vs), 1578, 1549, 1501, 1486, 1440(sh), 1418(sh), 1388(vs), 1352(m), 1322, 1296(vs), 1270(vs), 1239(sh), 1173(vs), 1139(s), 1088(s), 1009(s), 976(vs), 834, 803, 737(vw), 719(sh), 684(s), 659(m), 639, 584(vs), 530(vs), 518(vw), 472. ^{1}H NMR (DMSO-d_6): δ 9.07 [1H, C(1)], 7.68 [(1H, C(2)], 8.56 [(1H, C(4)], 2.34 [3H, C(6)], 8.38d [2H, C(12/14), J = 4.1], 7.36d [2H, C(16/20), J = 6.3], 6.74t [1H, C(13), J = 4.8], 6.35d [2H, C(17/19), J = 8.2], 5.56s [2H, (–NH_2)]. ^{13}CNMR (DMSO-d_6): δ 162.6 [C(12/14)], 158.7 [C(11)], 152.8 [C18], 151.5 [C(5)], 150.3 [C(1)], 137.4 [C(4)], 129.1 [C(16/20)], 126.4 [C(6)], 125.8 [C(15)], 121.2 [C(2)], 112.2 [C(13)], 111.5 [C(17/19)], 21.3 [C(6)].

3.4.22 Preparation of the complex $\{[Cd(smz)_2(H_2O)].DMF\}_n$ (22)

The cadmium precipitate of sulfamethazine was dissolved in DMF filtered and left for crystallization and after fifteen days white block crystals were obtained. The compound is soluble in DMF and DMSO but insoluble in water and all other organic solvents. Anal. Found: C, 54.25, H, 3.40; N, 11.10; Cd, 7.68. Calc. for $C_{32}H_{30}CdN_{10}O_4S_2$: C, 54.20, H, 3.48; N, 11.15; Cd, 7.79%. IR: (KBr disc), cm^{-1}, 3437(m), 3351(s), 3292(s), 2923, 2871, 1635(vs), 1597, 1582, 1560(vs), 1502(sh), 1433(vs), 1394, 1371, 1342 (m), 1303(vs), 1250(vs), 1177(sh), 1145(vs), 1127(s), 1083, 998(s), 973(vs), 876(vw), 834, 793, 732(vs), 679(s), 637(s), 599, 556, 524(vs). ^1H NMR (DMSO-d_6): δ 7.59d (2H, C(16/20), J = 8.4 Hz], 6.43d [2H, C(17/19), J = 8.0], 6.40s [1H, C(13)], 5.54s [2H (–NH_2)], 2.49s [6H, CH_3], ^{13}C NMR (DMSO-d_6): δ 167.5 [C11], 162.3 [C12/14], 151.2 [C18], 130.4 [C15], 129.8 [C16/20], 111.9 [C17/C19], 110.2 [C13], 23.3 [CH_3].

3.4.23 Preparation of the complex $\{[Cd(smz)_2(H_2O)].2H_2O\}_n$ (23)

The same precipitate was dissolved in a 1:1 water:ammonia mixture and stirred for 30 minutes. The solution was filtered and left for crystallisation. After five days white block crystals were obtained. The compound is soluble in DMF and DMSO but insoluble in water and all other organic solvents. Anal. Found: C, 54.25, H, 3.40; N, 11.10; Cd, 7.68. Calc. for $C_{32}H_{30}CdN_{10}O_4S_2$: C, 54.20, H, 3.48; N, 11.15; Cd, 7.79%. IR: (KBr disc), cm^{-1}, 3540, 3461(m), 3368(s), 3280(s), 3157, 1639(vs), 1598(vs), 1583, 1557, 1501, 1432(sh), 1397(sh), 1377(vs), 1345(m), 1298(vs), 1245(vs), 1209(sh), 1178(vs), 1142(s), 1125, 1080(s), 999(s), 980(vs),883(vw), 832, 804, 793(vw), 738(sh), 677(s), 636(m), 599(vs), 558(vs). ^1H NMR (DMSO-d_6): δ 7.61d (2H, C(16/20), J = 8.5 Hz], 6.45d [2H, C(17/19), J = 8.4], 6.38s [1H, C(13)], 5.59s [2H (–NH_2)], 2.50s [6H, CH_3], ^{13}C NMR (DMSO-d_6): δ 167.4 [C11], 162.2 [C12/14], 151.3 [C18], 130.2 [C15], 129.5 [C16/20], 111.8 [C17/C19], 110.3 [C13], 23.2 [CH_3].

3.4.24 Preparation of the complex [Cd(smz)$_2$(en)].2DMF (24)

To the DMF solution of the same precipitate, ethylenediamine (en) (1 mL) was added, stirred for 30 minutes. After seven days white block crystals were obtained. The compound is soluble in DMF and DMSO but insoluble in water and all other organic solvents. Anal. Found: C, 43.91, H, 5.47; N, 19.29%. Calc. for $C_{32}H_{48}CdN_{12}O_6S_2$: C, 43.97, H, 5.50; N, 19.24%. IR: (KBr disc), cm^{-1}, 3443(m), 3359(s), 3334, 3226(s), 3165, 3063, 2930, 2873,

2843, 1675(s), 1634(vs), 1595, 1579, 1562(vs), 1501(sh), 1432(sh), 1398, 1376, 1342(m), 1291(vs), 1262(vs), 1209, 1178(sh), 1139(vs), 1122(s), 1079(s), 994(s), 974(vs), 873(vw), 835, 794(vs), 743, 718, 675(s), 636(s), 596, 555. ^{1}H NMR (DMSO-d_6): δ 7.63d [2H, C(16/20), J = 8.5 Hz], 6.48d [2H, C(17/19), J = 8.6], 6.42s [1H, C(13)], 5.58s [2H (–NH_2)], 2.73s [4H, C(1/2)], 2.51s [6H, CH_3], ^{13}C NMR (DMSO-d_6): δ 167.7 [C(11)], 162.2 [C(12/14)], 151.5 [C(18)], 130.0 [C(15)], 129.9 [C(16/20)], 112.0 [C(17/C19)], 110.2 [C(13)], 45.3 [C(1/2)], 23.4 [CH_3].

3.4.25 Preparation of the complex [Hg(sdz)$_2$(dmf)$_2$] (25)

To the DMF solution of mercury precipitate of sulfadiazine, a few drops of ammonia was added and stirred for 30 minutes. A few days later, white block crystals were obtained. The compound is soluble in DMF and DMSO but insoluble in water, alcohol and acetonitrile. Anal. Found: C, 36.89, H, 3.85; N, 16.53%. Calc. for $C_{26}H_{32}HgN_{10}O_6S_2$: C, 36.94; H, 3.82; N, 16.57%. IR: (KBr disc): cm^{-1}, 3467(s), 3365(s), 3048(m), 2930, 1655(s), 1614(vs), 1588(vs), 1557(vs), 1506(vs), 1440(sh), 1414(vs), 1342(s), 1291(vs), 1184(w), 1127(sh), 1086(s), 994(w), 958(w), 907(s), 820, 682(s), 651(w), 574(vs), 547(vs), 518(vw), 457(vw), 416(w). ^{1}H NMR (DMSO-d_6): δ 8.50d [2H, C(12/14), J = 4.9], 7.78d [2H, C(16/20), J = 8.5], 6.98t [1H, C(13), J = 4.8], 6.56d [2H, C(17/19), J = 8.6], 5.92s [2H, (–NH_2)]. ^{13}C NMR (DMSO-d_6): δ 162.7 [C(12/14)], 158.8 [C(11)], 153.0 [C18], 130.6 [C(16/20)], 126.1 [C(15)], 114.7 [C(13)], 112.4 [C(17/19)].

3.4.26 Preparation of the complex [Hg(smr)$_2$] (26)

To the DMF solution of mercury precipitate of sulfamerazine, a few drops of ammonia was added and stirred for 30 minutes. A few days later, white block crystals were obtained. The compound is soluble in DMF and DMSO but insoluble in water, alcohol and acetonitrile. Anal. Found: C, 36.89, H, 3.85; N, 16.53%. Calc. for $C_{22}H_{32}HgN_8O_4S_2$: C, 36.94; H, 3.82; N, 16.57%. IR: (KBr disc): cm^{-1}, 3436(s), 3317(s), 3228(m), 1632(vs), 1598(vs), 1571(vs), 1501(vs), 1465(sh), 1435(vs), 1392(vs), 1371(s), 1332(m), 1310(sh), 1281(vs), 1259(m), 1189(m), 1135(sh), 1093(s), 1010(w), 971(w), 945(w), 917(s), 869(w), 823, 792(s), 769(vw), 716(vw), 689(s), 635(w), 582 (vs) and 546. ^{1}H NMR (DMSO-d_6): δ 8.37d [1H, C(14), J = 5.1], 7.84d [2H, C(16, 20), J = 8.5], 6.92d [2H, C(17, 19), J = 5.1], 6.63d[1H, C(13), J = 8.8], 5.97s [2H (–NH_2)], 2.39s [3H (CH_3)]. ^{13}CNMR (DMSO-d_6): δ

168.4 [C(11)], 161.4 [C(12)], 158.3 [C(14)], 152.9 [C(18)], 130.8 [C(15)], 126.2 [C(16/20)], 114.1 [C(17/19)], 112.2 [C(13)], 23.6 [CH_3].

3.4.27 Preparation of the complex [Hg(smr)$_2$(bpy)] (27)

To the DMF solution of mercury precipitate of sulfamerazine, 2,2'-bipyridine (0.157g, 1 mmol) was added, stirred for 30 minutes. After seven days, white block crystals were obtained. The compound is soluble in DMF and DMSO but insoluble in water, alcohol and acetonitrile. Anal. Found: C, 43.55, H, 3.40; N, 15.90%. Calc. for $C_{32}H_{30}HgN_{10}O_4S_2$: C, 43.51; H, 3.42; N, 15.86%. IR: (KBr disc): cm^{-1}, 3445 (s), 3349 (s), 3241 (m), 1637 (vs), 1599 (vs), 1577(vs), 1504(vs), 1459 (sh), 1432 (vs), 1389(vs), 1370(s), 1333(m), 1309(sh), 1286 (vs), 1258(m), 1194 (w), 1180 (m), 1131(sh), 1093(s), 1009 (w), 971(w), 944 (w), 915 (s), 869(w), 823, 792(s), 769 (vw), 716 (vw), 693 (w), 682 (s), 635 (w), 582 (vs), 546 (vs). ^{1}H NMR (DMSO-d_6): δ 8.32d [1H, C(14), J = 4.9], 7.77d [2H, C(16, 20), J = 8.3], 6.87d [2H, C(17, 19), J = 5.0], 6.57d[1H, C(13), J = 8.4], 5.90s [2H (–NH_2)], 2.33s [3H (CH_3)]. ^{13}CNMR (DMSO-d_6): δ 167.9 [C(11)], 159.9 [C(12)], 157.7 [C(14)], 152.8 [C(18)], 130.1 [C(15)], 126.7 [C(16/20)], 113.1 [C(17/19)], 111.8 [C(13)], 23.2 [CH_3].

3.4.28 Preparation of the complex [Hg(smz)$_2$(DMF)$_2$] (28)

To the DMF solution of mercury precipitate of sulfamethazine, a few drops of ammonia was added and stirred for 30 minutes. After three weeks, white block crystals were obtained, filtered and dried over silica gel. The compound is soluble in DMF and DMSO but insoluble in water, alcohol and acetonitrile. Anal. Found: C, 34.62, H, 3.58; N, 15.54%. Calc. for $C_{26}H_{32}HgN_{10}O_6S_2$: C, 34.65; H, 3.51; N, 15.50%. IR: (KBr disc): cm^{-1}, 3457(s), 3360(s), 3247(m), 2919, 1660(vs), 1599(vs), 1577(vs), 1547(vs), 1506, 1429(sh), 1393(vs), 1373(s), 1332(m), 1292(vs), 1258(m), 1194 (w), 1137(sh), 1086(s), 994(w), 965, 897(w), 820, 779(vw), 682(s), 635(w), 589(vs), 549(vs). ^{1}H NMR (DMSO-d_6): δ 7.80d [2H, C(16/20), J = 8.6 Hz], 6.57d [2H, C(17/19), J = 8.7], 6.69s [1H, C(13)], 5.90s [2H (–NH_2)], 2.51s [6H, CH_3]. ^{13}C NMR (DMSO-d_6): δ 167.9 [C(11)], 159.6 [C(12/14)], 152.8 [C(18)], 131.0 [C(15)], 126.3 [C(16/20)], 113.1 [C(17/C19)], 112.0 [C(13)], 23.5 [CH_3].

Chapter 4

RESULTS AND DISCUSSION OF METAL COMPLEXES OF TRIPLE SULFA DRUGS WITH SECONDARY LIGANDS

RESULTS AND DISCUSSION

The complexes were characterized by analytical and spectroscopic methods such as IR, EPR and NMR as well as by X-ray diffraction methods.

4.1 IR spectra

The infrared spectra of the complexes taken in the region 4000 – 400 cm^{-1} were compared with those of the free ligands. The bands that appear between 3500 and 3400 cm^{-1} due to *asym*(NH_2) and *sym*(NH_2) vibrations of the amino (–NH_2) group[1,2] are modified with respect to those of the free respective ligands. In general, these vibration modes appear at higher and lower wave numbers, compared with those of the free ligands. When the amino nitrogen atom does not interact with the metal ions, these modifications are consequently due to the hydrogen bonds involving the amino groups. The vibrations for the water molecule present in the complexes appear in the same region as well.

The peak for the sulfonamidic (N–H) group in the free ligands at around 3125 cm^{-1}, are not present in the spectra of the complexes, confirming the deprotonation of the –SO_2NH– moiety. The scissoring vibrations for the amino (–NH_2) groups appear in the range of 1614 – 1662 cm^{-1} and peaks due to phenyl ring appear at around 1547 and 1600 cm^{-1}. The peaks around 1325 and 1331 cm^{-1} are assigned to $\nu_{as}(SO_2)$, and those at 1155 – 1157 cm^{-1} to $\nu_{sy}(SO_2)$, show important changes upon complexation. The first one splits into two peaks at 1291 – 1386 cm^{-1} and the second one appears at around 1131 – 1194 cm^{-1} in the complexes.

The 945–965 cm^{-1} bands in the ligands are assigned to ν(S–N)[2,3] and changed to higher frequencies (958 – 1046 cm^{-1}) in all cases as a consequence of coordination to the metal. This shift to higher frequencies is in accordance with the shortening of the S–N bond lengths, which have been observed in the crystal structures of complexes.

Table 4.1: The IR spectra of the compounds 1 – 28

compds	NH_2/H_2O	NH_2	Phenyl rings	$(SO_2)as$	$(SO_2)sy$	S–N
1	3461, 3365	1625		1325	1157	945
2	3468, 3370	1630	1570	1331	1153	965
3	3435, 3353	1665	1598	1344, 1301	1144	999, 974
4	3441, 3332	1643	1596, 1581	1348, 1298	1134	1011, 975
5	3438, 3349	1632	1595, 1551	1351, 1295	1131	1011, 973
6	3439, 3341	1641	1599, 1584	1347, 1297	1158	1002, 977
7	3452, 3379	1629	1598, 1578	1362, 1301	1173	1000, 968
8	3523, 3387	1662	1597, 1576	1365, 1294	1178	1008, 971
9	3524, 3387	1660	1597, 1576	1363, 1294	1178	1010, 971
10	3423, 3346	1636	1597, 1554	1386, 1282	1177	1046, 971
11	3420, 3341	1639	1596, 1552	1383, 1281	1178	1045, 974
12	3345, 3210	1625	1598, 1570	1350, 1294	1182	1020, 982
13	3436, 3350	1629	1597, 1581	1372, 1300	1184	999, 975
14	3544, 3365	1640	1599, 1557	1378, 1306	1184	1010, 978
15	3464, 3387	1629	1593, 1552	1383, 1296	1134	1009, 979
16	3436, 3350	1665	1593, 1547	1357, 1317	1178	1015, 979
17	3444, 3345	1645	1597, 1581	1361, 1294	1181	1007, 976
18	3409, 3334	1645	1599, 1583	1349, 1299	1180	1010, 978
19	3431, 3339	1638	1598, 1553	1351, 1294	1178	1011, 978
20	3421, 3353	1669	1600, 1578	1360, 1296	1173	1009, 976
21	3438, 3345	1631	1596, 1583	1352, 1299	1179	1012, 978
22	3437, 3351	1635	1597, 1582	1342, 1303	1177	998, 973
23	3540, 3461	1639	1598, 1583	1345, 1298	1178	999, 980
24	3443, 3359	1634	1595, 1579	1342, 1291	1178	994, 974
25	3467, 3365	1614	1588, 1557	1342, 1291	1184	994, 958
26	3436, 3317	1632	1598, 1571	1371, 1281	1189	1010, 971
27	3445, 3349	1637	1599, 1577	1370, 1309	1180	1009, 971
28	3457, 3360	1660	1599, 1577	1373, 1292	1194	994, 965

4.2 Electron Paramagnetic Resonance

Figure 4.4 shows that the X-band EPR spectra obtained from the complexes (**8**), (**9**) and (**12**) in a DMF-d_7/toluene-d_8 frozen solution at 10K suggests that the copper ions are in a very similar molecular environments in all the complexes and in these cases each copper ion is surrounded by four nitrogen atoms and two oxygen atoms with the general formula of CuN_4O_2. Acceptable simulations of the X-band spectra obtained for the complexes (**8**), (**9**) and (**12**) are shown in Figure 4.1.

The simulation of the complex (**9**) is shown in Figure 4.2 and the Q-band spectrum for the complex (**12**) is shown in Figure 4.3. The spin Hamiltonian parameters were: $g_{\|}$ = 2.208, $g_{\perp}$ = 2.042, $A_{\|}(^{63}Cu)$ = 185 Gauss, $A_{\perp}(^{63}Cu)$ = 25 Gauss, $A_{\|}(^{65}Cu)$ = 197.7Gauss, $A_{\perp}(^{65}Cu)$

= 26.7 Gauss, 4 × ^{14}N $A_{\perp}$ = 14 Gauss. The perpendicular hyperfine values for both the copper and the nitrogen nuclei must be considered approximate due to the low resolution in the perpendicular region of the spectrum; the ^{14}N value for the parallel features was set to an arbitrary value of 1 Gauss.

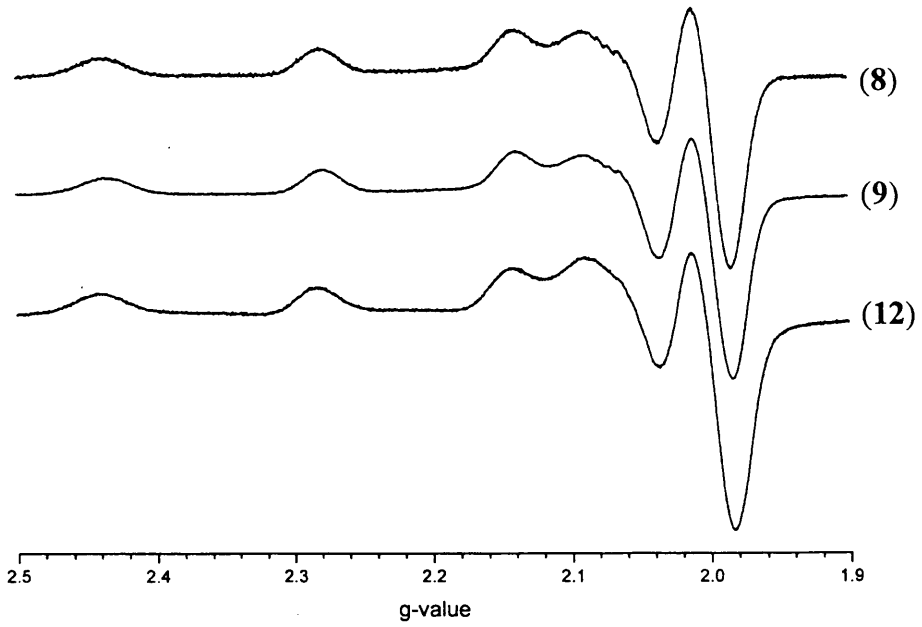

Figure 4.1
The X-band EPR spectra for the complexes (8), (9) and (12) in DMF-d_7/toluene-d_8

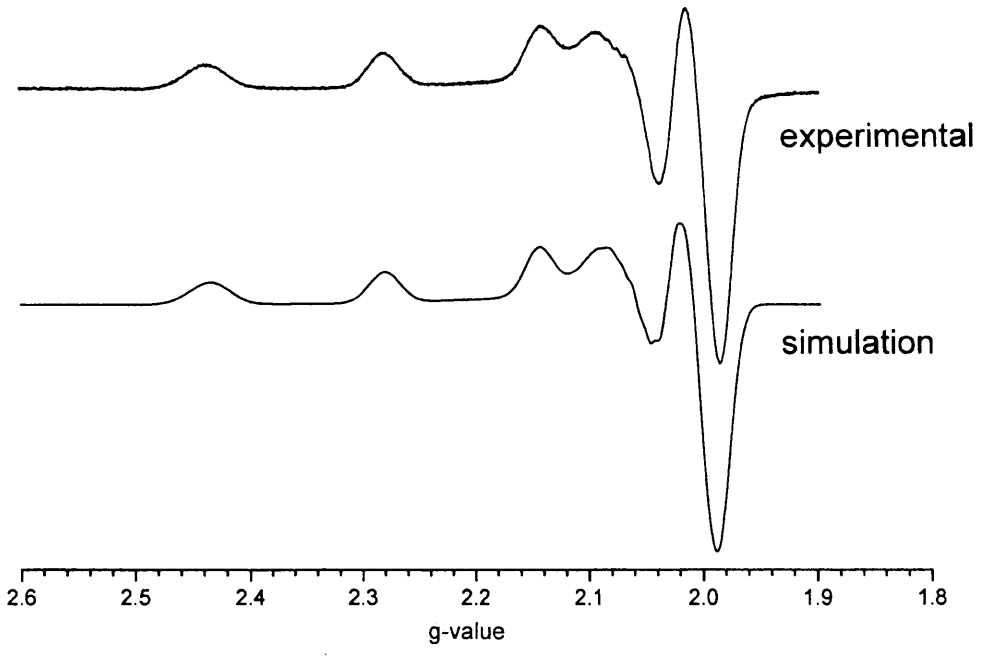

Figure 4.2
The X-band simulated EPR for the complex (8)

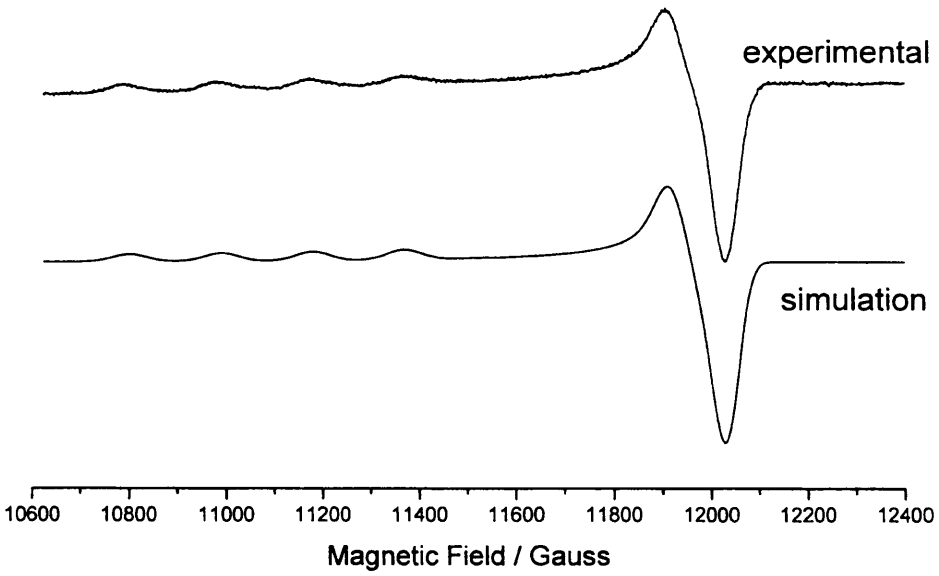

Figure 4.3
The Q-band EPR spectrum and simulation of the complex $[Cu(smz)_2(apen)].3H_2O.CH_3OH$ ***(12)***

In order to obtain accurate coupling constants for the nitrogen nuclei, X-band ENDOR spectra of the complex were recorded. For brevity, only the ENDOR spectra for (**9**) and (**12**) are shown in Figures 4.4 and 4.5 respectively. These spectra were complex with features arising from protons covering a wide frequency range and thus likely to obscure any features arising from ^{14}N nuclei. The Q-band spectra only showed features arising from protons; the nitrogen signals, presumably being too weak and broad for detection by c.w. techniques in this instance and therefore did not provide any additional information.

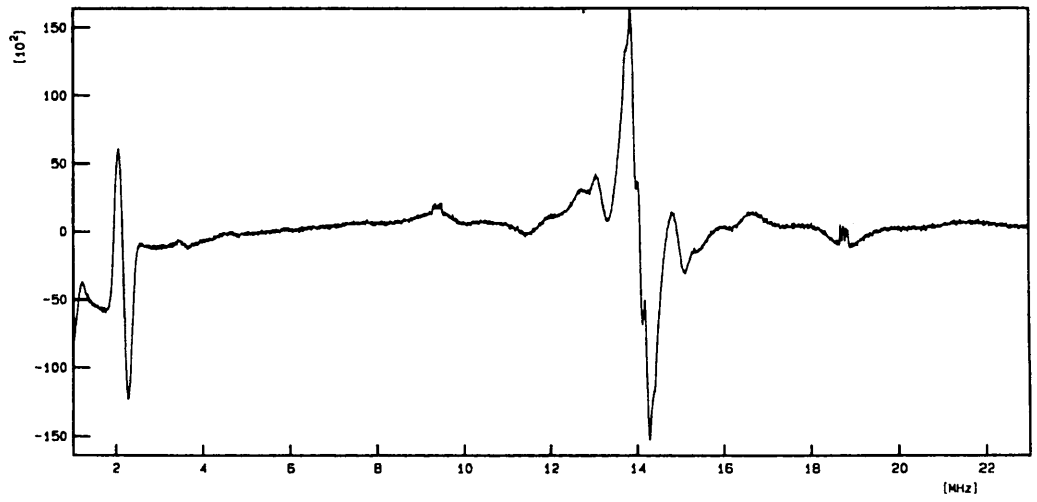

Figure 4.4
The X-band simulated ENDOR spectrum for the complex ***(9)***

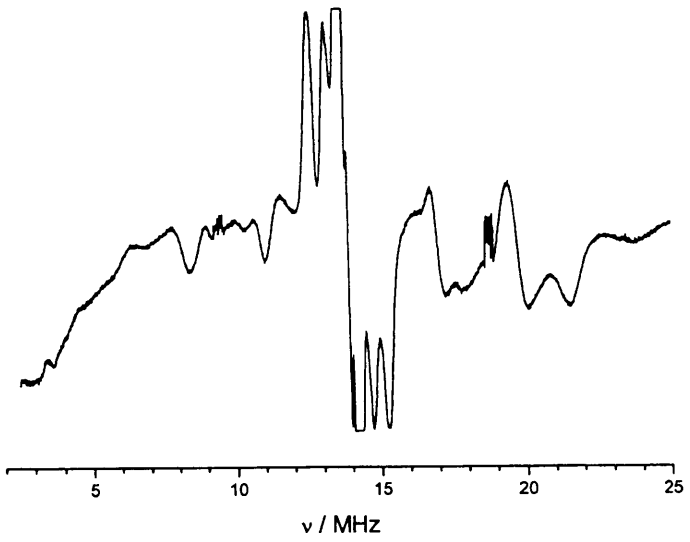

Figure 4.5
The X-band ENDOR spectrum of the complex $[Cu(smz)_2(apen)].3H_2O.CH_3OH$ (12) showing overlapping couplings to the ^1Hs and ^{14}N nuclei

In order to determine which features, if any, were due to ^{14}N, a second set of spectra were recorded at Q-band (Figure 4.6). These spectra, however, only showed features arising from protons; the nitrogen signals, presumably being too weak and broad for detection by c. w. techniques in this instance.

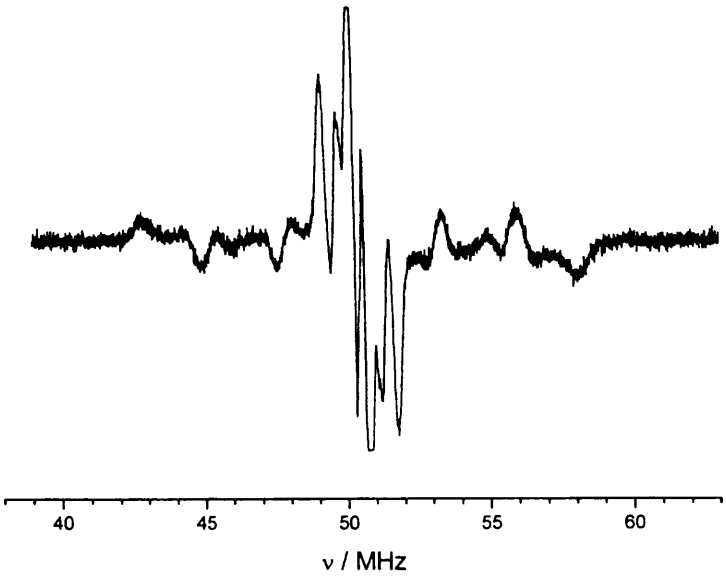

Figure 4.6
The Q-band ENDOR spectrum of the complex $[Cu(smz)_2(apen)].3H_2O.CH_3OH$ (12) showing couplings to the ^1H only

Nevertheless, the above spin Hamiltonian data confirms the X-ray structures obtained from the complex. The '*g*' and hyperfine splitting values are characteristic of a copper (II)

complex with octahedral symmetry distorted by a large Jahn-Teller elongation in the *z*-direction. It is interesting to note that the two copper atoms in the complex (**9**) are exactly equivalent and there does not appear to be any identifiable magnetic interaction between them.

For the complex (**9**) we also got four lines according to the following equation:

No of lines = $2nI + 1$

where n = the number of equivalent nuclei the electron couples to and I = nuclear spin and for the copper atom it is $^3/_2$.

So the number of lines for the complex (**9**) is $2.1.^3/_2 + 1 = 4$ as there are two unidentifiable copper ions in the complex. If there were two identifiable copper ion then we got the number of lines $2.2.^3/_2 + 1 = 7$.

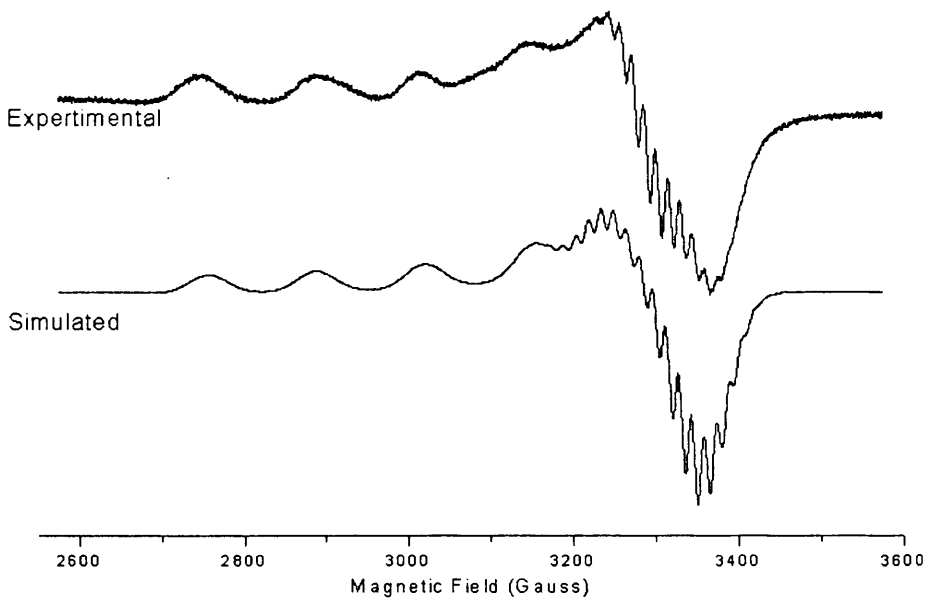

Figure 4.7
The X-band EPR spectrum and simulation of the complex $[Cu(smz)_2(NH_3)].2H_2O$ (13)

The experimental and simulated X-band EPR spectrum of (**13**) is shown in Figure 4.7. Owing to the complexity of the system (i.e., six interacting nitrogen nuclei in the complex) the EPR spectrum was very difficult to simulate accurately. This was particularly the case in the perpendicular region of the spectrum, where the number of superhyperfine lines originating from six interacting nitrogen nuclei (with slightly different environments and therefore slightly different couplings) was very difficult to reproduce. Nevertheless, a

qualitative simulation is shown in Figure 4.8 based on the spin Hamiltonian parameters of $g_{||}$ = 2.285, $g_{\perp}$ = 2.04, $A_{||}(^{63}Cu)$ = 132G, $A_{\perp}(^{63}Cu)$ = 25G, $A_{||}(^{65}Cu)$ = 142G, $A_{\perp}(^{65}Cu)$ = 26G, 6 x ^{14}N $A_{\perp}$ = 14.7G. It should be noted that these parallel values for complex (**13**) are significantly different compared to those observed for complexes (**8**), (**9**) and (**12**). In the latter case parallel components of $g_{||}$ = 2.208, $A_{||}(^{63}Cu)$ = 185G, $A_{||}(^{65}Cu)$ = 197G, were observed. These values are typical of Cu^{2+} complexes containing four interacting nitrogen atoms.[14] In the case of (**13**), the parallel components are very different [$g_{||}$ = 2.285, $A_{||}(^{63}Cu)$ = 132G, $A_{||}(^{65}Cu)$ = 142G] and suggestive of a higher symmetry for the ion which is consistent with the crystal structure.

Since in the complexes (**10**) and (**11**), the copper ions have five coordination numbers and one is metal-metal bonded, so there are no unpaired electrons and the complexes are EPR silent. This is due to the very strong spin-spin interactions that occur between the two copper centres, causing large zero field splitting terms are not visible in the X-ban measurements.

4.3 ^{1}H NMR and ^{13}C NMR spectra

^{1}H and ^{13}C NMR spectra were obtained from a solution of the sulfa drug molecules and the complexes in d^{6}-DMSO. The chemical shifts are expressed in ppm relative to internal TMS. The compounds present simple NMR spectra with two equivalent sulfa drug molecules and secondary ligands where applicable.

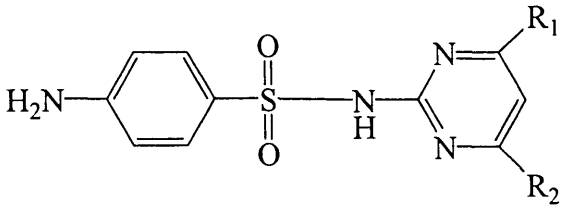

Sulfadiazine when R_1 and R_2 are hydrogen (H)

Sulfamerazine when R_1 is H and R_2 is methyl group (CH_3)

Sulfamethazine when R_1 and R_2 are methyl group (CH_3)

The ^{1}H spectra of the complexes are consistent with the X-ray structure obtained. The spectra consist of two doublets for the para substituted phenyl ring and one singlet for the amino group on the phenyl ring in all the complexes.

The pyrimidine ring of sulfadiazine showed one doublet integrating for two hydrogen atoms and one triplet integrating for one hydrogen atom, sulfamerazine showed two doublets for one hydrogen atom each and one singlet for substituted methyl group and sulfamethazine showed one singlet for pyrimido hydrogen atom and one singlet for substituted two methyl groups. All integrals are consistent with this assignment. Small shifts in resonances are observed for the complexes compared to the parent ligands.

In each case the N(11)–H peak has disappeared upon complexation with metal(II) ion and a downfield shift was observed for the C(11) resonance of sulfa drug molecules and from this observation it is probable that the metal(II) ions are bonded to the N(11) atom. Due to the complexation, the shift in signal for the aromatic protons occurred as observed in the ^{1}H NMR spectra of the metal complexes.

The ^{13}C NMR spectra (d^{6}–DMSO) of the complexes are relatively simple to interpret and are similar to those observed for the free ligands with seven peaks for sulfadiazine, nine for sulfamerazine and eight for sulfamethazine.

In the zinc complex $[Zn(smz)_2(NH_3)_2]$ (**14**) there are two molecules of ammonia as secondary ligands and it showed the spectra for the sulfamethazine molecules.

Table 4.2: ^{1}H NMR and ^{13}C NMR shift assignment of sulfamethazine and its zinc complex $[Zn(smz)_2(NH_3)_2]$ (14) in DMSO-d_6[a]

Assignment	^{1}H(smzH)	^{1}H(**14**)	^{13}C(smzH)	^{13}C(**14**)	Δδ (H)[b]	Δδ (C)[b]
N(11)-H	11.20					
C(11)			165.6	167.5		+1.9
C(12)/C(14)			157.0	162.3		+5.3
C(13)–H	6.45	6.33	112.3	110.3	–0.12	–2.3
C(15)			130.8	130.3		–0.5
C(16)–H/C(20)–H	7.69	7.58	125.4	129.8	–0.11	+4.4
C(17)–H/C(19)–H	6.60	6.42	114.0	111.9	–0.18	–2.1
C(18)			153.2	151.2		–2.0
NH_2	5.98	5.50			–0.48	
CH_3	2.22	2.49	23.4	23.3	+0.27	–0.1

[a] Relative to TMS with DMSO-d_6 peak as reference (^{1}H, 2.60 ppm, ^{13}C, 43.5 ppm).
[b] $\Delta\delta = \delta_{(complex)} - \delta_{(smz)}$

Due to the presence of pyridine molecules, the ^{1}H NMR spectrum of the complex $[Zn(smz)_2(py)_2].2py$ (**15**) shows two additional triplets for the *meta*- and *para*- hydrogen atoms and one doublet for *ortho*-hydrogen atoms.

Table 4.3: ^{1}H NMR and ^{13}C NMR shift assignment of sulfamethazine and pyridine and their zinc complex [Zn(smz)$_2$(py)$_2$].2py (15) in DMSO-d_6[a]

Assignment	^{1}H(smzH)	^{1}H(**15**)	^{13}C(smzH)	^{13}C(**15**)	Δδ (H)[b]	Δδ (C)[b]
N(11)-H	11.20					
C(11)			165.6	166.9		+1.4
C(12)/C(14)			157.0	162.4		+5.4
C(13)–H	6.45	6.32	112.3	110.5	–0.13	–1.8
C(15)			130.8	130.1		–0.7
C(16)–H/C(20)–H	7.69	7.57	125.4	129.2	–0.12	+3.8
C(17)–H/C(19)–H	6.60	6.43	114.0	111.7	–0.17	–2.3
C(18)			153.2	151.2		–2.0
NH_2	5.98	5.56			–0.42	
CH_3	2.22	2.41	23.4	23.0	+0.19	–0.4
	Py					
C(1)/C(5)	8.59	8.68	150.0	149.9	+0.09	–0.1
C(2)/C(4)	7.35	7.45	124.2	124.4	+0.10	+0.2
C(3)	7.73	7.85	136.4	137.4	+0.12	+1.0

[a] Relative to TMS with DMSO-d_6 peak as reference (^{1}H, 2.60 ppm, ^{13}C, 43.5 ppm).
[b] $\Delta\delta = \delta_{(complex)} - \delta_{(smz)}$

The ^{13}C NMR spectra showed two peaks for diene molecule for the complexes [Cd(sdz)$_2$(dien)].DMF (**16**) and [Cd(smr)$_2$(dien)].H_2O (**17**) at 31.1 and 38.8 ppm respectively for α–carbon and 48.3 and 47.6 ppm respectively for β–carbon atoms (Tables 4.4 and 4.5).

Table 4.4: ^{1}H NMR and ^{13}C NMR shift assignment of sulfadiazine and dien and their Cd complex [Cd(sdz)$_2$(dien)].DMF (16) in DMSO-d_6[a]

Assignment	^{1}H(sdzH)	^{1}H(**16**)	^{13}C(sdzH)	^{13}C(**16**)	Δδ (H)[b]	Δδ (C)[b]
N(11)-H	11.35					
C(11)			158.6	164.5		+5.9
C(12)–H/ C(14)–H	8.50	8.11	157.5	157.5	–0.39	+0.0
C(13)–H	7.00	6.40	115.9	112.1	–0.60	–3.8
C(15)			125.1	128.8		+3.7
C(16)–H/C(20)–H	7.75	7.47	130.3	133.3	–0.28	+3.0
C(17)–H/C(19)–H	6.58	6.45	112.6	109.7	–0.13	–2.9
C(18)			153.4	150.3		–2.9
NH_2	6.00	5.39			–0.61	
	dien					
C(1)/C(4)	2.84	2.73	41.9	31.1	–0.11	–10.8
C(2)/C(3)	2.97	2.89	52.9	48.3	–0.08	–4.6

[a] Relative to TMS with DMSO-d_6 peak as reference (^{1}H, 2.60 ppm, ^{13}C, 43.5 ppm)
[b] $\Delta\delta = \delta_{(complex)} - \delta_{(sulfadiazine)}$

Table 4.5: ^{1}H NMR and ^{13}C NMR shift assignment of sulfamerazine and its Cd complex [Cd(smr)$_2$(dien)].H$_2$O (17) in DMSO-d_6[a]

Assignment	^{1}H(smrH)	^{1}H(**17**)	^{13}C(smrH)	^{13}C(**17**)	Δδ (H)[b]	Δδ (C)[b]
N(11)-H	11.20					
C(11)			164.3	167.9		+3.6
C(12)			157.5	162.5		+5.0
C(13)–H	6.62	6.53	112.1	110.1	–0.09	–2.0
C(14)–H	8.37	8.24	156.8	157.1	–0.13	–0.3
C(15)			130.1	130.1		0.0
C(16)–H/C(20)–H	7.69	7.76	124.9	126.7	+0.07	+1.8
C(17)–H/C(19)–H	6.95	6.83	114.7	111.8	–0.12	–2.9
C(18)			152.9	152.8		–0.1
NH_2	6.07	5.90			–0.17	
CH_3	2.41	2.37	23.3	23.6	–0.04	+0.3
	dien					
C(1)/C(4)	2.84	2.79	41.9	38.8	–0.05	–3.1
C(2)/C(3)	2.97	2.88	52.9	47.6	–0.09	–5.3

[a] Relative to TMS with DMSO-d_6 peak as reference (^{1}H, 2.60 ppm, ^{13}C, 43.5 ppm).
[b] $\Delta\delta = \delta_{(complex)} - \delta_{(smr)}$

Due to the presence of 2,2′-bipyridine in the complex [Cd(sdz)$_2$(bpy)] (**18**) two additional doublets and two triplets were observed in the ^{1}H NMR spectrum.

Table 4.6: ^{1}H NMR and ^{13}C NMR shift assignment of sulfadiazine, 2,2′-bipyridine and their Cd complex [Cd(sdz)$_2$(bpy)] (18) in DMSO-d_6[a]

Assignment	^{1}H(sdzH)	^{1}H(**18**)	^{13}C(sdzH)	^{13}C(**18**)	Δδ (H)[b]	Δδ (C)[b]
N(11)-H	11.35					
C(11)			158.6	162.9		+4.3
C(12)–H/ C(14)–H	8.50	8.38	157.5	158.8	–0.12	+1.3
C(13)–H	7.00	6.75	115.9	112.2	–0.25	–3.7
C(15)			125.1	125.8		+0.7
C(16)–H/C(20)–H	7.75	7.37	130.3	129.1	–0.38	–1.2
C(17)–H/C(19)–H	6.58	6.35	112.6	111.8	–0.23	–0.8
C(18)			153.4	151.5		–1.9
NH_2	6.00	5.58			–0.42	
	^{1}H(bpy)		^{13}C(bpy)			
C(1)–H	8.70	9.15	149.2	140.4	+0.45	–8.8
C(2)–H	7.45	7.78	120.4	121.2	+0.33	+0.8
C(3)–H	7.95	8.25	124.0	124.9	+0.30	+0.9
C(4)–H	8.40	8.65	137.1	140.0	+0.25	+2.9
C(5)			152.2	151.4		–0.8

[a] Relative to TMS with DMSO-d_6 peak as reference (^{1}H, 2.60 ppm, ^{13}C, 43.5 ppm).
[b] $\Delta\delta = \delta_{(complex)} - \delta_{(sulfadiazine\ or\ bpy)}$

The ^{1}H NMR spectra of complexes [Cd(sdz)$_2$(phen)] (**19**) and [Cd(smr)$_2$(phen)] (**20**) exhibited one singlet, one doublet and two triplets for the 1,10-phenanthroline molecules.

Table 4.7: ^{1}H NMR and ^{13}C NMR shift assignment of sulfadiazine, 1,10-phenanthroline and their Cd complex [Cd(sdz)$_2$(phen)] (19) in DMSO-d_6[a]

Assignment	^{1}H(sdzH)	^{1}H(**19**)	^{13}C(sdzH)	^{13}C(**19**)	Δδ (H)[b]	Δδ (C)[b]
N(11)–H	11.35					
C(11)			158.6	162.7		+4.1
C(12)–H/ C(14)–H	8.50	8.45	157.5	158.8	–0.05	+1.3
C(13)–H	7.00	6.78	115.9	112.2	–0.22	–3.7
C(15)			125.1	125.7		+0.6
C(16)–H/C(20)–H	7.75	7.30	130.3	129.1	–0.45	–1.2
C(17)–H/C(19)–H	6.58	6.30	112.6	111.9	–0.28	–0.7
C(18)			153.4	152.8		–0.6
NH_2	6.00	5.58			–0.42	
	^{1}H(phen)		^{13}C(phen)			
C(1)–H	9.05	9.60	145.6	150.8	+0.55	+0.6
C(2)–H	8.45	8.90	123.2	121.2	+0.45	+0.8
C(3)–H	7.95	8.25	126.6	124.9	+0.30	+0.9
C(4)			136.1	138.4		+1.3
C(5)			149.9	151.5		0.0
C(6)–H	7.75	8.18	128.4	127.4	+0.45	

[a] Relative to TMS with DMSO-d_6 peak as reference (^{1}H, 2.60 ppm, ^{13}C, 43.5 ppm).

[b] $\Delta\delta = \delta_{(complex)} - \delta_{(sulfadiazine\ or\ phen)}$

Table 4.8: ^{1}H NMR and ^{13}C NMR shift assignment of sulfamerazine and its Cd complex [Cd(smr)$_2$(phen)] (20) in DMSO-d_6[a]

Assignment	^{1}H(smrH)	^{1}H(**20**)	^{13}C(smrH)	^{13}C(**20**)	Δδ (H)[b]	Δδ (C)[b]
N(11)-H	11.20					
C(11)			164.3	167.1		+2.8
C(12)			157.5	163.4		+5.9
C(13)–H	6.62	6.51	112.1	110.3	–0.11	–1.8
C(14)–H	8.37	8.30	156.8	156.2	–0.07	–0.6
C(15)			130.1	130.5		+0.4
C(16)–H/C(20)–H	7.69	7.72	124.9	129.1	+0.03	+4.2
C(17)–H/C(19)–H	6.95	6.81	114.7	112.5	–0.14	–2.2
C(18)			152.9	151.5		–1.4
NH_2	6.07	5.87			–0.20	
CH_3	2.41	2.36	23.3	23.3	–0.05	0.0
	^{1}H(phen)		^{13}C(phen)			
C(1)–H	9.05	9.26	145.6	148.8	+0.55	+0.6
C(2)–H	8.45	8.69	123.2	121.6	+0.45	+0.8
C(3)–H	7.95	8.15	126.6	124.7	+0.20	+0.9
C(4)			136.1	138.3		+1.3
C(5)			149.9	150.3		0.0
C(6)–H	7.75	8.03	128.4	127.3	+0.28	

[a] Relative to TMS with DMSO-d_6 peak as reference (^{1}H, 2.60 ppm, ^{13}C, 43.5 ppm)

[b] $\Delta\delta = \delta_{(complex)} - \delta_{(smr)}$

In complex $[Cd(sdz)_2(dmbpy)]$ (**21**) two doublets and two singlets were observed for 4,4′-dimethyl-2,2′-bipyridine molecule as shown in Figure 4.9.

Table 4.9: ^{1}H NMR and ^{13}C NMR shift assignment of sulfadiazine, 4,4′-dimethyl-2,2′-bipyridine and their Cd complex $[Cd(sdz)_2(dmbpy)]$ (21) in DMSO-d_6[a]

Assignment	^{1}H(sdzH)	^{1}H(**21**)	^{13}C(sdzH)	^{13}C(**21**)	Δδ (H)[b]	Δδ (C)[b]
N(11)-H	11.35					
C(11)			158.6	162.6		+4.0
C(12)–H/ C(14)–H	8.50	8.38	157.5	158.7	–0.12	+1.2
C(13)–H	7.00	6.74	115.9	112.2	–0.26	–3.7
C(15)			125.1	125.8		+0.7
C(16)–H/C(20)–H	7.75	7.36	130.3	129.1	–0.39	–1.2
C(17)–H/C(19)–H	6.58	6.35	112.6	111.5	–0.23	–1.1
C(18)			153.4	152.8		–0.5
NH_2	6.00	5.56			–0.44	
	^{1}H(dmbpy)		^{13}C(dmbpy)			
C(1)–H	8.73	9.07	149.9	150.3	+0.34	+0.4
C(2)–H	7.62	7.68	121.4	121.2	+0.06	–0.2
C(3)			126.4	124.9		+1.5
C(4)–H	8.41	8.56	137.1	137.4	+0.15	+0.3
C(5)			151.2	151.5		+0.3
C(5)	2.31	2.34	21.0	21.3	+0.03	+0.3

[a] Relative to TMS with DMSO-d_6 peak as reference (^{1}H, 2.60 ppm, ^{13}C, 43.5 ppm).
[b] $\Delta\delta = \delta_{(complex)} - \delta_{(sulfadiazine\ or\ dmbpy)}$

The polymeric cadmium complexes $\{[Cd(smz)_2(H_2O)].DMF\}_n$ (**22**) and $\{[Cd(smz)_2(H_2O)].2H_2O\}_n$ (**23**) showed characteristic peaks for the sulfamethazine molecules.

Table 4.10: ^{1}H NMR and ^{13}C NMR shift assignment of sulfamethazine and its cadmium complex $\{[Cd(smz)_2(H_2O)].DMF\}_n$ (22) in DMSO-d_6[a]

Assignment	^{1}H(smzH)	^{1}H(**22**)	^{13}C(smzH)	^{13}C(**22**)	Δδ (H)[b]	Δδ (C)[b]
N(11)-H	11.20					
C(11)			165.6	167.5		+1.9
C(12)/C(14)			157.0	162.7		+5.7
C(13)–H	6.45	6.40	112.3	110.2	-0.05	-2.1
C(15)			130.8	130.4		-0.4
C(16)–H/C(20)–H	7.69	7.59	125.4	129.8	-0.11	-4.4
C(17)–H/C(19)–H	6.60	6.43	114.0	111.9	-0.17	-2.1
C(18)			153.2	151.2		-2.0
NH_2	5.98	5.54			-0.44	
CH_3	2.22	2.49	23.4	23.3	+0.27	-0.1

[a] Relative to TMS with DMSO-d_6 peak as reference (^{1}H, 2.60 ppm, ^{13}C, 43.5 ppm).
[b] $\Delta\delta = \delta_{(complex)} - \delta_{(smz)}$

Table 4.11: ^{1}H NMR and ^{13}C NMR shift assignment of sulfamethazine and its cadmium complex {[Cd(smz)$_2$(H$_2$O)].2H$_2$O}$_n$ (23) in DMSO-d_6[a]

Assignment	^{1}H(smzH)	^{1}H(**23**)	^{13}C(smzH)	^{13}C(**23**)	Δδ (H)[b]	Δδ (C)[b]
N(11)-H	11.20					
C(11)			165.6	167.4		+1.8
C(12)/C(14)			157.0	162.2		+5.2
C(13)–H	6.45	6.38	112.3	110.3	–0.17	–2.0
C(15)			130.8	130.2		–0.6
C(16)–H/C(20)–H	7.69	7.61	125.4	129.5	–0.08	–4.1
C(17)–H/C(19)–H	6.60	6.45	114.0	111.8	–0.15	–2.2
C(18)			153.2	151.3		–1.9
NH_2	5.98	5.59			–0.39	
CH_3	2.22	2.50	23.4	23.2	+0.28	–0.2

[a] Relative to TMS with DMSO-d_6 peak as reference (^{1}H, 2.60 ppm, ^{13}C, 43.5 ppm).
[b] $\Delta\delta = \delta_{(complex)} - \delta_{(smz)}$

The ethylenediamine molecule in complex [Cd(smz)$_2$(en)].DMF (**24**) showed one singlet at 2.51 ppm indicating a downfield shift due to complexation with the cadmium ion.

Table 4.12: ^{1}H NMR and ^{13}C NMR shift assignment of sulfamethazine and its cadmium complex [Cd(smz)$_2$(en)].DMF (24) in DMSO-d_6[a]

Assignment	^{1}H(smzH)	^{1}H(**24**)	^{13}C(smzH)	^{13}C(**24**)	Δδ (H)[b]	Δδ (C)[b]
N(11)-H	11.20					
C(11)			165.6	167.7		+2.1
C(12)/C(14)			157.0	162.2		+5.2
C(13)–H	6.45	6.42	112.3	110.2	–0.03	–2.1
C(15)			130.8	130.0		–0.8
C(16)–H/C(20)–H	7.69	7.96	125.4	129.9	+0.30	+4.5
C(17)–H/C(19)–H	6.60	6.48	114.0	112.0	–0.12	–2.0
C(18)			153.2	151.5		–2.3
NH_2	5.98	5.58			–0.40	
CH_3	2.22	2.51	23.4	23.4	+0.29	–0.0
	en					
C(1)/C(2)	2.48	2.73	45.3	40.9	+0.25	–4.4

[a] Relative to TMS with DMSO-d_6 peak as reference (^{1}H, 2.60 ppm, ^{13}C, 43.5 ppm).
[b] $\Delta\delta = \delta_{(complex)} - \delta_{(smz)}$

The complex $[Hg(sdz)_2(DMF)_2]$ (**25**) displayed peaks for the sulfadiazine ligand only.

Table 4.13: ^{1}H NMR and ^{13}C NMR shift assignment of sulfadiazine and its Hg complex $[Hg(smr)_2(DMF)_2]$ (25) in DMSO-d_6[a]

Assignment	^{1}H(HsdzH)	^{1}H(**25**)	^{13}C(HsdzH)	^{13}C(**25**)	Δδ (H)[b]	Δδ (C)[b]
N(11)-H	11.35					
C(11)			158.6	162.7		+4.1
C(12)–H/C(14)–H	8.50	8.48	157.5	158.8	–0.02	+1.3
C(13)–H	7.00	6.98	115.9	114.7	–0.02	–1.2
C(15)			125.1	126.1		+1.8
C(16)–H/C(20)–H	7.75	7.78	130.3	130.6	+0.03	+0.3
C(17)–H/C(19)–H	6.58	6.56	112.6	112.4	–0.02	–0.2
C(18)			153.4	153.0		–0.4
NH_2	6.00	5.92			+0.08	

[a] Relative to TMS with DMSO-d_6 peak as reference (^{1}H, 2.60 ppm, ^{13}C, 43.5 ppm).
[b] $\Delta\delta = \delta_{(complex)} - \delta_{(sdz)}$

The complex $[Hg(smr)_2]$ (**26**) showed the peaks for the sulfadiazine only.

Table 4.14: ^{1}H NMR and ^{13}C NMR shift assignment of sulfamerazine and its Hg complex $[Hg(smr)_2]$ (26) in DMSO-d_6[a]

Assignment	^{1}H(smrH)	^{1}H(**26**)	^{13}C(smrH)	^{13}C(**26**)	Δδ (H)[b]	Δδ (C)[b]
N(11)-H	11.20					
C(11)			164.3	168.4		+4.1
C(12)			157.5	161.4		+3.9
C(13)–H	6.62	6.63	112.1	112.2	+0.01	+0.1
C(14)–H	8.37	8.37	156.8	158.3	0.00	+1.5
C(15)			130.1	130.8		+0.7
C(16)–H/C(20)–H	7.69	7.84	124.9	126.2	+0.15	+1.3
C(17)–H/C(19)–H	6.95	6.92	114.7	114.1	–0.03	–0.6
C(18)			152.9	152.9		0.0
NH_2	6.07	5.97			–0.10	
CH_3	2.41	2.39	23.3	23.6	–0.02	+0.3

[a] Relative to TMS with DMSO-d_6 peak as reference (^{1}H, 2.60 ppm, ^{13}C, 43.5 ppm)
[b] $\Delta\delta = \delta_{(complex)} - \delta_{(smr)}$

The ^{1}H and ^{13}C NMR spectra of $[Hg(smr)_2(bpy)]$ (**27**) are comparable to those observed for the complex $[Cd(sdz)_2(bpy)]$ (**18**).

Table 4.15: ^{1}H NMR and ^{13}C NMR shift assignment of sulfamerazine and its Hg complex [Hg(smr)$_2$(bpy)] (27) in DMSO-d_6[a]

Assignment	^{1}H(smrH)	^{1}H(**27**)	^{13}C(smrH)	^{13}C(**27**)	Δδ (H)[b]	Δδ (C)[b]
N(11)-H	11.20					
C(11)			164.3	167.9		+3.6
C(12)			157.5	159.9		+2.4
C(13)–H	6.62	6.57	112.1	111.8	–0.05	–0.3
C(14)–H	8.37	8.22	156.8	157.7	–0.15	+0.9
C(15)			130.1	130.1		0.0
C(16)–H/C(20)–H	7.69	7.77	124.9	126.7	+0.08	+1.8
C(17)–H/C(19)–H	6.95	6.87	114.7	113.5	–0.08	–1.2
C(18)			152.9	152.8		–0.1
NH_2	6.07	5.90			–0.17	
CH_3	2.41	2.36	23.3	23.2	–0.05	–0.1
	^{1}H(bpy)		^{13}C(bpy)			
C(1)–H	8.70	8.81	149.2	149.8	+0.11	+0.6
C(2)–H	7.45	7.77	120.4	121.2	+0.32	+0.8
C(3)–H	7.95	8.03	124.0	124.9	+0.08	+0.9
C(4)–H	8.40	8.47	137.1	138.4	+0.07	+1.3
C(5)			152.2	152.2		0.0

[a] Relative to TMS with DMSO-d_6 peak as reference (^{1}H, 2.60 ppm, ^{13}C, 43.5 ppm).
[b] $\Delta\delta = \delta_{(complex)} - \delta_{(smr)}$

The complex [Hg(smz)$_2$(DMF)$_2$] (**28**) exhibited peaks for the sulfamethazine ligand only.

Table 4.16: ^{1}H NMR and ^{13}C NMR shift assignment of sulfamethazine and its mercury complex (28) in DMSO-d_6[a]

Assignment	^{1}H(smzH)	^{1}H(**28**)	^{13}C(smzH)	^{13}C(**28**)	Δδ (H)[b]	Δδ (C)[b]
N(11)-H	11.20					
C(11)			165.6	167.9		+2.3
C(12)/C(14)			157.0	159.6		+2.6
C(13)–H	6.45	6.57	112.3	113.1	+0.12	+0.8
C(15)			130.8	131.0		–0.3
C(16)–H/C(20)–H	7.69	7.80	125.4	126.3	+0.11	+0.9
C(17)–H/C(19)–H	6.60	6.69	114.0	112.0	–0.09	–2.0
C(18)			153.2	152.8		–0.4
NH_2	5.98	5.90			–0.08	
CH_3	2.22	2.51	23.4	23.5	+0.29	+0.1

[a] Relative to TMS with DMSO-d_6 peak as reference (^{1}H, 2.60 ppm, ^{13}C, 43.5 ppm).
[b] $\Delta\delta = \delta_{(complex)} - \delta_{(smz)}$

4.4 Structure of sulfadiazine (1) and sulfamerazine (2)

We solved the crystal structure for sulfadiazine with a lower *R*-factor and synthesized a new polymorph for sulfamerazine. These were characterized by X-ray diffraction methods. The crystal data and refinement details for sulfadiazine (**1**) and sulfamerazine (**2**) are summarized in Table 4.17.

Table 4.17: Crystal data and details of data collection and structure refinement for sulfadiazine (1) and sulfamerazine (2)

	Sulfadiazine (1)	**Sulfamerazine (2)**
Empirical formula	$C_{10}H_{10}N_4O_2S$	$C_{11}H_{12}N_4O_2S$
Formula weight	250.28	264.31
Temperature (K)	150(2)	150(2)
Wavelength (Å)	0.71073	0.71073
Crystal system	Monoclinic	Monoclinic
Space group	$P\,2_1/c$	$P\,2_1/c$
a (Å)	13.6881(6)	11.0966(5)
b (Å)	5.8485(3)	8.3152(5)
c (Å)	14.8657(8)	13.9640(7)
β (°)	114.946(2)	99.327(4)
V(Å^{-3})	1079.04(9)	1271.43 (11)
Z	4	4
Calculated density (Mg/m^3)	1.541	1.381
Absorption coefficient (mm^{-1})	0.295	0.255
F(000)	520	552
Crystal size/mm	0.15 × 0.12 × 0.10	0.22 × 0.20 × 0.18
θ-Range for data collection (°)	3.28 – 27.50	2.96 – 27.47
Reflections collected	7910	11168
Unique reflections	2444	2872
Rint	0.0617	0.0910
Index ranges	−17<=h<=15 −7 <=k<=7 −19<=l<=19	−11<=h<=11 −15<=k<=15 −20<=l<=20
Max. and min. transmission	0.9711 and 0.9570	0.9556 and 0.9461
Goodness-of-fit on F^2	1.078	1.043
Data / parameters in the refinement	2444/162	2872/176
Final R indices [$(I > 2\sigma(I)$]	0.0446/0.1115	0.0522/0.1160
R indices (all data)	0.0554/0.1182	0.0778/0.1288
Largest diff. peak and hole (e.Å^{-3})	0.414 and −0.616	0.290 and −0.549

The numbering scheme and the geometry of the sulfadiazine (**1**) and sulfamerazine (**2**) molecules are shown in Figures 4.8 and 4.9 together with the crystallographic atom numbering scheme used. The bond lengths and angles of the compounds are listed in Table 4.18.

Table 4.18: Selected bond lengths [Å] and angles [°] in (1) and (2)

Bond	(1) (Å)	(2) (Å)	Angle	(1) (°)	(2) (°)
S(11)-O(11)	1.429(2)	1.429(2)	O(11)-S(11)-O(12)	119.26(9)	119.2(1)
S(11)-O(12)	1.437(2)	1.440(2)	O(11)-S(11)-N(11)	110.01(8)	109.0(1)
S(11)-N(11)	1.650(2)	1.654(2)	O(12)-S(11)-N(11)	101.68(8)	102.3(1)
S(11)-C(15)	1.740(2)	1.733(2)	O(11)-S(11)-C(15)	108.82(9)	109.5(1)
N(11)-C(11)	1.386(2)	1.389(3)	O(12)-S(11)-C(15)	109.82(9)	109.2(1)
N(12)-C(12)	1.340(2)	1.345(2)	N(11)-S(11)-C(15)	106.42(9)	106.7(1)
N(12)-C(11)	1.344(2)	1.327(2)	C(11)-N(11)-S(11)	125.90(13)	126.1(2)
N(13)-C(11)	1.334(2)	1.337(2)	C(12)-N(12)-C(11)	115.93(16)	116.1(2)
N(13)-C(14)	1.342(3)	1.336(3)	C(11)-N(13)-C(14)	115.06(17)	114.6(2)
N(14)-C(18)	1.384(2)	1.367(3)	N(13)-C(11)-N(12)	126.86(17)	127.5(2)

The bond lengths and angles are comparable with those found in the previously reported structures. The shortening of the C(18)–N(14), S(11)–C(15) and S(11)–N(11) bond lengths from the expected single bond distances have been attributed to dπ–pπ interactions. The C(18)–N(14) bond distances of 1.384(2)Å for (**1**) and 1.367(3)Å for (**2**) are comparable with the values of [1.43(3)Å][4] and [1.386(8)Å][5] in sulfadiazine, [1.363(12)Å][6], [1.357(7)Å][7] and [1.354(7)Å][7] in sulfamerazine and [1.367(3)Å][8] and [1.36(1)Å][9] in sulfamethazine molecules which are shorter than the value of [1.470(5)Å][10] for the length of a C(sp^2)–N(sp^2) single bond.

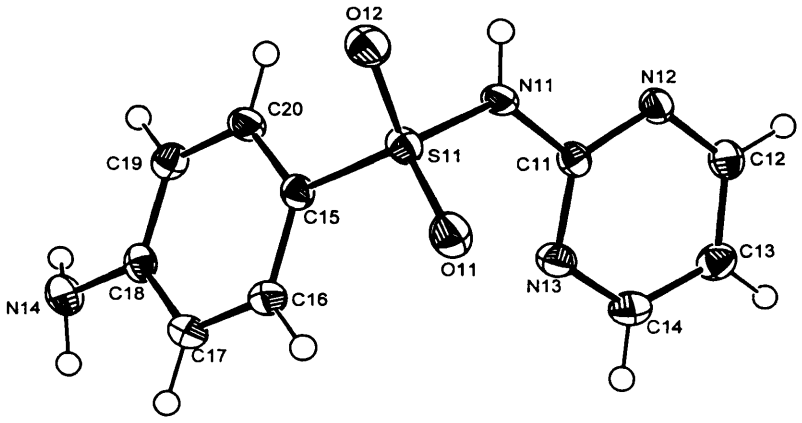

Figure 4.8
X-ray structure of sulfadiazine (1) showing crystallographic atom numbering scheme used. Thermal ellipsoids are drawn at 50% probability level.

The S(11)–C(15) bond distances of 1.740(2)Å for (**1**) and 1.733(2)Å for (**2**) are comparable with the values of [1.74(2)Å][4] and [1.736(5)Å][5] in sulfadiazine, [1.357(7)Å][6], [1.732(4)Å][7] and [1.736(4)Å][7] in sulfamerazine and [1.746(3)Å][8] and [1.765(9)Å][9] in sulfamethazine molecules and are in good agreement with the theoretical value of 1.75Å calculated from

the atomic radii and electronegativities[11] and 1.750(18)Å in β-sulfanilamide[12] and the S(11)–N(11) bond distances of 1.650(2)Å for (**1**) and 1.654(2)Å for (**2**) are in agreement with the values of other sulfa drugs reported in the literatures.[4–9, 13]

The endocyclic angle at C(11) of 126.85(2)° for (**1**) and 127.5(2)° for (**2**) are comparable with the corresponding values in the other sulfa drugs and these are considerably larger than the value usually observed for a pyrimidine ring.

The planes of the benzene and pyrimidine rings are inclined to each other at 74.63(20)° for (**1**) and 64.39(2)° for (**2**) which is compared to the values of [77°][1], [78.6(3)°][2] and [75.7°][13] in sulfadiazine, [71(1)°][6], [61.5(5)°][7] and [58.5(5)°][7] in sulfamerazine and [83.0(3)°][8] and [78.16(6)°][9] in sulfamethazine. These indicate that the molecules adopt *gauche* conformation when viewed along the S–N axis.

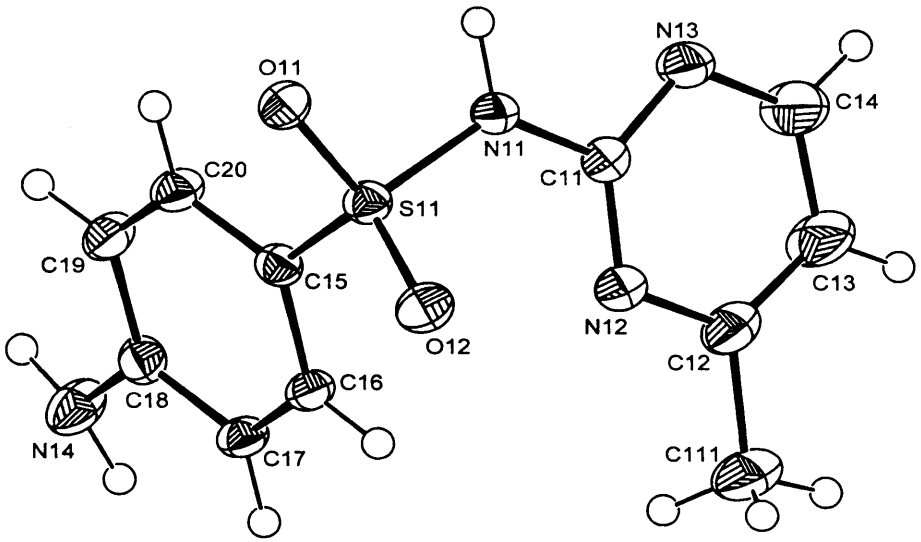

Figure 4.9
*X-ray structure of the new polymorph of sulfamerazine (**10**) showing crystallographic atom numbering scheme used. Thermal ellipsoids are drawn at 50% probability level.*

The S(11)–O bond distances of 1.429(2) and 1.437(2)Å for (**1**) and 1.429(2) and 1.440(2)Å for (**2**) are also comparable with the corresponding values of other sulfa drugs reported in the literatures.[4–9]

The tetrahedral geometry around the S(11) atom is distorted and this is evident from the deviations in the values of the bond angles around the S(11) atom from 109.5°.

The crystal structure is stabilized by the network of hydrogen bonds and van der Waals' forces. The interesting point here is to note that the sulfonamidic nitrogen atom is involved in hydrogen bonding with one of the pyrimido nitrogen atoms of its symmetry generated molecules by $-x+1, -y+1, -z+1$ in sulfadiazine (**1**) and $-x+1, -y, -z$ in sulfamerazine (**2**).

Two centrosymmetrically related molecules in the crystal form a dimer through a pair of hydrogen bonds N(11)–H(11)···N(12′) and N(11′)–H(11′)···N(12) in (**1**) and N(11)–H(11)---N(13′) and N(11′)–H(11′)---N(13) in (**2**) as shown in Figures 4.10 and 4.11 respectively.

These hydrogen bonds are fairly strong as indicated by the dimensions of H(11)–N(12′) or H(11′)–N(12) = 2.108(3)Å and ∠N(11)–H(11)–N(12′) or ∠N(11′)–H(11′)–N(12) = 158.39(1)° for sulfadiazine (**1**) and H(11)–N(13′) or H(11′)–N(13) = 1.964(4)Å and ∠N(11)–H(11)–N(13′) or ∠N(11′)–H(11′)–N(13) = 174.46(4)° sulfamerazine (**2**) which indicates the linearity of the hydrogen bond.

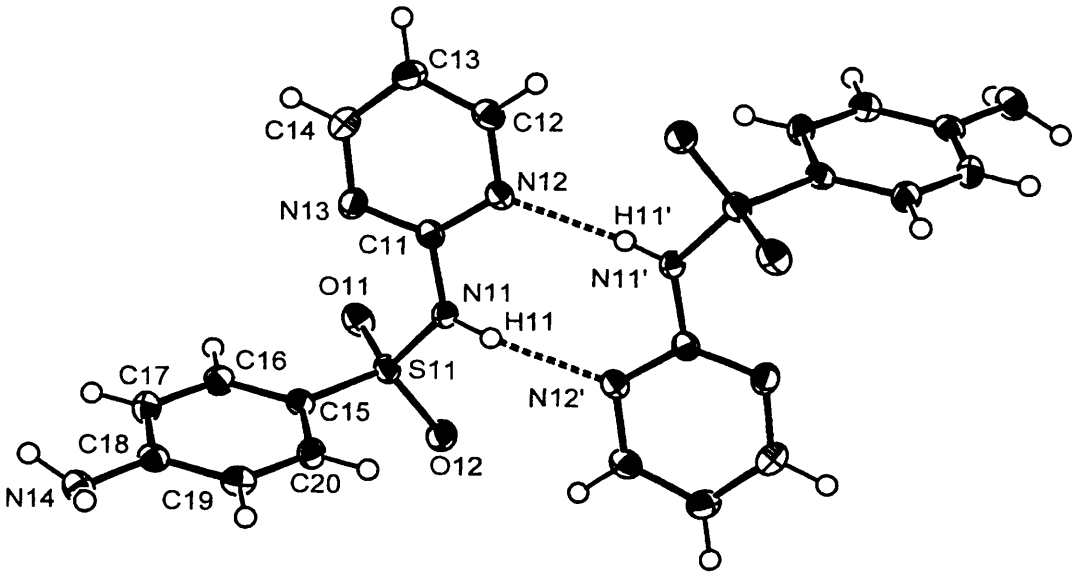

Figure 4.10
X-ray structure of sulfadiazine molecules showing the formation of dimer through N(11)-H(11) ...N (12′) hydrogen bonds with the symmetry –x+1, –y+1, –z+1.

The present structure of sulfamerazine crystallises in the monoclinic crystal system with the space group of $P2_1/c$, but two others were crystallised in the orthorhombic form.[3,4]

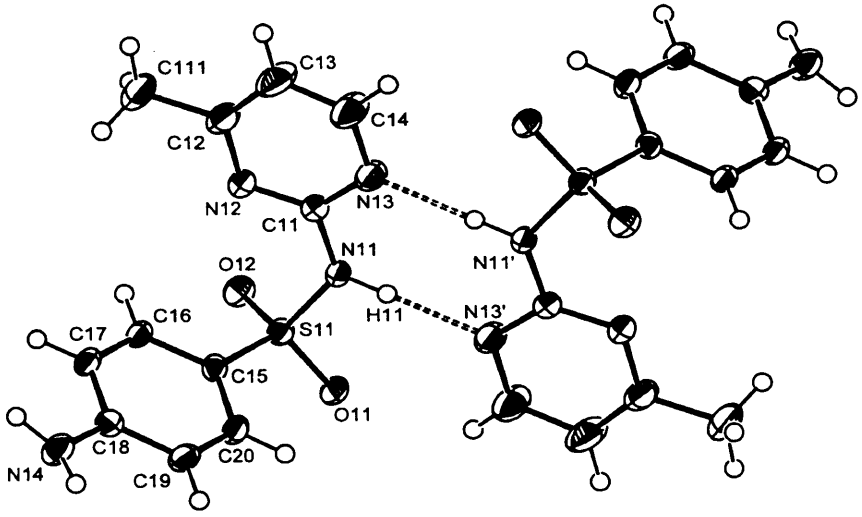

Figure 4.11
Two centrosymmetrically related molecules in the crystal form a dimer through a pair of hydrogen bonds with the symmetry –x+1, –y, –z.

The packing diagrams are shown in Figures 4.12 and 4.13 for sulfadiazine and sulfamerazine molecules respectively where the various hydrogen bonds and short contacts are shown by dashed lines.

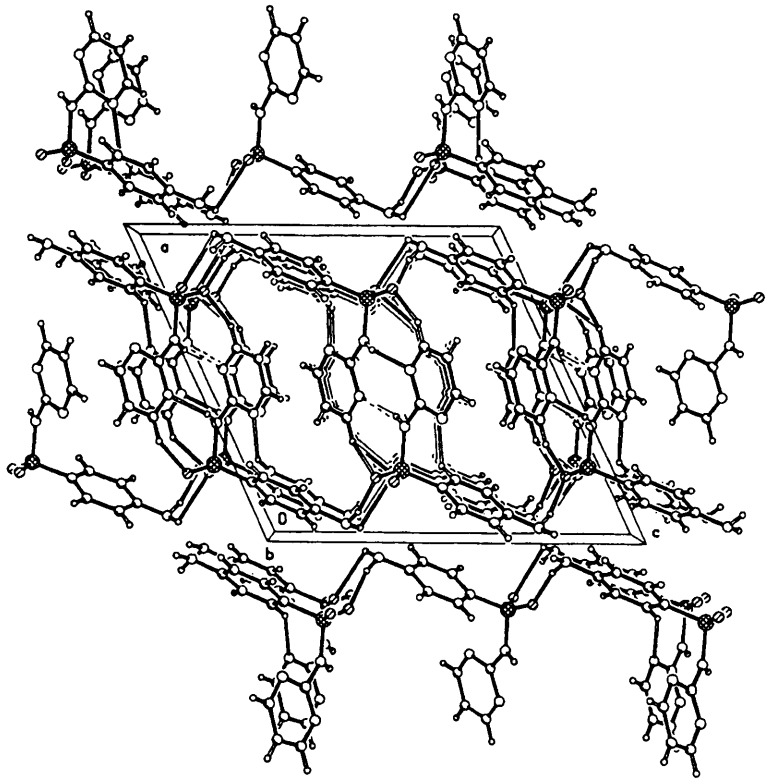

Figure 4.12
The packing diagram of sulfadiazine (1) where hydrogen bonds are shown by dashed lines

Table 4.19: Possible hydrogen bonds in sulfadiazine (1) and angles given in Å and deg respectively.

Donor-H	Donor...Acceptor	H...Acceptor	Donor-H.....Acceptor
N11 -H11	N11 ....N12 (1)	H11 ...N12 (1)	N11 -H11 ...N12 (1)
0.860(2)	2.924(4)	2.108(3)	158.39(1)
N14 -H14A	N14 ....O12 (2)	H14A...O12 (2)	N14 -H14A...O12 (2)
0.948(2)	2.975(3)	2.046(3)	166.23(1)

Equivalent positions:
(1) –x+1, –y+1, –z+1; (2) x, –y+½,+z+½

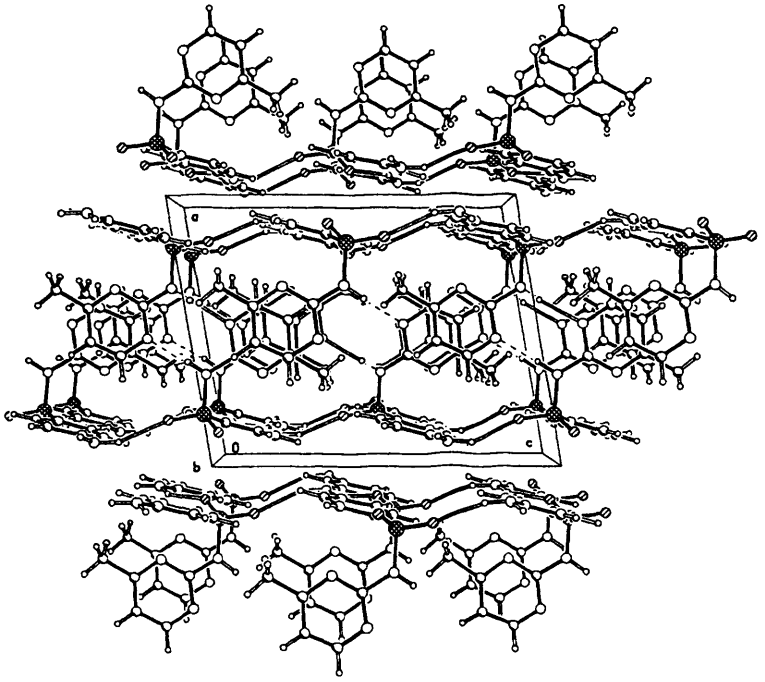

Figure 4.13
The packing diagram of sulfamerazine (2) molecule where hydrogen bonds are shown by dashed lines.

Table 4.20: Possible hydrogen bonds in sulfamerazine (2) (distances and angles given in Å and deg respectively)

Donor-H	**Donor...Acceptor**	**H...Acceptor**	**Donor-H.....Acceptor**
N11 -H11	N11 ....N13 (1)	H11 ...N13 (1)	N11 -H11 ...N13 (1)
0.950(4)	2.911(4)	1.964(4)	174.46(4)
N14 -H14A	N14 ....O12 (2)	H14A...O12 (2)	N14 -H14A...O12 (2)
0.947(2)	2.985(1)	2.111(1)	152.75(2)
N14 -H14B	N14 ....O11 (3)	H14B...O11 (3)	N14 -H14B...O11 (3)
0.946(1)	3.091(1)	2.241(1)	149.01(4)

Equivalent positions: (1) -x+1, -y, -z; (2) x, +y-1, +z; (3) x, -y-½, +z+½

4.5 Cobalt complex $\{[Co(smz)_2(H_2O)].DMF\}_n$ (3)

This is a new polymeric cobalt complex of sulfamethazine and has been characterised by analytical and spectroscopic data as well as by single crystal X-ray diffraction methods. The crystal data and refinement details for the complex (**3**) are summarized in Table 4.21.

Table 4.21: Crystal data and details of data collection and structure refinement for $\{[Co(smz)_2(H_2O)].DMF\}_n$ (3)

	(3)
Empirical formula	$C_{27}H_{35}CoN_9O_6S_2$
Formula weight	704.69
Crystal system	Monoclinic
Space group	$P2_1/c$
a (Å)	16.4001(4)
b (Å)	14.6508(3)
c (Å)	13.1430(3)
β (°)	100.8292(10)
V (Å^3)	3101.69(12)
Z	4
Crystal size/mm	0.18 × 0.15 × 0.12
θ-Range for data collection (°)	3.05 – 27.47
Reflections collected	28696
Unique reflections	7084
R_{int}	0.0989
Index ranges	−18<=h<=21 −19<=k<=18 −17<=l<=16
Data/parameters	7084/428
Final R indices [$(I > 2\sigma(I)$]	0.0506/0.1060
R indices for all data	0.0857/0.1219
Largest diff. peak and hole (e.Å^{-3})	0.437 and – 0.545

The asymmetric unit of the crystal structure of the complex $\{[Co(smz)_2(H_2O)].DMF\}_n$ (**3**) is shown in Figure 4.14 together with the crystallographic atom numbering scheme used. The polymeric form and the packing diagram of the complex is shown in Figures 4.15 and 4.16 respectively. The selected bond lengths and angles are given in Table 4.22 and the possible hydrogen bond dimensions are given in Table 4.23.

The complex $[Co(smz)_2(H_2O)].DMF$ (**3**) consists of an independent polymeric crystal structure of $\{[Co(smz)_2(H_2O)].DMF\}_n$ held together in the crystal by very strong hydrogen bonds and van der Waals' interactions. The cobalt ion in the complex exhibits a distorted

octahedral geometry, being coordinated to the sulfonamidic [N(11) and N(21)] and pyrimido [N(12) and N(22)] nitrogen atoms of two bidentate sulfamethazine ligands generating four-membered rings. The nitrogen [N(24)] atom from the terminal amino group of a third sulfamethazine, which is bonded to the adjacent Co(II) ion, and the O(1) atom of water molecule complete the coordination sphere. The N(14)–C(18) bond distance of 1.385(4)Å is shorter than the N(24)–C(28) bond distance with the value of 1.428(4)Å which is comparable with the corresponding value of 1.413(9)Å in the polymeric complex $\{[Cd(smz)_2(H_2O)].2H_2O\}_n$[1] and is longer than the corresponding distances in the free ligand [1.384(6)Å], which is consistent with the coordination of the terminal amino group [N(24)] to the adjacent Co(II) ion. The bond lengths and angles of the phenyl rings conform well to those found in the free sulfamethazine.[9,10]

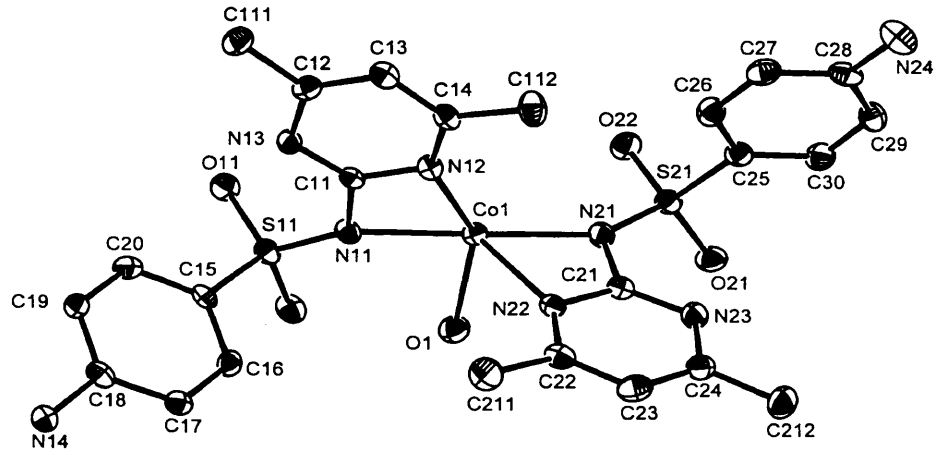

Figure 4.14
X-ray structure of the complex $[Co(smz)_2(H_2O)].DMF$ (3) showing crystallographic atom numbering scheme used. Thermal ellipsoids are drawn at 50% probability level. The hydrogen atoms and DMF molecule are omitted for clarity.

The packing of the complex units is governed by the long chains formed by the bridging ligands which are bound to Co(II) via N(24) nitrogen atom of the amino group [N(24)–Co = 2.225(2)Å]

In the complex units, the intramolecular hydrogen bonds exist between the amino ($-NH_2$) groups and the sulfonyl oxygen atoms of different ligands, and between the sulfonyl oxygen atoms and the coordinated water molecule and DMF molecule.

Table 4.22: Selected bond lengths [Å] and angles [°] in $\{[Co(smz)_2(H_2O)].DMF\}_n$ (3)

Bond	(Å)	Bond	(Å)
Co(1)-O(1)	2.112(2)	Co(1)-N(11)	2.142(2)
Co(1)-N(21)	2.147(2)	Co(1)-N(12)	2.187(2)
Co(1)-N(22)	2.200(2)	Co(1)-N(24)#1	2.225(2)
S(11)-O(12)	1.447(2)	S(11)-O(11)	1.451(2)
S(11)-N(11)	1.595(2)	S(11)-C(15)	1.757(3)
S(21)-O(22)	1.446(2)	S(21)-O(21)	1.457(2)
S(21)-N(21)	1.590(2)	S(21)-C(25)	1.764(3)
N(11)-C(11)	1.380(4)	N(14)-C(18)	1.385(4)
N(21)-C(21)	1.374(3)	N(24)-C(28)	1.428(4)
Angle	**(°)**	**Angle**	**(°)**
O(1)-Co(1)-N(11)	93.36(8)	O(1)-Co(1)-N(21)	87.51(8)
N(11)-Co(1)-N(21)	179.10(9)	O(1)-Co(1)-N(12)	87.34(8)
N(11)-Co(1)-N(12)	61.72(8)	N(21)-Co(1)-N(12)	118.57(9)
O(1)-Co(1)-N(22)	145.01(8)	N(11)-Co(1)-N(22)	117.88(9)
N(21)-Co(1)-N(22)	61.35(8)	N(12)-Co(1)-N(22)	93.79(8)
O(1)-Co(1)-N(24)#1	103.79(8)	N(11)-Co(1)-N(24)#1	90.70(9)
N(21)-Co(1)-N(24)#1	88.88(9)	N(12)-Co(1)-N(24)#1	151.10(9)
N(22)-Co(1)-N(24)#1	91.89(8)	O(12)-S(11)-O(11)	114.84(12)
O(12)-S(11)-N(11)	113.57(12)	O(11)-S(11)-N(11)	105.66(12)
O(12)-S(11)-C(15)	107.61(13)	O(11)-S(11)-C(15)	108.17(13)
N(11)-S(11)-C(15)	106.60(13)	O(22)-S(21)-O(21)	115.20(12)
O(22)-S(21)-N(21)	113.96(12)	O(21)-S(21)-N(21)	104.90(12)
O(22)-S(21)-C(25)	108.05(13)	O(21)-S(21)-C(25)	106.76(12)
N(21)-S(21)-C(25)	107.52(12)	C(28)-N(24)-Co(1)#2	115.05(16)
N(13)-C(11)-N(12)	127.0(3)	N(23)-C(21)-N(22)	126.6(2)

Symmetry transformations used to generate equivalent atoms: #1 –x, y+½, –z+½; #2 –x, y–½, –z+½

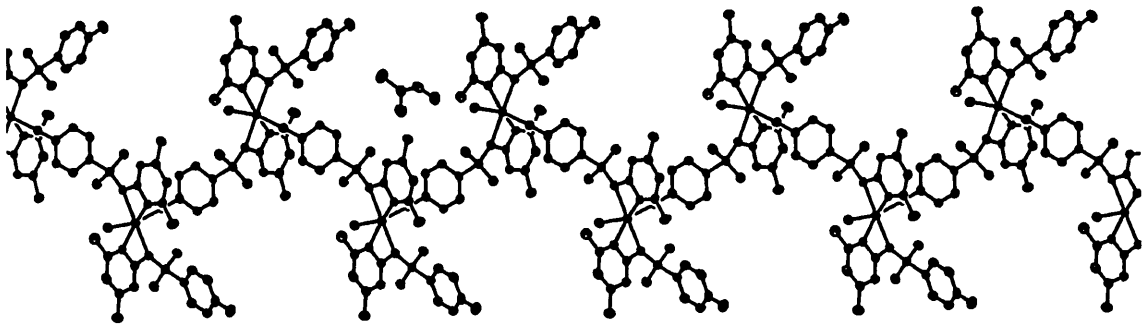

Figure 4.15
Structure of $[Co(smz)_2(H_2O)].DMF$ (3) in the polymeric form where cobalt ion is bonded to the terminal N(24) atom of the adjacent cobalt ion.

The ligands are chelated to cobalt atoms symmetrically in the octahedral structure. The Co–N(11) and Co–N(21) bond distances of 2.142(2) and 2.147(2)Å respectively are comparable with those in the 2,2′-bipyrimidine cobalt(II) complex $[Co(bipym)(H_2O)_2][(NO_3)_2]$ [2.176(5) and 2.177(5)Å], and $[Co_2(bipym)_3(H_2O)_4][(NO_3)_4]$ [2.140(2), 2.144(2) and 2.125(2)Å] and $[Co_2(bipym)_3(H_2O)_2(SO_4)_2].12H_2O$ [2.155(2), 2.146(2)Å and 2.131(2)Å] reported by Munno *et al.*[15] and Co–O(1) distance of 2.112(2)Å is longer than the value of 2.053(5) and 2.046(5)Å in $[Co(bipym)(H_2O)_2][(NO_3)_2]$, 2.049(2) and 2.068(2)Å in $Co_2(bipym)_3(H_2O)_4][(NO_3)_4]$ and 2.093(2) and 2.031(2)Å in $[Co_2(bipym)_3(H_2O)_2(SO_4)_2].12H_2O$ due to the formation of polymer. Co–N(12) and Co–N(22) distances of 2.187(2) and 2.200(2)Å respectively are also comparable with the values of 2.173(3) – 2.197Å in the polymeric cobalt complex $\{[Co(C_{10}H_8N_2)(H_2O)_4](C_8H_4O_4)\cdot 2H_2O\}_n$[16]. The Co–N(11)/N(21) bond distance is shorter than the Co–N(12)/N(22) bond in the complex.

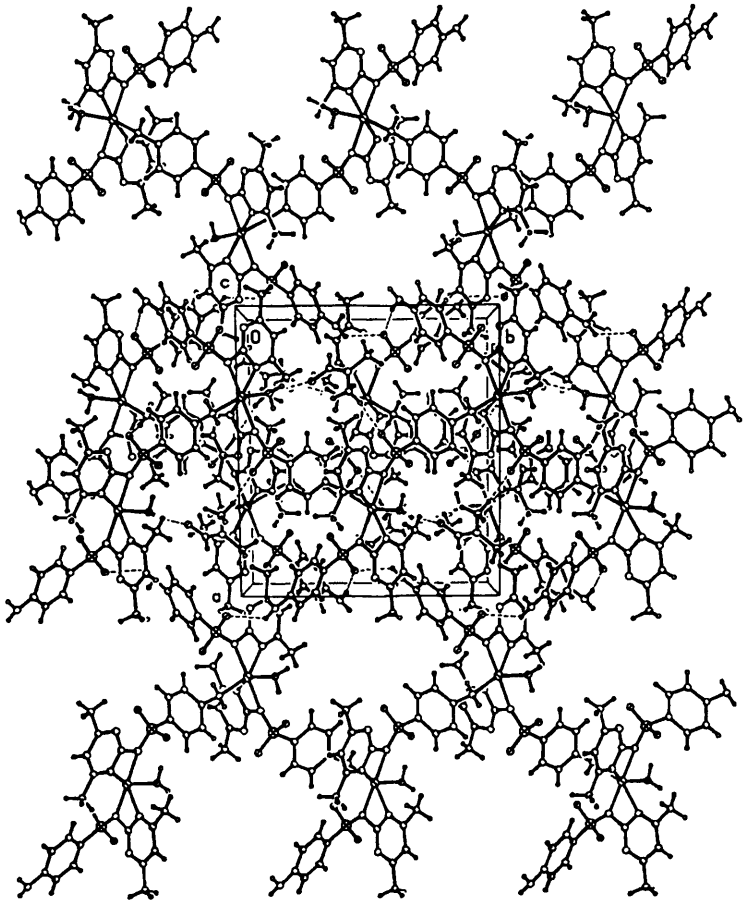

Figure 4.16
Packing diagram of the complex $[Co(smz)_2(H_2O)].DMF$ (3) where the hydrogen bonds are shown by dashed lines

In this polymeric complex there are several hydrogen bonds which are shown by dashed lines between the acceptors and hydrogen atoms in the packing diagram (Figure 4.16) and the hydrogen bonds are listed in Table 4.23.

Table 4.23: The hydrogen bonds in [Cu(smz)$_2$(H$_2$O)].DMF (3) (distances and angles given in Å and (°) respectively)

Donor-H	Donor...Acceptor	H...Acceptor	Donor-H.....Acceptor
O1 -H1A	O1 ....O2 (0)	H1A ...O2 (0)	O1 -H1A ...O2 (0)
0.971(2)	2.769(2)	1.842(4)	158.68(1)
O1 -H1B	O1 ....O21 (0)	H1B ...O21 (0)	O1 -H1B ...O21 (0)
0.886(5)	2.748(8)	1.925(6)	154.01(4)
N14 -H14A	N14 ....O12 (1)	H14A...O12 (1)	N14 -H14A...O12 (1)
0.949(7)	3.057(8)	2.128(7)	166.05(4)
N14 -H14B	N14 ....O12 (2)	H14B...O12 (2)	N14 -H14B...O12 (2)
0.949(8)	2.966(2)	2.263(4)	130.19(2)
N24 -H24A	N24 ....O11 (3)	H24A...O11 (3)	N24 -H24A...O11 (3)
0.948(8)	2.922(9)	2.009(9)	161.08(4)
N24 -H24B	N24 ....O22 (4)	H24B...O22 (4)	N24 -H24B...O22 (4)
0.948(4)	3.001(2)	2.117(9)	154.57(2)

Equivalent positions:
(0) x, y, z; (1) x,-y+½+1, +z+½; (2) -x+1,+y+½,-z+½; (3) -x,+y-½,-z+½; (4) x,-y+½,+z+½

4.6 Nickel complexes of triple sulfa drugs

The nickel complexes $[Ni(en)_3][(sdz)_2].H_2O$ (**4**) and $[Ni(smr)_2(py)_2].4py$ (**5**) are new compounds. The crystal data, details of data collection and structure refinement for complexes $[Ni(en)_3][(sdz)_2].H_2O$ (**4**) and $[Ni(smr)_2(py)_2].4py$ (**5**) are given in Table 4.24.

Table 4.24: Crystal data and details of data collection and structure refinement for complexes $[Ni(en)_3][(sdz)_2].H_2O$ (4) and $[Ni(smr)_2(py)_2].4py$ (5)

	(4)	(5)
Empirical Formula	$C_{26}H_{44}N_{14}NiO_5S_2$	$C_{52}H_{52}N_{14}NiO_4S_2$
Formula Weight	755.58	1059.91
Crystal System	Orthorhombic	Triclinic
Space Group	*Pbcn*	$P\bar{1}$
a(Å)	7.7894(1)	9.9781(2)
b(Å)	15.8762(3)	10.0610(2)
c(Å)	27.7420(5)	13.2582(4)
$\alpha(^\circ)$	90	89.7440(8)
$\beta(^\circ)$	90	82.2380(8)
$\gamma(^\circ)$	90	84.1440(13)
V/Å^3	3430.74(10)	1311.85(5)
Z	4	1
T/K	150 (2)	150 (2)
Crystal Size/mm	0.15 × 0.12 × 0.12	0.18 × 0.16 × 0.16
Shape	Block	Block
Colour	Pink	Pink
θ-range for data collection	2.91 – 27.48	3.03 – 27.48
Reflection Collected	19897	24079
Unique Reflections	3931	5955
R_{int}	0.0711	0.1594
Index ranges	−6<=h<=10 −20<=k<=20 −35<=l<=35	−12<=h<=12 −13<=k<=13 −17<=l<=17
Data/parameters	3931/219	5955/340
Final R indices (all data)	0.0416/0.0955	0.0530/0.1299
R indices [$I>2\sigma(I)$]	0.0677/0.1063	0.0746/0.1407
Largest diff. peak and hole (e. Å^{-3})	0.526 and -0.518	0.514 and −1.108

4.6.1 Nickel complex of sulfadiazine $[Ni(en)_3][(sdz)_2].H_2O$ (4)

The crystal structure of the complex $[Ni(en)_3][(sdz)_2].H_2O$ (**4**) is shown in Figure 4.17 together with the crystallographic atom numbering scheme used. The bond lengths and angles are given in Table 4.25. The complex consists of discrete molecules of $[Ni(en)_3]^{2+}$ cation, $[sdz]^-$ anion and the lattice water molecule in the ratio of 1:2:1, held together by hydrogen bonds and van der Waals' interactions. In the cation the Ni(II) ion is *N,N'*-

chelated by three neutral ethylenediamine molecules, it lies in a three fold axis and has a slightly distorted octahedral geometry being coordinated by six nitrogen atoms from three ethylenediamine molecules.

The three ethylenediamine molecules in the $[Ni(en)_3]^{2+}$ cation are oriented around the Ni atom in a $(lel)_3$ conformation thus the cation exists either in $\Delta(\lambda\lambda\lambda)$ or $\Lambda(\delta\delta\delta)$ form.

The average atom distance between the two N-atoms of the ethylenediamine molecule is 2.79Å and the average bond angle is 82.15°. These values are in good agreement with those reported previously.[17-23]

In this complex, the $[Ni(en)_3]^{2+}$ cation has an octahedral geometry around the Ni(II) atom with three bidentate ethylenediamine molecules. The sulfadiazinato anions remain in the ionic form in the structure and these are joined with lattice water through the hydrogen bonding of O(11)...O(1)–H(1E) (lattice water).

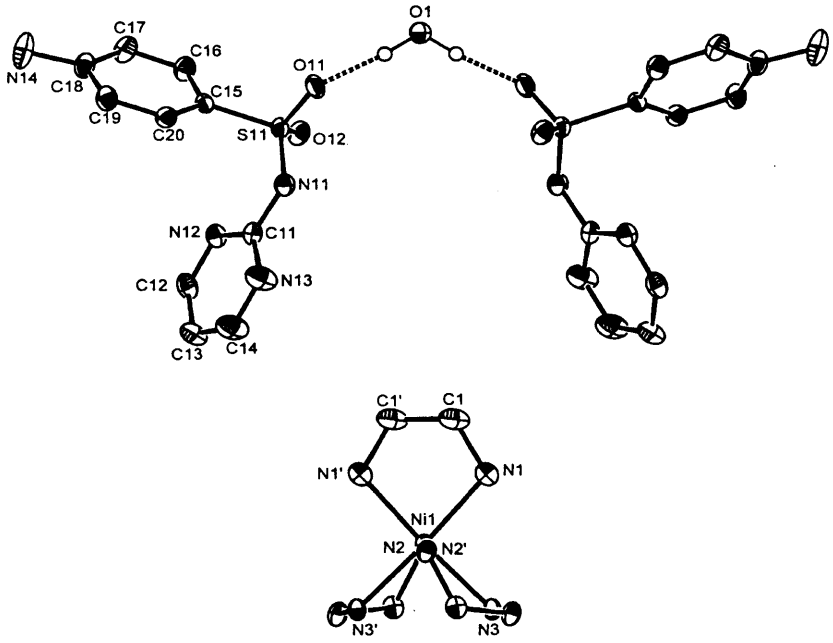

Figure 4.17
*X-ray structure of the complex $[Ni(en)_3][(sdz)_2].H_2O$ (**4**). Thermal ellipsoids are drawn at 50% probability level. The hydrogen atoms are omitted for clarity. The hydrogen bonds between water molecule and sulfadiazinato anions are shown by dashed lines.*

The octahedral geometry around Ni atom is distorted showing only minor variations from ideal geometry of the mutually *cis* 90° and *trans* 180° angles. This is evident from the values of the *trans* angles range between 170.94(10) and 174.40(7)° and also from the *cis* angles which vary from 82.15(11) to 94.30(8)°.

The Ni–N(en) distances of the complex are Ni–N(1) = 2.123(2), Ni–N(2) = 2.117(2) and Ni–N(3) = 2.128(2)Å are comparable with the corresponding bonds of the values of 2.121(6) – 2.139(1)Å in the complex $[Ni(en)_3][N(NO_2)_2]_2$[24] and 2.099(3) – 2.135(2)Å in the complex tris(ethylenediamine-*N*,*N*')nickel(II) tetrathiomolybdate $[Ni(en)_3][MoS_4]_2$[25] and 2.113(4) – 2.150(5)Å in $[Ni(en)_3][L]$[26] (L = 2,4-bis(4-methoxyphenyl)-1,3,2,4-dithiadiphosphetane-2,4-disulfide).

Table 4.25: Selected bond lengths [Å] and angles [deg] in $[Ni(en)_3][(sdz)_2].H_2O$ (4)

Bond	(Å)	Bond	(Å)
Ni(1)-N(2)	2.117(2)	Ni(1)-N(1)	2.123(2)
Ni(1)-N(3)	2.128(2)	S(11)-O(12)	1.448(2)
S(11)-O(11)	1.461(2)	S(11)-N(11)	1.575(2)
S(11)-C(15)	1.766(2)	N(11)-C(11)	1.371(3)
N(12)-C(12)	1.331(3)	N(12)-C(11)	1.351(3)
N(13)-C(14)	1.337(3)	N(13)-C(11)	1.348(3)
N(14)-C(18)	1.375(3)		
Angle	**(°)**	**Angle**	**(°)**
N(2')-Ni(1)-N(2)	170.94(10)	N(2')-Ni(1)-N(1)	91.30(6)
N(2)-Ni(1)-N(1)	82.25(6)	N(1')-Ni(1)-N(1)	89.55(10)
N(2)-Ni(1)-N(3')	93.24(7)	N(1)-Ni(1)-N(3')	94.30(8)
N(2')-Ni(1)-N(3)	93.24(7)	N(2)-Ni(1)-N(3)	93.58(7)
N(1')-Ni(1)-N(3)	94.30(8)	N(1)-Ni(1)-N(3)	174.40(7)
N(3')-Ni(1)-N(3)	82.15(11)	O(12)-S(11)-O(11)	113.51(9)
O(12)-S(11)-N(11)	115.37(10)	O(11)-S(11)-N(11)	104.33(10)
O(12)-S(11)-C(15)	107.17(10)	O(11)-S(11)-C(15)	106.75(10)
N(11)-S(11)-C(15)	109.38(10)	C(11)-N(11)-S(11)	121.79(15)
N(13)-C(11)-N(12)	124.6(2)	N(13)-C(11)-N(11)	122.25(19)

Symmetry transformations used to generate equivalent atoms: (') $-x, y, -z+½$

It can be seen that in the $[Ni(en)_3]$ ion, four N-atoms exist in the equatorial position forming a parallelogram and two other N-atoms occupying the axial sites.

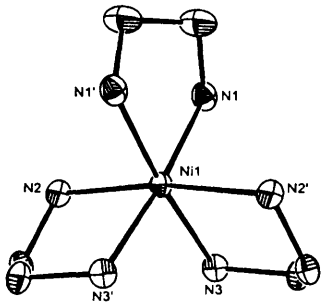

Figure 4.18
Octahedral structure of the cation $[Ni(en)_3]^{2+}$ in the complex (4)

The several hydrogen bonds are shown in Table 4.26 and the intermolecular hydrogen bondings are shown by open bonds in the packing diagram (Figure 4.19). The hydrogen bonds are very strong with short donor-acceptor distances and the linearity of the angles.

Table 4.26: Possible hydrogen bonds in $[Ni(en)_3(sdz)_2]\cdot H_2O$ (4) (distances and angles given in Å and deg respectively)

Donor-H	Donor...Acceptor	H...Acceptor	Donor-H.....Acceptor
O1 -H1E	O1 ....O11 (0)	H1E ...O11 (0)	O1 -H1E ...O11 (0)
0.948(12)	2.723(1)	1.781(2)	172.25(5)
N14 -H14A	N14 ....N12 (1)	H14A...N12 (1)	N14 -H14A...N12 (1)
0.948(3)	3.238(4)	2.455(4)	139.88(1)
N1 -H1A	N1 ....O12 (2)	H1A ...O12 (2)	N1 -H1A ...O12 (2)
0.920(2)	3.066(3)	2.268(2)	144.78(4)
N3 -H3B	N3 ....N13 (3)	H3B ...N13 (3)	N3 -H3B ...N13 (3)
0.920(2)	3.101(3)	2.279(2)	148.58(3)
N1 -H1B	N1 ....O11 (3)	H1B ...O11 (3)	N1 -H1B ...O11 (3)
0.920(2)	3.210(3)	2.333(2)	159.14(1)
N2 -H2B	N2 ....N11 (3)	H2B ...N11 (3)	N2 -H2B ...N11 (3)
0.920(1)	3.250(1)	2.362(5)	162.35(2)
N2 -H2A	N2 ....O12 (4)	H2A ...O12 (4)	N2 -H2A ...O12 (4)
0.920(1)	3.130(7)	2.315(3)	147.58(2)
N3 -H3A	N3 ....O1 (5)	H3A ...O1 (5)	N3 -H3A ...O1 (5)
0.920(1)	2.986(.004)	2.125(3)	155.35(2)
N3 -H3A	N3 ....O1 (6)	H3A ...O1 (6)	N3 -H3A ...O1 (6)
0.920(1)	2.986(4)	2.125(3)	155.35(2)

Equivalent positions:
(0) x, y, z; (1) x+½,-y+½,-z; (2) x-½,+y+½,-z+½; (3) -x-½,+y+½,+z; (4) x,+y+1,+z; (5) -x,+y+1,-z+½; (6) x+½, +y-½, -z+½

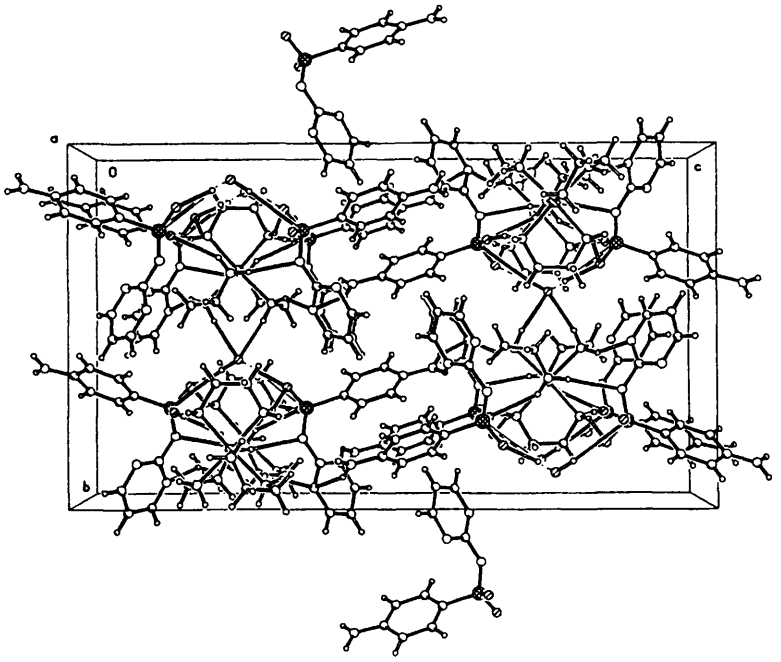

Figure 4.19
Packing diagram of the complex $[Ni(en)_3][(sdz)_2].H_2O$ (4) showing the hydrogen bonds by open line between the atoms.

4.6.2 Nickel complex of sulfamerazine $[Ni(smr)_2(py)_2].4py$ (5)

The structure of the complex $[Ni(smr)_2(py)_2].4py$ (**5**) is shown in Figure 4.20 together with the crystallographic atom numbering scheme used. The numbering of atoms with prime (') indicates that these atoms are generated from the original atoms by an inversion centre. Selected bond lengths and angles are given in Tables 4.27 and the possible hydrogen bond dimensions and short contacts are listed in Table 4.28.

The nickel atom in the complex (**5**) sits on a centre of symmetry, and is a distorted octahedral structure with two bidentate *N*-coordinated sulfamerazinato anions and two pyridine molecules in *trans* positions making up the coordination sphere and the lattice four pyridine molecules are hydrogen bonded with the terminal amino ($-NH_2$) group of the sulfamerazine molecules. The sulfamerazine molecule coordinates to Ni(II) as a mono-negative bidentate ligand with pyrimido nitrogen and sulfonamidic nitrogen atoms.

The relative orientations of the sulfamerazine and the pyridine molecules are such that they are nearly perpendicular to each other. Such orientations of the ligands around the nickel atom appear to be dictated more by steric considerations than any other factors.

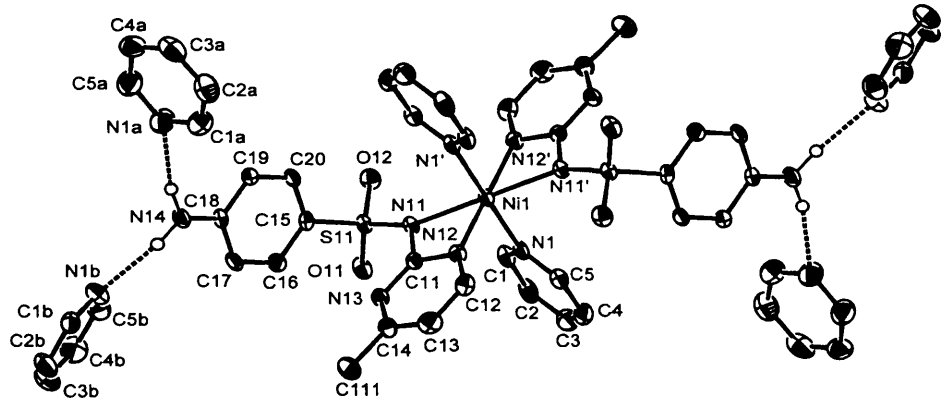

Figure 4.20
X-ray structure of the complex [Ni(smr)$_2$(py)$_2$].4py (5) showing crystallographic atom numbering scheme used. Thermal ellipsoids are drawn at 50% probability level. The hydrogen atoms are omitted for clarity. The hydrogen bonds are shown by dashed lines.

Table 4.27: Selected bond lengths (Å) and angles (°) for [Ni(smr)$_2$(py)$_2$].4py (5)

Bond	(Å)	Bond	(Å)
Ni(1)-N(1)	2.080(2)	Ni(1)-N(12)	2.100(2)
Ni(1)-N(11)	2.139(2)	S(11)-O(12)	1.443(2)
S(11)-O(11)	1.445(2)	S(11)-N(11)	1.614(2)
S(11)-C(15)	1.760(2)	N(11)-C(11)	1.358(3)
N(14)-C(18)	1.367(3)		
Angle	**(°)**	**Angle**	**(°)**
N(1')-Ni(1)-N(1)	180.00(11)	N(1')-Ni(1)-N(12)	92.00(7)
N(1)-Ni(1)-N(12)	88.00(7)	N(12')-Ni(1)-N(12)	180.0(9)
N(1)-Ni(1)-N(11')	90.37(7)	N(1)-Ni(1)-N(11)	89.63(7)
N(12')-Ni(1)-N(11)	116.66(7)	N(12)-Ni(1)-N(11)	63.34(7)
N(11')-Ni(1)-N(11)	180.00(10)	O(12)-S(11)-O(11)	116.68(10)
O(12)-S(11)-N(11)	104.93(10)	O(11)-S(11)-N(11)	111.74(10)
O(12)-S(11)-C(15)	108.80(10)	O(11)-S(11)-C(15)	107.20(10)
N(11)-S(11)-C(15)	107.11(10)	C(12)-N(11)-C(13)	125.2(2)

Symmetry transformations used to generate equivalent atoms: $-x, -y, -z$

The unique Ni–N bond distances, in the present complex involving the sulfonamidic nitrogen [N(11)], pyrimido nitrogen [N(12)] atoms and the pyridine molecules [N(1)] of 2.139(2), 2.100(2) and 2.080(2)Å respectively, are comparable with the corresponding Ni–N distances with the values of 2.117(2), 2.123(2) and 2.128(2)Å in the previous complex [Ni(en)$_3$][(sdz)$_2$].H_2O (**4**), 2.129(4)Å in [Ni(L)$_2$(py)$_2$].$2H_2O$ (where, L = 4,5-diazofluorene-9-one quinaldinoylhydrazone and py = pyridine)[27] and 2.127(3)Å in [Ni(i-pr$_2$dtp)$_2$(py)$_2$] (where dtp = dithiophosphate and pr = isopropyl)[28] which are also consistent with the value of 2.11(1)Å in [Ni(Et$_2$dtp)$_2$(py)$_2$][29], 2.116(4)Å in [Ni(Bu$_2$dtp)$_2$(py)$_2$][30] and 2.100(5) –

2.123(5)Å in the complex $[Ni(L)(py)_2]$[31] (L = 6-phenyl-15-aza-6-phospha-3,9-dithiabicyclo[9,3,1]pentadeca-1(15),11,13-triene).

The S(11) atoms are sp^3 hybridised and this is distorted as in the case of sulfamerazine molecule. The endocyclic angle at C(11) of pyrimidine ring of sulfamerazine in the complex is 125.2(2)° which is decreased compared to the corresponding angle in pure sulfamerazine 127.5(2)° due to the formation of bonds of sulfonamidic and pyrimido nitrogen atom with the nickel atom.

In the packing diagram (Figure 4.21), the several hydrogen bonds and short contacts are shown by dashed lines.

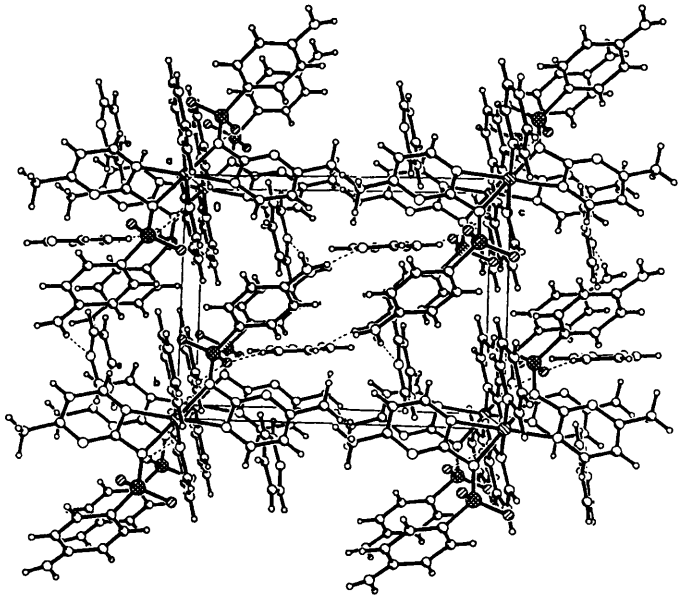

Figure 4.21
Packing diagram of the complex (5) showing the hydrogen bonds with dashed lines

Table 4.28: Possible hydrogen bonds and short interactions for $[Ni(smr)_2(py)_2].4py$ (5)

Donor-H	Donor...Acceptor	H...Acceptor	Donor-H...Acceptor
N14 -H14A 0.949(3)	N14 ....N1B (0) 3.065(3)	H14A...N1B (0) 2.135(3)	N14 -H14A...N1B (0) 166.25(4)
N14 -H14B 0.947(4)	N14 ....N1A (0) 3.029(5)	H14B...N1A (0) 2.094(4)	N14 -H14B...N1A (0) 168.91(3)
C2 -H2 0.950(4)	C2 ....O11 (1) 3.108(4)	H2 ...O11 (1) 2.414(2)	C2 -H2 ...O11 (1) 129.72(4)
C3B -H3B 0.950(4)	C3B ....O11 (2) 3.284(5)	H3B ...O11 (2) 2.340(2)	C3B -H3B ...O11 (2) 172.42(4)

Equivalent positions: (0) x, y, z; (1) -x+1, -y, -z; (2) -x+1, -y+1, -z-1

4.7 Copper complexes of triple sulfa drugs

In this section, we will discuss the copper complexes of four coordinate with square planar geometry $[Cu(en)_2][(sdz)_2]$ (**6**), five coordinate with square pyramidal containing a metal-metal bond $[Cu_2(smr)_4].2DMF$ (**10**) and $[Cu_2(smr)_4].2DMSO$ (**11**) and six coordinate with octahedral $[Cu(dien)(sdz)_2]$ (**7**), $[Cu(en)_2(H_2O)_2][(smr)_2]$ (**8**), $[Cu(en)_2(H_2O)_2][(smr)_2]_2.H_2O$ (**9**), $[Cu(smz)_2(apen)].3H_2O.CH_3OH$ (**12**) and $\{[Cu(smz)_2(NH_3)].2H_2O\}_n$ (**13**) around the copper centres. The crystal data for the complexes are listed in Table 4.29.

4.7.1 Crystal Structure of $[Cu(en)_2][(sdz)_2]$ (6)

The crystal structure of the complex (**6**) is shown in Figure 4.23 together with the crystallographic atom numbering scheme used. Selected bond lengths and angles are given in Table 4.30 and the hydrogen bond dimensions are given in Table 4.31.

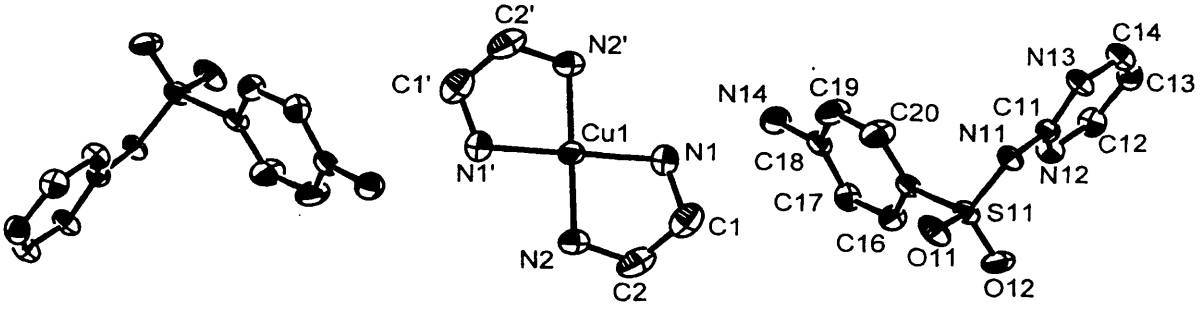

Figure 4.23
X-ray structure of the complex $[Cu(en)_2][(sdz)_2]$ (6) showing crystallographic atom numbering scheme used. Thermal ellipsoids are drawn at 50% probability level. The hydrogen atoms are omitted for clarity.

The X-ray structure of the complex $[Cu(en)_2][(sdz)_2]$ (**6**) shows the formation of a "cation-anion pair" involving the $[Cu(en)_2]^{2+}$ cation and $[sdz]^-$ anions which are held together in the crystal by very strong intermolecular hydrogen bonds and van der Waals' interactions.

The structure has a distorted square planar geometry around the Cu(II) atom with four nitrogen atoms from the two ethylenediamine molecules. The N–Cu–N *trans* angles N(1)–Cu(1)–N(1′) and N(2)–Cu(1)–N(2′) are 180° and the *cis* angles have the values ranging from 84.87(12) to 95.13(12)° showing small variations from the ideal value of 90°.

Table 4.29: Crystal data and details of data collection and structure refinement for $[Cu(en)_2(sdz)_2]$ (6), $[Cu(dien)(sdz)_2]$ (7), $[Cu(en)_2(H_2O)_2][(smr)_2]$ (8) and $[Cu(en)_2(H_2O)_2][(smr)_2]_2.H_2O$ (9), $[Cu_2(smr)_4].2DMF$ (10), $[Cu_2(smr)_4].2DMSO$ (11), $[Cu(smz)_2(apen)].3H_2O.CH_3OH$ (12) and $\{[Cu(smz)_2(NH_3)].2H_2O\}_n$ (13)

	(6)	(7)	(8)	(9)	(10)	(11)	(12)	(13)
Empirical Formula	$C_{24}H_{34}CuN_{12}O_4S_2$	$C_{28}H_{44}CuN_{14}O_4S_2$	$C_{26}H_{42}CuN_{12}O_6S_2$	$C_{26}H_{44}CuN_{12}O_7S_2$	$C_{50}H_{58}Cu_2N_{18}O_{10}S_4$	$C_{26}H_{34}CuN_8O_6S_4$	$C_{33}H_{60}CuN_{12}O_8S_2$	$C_{24}H_{33}CuN_9O_6S_2$
Formula Weight	682.29	768.43	746.38	764.39	1326.46	746.39	880.59	671.25
Crystal System	Monoclinic	Monoclinic	Triclinic	Triclinic	Orthorhombic	Rhombohedral	Monoclinic	Monoclinic
Space Group	$P2_1/c$	$P2_1/c$	$P\bar{1}$	$P\bar{1}$	$P2_1/n$	$P2_1/n$	$P2_1/c$	P2(1)/n
a(Å)	10.8610(5)	14.5950(3)	7.5224(2)	7.56470(10)	13.63740(10)	18.8480(8)	9.4530(10)	13.6802(4)
b(Å)	10.6329(4)	7.8230(2)	8.1435(2)	15.0976(3)	32.7241(3)	18.8480(8)	12.3456(10)	13.8369(5)
c(Å)	12.5227(6)	15.9670(5)	14.7025(4)	16.0079(3)	13.78540(10)	8.9830(4)	34.7476(5)	15.8383(6)
α(°)	90	90	75.8094(9)	104.5786(13)	90	90	90	90
β(°)	93.3022(17)	111.0650(12)	82.9174(9)	99.8549(11)	113.9274(4)	90	90.8372(4)	96.3389(11)
γ(°)	90	90	79.4520(9)	91.8427(9)	90	90	90	90
V/Å^3	1443.77(11)	1701.23(8)	855.51(4)	1737.84(5)	5623.33(8)	3191.2(2)	4054.71(8)	2979.73(18)
Z	4	2	1	2	4	4	4	4
T/K	150	150	150	150	150	150	150	150
Crystal Size/mm	0.15 ×0.12 ×0.12	0.12 ×0.10 ×0.08	0.18 ×0.15 ×0.12	0.12 ×0.08 ×0.08	0.20 ×0.15 ×0.06	0.50 ×0.45 ×0.42	0.15 ×0.12 ×0.10	0.20 ×0.18 ×0.18
Shape	Block	Block	Block	Block	Prism	Prism	Block	Prism
Colour	Blue	Blue	Blue	Blue	Green	Green	Blue	Green
θ-range data collection	3.08 – 27.47	2.94 - 27.52	3.01 – 27.52	2.98 – 27.51	2.97 – 27.50	3.06 – 27.45	2.94 - 27.71	2.94 - 27.58
Reflection Collected	9385	12097	14556	30508				
Unique Reflections	3290	3882	3889	7900	12633	3387	9033	6811
R_{int}	0.0892	0.0609	0.1014	0.0812	0.0950	0.0698	0.0572	0.0571
Index ranges	−14<=h<=13, −13<=k<=13 −14<=l<=16	−18<=h<=15 −9<=k<=8 −20<=l<=18	−9<=h<=9 −10<=l<=10 −19<=k<=19	−9<=h<=9 −19<=k<=19 −20<=l<=20	−16<=h<=17 −42<=k<=42 −17<=l<=14	−18<=h<=24 −16<=k<=24 −11<=l<=11	−12<=h<=11 −15<=k<=15 −44<=l<=45	−17<=h<=15 −16<=k<=17 −20<=l<=20
Data/parameters	3290/196	3882/231	3889/231	7900/480	12633	3387	9033	6811/383
Final R indices [I>2σ(I)]	0.0547/0.1295	0.0436/0.0927	0.0393/0.0951	0.0437/0.1068	0.0504/0.1121	0.0565/0.1260	0.0479/0.1179	0.0605/0.1685
R indices (all data)	0.0808/0.1446	0.0721/0.1130	0.0479/0.1008	0.0679/0.1182	0.0856/0.1286	0.0849/0.1562	0.0706/0.1368	0.0842/0.1841
Largest diff. peak/hole (e.Å^{-3})	0.779 and -0.491	0.366 and -0.615	0.336 and -0.669	0.413 and -0.653	1.424 and -0.721	0.583 and -0.457	0.546 and -0.871	1.674 and -0.535

The bond lengths within the sulfadiazine and ethylenediamine are as expected. The Cu–N distances of 2.005(3) and 2.013(3)Å, involving the ethylenediamine molecules, are comparable with the corresponding values in the complex bis(ethylenediamine)copper(II) tetracyanonickelate $[Cu(en)_2][Ni(CN)_4]$ [1.997(3) and 2.001(3)Å][32], in diaqua-bis(ethylenediamine)copper(II) sulfathiazolate $[Cu(en)_2(H_2O)_2]$-$[(stz)_2].2H_2O$ [2.033(3) and 2.042(3)Å][33], in diaqua-bis-(ethylenediamine)copper(II) ethylenediaminebicarboxylate $[Cu(en)_2(H_2O)_2][(OOCNH\text{-}CH_2CH_2NHCOO)].2H_2O$ [1.996(2) and 2.022(3)Å][34], in diaqua-bis(ethylenedi-amine)copper(II) *N*-carboxyglycynate $[Cu(en)_2(H_2O)_2]$-$[(OOCCH_2NHCOO)].H_2O$ [2.007(3) – 2.024(3)Å][34], in bis(ethylenediamine)copper(II)-bis(*O*,*O*'-diethyl dithiophosphate) $[Cu(C_2H_8N_2)_2]$-q$[(C_4H_{10}O_2PS_2)_2]$ [2.016(2) and 2.019(2)Å][35], in *trans*-Bis(ethylenediamine)bis(*p*-nitrobenzoxasulfamato)copper(II) $[Cu(nbs)_2(en)_2]$ [2.007(3) and 2.010(3)Å][36] [where nbs is the *p*-nitrobenzoxasulfamate anion $(C_6H_3N_2O_5S)^-$].

Table 4.30: Selected bond lengths [Å] and angles [deg] in $[Cu(en)_2][(sdz)_2]$ (3)

Bond	(Å)	Bond	(Å)
Cu(1)–N(2)	2.005(3)	Cu(1)–N(1)	2.013(3)
S(11)–O(12)	1.449(3)	S(11)–O(11)	1.458(2)
S(11)–N(11)	1.589(3)	S(11)–C(15)	1.765(3)
N(11)–C(11)	1.372(4)	N(14)–C(18)	1.390(4)
Angle	**(°)**	**Angle**	**(°)**
N(2')-Cu(1)-N(2)	180.0	N(2)-Cu(1)-N(1)	84.87(12)
N(2)-Cu(1)-N(1')	95.13(12)	N(1)-Cu(1)-N(1')	180.0
O(12)-S(11)-O(11)	113.36(15)	O(12)-S(11)-N(11)	115.92(15)
O(11)-S(11)-N(11)	105.23(14)	O(12)-S(11)-C(15)	107.32(15)
O(11)-S(11)-C(15)	106.62(15)	N(11)-S(11)-C(15)	107.93(14)
N(13)-C(11)-N(12)	124.2(3)		

Symmetry transformations used to generate equivalent atoms: (') $-x, -y, -z+1$

The S(11)-O bond distances of 1.458(3) and 1.449(3)Å are longer than the corresponding bonds in the pure sulfadiazine (**1**) with the values of 1.429(2) and 1.437(2)Å. The sulfonyl SO_2 and amino NH_2 groups of sulfadiazine and NH_2 groups of ethylenediamine molecules appear to be hydrogen bonded. The hydrogen bonds and short contacts have week interactions between donor and acceptors as the angles don't show any linearity. The hydrogen bondings are shown in the packing diagram, Figure 4.24, by open bonds between the atoms.

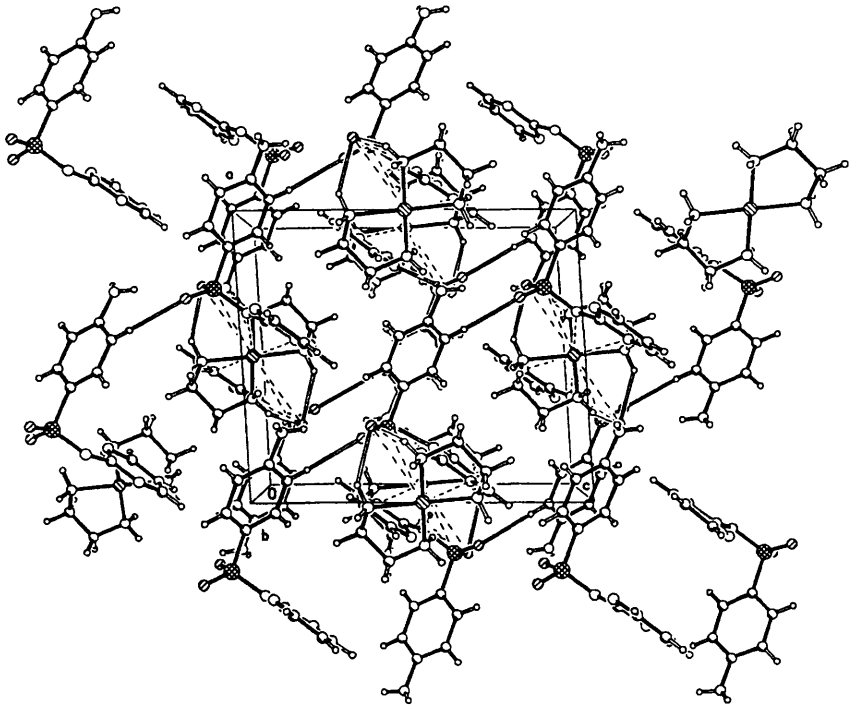

Figure 4.24:
The packing diagram of the complex $[Cu(en)_2(sdz)_2]$ (6) where the hydrogen bonds are shown by dashed lines.

Table 4.31: Possible hydrogen bonds and short interactions for $[Cu(en)_2(sdz)_2]$ (6) (distances and angles given in Å and deg respectively)

Donor-H	Donor...Acceptor	H...Acceptor	Donor-H.....Acceptor
N14 -H14B 0.800(2)	N14 ....N12 (1) 3.116(3)	H14B...N12 (1) 2.415(1)	N14 -H14B...N12 (1) 147.02(3)
C19 -H19 0.930(3)	C19 ....O12 (2) 3.293(4)	H19 ...O12 (2) 2.448(2)	C19 -H19 ...O12 (2) 151.10(4)
N1 -H1A 0.900(4)	N1 ....O11 (3) 2.959(3)	H1A ...O11 (3) 2.167(2)	N1 -H1A ...O11 (3) 146.35(2)
N2 -H2B 0.900(2)	N2 ....N13 (3) 3.021(1)	H2B ...N13 (3) 2.269(4)	N2 -H2B ...N13 (3) 140.84(2)
N2 -H2A 0.900(5)	N2 ....O11 (4) 3.070(7)	H2A ...O11 (4) 2.305(5)	N2 -H2A ...O11 (4) 142.71(8)

Equivalent positions:
(1) -x+1,-y+1,-z+1; (2) x-½,-y+½,+z-½; (3) -x+1,-y,-z+1; (4) x-1,+y,+z

4.7.2 Crystal structure of [Cu(dien)(sdz)$_2$] (7)

The crystal structure of [Cu(dien)(sdz)$_2$] (**7**) is shown in Figure 4.25 together with the crystallographic atom numbering scheme used. The bond lengths and angles are given in Table 4.32 and the hydrogen bond dimensions are given in Table 4.33.

In this complex, the $[Cu(dien)_2]^{2+}$ cation has an octahedrally arrangement around the Cu(II) atom with the two tridentate diethylenetriamine molecules. In the complex the sulfadiazinato anions do not coordinate to the copper centre and are joined through the hydrogen bonding of sulfonyl oxygen O(12) atom with the hydrogen atoms of amino groups of the diethylenetriamine molecules.

The Cu–N distances in the present complex involving the diethylenetriamine molecules are Cu–N(1) = 2.339(3), Cu–N(2) = 2.031(2) and Cu–N(3) = 2.116(2)Å. The Cu–N(2) is the shortest bond formed by the central –NH– group of dien molecule with the copper atom. The Cu–N(dien) bond distances are shorter than the corresponding bonds of the values of 2.459(26), 2.040(23) and 2.350(28)Å in the complex $[Cu(dien)_2][Br_2].H_2O$[37] and than the values of 2.098(15) – 2.140(9)Å in the complex $[Cu(dien)(OAc)]_n[(ClO4)_n]$[38], 1.998(4) – 2.019(4)Å in $[Cu(dien)(cnge)(ONO_2)_2]$[39], 1.98(2) – 2.05(2)Å in $[Cu(bimH_2)(dien)][(ClO_4)_2]$[40], 2.002(10) – 2.265(23)Å in $[Cu(dien)_2]$ cation[41] and 2.014(3) – 2.032(3)Å in $[Cu(dien)Ag(CN)_2]$[42] but the middle Cu–N(dien) bond are similar with the corresponding bonds in related the complexes.[37–42]

It is seen that in this complex the Cu–N bonds of 2.339(3)Å are longer compared to the four short bonds in a square planar arrangement, so that the overall geometry is highly distorted octahedral and the origin of this type of distortion is attributed to the Jahn-Teller effect.

The octahedral geometry around the Cu atom is distorted from the ideal geometry and this is evident from the values of three *trans* angles of 180.0° and also from the *cis* angles which vary from 80.49(9) to 99.51(9)°.

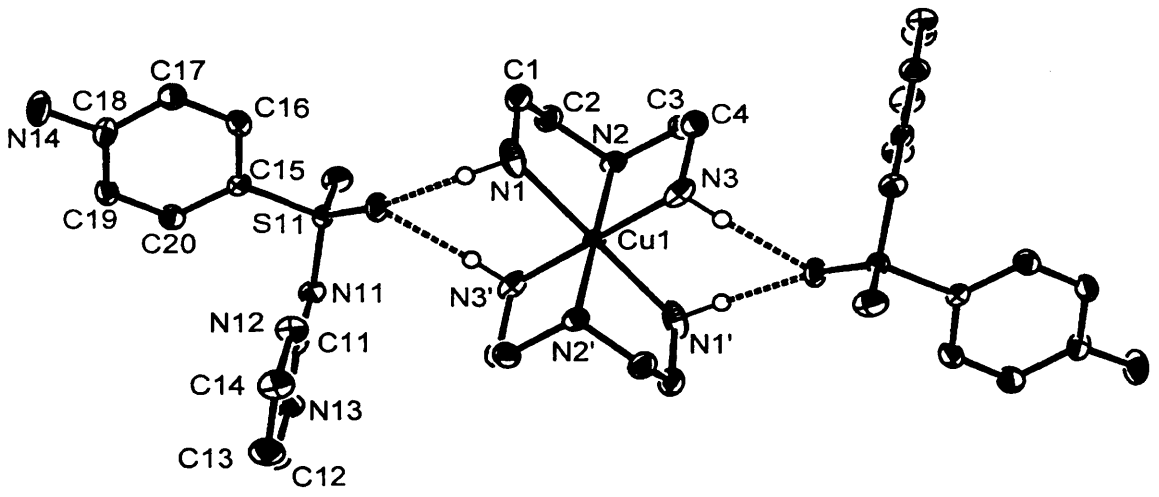

Figure 4.25
X-ray structure of the complex [Cu(dien)$_2$][(sdz)$_2$] (7) showing crystallographic atom numbering scheme used. Thermal ellipsoids are drawn at 50% probability level. The ring hydrogens are omitted for clarity. The hydrogen bonds are shown by dashed line.

Table 4.32: Selected bond lengths [Å] and angles [°] in [Cu(dien)$_2$][(sdz)$_2$] (7)

Bond	(Å)	Bond	(Å)
Cu(1)-N(2)	2.031(2)	Cu(1)-N(3)	2.116(3)
Cu(1)-N(1)	2.339(3)	S(11)-O(11)	1.446(2)
S(11)-O(12)	1.456(2)	S(11)-N(11)	1.587(2)
S(11)-C(15)	1.762(3)	N(11)-C(11)	1.368(3)
N(13)-C(11)	1.366(3)	N(14)-C(18)	1.370(4)
Angle	**(°)**	**Angle**	**(°)**
N(2')-Cu(1)-N(2)	180.0	N(2')-Cu(1)-N(3)	95.64(9)
N(2)-Cu(1)-N(3)	84.36(9)	N(3')-Cu(1)-N(3)	180.00(14)
N(3)-Cu(1)-N(1')	91.90(9)	N(2')-Cu(1)-N(1)	99.51(9)
N(2)-Cu(1)-N(1)	80.49(9)	N(3)-Cu(1)-N(1)	88.10(9)
N(1')-Cu(1)-N(1)	180.0	O(11)-S(11)-O(12)	113.72(13)
O(11)-S(11)-N(11)	105.92(12)	O(12)-S(11)-N(11)	113.96(12)
O(11)-S(11)-C(15)	107.02(12)	O(12)-S(11)-C(15)	106.70(12)
N(11)-S(11)-C(15)	109.28(12)	N(12)-C(11)-N(13)	124.5(3)

Symmetry transformations used to generate equivalent atoms: (') $-x, -y+1, -z+1$

This complex also forms a "cation-anion pair" involving the $[Cu(dien)_2]^{2+}$ cation and two sdz^- anions. This is affected by the formation of strong hydrogen bonds involving the coordinated dien molecules [N(1) and N(3)] and the sulfonyl oxygen [O(12)] atom anions which are shown in the packing diagram of the complex in Figure 4.26.

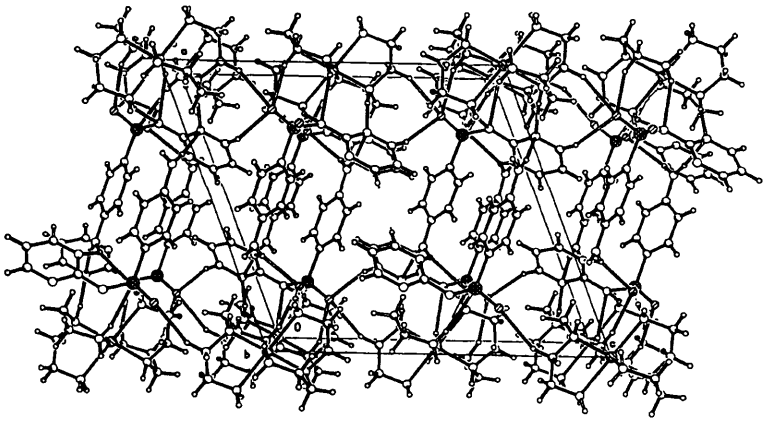

Figure 4.26
The packing diagram of the complex [Cu(dien)$_2$(sdz)$_2$] (7) where the hydrogen bonds are shown by open bonds.

Table 4.33: Possible hydrogen bonds and short interactions in [Cu(dien)$_2$][(sdz)]$_2$ (7) (distances and angles given in Å and deg respectively)

Donor-H	Donor...Acceptor	H...Acceptor	Donor-H.....Acceptor
N1 -H1A 0.920(5)	N1 ....O12 (0) 2.887(4)	H1A ...O12 (0) 2.061(1)	N1 -H1A ...O12 (0) 148.65(1)
N14 -H14A 0.898(4)	N14 ....N13 (1) 3.438(4)	H14A...N13 (1) 2.558(4)	N14 -H14A...N13 (1) 166.37(2)
N14 -H14B 0.948(5)	N14 ....N12 (2) 3.160(14)	H14B...N12 (2) 2.433(7)	N14 -H14B...N12 (2) 133.32(1)
N1 -H1B 0.920(4)	N1 ....N11 (3) 3.121(4)	H1B ...N11 (3) 2.237(3)	N1 -H1B ...N11 (3) 161.06(1)
N3 -H3A 0.920(6)	N3 ....N11 (3) 3.283(9)	H3A ...N11 (3) 2.441(6)	N3 -H3A ...N11 (3) 152.15(3)
C4 -H4B 0.990(5)	C4 ....O11 (3) 3.361(8)	H4B ...O11 (3) 2.461(5)	C4 -H4B ...O11 (3) 150.89(3)
N2 -H2 1.008(4)	N2 ....N13 (4) 3.065(7)	H2 ...N13 (4) 2.061(5)	N2 -H2 ...N13 (4) 174.06(1)
N3 -H3B 0.920(3)	N3 ....O12 (5) 3.071(6)	H3B ...O12 (5) 2.201(4)	N3 -H3B ...O12 (5) 157.24(3)
C2 -H2B 0.990(6)	C2 ....O11 (6) 3.340(9)	H2B ...O11 (6) 2.416(6)	C2 -H2B ...O11 (6) 155.15(6)

Equivalent positions:
(0) x, y, z; (1) -x-1,+y+½,-z+½; (2) -x-1,+y-½,-z+½; (3) x,+y+1,+z; (4) -x,-y,-z+1; (5) -x,-y+1,-z+1; (6) -x,+y+½,-z+½

4.7.3 Structures of the complexes $[Cu(en)_2(H_2O)_2].2[smr]^-$ (8) and $\{[Cu(en)_2(H_2O)_2].[(smr)_2]\}_2.H_2O$ (9)

The complexes consist of discrete molecules of the $[Cu(en)_2(H_2O)_2]^{2+}$ cation and $[smr]^-$ anions and are held together by very strong hydrogen bonds and van der Waals' interactions. In the complexes, the $[Cu(en)_2(H_2O)_2]^{2+}$ cation has a distorted octahedral arrangement of copper(II) atom with two ethylenediamine and two water molecules which are in the *trans* position and the sulfamerazinato anions are bonded through the hydrogen bonding. The selected bond lengths and angles for the complexes (**8**) and (**9**) are given in Table 4.6.

Table 4.34: Selected bond lengths [Å] and angles [°] in the complexes (8) and (9)

Bond	(8) [Å]	(9) [Å]		Angle	(8) [°]	(9) [°]	
Cu(1)-N(1)	2.034(2)	2.030(2)	2.029(2)	N(1)-Cu(1)-N(1′)	180.0	180.0(1)	180.0(1)
Cu(1)-N(2)	2.006(2)	2.001(2)	2.009(2)	N(2)-Cu(1)-N(2′)	180.0	180.0(2)	180.0(2)
Cu(1)-O(1)	2.501(2)	2.506(2)	2.509(2)	N(2)-Cu(1)-N(1)	85.3(1)	94.7(1)	84.7(1)
S(11)-O(11)	1.460(2)	1.464(2)	1.460(2)	N(2′)-Cu(1)-N(1)	94.7(1)	85.3(1)	95.3(1)
S(11)-O(12)	1.454(2)	1.462(2)	1.462(2)	O(1)-Cu(1)-O(1′)	179.9(1)	180.0(1)	180.0(1)
S(11)-N(11)	1.584(2)	1.580(2)	1.588(2)	O(1)-Cu(1)-N(1)	91.4(1)	91.92(1)	86.35(1)
S(11)-C(15)	1.760(2)	1.759(2)	1.762(2)	O(1)-Cu(1)-N(2′)	97.6(1)	96.78(1)	88.67(1)
N(11)-C(11)	1.376(3)	1.380(3)	1.377(3)	O(1)-Cu(1)-N(1′)	88.6(1)	88.08(1)	88.62(1)
N(14)-C(18)	1.375(3)	1.366(3)	1.366(3)	N(12)-C(11)-N(13)	125.1(2)	124.9(2)	125.3(2)

Symmetry transformations used to generate equivalent atoms: (*a*) $-x, -y, -z$, (*b*) $-x, -y, -z+1$

The crystal structures of the complexes (**8**) and (**9**) are shown in Figures 4.27 and 4.28 together with the crystallographic atom numbering scheme used.

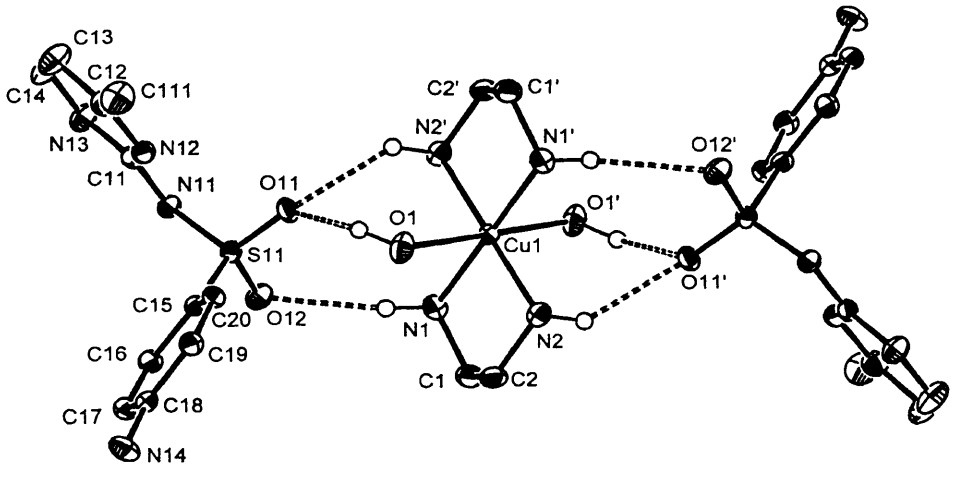

Figure 4.27
X-ray structure of the complex $[Cu(smr)_2(H_2O)_4]\cdot 2[smr]^-$ (8) showing the crystallographic atom numbering scheme used. Thermal ellipsoids are drawn at 50% probability level. The hydrogen except bonding hydrogen atoms are omitted for clarity.

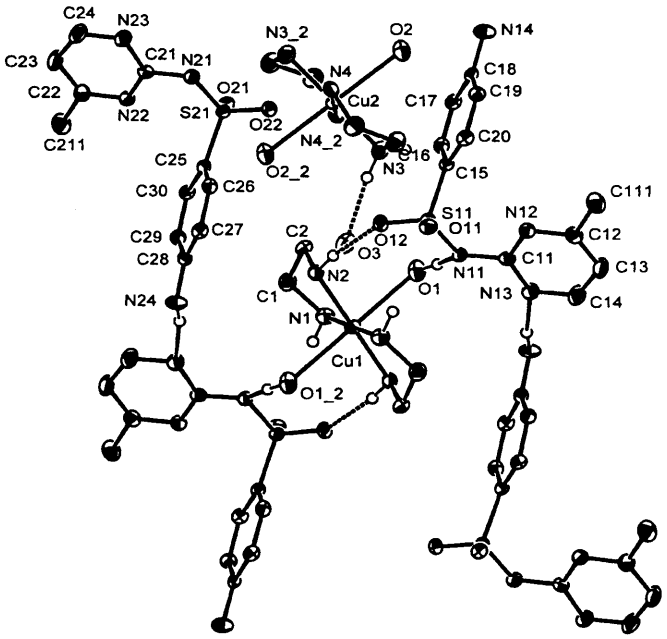

Figure 4.28
X-ray structure of $[Cu(en)_2(H_2O)_2][smr)_2].H_2O$ (9) showing crystallographic atom numbering scheme used. Thermal ellipsoids are drawn at 50% probability level. The hydrogen atoms are omitted for clarity.

In the complex (**9**), there are two Cu(II) ions in the structure although both the Cu ions are of the same symmetry which is proved by the EPR data. The ethylenediamine molecules are chelated to the Cu atoms symmetrically in the octahedral structure.

The Cu(II) ion in the complexes is coordinated to two ethylenediamine molecules and two oxygen atoms from the water molecules, forming the tetragonally distorted octahedral structures. In the complexes the sulfamerazine molecules are bonded through the H-bondings. These structures show that the Cu(II) ions are six coordinated with four nitrogen atoms [N(1)/N(2)] from two ethylenediamine molecules and two oxygen [O(1)] atoms from two coordinated water molecules. The oxygen atoms are coordinated with longer interactions [Cu–O(1) = 2.501(2)Å in (**8**) and 2.506(2)Å in (**9**)] compared to the Cu–N bonds of the distances of 2.034(2) – 2.006(2)Å in (**8**) and 2.001(2) – 2.030(2)Å in (**9**) and this is attributed to the Jahn-Teller effect.

The Cu–N(en) distances are comparable with the corresponding values of 2.013(3) and 2.005(3)Å in the previous copper ethylenediamine complex $[Cu(en)_2][(sdz)_2]$ (**6**) and the other complexes[32–36], 1.996(2) and 2.022(3)Å in diaquabis-(ethylenediamine)copper(II) ethylenediaminebicarboxylate $[Cu(en)_2(H_2O)_2][(OOCNH\text{-}CH_2CH_2NHCOO)].2H_2O$ and

2.007(3) – 2.024(3)Å in diaqua-bis(ethylenediamine)copper(II) *N*-carboxyglcynate $[Cu(en)_2(H_2O)_2][(OOCCH_2NHCOO)].H_2O$[43] and 2.018(4) – 2.021(4)Å in diaqua-bis(ethylenediamine)copper(II) bis(4-fluorobenzoate) $[Cu(C_2H_8N_2)(H_2O)_2](C_7H_4FO_2)_2$.[44]

The Cu–O distances of 2.507(2)Å are comparable with the values of 2.556(2)Å in diaqua-bis(ethylenediamine)copper(II) ethylenediaminebicarboxylate $[Cu(en)_2(H_2O)_2][(OOCNH-CH_2CH_2NHCOO)].2H_2O$ and 2.591(3) and 2.741(3)Å in of *N*-carboxyglycinate $[Cu(en)_2(H_2O)_2][(OOCCH_2NHCOO)].H_2O$[34], 2.0579(4)Å in diaqua-bis-(ethylenediamine)-copper(II) bis(4-fluorobenzoate) $[Cu(C_2H_8N_2)(H_2O)_2](C_7H_4FO_2)_2$.[44]

The complexes form "cation-anion pair" involving the $[Cu(en)_2(H_2O)_2]^{2+}$ cation and two $[smr]^-$ anions which are affected by the formation of strong hydrogen bonds involving the coordinated and lattice water molecules [O(1) in (**8**) and O(1), O(2) and O(3) in (**9**)], ethylenediamine molecules [N(1) and N(2)] and the sulfonyl oxygen [O(11) and O(12)] atoms and pyrimido and terminal amino nitrogen atoms of the $[smr]^-$ anions in (**9**).

The O(1)–H(1A)···O(11), N(1)–H(1A)···O(12) and N(2)–H(2A)···O(11) hydrogen bonds in the complexes present very short donor-acceptor distances and nearly linear donor-acceptor angles indicating strong interactions.

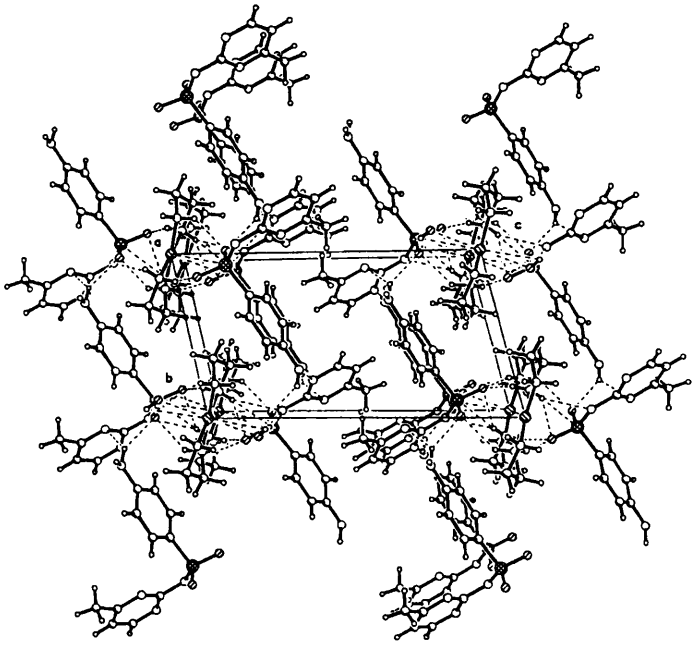

Figure 4.29
*The packing diagram of the complex $[Cu(en)_2(H_2O)_2][(smr)_2]$ (**8**) where the hydrogen bonds are shown by dashed lines.*

Table 4.35: Possible hydrogen bonds in (8) (distances and angles given in [Å] and [°] respectively)

Donor-H	Donor...Acceptor	H...Acceptor	Donor-H.....Acceptor
N1 -H1A 0.900(1)	N1 ....O12 (0) 3.250(2)	H1A ...O12 (0) 2.448(2)	N1 -H1A ...O12 (0) 148.64(3)
O1 -H1C 0.948(2)	O1 ....O11 (0) 2.816(2)	H1C ...O11 (0) 1.941(2)	O1 -H1C ...O11 (0) 152.49(4)
N14 -H14A 0.948(2)	N14 ....N13 (1) 2.981(3)	H14A...N13 (1) 2.036(2)	N14 -H14A...N13 (1) 174.15(5)
N14 -H14B 0.864(1)	N14 ....O11 (2) 2.975(1)	H14B...O11 (2) 2.255(1)	N14 -H14B...O11 (2) 140.86(2)
N1 -H1B 0.900(1)	N1 ....O12 (3) 3.207(2)	H1B ...O12 (3) 2.418(1)	N1 -H1B ...O12 (3) 146.55(2)
N2 -H2A 0.900(1)	N2 ....O11 (5) 3.161(1)	H2A ...O11 (5) 2.403(1)	N2 -H2A ...O11 (5) 142.03(2)
N2 -H2B 0.900(2)	N2 ....O12 (6) 3.015(2)	H2B ...O12 (6) 2.142(1)	N2 -H2B ...O12 (6) 163.44(3)
O1 -H1D 0.983(1)	O1 ....N11 (7) 2.859(2)	H1D ...N11 (7) 1.892(2)	O1 -H1D ...N11 (7) 167.08(3)

Equivalent positions:
(0) x,y,z; (1) x-1,+y+1,+z; (2) x,+y+1,+z; (3) -x+1,-y,-z; (4) x+1,+y,+z; (5) -x,-y,-z; (6) x-1,+y,+z; (7) -x-1,-y,-z

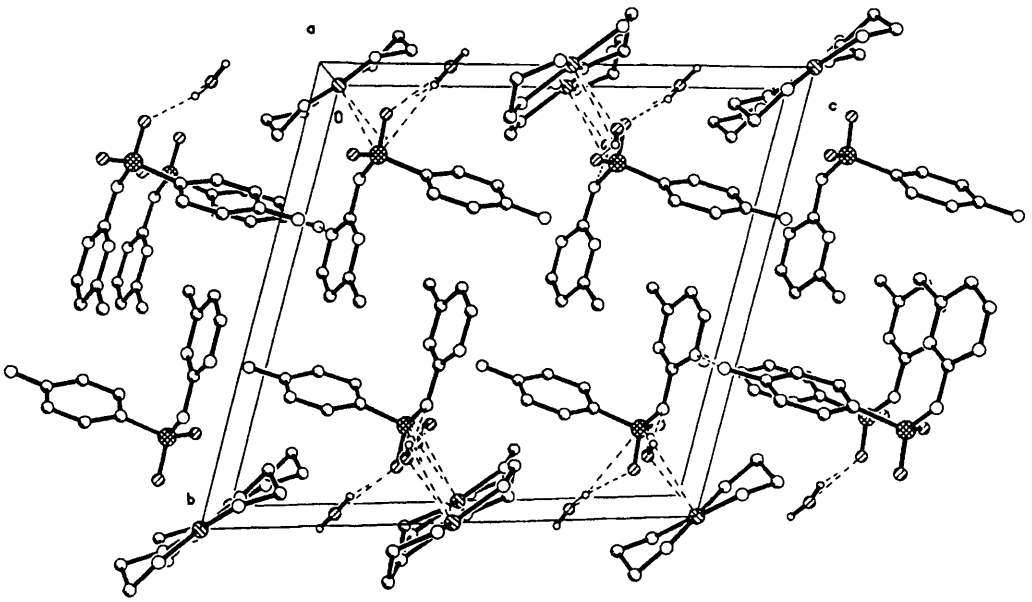

Figure 4.30
*The packing diagram of the complex {[Cu(en)$_2$(H$_2$O)$_2$][(smr)$_2$]}$_2$.H$_2$O (**9**) where the hydrogen bonds are shown by dashed lines.*

Table 4.36: Possible hydrogen bonds in the complex $[Cu(en)_2(H_2O)_2][(smr)_2].H_2O$ (9) (distances and angles are given in Å and deg respectively)

Donor-H	Donor...Acceptor	H...Acceptor	Donor-H....Acceptor
O1 -H1A 0.894(2)	O1 ....N11 (0) 2.896(4)	H1A ...N11 (0) 2.036(3)	O1 -H1A ...N11 (0) 160.87(4)
N2 -H2D 0.920(2)	N2 ....O12 (0) 3.002(3)	H2D ...O12 (0) 2.091(2)	N2 -H2D ...O12 (0) 170.56(3)
N3 -H3A 0.920(1)	N3 ....O3 (0) 2.988(2)	H3A ...O3 (0) 2.080(2)	N3 -H3A ...O3 (0) 168.47(2)
N4 -H4B 0.920(1)	N4 ....O21 (0) 3.075(1)	H4B ...O21 (0) 2.195(5)	N4 -H4B ...O21 (0) 159.81(2)
O1 -H1B 0.919(3)	O1 ....O11 (1) 2.844(4)	H1B ...O11 (1) 2.006(3)	O1 -H1B ...O11 (1) 150.91(5)
O3 -H3E 0.944(2)	O3 ....O22 (1) 2.847(2)	H3E ...O22 (1) 1.911(1)	O3 -H3E ...O22 (1) 171.21(2)
O3 -H3F 0.967(2)	O3 ....O12 (1) 2.888(2)	H3F ...O12 (1) 1.987(1)	O3 -H3F ...O12 (1) 154.05(2)
N24 -H24B 0.880(2)	N24 ....O11 (2) 3.016(2)	H24B...O11 (2) 2.376(1)	N24 -H24B...O11 (2) 129.84(3)
N24 -H24B 0.880(2)	N24 ....N12 (2) 3.150(4)	H24B...N12 (2) 2.371(3)	N24 -H24B...N12 (2) 147.72(3)
N2 -H2C 0.920(2)	N2 ....O11 (2) 3.160(2)	H2C ...O11 (2) 2.343(1)	N2 -H2C ...O11 (2) 147.75(2)
N24 -H24A 0.880(3)	N24 ....N13 (3) 2.969(5)	H24A...N13 (3) 2.150(3)	N24 -H24A...N13 (3) 154.48(5)
N14 -H14A 0.880(3)	N14 ....N23 (4) 2.984(5)	H14A...N23 (4) 2.149(3)	N14 -H14A...N23 (4) 158.17(5)
N4 -H4A 0.920(2)	N4 ....O22 (5) 2.972(2)	H4A ...O22 (5) 2.067(1)	N4 -H4A ...O22 (5) 167.17(2)
N14 -H14B 0.880(2)	N14 ....O21 (5) 2.971(2)	H14B...O21 (5) 2.292(1)	N14 -H14B...O21 (5) 133.93(3)
O2 -H2A 1.022(2)	O2 ....N21 (5) 2.900(4)	H2A ...N21 (5) 1.901(3)	O2 -H2A ...N21 (5) 165.06(4)
O2 -H2B 0.986(3)	O2 ....O21 (6) 2.924(4)	H2B ...O21 (6) 1.954(3)	O2 -H2B ...O21 (6) 167.41(5)

Equivalent positions:
(0) x,y,z; (1) x-1,+y,+z; (2) -x+1,-y,-z; (3) -x,-y,-z; (4) -x+2,-y,-z+1; (5) -x+1,-y,-z+1; (6) -x,-y,-z+1

4.7.4 Structures of $[Cu_2(smr)_4]$.DMF (10) and $[Cu_2(smr)_4]$.DMSO (11)

These complexes contain dimeric copper atoms where a metallic Cu – Cu bond exists. The bond lengths and angles are for the complexes are shown in Table 4.37.

Table 4.37: Selected bond lengths [Å] and angles [°] in $[Cu_2(smr)_4]$.2DMF (10) and $[Cu_2(smr)_4]$.2DMSO (11)

Bonds	(10)	(11)	Angles	(10)	(11)
Cu–N_{sulf}	2.052(3)	2.040(5)	N_{pyr}–Cu–N_{sulf}	90	90
Cu–N_{pyr}	1.984(3)	1.998(5)	N_{pyr}–Cu–N_{pyr}	176.77(11)	178.3(3)
Cu–Cu	2.609(5)	2.614(5)	N_{sulf}–Cu–N_{sulf}	158.82(11)	161.8(3)
S–O	1.446(2)	1.444(4)	N_{pyr}–Cu–Cu	91.63(8)	90.85(14)
S(11)–N(11)	1.621(3)	1.641(5)	N_{sulf}–Cu–Cu	79.46(8)	80.90(13)
S(11)–C(15)	1.755(3)	1.754(6)	N(12)-C(11)-N(13)	123.9(3)	123.2(5)
N(11)–C(11)	1.366(4)	1.360(7)			
N(14)–C(18)	1.378(5)	1.362(8)			

Symmetry transformations used to generate equivalent atoms: #1 -x,-y+1,z #2 y-½,-x+½,-z+1½ #3 -y+½,x+½,-z+1½

The X-ray structures showed that in the complexes $[Cu_2(smr)_4]$.DMF (**10**) and $[Cu_2(smr)_4]$.DMSO (**11**) the Cu(II) atoms adopt a square pyramidal geometry arrangement and the five coordinate geometry consisted of four nitrogen atoms from the bridging sulfamerazine molecules occupying the basal plane and the other Cu(II) atom in an elongated apical site completes the coordination sphere.

The Cu–Cu distances of 2.609(5) and 2.614(2)Å respectively in the complexes (**10**) and (**11**) are longer than those found in the dinuclear copper complex of sulfamethazine [2.5412(6)Å][43] but shorter than that found in adenine complexes[45] and in $[Cu_2(stz)_4]$ [2.671(2)Å][46] (where stzH = sulfathiazole).

The Cu-N distances involving the four sulfamerazinato ligands are 1.977(3) – 2.061(3)Å in (**10**) and 2.077(2) – 2.082(2)Å in (**11**) are very similar with the values of 1.922(5) – 2.100(5)Å in $[Cu_2(stz)_4]$[46] and 2.02(1) – 2.36(1)Å in $[Cu(B\text{-}ats)(NH_3)_2]_2$[47], 1.951(6) – 2.043(6)Å in the sulfonamidic complex[48] and also in the related systems.[49,50]

The structure of the complex $[Cu_2(smr)_4]$.DMF (**10**) is shown in Figure 4.31 together with the crystallographic atom numbering scheme used.

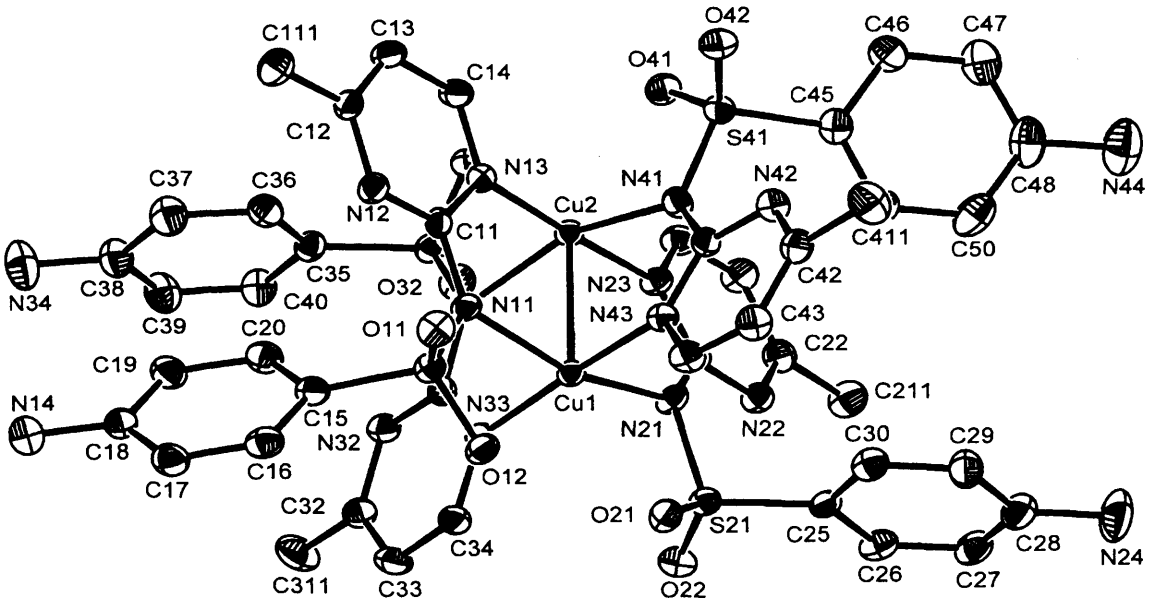

Figure 4.31
*X-ray structure of the complex $[Cu_2(smr)_4]$.DMF (**10**) showing crystallographic atom numbering scheme used. Thermal ellipsoids are drawn at 50% probability level. The ring hydrogen atoms and DMF molecules are omitted for clarity.*

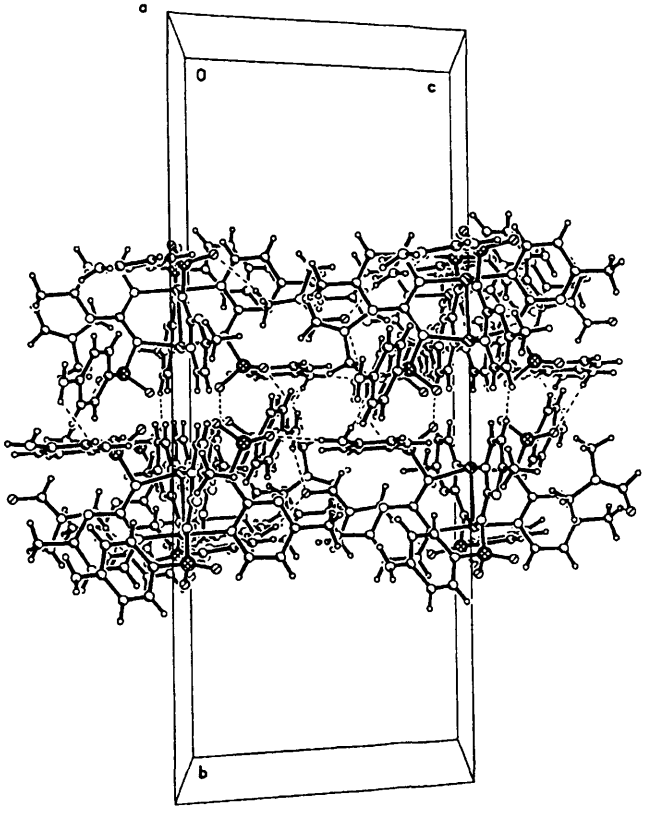

Figure 4.32
*The packing diagram of the complex $[Cu_2(smr)_4]$.2DMF (**10**) where the hydrogen bonds are shown by dashed lines.*

Table 4.38: Possible hydrogen bonds and short interactions in $[Cu_2(smr)_4]$.2DMF (10) (distances and angles given in Å and [°] respectively)

Donor-H	Donor...Acceptor	H...Acceptor	Donor-H.....Acceptor
N14 -H14A	N14 ....O2 (0)	H14A...O2 (0)	N14 -H14A...O2 (0)
0.933(5)	3.100(5)	2.247(3)	151.53(8)
N34 -H34A	N34 ....O2 (0)	H34A...O2 (0)	N34 -H34A...O2 (0)
0.940(7)	2.983(8)	2.064(8)	165.23(2)
N44 -H44A	N44 ....O1 (0)	H44A...O1 (0)	N44 -H44A...O1 (0)
0.930(9)	2.959(6)	2.137(5)	146.73(1)
N24 -H24A	N24 ....O11 (1)	H24A...O11 (1)	N24 -H24A...O11 (1)
0.926(1)	3.134(3)	2.226(9)	166.46(2)
C43 -H43	C43 ....O21 (2)	H43 ...O21 (2)	C43 -H43 ...O21 (2)
0.950(4)	3.253(8)	2.359(5)	156.53(5)
N34 -H34B	N34 ....O42 (3)	H34B...O42 (3)	N34 -H34B...O42 (3)
0.938(8)	3.024(1)	2.145(8)	155.35(3)
C23 -H23	C23 ....O31 (4)	H23 ...O31 (4)	C23 -H23 ...O31 (4)
0.950(8)	3.191(3)	2.353(2)	146.83(1)

Equivalent positions:
(0) x,y,z; (1) -x,-y,-z+1; (2) x+1,+y,+z; (3) x,-y+½,+z+½; (4) x,+y,+z-1

The crystal structure of the complex $[Cu_2(smr)_4]$.DMSO (**11**) is shown in Figure 4.33 together with the crystallographic atom numbering scheme used.

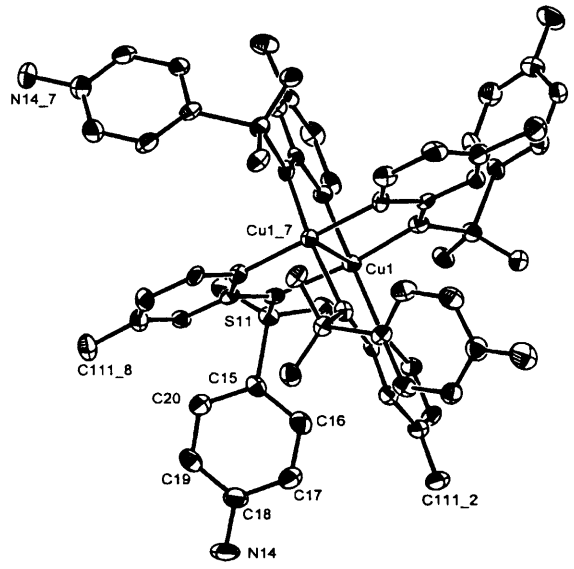

Figure 4.33
X-ray structure of the complex $[Cu_2(smr)_4]$.DMSO (11) showing crystallographic atom numbering scheme used. Thermal ellipsoids are drawn at 50% probability level. The hydrogen atoms and DMSO molecules are omitted for clarity.

Several hydrogen bonds exist in the complex (**11**), listed in Table 4.39, and in the packing diagram (Figure 4.34) these are shown by dashed lines.

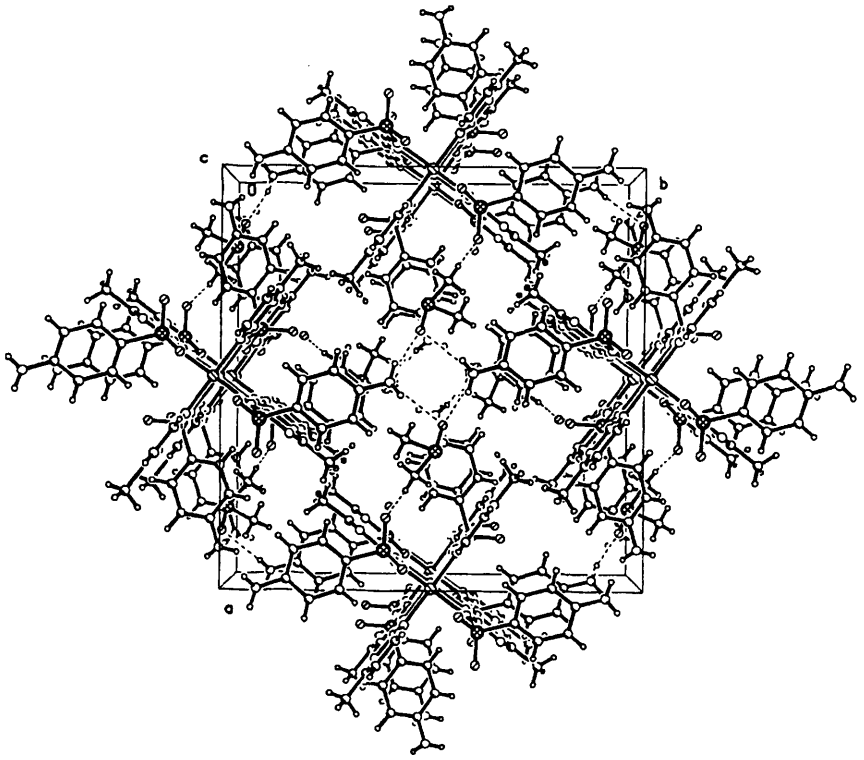

Figure 4.34
The packing diagram of the complex [$Cu_2(smr)_4$].2DMSO (11) where the hydrogen bonds are shown by dashed lines.

Table 4.39: Possible hydrogen bonds and short interactions in [$Cu_2(smr)_4$].DMSO (11) (distances and angles given in Å and deg respectively)

Donor-H	Donor...Acceptor	H...Acceptor	Donor-H.....Acceptor
N14 -H14A 0.945(3)	N14 ....O1 (1) 2.825(2)	H14A...O1 (1) 1.925(6)	N14 -H14A...O1 (1) 158.26(4)
N14 -H14B 0.938(3)	N14 ....O1 (2) 3.169(3)	H14B...O1 (2) 2.309(6)	N14 -H14B...O1 (2) 152.14(6)
C14 -H14 0.930(1)	C14 ....O11 (3) 3.320(4)	H14 ...O11 (3) 2.425(2)	C14 -H14 ...O11 (3) 161.59(2)
C2 -H2C 0.960(2)	C2 ....O12 (4) 3.351(2)	H2C ...O12 (4) 2.433(6)	C2 -H2C ...O12 (4) 159.87(3)

Equivalent positions:
(1) y-1,-x,-z+1; (2) -y,+x+1,-z+1; (3) y-½,-x+½,-z+½; (4) -y+½,+x+½,-z+½+1

The square pyramidal geometry around the Cu atoms in both the complexes is distorted showing a small variation from ideal geometry of the mutually *cis* 90° and *trans* 180°

angles. This is evident from the values of the *trans* angles vary from 158.67(11) to 176.82(11) and also from the *cis* angles which vary from 88.85(11) to 93.72(8)° in complex (**10**) and from 161.8(3) to 178.3(3) and also from the *cis* angles which vary from 89.7(2) to 90.85(14)° in complex (**11**).

The Cu-Cu bonding and their environment in both the complexes have the same arrangement and the pattern of the complex (**10**) is shown only.

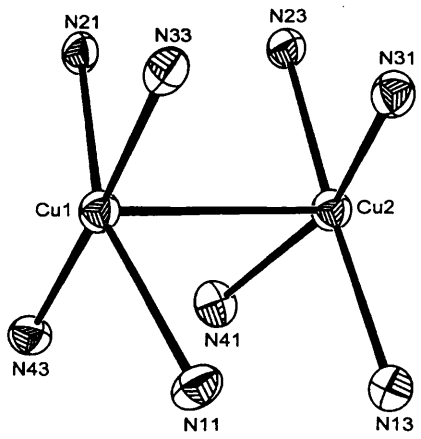

Figure 4.35
*The metal-metal bond in the complex $[Cu_2(smr)_4].2DMF$ (**10**) showing only bonded nitrogen atoms*

The interesting aspect of the present structures is the formation of a "metal-metal bond" involving two copper atoms in the complexes. The solvent DMF molecule in (**10**) and DMSO in (**11**) are attached to the complex by the formation of strong hydrogen bonds involving the terminal amino group [N(14), N(24), N(34) and N(44) atoms of $[smr]^-$ anion in (**10**) and N(14) in the complex (**11**)]. Additional hydrogen bonds and van der Waals' interactions hold the whole crystal together.

The copper atoms in the complexes bind with the sulfonamidic nitrogen atom of one sulfamerazine molecule and pyrimido nitrogen atom of the other sulfamerazine molecules, *i.e.*, the sulfonamidic nitrogen atom binds to one copper atom and at the same time the pyrimido nitrogen atom binds to other copper atom. In the complexes the sulfamerazinato anions behave as bridging ligands similar to that found in the acetate dimers such as in the compounds $[Cu_2(OCOCH_3)_4].2L$ where L is acetic acid,[51] methanol,[51] DMF,[51] water,[52] urea,[53] pyridine[54,55] and quinoline.[56] Each copper atom is surrounded by four nitrogen

atoms forming square planar geometry which are eclipsed with each other shown in Figure 4.36.

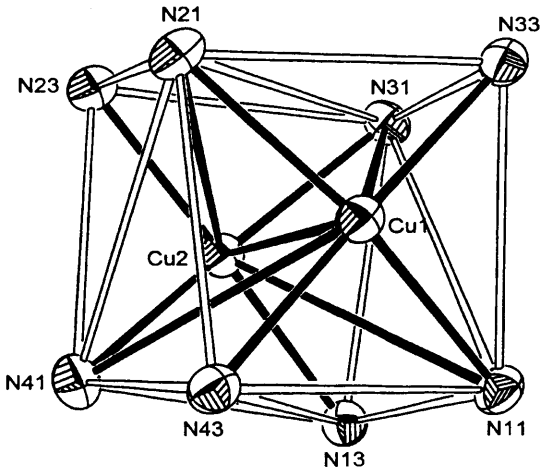

Figure 4.36
*The square planar geometries on the copper atoms are eclipsed with each other in the complex [$Cu_2(smr)_4$].2DMF (**10**)*

4.7.5 Structure of the complex [$Cu(smz)_2(apen)$].3H_2O.CH_3OH (12)

The crystal structure of the complex [$Cu(smz)_2(apen)$].3H_2O.CH_3OH (**12**) is shown in Figure 4.37 together with the crystallographic atom numbering scheme used. The selected bond lengths and angles are collected together in Table 4.40 and the dimensions of the hydrogen bonds are listed in Table 4.41.

In the complex, the [$Cu(smz)_2(apen)$] molecule has a distorted octahedral arrangement around copper(II) atom with one apen [*N,N'*(3-aminopropyl)-bis-(ethylenediamine)] molecule in which the bonds are through the four nitrogen atoms and the sulfamethazinato anions are bonded through the sulfonyl oxygen atoms.

Equatorial N4 ligation is provided by the apen molecule, while apical Cu-O bonds result from coordination of two sulfonyl oxygen atoms from sulfamethazine molecules.

The observed Cu-O bond lengths of 2.351(4) and 2.621(4)Å differ significantly; the longer length just falls within the range of 2.575 (6)-2.676 (10) A in related complexes containing CuN_4O_2 chromophores.[59]

The Cu–N(apen) distances in the present complex involving all the *N,N'*(3-aminopropyl)-bis-(ethylenediamine) ligand are similar and lie between 2.018(2) and 2.058(2)Å which are comparable with the corresponding bonds with the values 2.010(8) – 2.038(8)Å in $[Cu(apen)(ClO_4)_2].H_2O$,[57] 2.012(8) – 2.031(8)Å in $[Cu(apen)(ClO_4)].ClO_4.½H_2O$,[58] and 2.016(6)–2.032(6)Å in $[Cu(apen)(ClO_4)_2]$.[59]

Table 4.40: Bond lengths [Å] and angles (°) in $[Cu(smz)_2(apen)].3H_2O.CH_3OH$ (12)

Bond	(Å)	Bond	(Å)
Cu(1)-N(1)	2.018(5)	Cu(1)-N(4)	2.040(6)
Cu(1)-N(3)	2.044(5)	Cu(1)-N(2)	2.058(6)
Cu(1)-O(11)	2.351(4)	Cu(1)-O(21)	2.621(4)
S(11)-O(12)	1.452(5)	S(11)-O(11)	1.463(5)
S(11)-N(11)	1.575(5)	S(11)-C(15)	1.766(6)
N(11)-C(11)	1.385(8)	N(14)-C(18)	1.379(8)
S(21)-O(22)	1.457(5)	S(21)-O(21)	1.460(4)
S(21)-N(21)	1.594(5)	S(21)-C(25)	1.763(6)
N(21)-C(21)	1.370(8)	N(24)-C(28)	1.377(8)
Angle	**(°)**	**Angle**	**(°)**
N(1)-Cu(1)-N(4)	88.6(2)	N(1)-Cu(1)-N(3)	177.0(2)
N(4)-Cu(1)-N(3)	94.1(2)	N(1)-Cu(1)-N(2)	93.1(2)
N(4)-Cu(1)-N(2)	174.6(2)	N(3)-Cu(1)-N(2)	84.3(2)
N(1)-Cu(1)-O(11)	87.6(2)	N(4)-Cu(1)-O(11)	97.3(2)
N(3)-Cu(1)-O(11)	90.6(2)	N(2)-Cu(1)-O(11)	87.8(2)
O(21)-Cu(1)-O(11)	171.3(2)	O(21)-Cu(1)-N(3)	85.5(2)
O(21)-Cu(1)-N(1)	95.9(2)	O(21)-Cu(1)-N(2)	84.1(2)
N(2)-Cu(1)-O(11)	171.33(2)	O(12)-S(11)-O(11)	112.9(3)
O(12)-S(11)-N(11)	117.4(3)	O(11)-S(11)-N(11)	105.2(3)
O(12)-S(11)-C(15)	107.7(3)	O(11)-S(11)-C(15)	106.2(3)
N(11)-S(11)-C(15)	106.7(3)	S(11)-O(11)-Cu(1)	133.3(3)
N(12)-C(11)-N(13)	125.6(6)	O(22)-S(21)-O(21)	113.9(3)
O(22)-S(21)-N(21)	113.5(3)	O(21)-S(21)-N(21)	105.0(3)
O(22)-S(21)-C(25)	107.2(3)	O(21)-S(21)-C(25)	106.7(3)
N(21)-S(21)-C(25)	110.4(3)	N(22)-C(21)-N(23)	124.7(6)

The Cu–O(11) distance, involving the sulfonyl oxygen atom of the sulfamethazinato anion, of 2.351(4)Å is shorter than the second Cu–O(21) bond distance with the value of 2.621(4)Å in this complex which is comparable with the values 2.66(2)Å in $[Cu(apen)(ClO_4)_2].H_2O$,[57] 2.539(7)Å in $[Cu(apen)(ClO_4)].ClO_4.½H_2O$,[58] and 2.667(5) and 2.527(5)Å in $[Cu(apen)(ClO_4)_2]$[59] and all these complexes are bonded through the oxygen atom of the perchlorate anion. The octahedral geometry around the Cu atom is distorted with longer Cu–O bond lengths due to the Jahn-Teller effect which is also confirmed by the EPR spectroscopy.

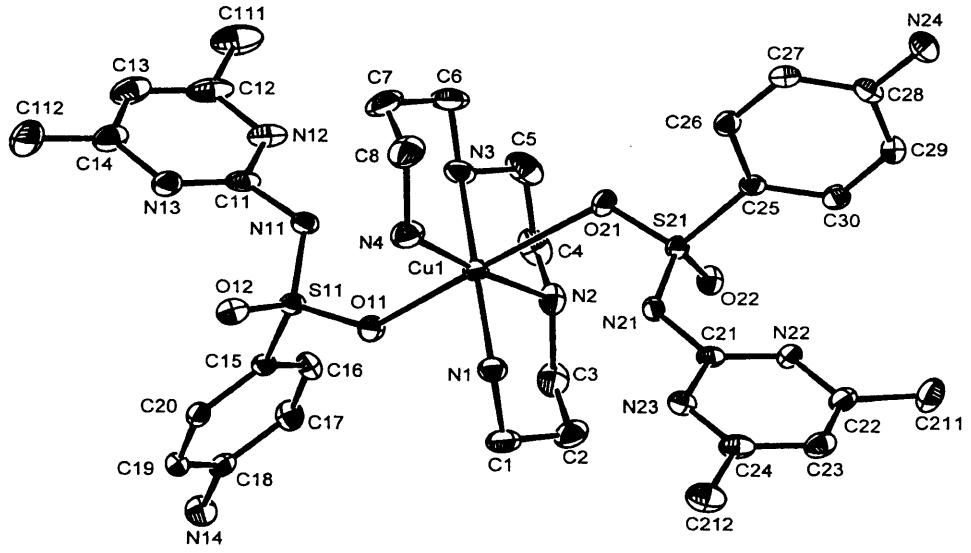

Figure 4.37
*X-ray structure of [Cu(smz)$_2$(apen)].3H$_2$O.CH$_3$OH (**12**) showing crystallographic atom numbering scheme used. Thermal ellipsoids are drawn at 50% probability level. The ring hydrogens are omitted for clarity.*

The complex forms several hydrogen bonds involving the coordinated *N,N'*(3-aminopropyl)-bis-(ethylenediamine) molecule and sulfamethazine molecule which are listed in Table 4.41.

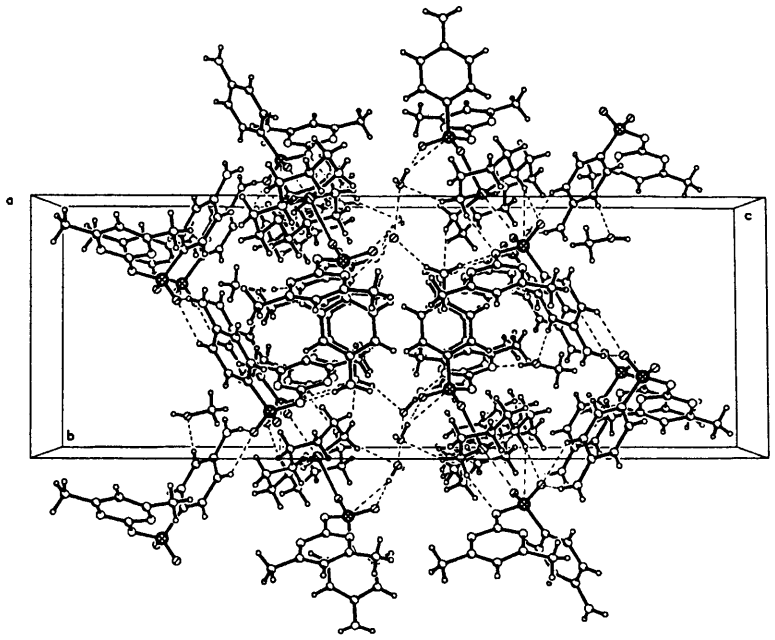

Figure 4.38
*The packing diagram of the complex [Cu(smz)$_2$(apen)].3H$_2$O.CH$_3$OH (**12**) where the hydrogen bonds are shown by dashed lines.*

Table 4.41: The hydrogen bonds in the complex $[Cu(smz)_2(apen)].3H_2O.CH_3OH$ (12) (distances and angles given in Å and deg respectively)

Donor-H	Donor...Acceptor	H...Acceptor	Donor-H.....Acceptor
N1 -H1A 0.900(1)	N1 ....O12 (0) 3.250(2)	H1A ...O12 (0) 2.448(2)	N1 -H1A ...O12 (0) 148.64(3)
O1 -H1C 0.948(2)	O1 ....O11 (0) 2.816(2)	H1C ...O11 (0) 1.941(2)	O1 -H1C ...O11 (0) 152.49(4)
N14 -H14A 0.948(2)	N14 ....N13 (1) 2.981(3)	H14A...N13 (1) 2.036(2)	N14 -H14A...N13 (1) 174.15(5)
N14 -H14B 0.864(1)	N14 ....O11 (2) 2.975(1)	H14B...O11 (2) 2.255(1)	N14 -H14B...O11 (2) 140.86(2)
N14 -H14B 0.864(1)	N14 ....N12 (2) 3.190(2)	H14B...N12 (2) 2.478(2)	N14 -H14B...N12 (2) 140.12(2)
N1 -H1B 0.900(1)	N1 ....O12 (3) 3.207(2)	H1B ...O12 (3) 2.418(1)	N1 -H1B ...O12 (3) 146.55(2)
N1 -H1B 0.900(1)	N1 ....N11 (4) 3.283(1)	H1B ...N11 (4) 2.492(1)	N1 -H1B ...N11 (4) 146.93(2)
N2 -H2A 0.900(1)	N2 ....O11 (5) 3.161(1)	H2A ...O11 (5) 2.403(1)	N2 -H2A ...O11 (5) 142.03(2)
N2 -H2B 0.900(2)	N2 ....O12 (6) 3.015(2)	H2B ...O12 (6) 2.142(1)	N2 -H2B ...O12 (6) 163.44(3)
O1 -H1D 0.983(1)	O1 ....N11 (7) 2.859(2)	H1D ...N11 (7) 1.892(2)	O1 -H1D ...N11 (7) 167.08(3)

Equivalent positions:
(0) x, y, z; (1) x-1,+y+1,+z; (2) x,+y+1,+z; (3) -x+1,-y,-z; (4) x+1,+y,+z; (5) -x,-y,-z; (6) x-1,+y,+z; (7) -x-1,-y,-z

4.7.6 Structure of the complex $\{[Cu(smz)_2(NH_3)].2H_2O\}_n$ (13)

The crystal structure of the complex $\{[Cu(smz)_2(NH_3)].2H_2O\}_n$ (**13**) is shown in Figure 4.39 together with the crystallographic atom numbering scheme used, the selected bond lengths are listed in Tables 4.42.

The copper ion in the complex exhibits a high distorted octahedral geometry, being coordinated to the two sulfonamidic [N(11)/N(21)] and two pyrimido N[(12)/(22)] nitrogen atoms of two bidentate sulfamethazine ligands generating four-membered rings. The

nitrogen atom N(14) from the terminal amino group of a third sulfamethazine, which is bonded to the adjacent Cu(II) ions, and the N(1) atom of the ammonia molecule complete the coordination sphere. Although both the ligands are bound to copper, only one sulfamethazine presents almost equivalent Cu–N bond distances [Cu(1)–N(11) and Cu(1)–N(12) are 2.044(3) and 2.035(3)Å respectively] and are comparable with the values of 2.083(13) and 2.071(11)Å in the complex $[Cu(sdz)_2(NH_3)_2]$.[32] The packing of the complex units is governed by long chains formed by the bridging sulfamethazine ligands which is bound to Cu(1) via N(21)/N(22) and Cu(2) via NH_2 [N(14)–Cu = 2.660(3)Å].

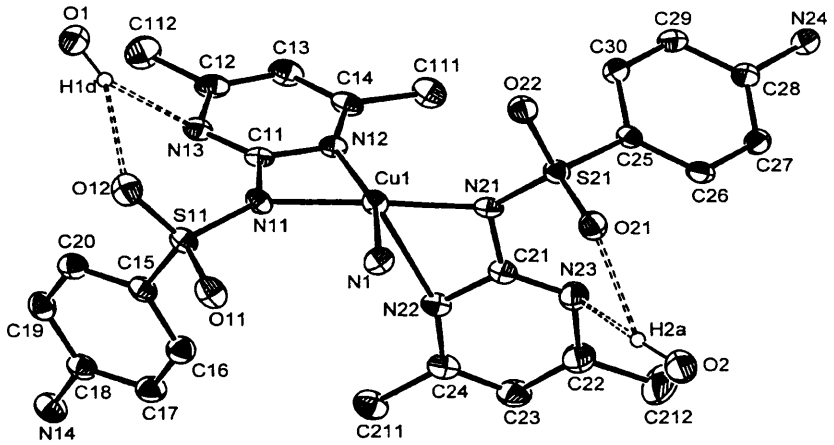

Figure 4.39
*X-ray structure of the complex $[Cu(smz)_2(NH_3)].2H_2O$ (**13**. Thermal ellipsoids are drawn at 50% probability level. The hydrogen atoms are omitted for clarity. The hydrogen bonds of water with sulfonyl oxygen and pyrimido nitrogen atoms are shown by dashed lines*

The complex $[Cu(smz)_2(NH_3)].H_2O$ (**13**) consists of an independent polymeric crystal structure of $\{[Cu(smz)_2(NH_3)].H_2O\}_n$ held together in the crystal by very strong hydrogen bonds and van der Waals' interactions shown in Figure 4.40.

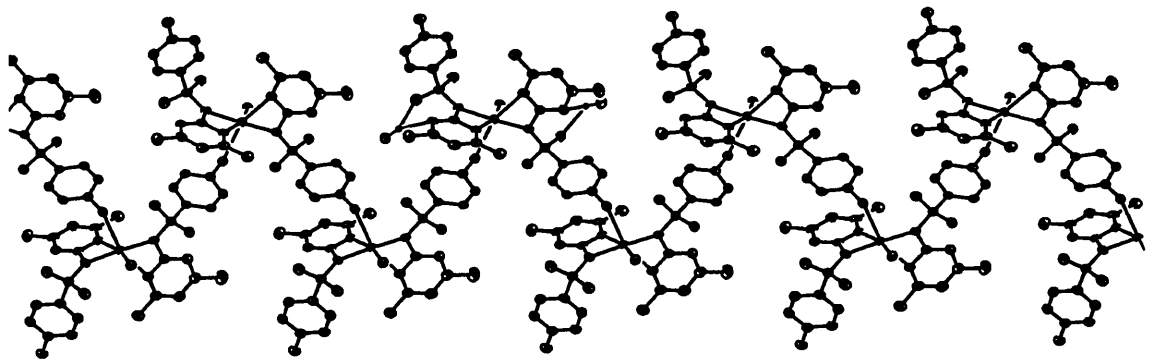

Figure 4.40

*Structure of $[Cu(smz)_2(NH_3)].2H_2O$ (**13**) in the polymeric form where cobalt ion is bonded to the terminal N(14) atom of the adjacent cobalt ion.*

Table 4.42: Selected bond lengths [Å] and angles [°] in $\{[Cu(smz)_2(NH_3)].2H_2O\}_n$ (13)

Bond	(Å)	Bond	(Å)
Cu(1)-N(1)	1.973(3)	Cu(1)-N(21)	2.007(4)
Cu(1)-N(12)	2.035(3)	Cu(1)-N(11)	2.044(3)
Cu(1)-N(22)	2.563(3)	Cu(1)-N(14′)	2.660(3)
S(11)-O(12)	1.426(3)	S(11)-O(11)	1.451(3)
S(11)-N(11)	1.603(3)	S(11)-C(15)	1.755(4)
N(11)-C(11)	1.365(5)	N(14)-C(18)	1.394(6)
S(21)-O(22)	1.441(3)	S(21)-O(21)	1.457(3)
S(21)-N(21)	1.610(4)	S(21)-C(25)	1.759(4)
N(21)-C(21)	1.393(5)	N(24)-C(28)	1.389(5)
Angle	**(°)**	**Angle**	**(°)**
N(1)-Cu(1)-N(21)	94.68(14)	N(1)-Cu(1)-N(12)	160.67(14)
N(21)-Cu(1)-N(12)	104.49(14)	N(1)-Cu(1)-N(11)	95.53(14)
N(21)-Cu(1)-N(11)	166.50(14)	N(12)-Cu(1)-N(11)	65.15(13)
N(1)-Cu(1)-N(22)	93.91(14)	N(22)-Cu(1)-N(12)	94.15(13)
N(14′)-Cu(1)-N(11)	86.11(13)	N(14′)-Cu(1)-N(22)	158.34(13)
O(12)-S(11)-O(11)	115.8(2)	O(12)-S(11)-N(11)	113.2(2)
O(11)-S(11)-N(11)	104.8(2)	O(12)-S(11)-C(15)	106.8(2)
O(11)-S(11)-C(15)	109.1(2)	N(11)-S(11)-C(15)	106.7(2)
N(12)-C(11)-N(13)	126.9(3)	N(23)-C(21)-N(22)	126.8(4)

Symmetry transformations used to generate equivalent atoms: (′) $-x, -y, z$

The Cu–N(22) distance of 2.563Å is longer than the corresponding bond with the value of 2.225(2)Å in the polymeric complex $\{Co(smz)_2(H_2O)\}.DMF$ (**3**). The N(14) atom, bonded to an adjacent copper atom to form a polymer, shows a weaker longer interaction. The N(14)–C(18) bond distance of 1.394(6)Å and the N(24)–C(28) of 1.389(7)Å are similar to each other and are also comparable with the corresponding distance in the free ligand [1.384(6)Å].

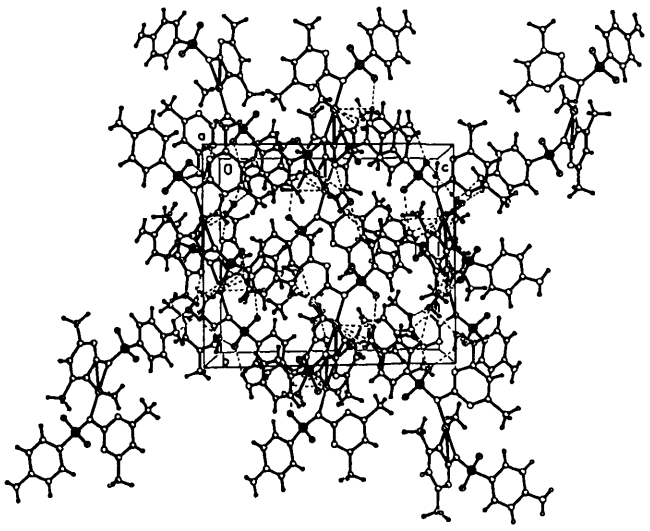

Figure 4.41
The packing diagram of the complex $[Cu(smz)_2(NH_3)].2H_2O$ (13) where the hydrogen bonds are shown by dashed lines.

In the complex unit there are hydrogen bonds between the NH_2 groups and SO_2 groups of different sulfamethazine and between SO_2 and ammonia molecules and between the lattice water molecules. The N(1)–H(1B)···O(11), O(1)–H(1E)···O(2), N(14)–H(14A)···O(21), N(24)–H(24A)···O(11) and N(24)–H(24B)···O(22) hydrogen bonds in the complex present very short donor-acceptor distances and nearly linear donor-acceptor angles, which indicate that these interactions are very strong.

Table 4.43: The hydrogen bonds in $[Cu(smz)_2(NH_3)].2H_2O$ (13) (distances and angles given in Å and deg respectively)

Donor-H	Donor...Acceptor	H...Acceptor	Donor-H.....Acceptor
N1 -H1B 0.912(1)	N1 ....O11 (0) 3.003(5)	H1B ...O11 (0) 2.121(6)	N1 -H1B ...O11 (0) 162.28(2)
O1 -H1D 0.950(3)	O1 ....N13 (0) 3.227(7)	H1D ...N13 (0) 2.355(6)	O1 -H1D ...N13 (0) 152.45(3)
O2 -H2A 0.987(4)	O2 ....O21 (0) 2.958(6)	H2A ...O21 (0) 2.280(2)	O2 -H2A ...O21 (0) 124.94(2)
O2 -H2A 0.987(4)	O2 ....N23 (0) 3.364(9)	H2A ...N23 (0) 2.480(8)	O2 -H2A ...N23 (0) 148.98(3)
N14 -H14A 0.955(5)	N14 ....O21 (1) 3.067(5)	H14A...O21 (1) 2.136(3)	N14 -H14A...O21 (1) 164.64(3)
N24 -H24B 0.924(1)	N24 ....O22 (2) 2.899(7)	H24B...O22 (2) 1.996(9)	N24 -H24B...O22 (2) 165.01(2)
N1 -H1C 0.890(7)	N1 ....O12 (4) 2.940(9)	H1C ...O12 (4) 2.102(6)	N1 -H1C ...O12 (4) 156.39(4)
O1 -H1E 0.959(3)	O1 ....O2 (5) 2.865(5)	H1E ...O2 (5) 1.910(4)	O1 -H1E ...O2 (5) 173.09(3)
O2 -H2B 0.966(9)	O2 ....O21 (6) 3.087(2)	H2B ...O21 (6) 2.171(7)	O2 -H2B ...O21 (6) 157.93(8)
N14 -H14B 0.999(5)	N14 ....O1 (7) 3.142(9)	H14B...O1 (7) 2.386(7)	N14 -H14B...O1 (7) 131.81(4)
N24 -H24A 0.881(6)	N24 ....O11 (8) 3.054(9)	H24A...O11 (8) 2.239(7)	N24 -H24A...O11 (8) 153.92(4)

Equivalent positions:
(0) x,y,z; (1) x+½,-y+½,+z+½; (2) -x+½,+y+½,-z+½; (3) -x+½,+y+½,-z+½+1; (4) -x,-y,-z+1; (5) x,+y-1,+z; (6) -x,-y+1,-z+1; (7) x+½,-y-½,+z+½; (8) x+½,-y+½,+z-½

4.8 Structure of the zinc complexes

The compounds $[Zn(smz)_2(NH_3)_2]$ (**14**) and $[Zn(smz)_2(py)_2].2py$ (**15**) are new complexes and have been characterised by independent analytical and spectroscopic data and also by X-ray diffraction methods. The crystal data and refinement details for the complexes (**14**) and (**15**) are summarized in Table 4.44.

Table 4.44: Crystal data and details of data collection and structure refinement for $[Zn(smz)_2(NH_3)_2]$ (14) and $[Zn(smz)_2(py)_2].2py$ (15)

	(14)	(15)
Empirical formula	$C_{24}H_{32}N_{10}O_4S_2Zn$	$C_{44}H_{46}N_{12}O_4S_2Zn$
Formula weight	654.09	880.59
Crystal system	Monoclinic	Monoclinic
Space group	$P2_1/c$	$C2/c$
a (Å)	37.6123(14)	9.45300(10)
b (Å)	6.2170(2)	12.34560(10)
c (Å)	25.4271(11)	34.7476(5)
β (°)	90.148(3)	90.8372(4)
V (Å^3)	5945.7(4)	4054.71(8)
Z	4	4
Crystal size/mm	0.15 × 0.12 × 0.10	0.18 × 0.15 × 0.12
θ-Range for data collection (°)	3.20 – 27.58	2.94 – 27.71
Reflections collected	11621	30461
Unique reflections	6197	9033
R_{int}	0.0609	0.0572
Index ranges	−22<=h<=48 −7<=k<=7 −32<=l<=33	−12<=h<=11 −15<=k<=15 −44<=l<=45
Data/parameters in the refinement	6197/414	9033/558
Goodness-of-fit on F^2	1.066	1.058
Final R indices [$I > 2\sigma(I)$]	0.0689/0.1720	0.0479/0.1179
R indices (all data)	0.1131/0.2001	0.0706/0.1368
Largest diff. peak and hole (e. Å^{-3})	1.876 and −0.821	1.025 and −0.498

4.8.1 Structure of the complex $[Zn(smz)_2(NH_3)_2]$ (14)

The crystal structure of the complex $[Zn(smz)_2(NH_3)_2]$ (**14**) is shown in Figure 4.42 together with the crystallographic atom numbering scheme used. The selected bond lengths and angles, and the possible hydrogen bond dimensions are given in Tables 4.45 and 4.46 respectively.

The complex (**14**) consists of the independent crystal structure of $[Zn(smz)_2(NH_3)_2]$ only and is held together in the crystal by very strong intermolecular hydrogen bonds and van

der Waals' interactions. The zinc ion is four coordinated and is bound to two nitrogen [N(11)/N(21)] atoms from two sulfamethazine ligands and two nitrogen [N(1)/N(2)] atoms from two ammonia molecules.

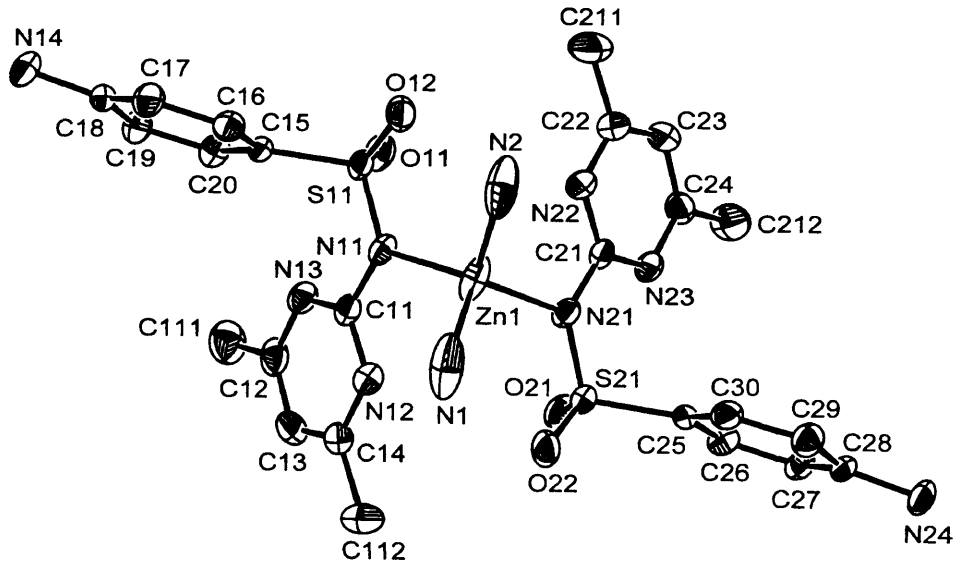

Figure 4.42
*X-ray structure of the complex $[Zn(smz)_2(NH_3)_2]$ (**14**) showing crystallographic atom numbering scheme used. Thermal ellipsoids are drawn at 50% probability level. The hydrogen atoms are omitted for clarity.*

Table 4.45: Selected bond lengths [Å] and angles [deg] in $[Zn(smz)_2(NH_3)_2]$ (14)

Bond	(Å)	Bond	(Å)
Zn(1)-N(1)	2.019(5)	Zn(1)-N(21)	2.036(3)
Zn(1)-N(2)	2.041(5)	Zn(1)-N(11)	2.045(3)
S(11)-O(12)	1.446(3)	S(11)-O(11)	1.450(3)
S(11)-N(11)	1.602(3)	S(11)-C(15)	1.765(4)
S(21)-O(22)	1.443(3)	S(21)-O(21)	1.446(3)
S(21)-N(21)	1.605(3)	S(21)-C(25)	1.761(4)
N(11)-C(11)	1.395(5)	N(14)-C(18)	1.398(5)
N(21)-C(21)	1.378(5)	N(24)-C(28)	1.390(5)
Angle	**(°)**	**Angle**	**(°)**
N(1)-Zn(1)-N(21)	110.1(2)	N(1)-Zn(1)-N(2)	100.1(3)
N(21)-Zn(1)-N(2)	114.2(2)	N(1)-Zn(1)-N(11)	113.2(2)
N(21)-Zn(1)-N(11)	108.7(2)	N(2)-Zn(1)-N(11)	110.4(2)
O(12)-S(11)-O(11)	114.6(2)	O(12)-S(11)-N(11)	105.9(2)
O(11)-S(11)-N(11)	112.6(2)	O(12)-S(11)-C(15)	106.9(2)
O(11)-S(11)-C(15)	107.4(2)	N(11)-S(11)-C(15)	109.3(2)
O(22)-S(21)-O(21)	115.4(2)	O(22)-S(21)-N(21)	105.0(2)
O(21)-S(21)-N(21)	112.7(2)	O(22)-S(21)-C(25)	107.1(2)
O(21)-S(21)-C(25)	107.6(2)	N(21)-S(21)-C(25)	108.8(2)
N(13)-C(11)-N(12)	126.6(4)	N(22)-C(21)-N(23)	125.3(4)

The geometry of the zinc complex (**14**) is tetrahedral with four nitrogen atoms. Both the ammonia and sulfamethazine molecules are bound to zinc, two Zn–N bonds are almost equivalent. The bond distances for the complex $[Zn(smz)_2(NH_3)_2]$ (**14**), Zn–N(amm) of 2.019(5) and 2.041(5)Å are comparable with the corresponding distances of 2.022(7) and 2.071(9)Å in the zinc tetrahedral complex $[Zn(sdz)_2(NH_3)_2]$[60] and 2.036(4) and 2.050(4)Å in the same complex $[Zn(sdz)_2(NH_3)_2]$[61] and the Zn–N(smz) distances of 2.045(3) and 2.036(3)Å, are also in good agreement with the distances of 2.087(8) and 2.100(6)Å in the complex $[Zn(sdz)_2(NH_3)_2]$[60] and 2.078(4) and 2.166(4)Å in the same complex $[Zn(sdz)_2(NH_3)_2]$[61], 2.017(3) and 2.060(2)Å in the complex $[Zn(sdz)_2]$[62] and 1.998(3)Å in the complex $Zn(L^{pr})$[63] (where $L^{pr}H$ is *N-n*-propylsacyaldimine).

There are several hydrogen bonds in the complex which are shown by dashed lines in the packing diagram shown in Figure 4.43.

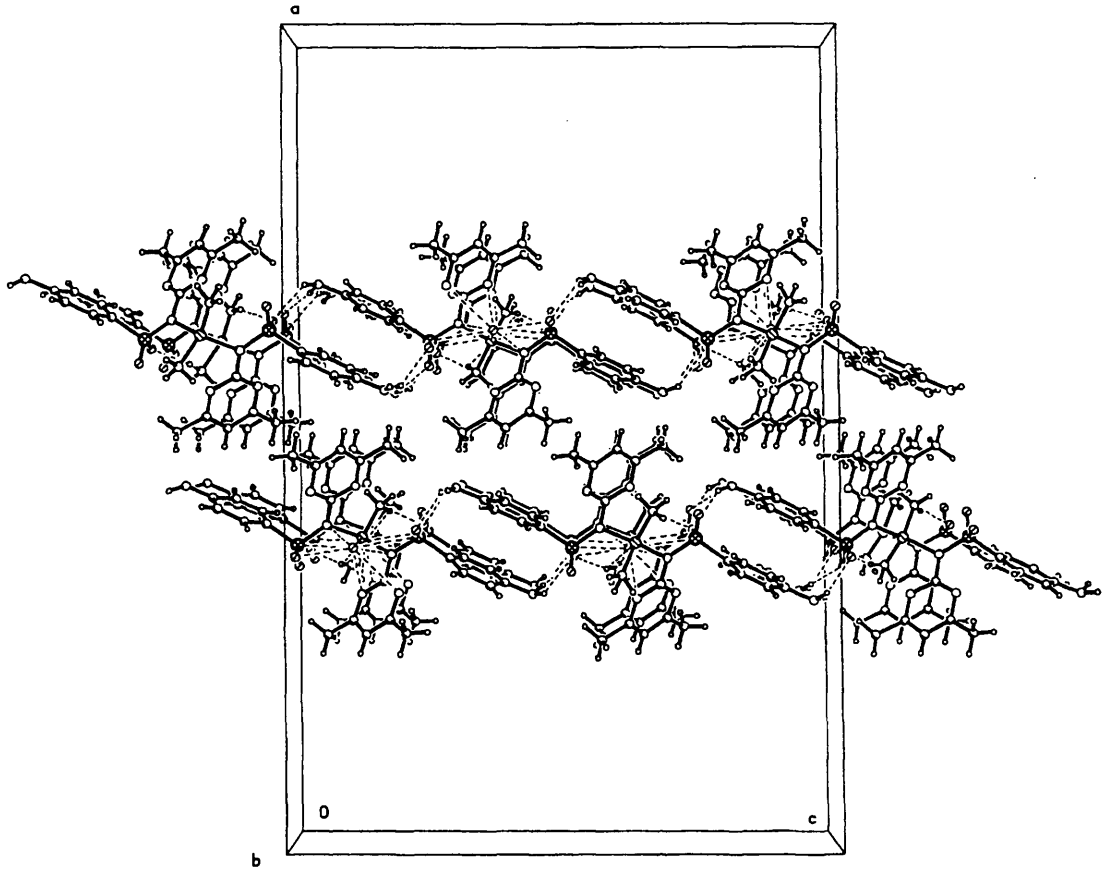

Figure 4.43
*Packing diagram of the complex $[Zn(smz)_2(NH_3)_2]$ (**14**) where the hydrogen bonds are shown by dashed lines*

Table 4.46: Possible hydrogen bonds in $[Zn(smz)_2(NH_3)_2]$ (14) (distances and angles given in Å and deg respectively)

Donor-H	Donor...Acceptor	H...Acceptor	Donor-H.....Acceptor
N1 -H1C 0.948(4)	N1 ...N12 (0) 3.011(7)	H1C ...N12 (0) 2.411(5)	N1 -H1C ...N12 (0) 120.98(3)
N2 -H2A 0.949(7)	N2 ...O12 (0) 2.920(6)	H2A ...O12 (0) 2.222(7)	N2 -H2A ...O12 (0) 129.63(6)
N14 -H14A 0.948(4)	N14 ...O21 (1) 3.194(5)	H14A ...O21 (1) 2.458(5)	N14 -H14A ...O21 (1) 134.30(3)
N14 -H14B 0.949(5)	N14 ...O22 (2) 3.008(5)	H14B ...O22 (2) 2.087(6)	N14 -H14B ...O22 (2) 163.45(4)
N24 -H24A 0.949(4)	N24 ...O12 (3) 3.075(5)	H24A ...O12 (3) 2.215(5)	N24 -H24A ...O12 (3) 150.19(3)
N24 -H24B 0.950(5)	N24 ...O11 (4) 3.230(5)	H24B ...O11 (4) 2.390(7)	N24 -H24B ...O11 (4) 147.22(5)
N1 -H1B 0.950(5)	N1 ...O21 (6) 2.964(6)	H1B ...O21 (6) 2.047(6)	N1 -H1B ...O21 (6) 161.66(4)
N2 -H2B 0.949(4)	N2 ...O11 (6) 2.933(6)	H2B ...O11 (6) 2.027(5)	N2 -H2B ...O11 (6) 159.12(4)
N1 -H1A 0.950(7)	N1 ...N13 (6) 3.434(7)	H1A ...N13 (6) 2.506(7)	N1 -H1A ...N13 (6) 165.69(5)

Equivalent positions:
(0) x, y, z; (1) x,-y+1,+z-½; (2) x,-y,+z-½; (3) x,-y,+z+½; (4) x,-y+1,+z+½; (5) x,+y-1,+z

4.8.2 Structure of the complex $[Zn(smz)_2(py)_2].2py$ (15)

The crystal structure of the complex $[Zn(smz)_2(py)_2].2py$ (**15**) is shown in Figure 4.44 together with the crystallographic atom numbering scheme used. The selected bond lengths and angles are given in Table 4.47 and the possible hydrogen bond dimensions and short interactions are given in Table 4.48.

The zinc ion lies on a two-fold axis in the complex and exhibits a highly distorted octahedral geometry, being coordinated to the sulfonamidic [N(11)] and pyrimido [N(12)] nitrogen atoms of two bidentate sulfamethazine ligands generating four-member rings. The nitrogen atoms N(1) from the pyridine molecules complete the coordination sphere. The octahedral geometry is highly distorted since the pyridine molecules lie on one side and the two larger sulfamethazine molecules lie on the other

The two Zn–N bonds are almost equivalent, the Zn(1)–N(1) and Zn(1)–N(11) bond distances of 2.108(3) and 2.122(3)Å respectively are very similar to those found in the previous complex $[Zn(smz)_2(NH_3)_2]$ (**14**) and are in good agreement of the bond lengths in the tetrahedral complex $[Zn(sdz)_2(NH_3)_2]$[61,62] but the Zn(1)–N(12) bond distance of 2.324(3)Å is longer indicating weak interaction.

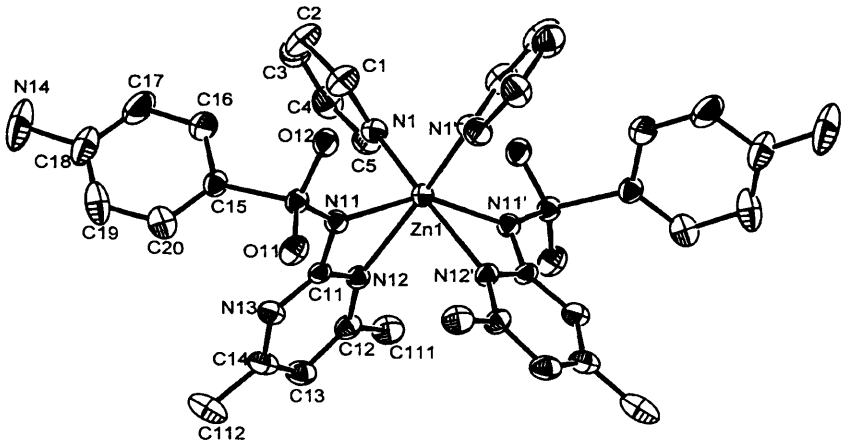

Figure 4.44
X-ray structure of the complex [Zn(smz)$_2$(py)$_2$].2py (15) showing crystallographic atom numbering scheme used. Thermal ellipsoids are drawn at 50% probability level. The hydrogen atoms and the lattice pyridine molecules are omitted for clarity.

Table 4.47: Selected bond lengths [Å] and angles [deg] in [Zn(smz)$_2$(py)$_2$].2py (15)

Bond	(Å)	Bond	(Å)
Zn(1)-N(1)	2.108(3)	Zn(1)-N(11)	2.122(3)
Zn(1)-N(12)	2.324(3)	S(11)-O(11)	1.443(3)
S(11)-O(12)	1.446(3)	S(11)-N(11)	1.600(3)
S(11)-C(15)	1.765(4)	N(11)-C(11)	1.367(4)
N(14)-C(18)	1.394(6)		
Angle	**(°)**	**Angle**	**(°)**
N(1)-Zn(1)-N(1′)	95.97(16)	N(1)-Zn(1)-N(11′)	106.48(11)
N(1)-Zn(1)-N(11)	95.56(11)	N(11′)-Zn(1)-N(11)	146.97(16)
N(1)-Zn(1)-N(12′)	165.75(11)	N(11)-Zn(1)-N(12′)	94.09(11)
N(1)-Zn(1)-N(12)	91.31(11)	N(1′)-Zn(1)-N(12)	165.75(11)
N(11)-Zn(1)-N(12)	60.49(10)	N(12′)-Zn(1)-N(12)	84.36(13)
O(11)-S(11)-O(12)	116.48(16)	O(11)-S(11)-N(11)	113.17(16)
O(12)-S(11)-N(11)	104.95(16)	O(11)-S(11)-C(15)	107.27(17)
O(12)-S(11)-C(15)	106.45(16)	N(11)-S(11)-C(15)	108.09(16)
N(13)-C(11)-N(12)	125.8(3)		

Symmetry transformations used to generate equivalent atoms: (′) $-x+1$, y, $-z+½$

The Zn–N(py) bond distance of 2.108(3)Å is shorter than the corresponding distance found in the complex $[Zn(smpz)_2(py)_2]$[43] (2.1841(17)Å) and is in agreement with the bond

distance of 2.079(9)Å in $[[Zn(S_2CNMe)_2(py)_2]$[64], 2.116(3) and 2.134(3)Å in $[Zn(Py)(chxn(Cl\text{-}sal)_2)]$[65] and 2.104(8) and 2.081(8)Å in the complex $[Zn(Py)(chxn(Br\text{-}sal)_2)]$[8] [where chxn is cyclohexanediamine and Cl-sal and Br-sal are 5-chloro- and 5-bromosalicylaldehyde respectively], 2.110(5)Å in $[Zn(TeR^1)_2(py)_2]$[66], 2.042(6) and 2.092(6)Å in $[Cr(acacen)py_2]$ $[ZnCl_3py]$[67], 2.049(3)Å in $[ZnCl_2(py)_2]$[68] and 2.13(1)Å in $[V(salen)(py)_2][ZnCl_2py]$[69] and 2.070(2)Å in $[Zn_2(C_{13}H_{22}N_3O_4)_2][ZnCl_3(py)]_2$.[70]

The complex is held together in the crystal by very strong intermolecular hydrogen bonds and van der Waals' interactions. The N(14)–H(14A)···N(1A) hydrogen bond in the complex is associated with very short donor-acceptor distance of 2.159(6)Å and nearly linear donor-acceptor angle of 161.35(7)°, indicating the very strong interaction and the packing diagram of the complex indicating the hydrogen bonds is shown in Figure 4.45.

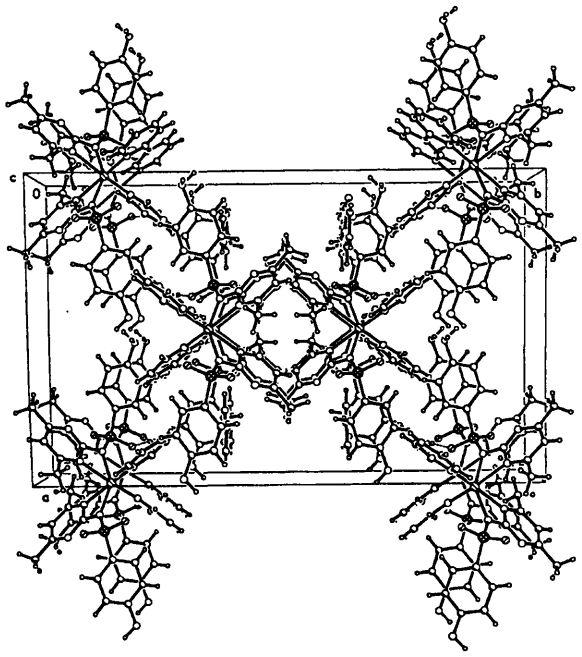

Figure 4.45
Packing diagram of the complex $[Zn(smz)_2(py)_2].2py$ (15) where the hydrogen bonds are shown by dashed lines

Table 4.48: Possible hydrogen bonds and short interactions in $[Zn(smz)_2(py)_2].2py$ (15) (distances and angles given in Å and deg respectively)

Donor-H	Donor...Acceptor	H...Acceptor	Donor-H.....Acceptor
N14 -H14A	N14 ....N1A (1)	H14A...N1A (1)	N14 -H14A...N1A (1)
0.949(5)	3.073(2)	2.159(6)	161.35(7)
C4 -H4	C4 ....O12 (2)	H4 ...O12 (2)	C4 -H4 ...O12 (2)
0.950(3)	3.409(2)	2.483(4)	164.57(9)

Equivalent positions:
(1) x+1, +y, +z; (2) x, +y, +z–1

4.9 Cadmium complexes

The crystal data and refinement details for the cadmium complexes $[Cd(sdz)_2(dien)].DMF$ (**16**), $[Cd(smr)_2(dien)].H_2O$ (**17**), $[Cd(sdz)_2(bpy)]$ (**18**), $[Cd(sdz)_2(phen)]$ (**19**), $[Cd(sdz)_2(dmbpy)].DMF$ (**20**), $[Cd(smr)_2(phen)]$ (**21**), $[Cd(smz)_2(H_2O)].DMF\}_n$ (**22**), $[Cd(smz)_2(H_2O)].2H_2O\}_n$ (**23**) and $[Cd(smz)_2(en)].DMF$ (**24**) are listed in Table 4.49.

4.9.1 Structures of the complexes (16) and (17)

The crystal structures of the complexes are shown in Figures 4.46 and 4.47 respectively for the complexes $[Cd(sdz)_2(dien)].DMF$ (**16**) and $[Cd(smr)_2(dien)].2H_2O$ (**17**). Selected bond lengths and angles for the complexes are given in Table 4.50.

The Cd(II) ions in the complexes are seven coordinate with one tridentate dien molecule and two bidentate sulfa drug molecules. The Cd–N distances involving the diethylenetriamine ligand [2.362(2), 2.389(2) and 2.373(2)Å for the complex (**16**) and 2.343(2), 2.398(2) and 2.334(2) for the complex (**17**)] are comparable with the corresponding Cd–N(dien) bond distances in the structure $[Cd_3(dien)_2(NCS)_6]_n.nH_2O$[71] with Cd–N(1) = 2.287(6), Cd–N(2) = 2.453(8) and Cd–N(3) = 2.31(2)Å, 2.340 – 2.425Å in the polymeric cluster $[Cd(dien)_2]\cdot[Cd(dien)_2]\cdot3(CN)\cdot[Cd_8(CN)_{19}]\cdot3H_2O$[72] and 2.327(5) – 2.401(4)Å in $[Cd(dien)_2]\cdot2sac$ (where sacH = saccharin).[73]

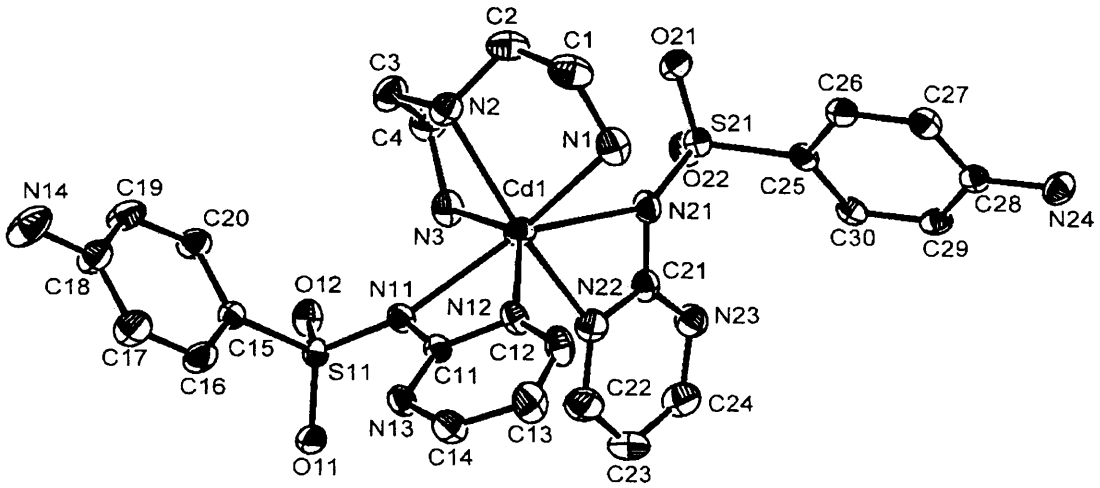

Figure 4.46
*X-ray structure of the complex $[Cd(sdz)_2(dien)].DMF$ (**16**) showing crystallographic atom numbering scheme used. Thermal ellipsoids are drawn at 50% probability level. The hydrogen atoms and DMF molecule are omitted for clarity.*

Table 4.49: Crystal data and details of data collection and structure refinement [Cd(sdz)$_2$(dien)].DMF (16), [Cd(smr)$_2$(dien)].H$_2$O (17), [Cd(sdz)$_2$(bpy)] (18), [Cd(sdz)$_2$(phen)] (19), [Cd(sdz)$_2$(dmbpy)].DMF (20), [Cd(smr)$_2$(phen)] (21), {[Cd(smz)$_2$(H$_2$O)].DMF}$_n$ (22), {[Cd(smz)$_2$(H$_2$O)].2H$_2$O}$_n$ (23) and [Cd(smz)$_2$(en)].DMF (24)

	(16)	(17)	(18)	(19)	(20)	(21)	(22)	(23)	(24)
Empirical Formula	$C_{27}H_{38}CdN_{12}O_5S_2$	$C_{26}H_{37}CdN_{11}O_5S_2$	$C_{30}H_{26}CdN_{10}O_4S_2$	$C_{32}H_{26}CdN_{10}O_4S_2$	$C_{38}H_{44}CdN_{12}O_6S_2$	$C_{34}H_{30}CdN_{10}O_4S_2$	$C_{27}H_{35}CdN_9O_6S_2$	$C_{24}H_{32}CdN_8O_7S_2$	$C_{32}H_{48}CdN_{12}O_6S_2$
Formula Weight	787.21	760.19	767.13	791.15	941.37	819.20	758.16	721.10	873.34
Crystal System	Triclinic	Triclinic	Orthorhombic	Orthorhombic	Monoclinic	Monoclinic	Monoclinic	Monoclinic	Orthorhombic
Space Group	$P\bar{1}$	$P\bar{1}$	*Pbcn*	*Pbcn*	*C2/c*	*C2/c*	P2(1)/c	$P2_1/c$	$P2_12_12$
a(Å)	8.31170(10)	8.3269(2)	16.7889(5)	16.7230(4)	17.4428(4)	19.4025(7)	16.6200(4)	15.3580(4)	11.9126(5)
b(Å)	14.2542(3)	10.8508(3)	15.5601(5)	16.0281(4)	16.2753(4)	15.6340(6)	14.6770(3)	15.0300(5)	22.7582(5)
c(Å)	14.7348(3)	18.9660(5)	11.9429(4)	11.9127(3)	16.3873(4)	11.3864(4)	13.2500(2)	13.2270(5)	7.09670(10)
α(°)	88.8394(6)	106.4840(16)	90	90	90	90	90	90	90
β(°)	76.4420(7)	90.8340(15)	90	90	118.3334(11)	97.699(2)	101.0440(8)	97.3810(14)	90
γ(°)	78.2833(11)	105.0620(9)	90	90	90	90	90	90	90
V/Å^3	2979.73 (18)	1579.53(7)	3119.93 (17)	3193.06(14)	4094.81(17)	3422.8(2)	3172.24(11)	3027.90(17)	1923.98(10)
Z	2	4	4	4	4	4	4	4	2
T/K	150	150	150	150	150	150	150	150	150
Crystal Size/mm	0.15×0.12×0.08	0.15×0.12×0.08	0.25×0.22×0.18	0.20×0.18×0.18	0.20×0.18×0.18	0.20×0.18×0.18	0.18×0.15×0.12	0.20×0.18×0.15	0.20×0.18×0.16
Shape	Block	Block	Block	Block	Block	Block	Block	Block	Block
Colour	White	White	White	White	White	White	White	White	White
θ-range for data collection	2.92 – 27.52	3.14 – 27.48	3.12 – 27.47	3.06 – 27.47	3.43 – 27.48	3.17 – 27.48	3.05 – 27.49	3.02 – 27.48	3.01 – 27.46
Reflection Collected	14955	23981	16696	32250	18995	14752	29768	20590	17156
Unique Reflections	3874	7103	3573	3653	4685	3910	7242	6895	4357
R_{int}	0.0722	0.0559	0.0827	0.0810	0.0704	0.0585	0.0839	0.0964	0.1128
Index ranges	−10<=h<=10 −18<=k<=18 −19<=l<=19	−10<=h<=10 −14<=k<=14 −23<=l<=24	−19<=h<=21 −20<=k<=20 −15<=l<=15	−21<=h<=21 −20<=k<=20 −15<=l<=14	−22<=h<=22 −20<=k<=21 −21<=l<=21	−25<=h<=24 −20<=k<=20 −12<=l<=14	−21<=h<=21 −19<=k<=19 −17<=l<=17	−19<=h<=19 −16<=k<=19 −17<=l<=14	−15<=h<=13 −29<=k<=29 −9<=l<=9
Data/parameters	3874/231	7103/437	3573/213	3653/230	4685/277	3910/227	7242/436	6895/423	4357/252
Final *R* indices [I>2σ(I)]	0.0360/0.0644	0.0388/0.0827	0.0490/0.1000	0.0358/0.0812	0.0397/0.0915	0.0420/0.0874	0.0466/0.1024	0.0545/0.1047	0.0462/0.1045
R indices (all data)	0.0508/0.0674	0.0548/0.0894	0.0781/0.1101	0.0548/0.0887	0.0531/0.0977	0.0591/0.0913	0.0784/0.1204	0.1053/0.1225	0.0575/0.1099
Largest diff. peak/hole(e.Å^{-3})	0.527 / −1.297	0.679 / −0.961	0.668 / −1.120	0.475 / −0.681	0.897 / −0.576	1.086 / −0.806	0.654 / −0.744	0.568 / −0.780	1.714 / −0.674

The Cd–N(sdz) bond distances are Cd–N(11) = 2.495(2), Cd–N(12) = 2.403(2), Cd–N(21) = 2.738(2) and Cd–N(22) = 2.317(2)Å in (**16**) and the corresponding Cd–N(smr) distances are Cd–N(11) = 2.434(2), Cd–N(13) = 2.416(2), Cd–N(21) = 2.371(2) and Cd–N(23) = 2.753(2)Å in (**17**), which are longer than the Cd–N bond distance of 2.240(2)Å in the complex $[Cd(sdz)].2H_2O$[74] where Hsdz is sulfadiazine due to the formation of a four membered ring and a high coordination number around the cadmium(II) ion. The pyrimido nitrogen N(22) in (**16**) and N(23) atom in (**17**) have a weak interaction with the cadmium ion in the complexes casing the Cd–N(pyrimido) bond distances to be longer than the others.

Table 4.50: Selected bond lengths [Å] and angles [deg] in $[Cd(sdz)_2(dien)_2].DMF$ (16) and $[Cd(smr)_2(dien)].2H_2O$ (17)

Bond	(16)	(17)	Angle	(16)	(17)
Cd(1)-N(11)	2.495(2)	2.434(2)	N(22)-Cd(1)-N(1)	109.68(8)	95.31(8)
Cd(1)-N(12)	2.403(2)	2.416(2)	N(22)-Cd(1)-N(3)	84.49(8)	136.64(8)
Cd(1)-N(21)	2.317(2)	2.371(2)	N(1)-Cd(1)-N(3)	128.00(8)	105.10(9)
Cd(1)-N(22)	2.738(2)	2.753(2)	N(22)-Cd(1)-N(2)	154.95(8)	74.73(8)
Cd(1)-N(1)	2.362(2)	2.343(2)	N(1)-Cd(1)-N(2)	74.81(8)	75.32(8)
Cd(1)-N(2)	2.389(2)	2.398(2)	N(3)-Cd(1)-N(2)	74.38(8)	74.16(8)
Cd(1)-N(3)	2.373(2)	2.334(2)	N(22)-Cd(1)-N(12)	91.99(8)	74.51(8)
S(11)-O(11)	1.446(2)	1.449(2)	N(1)-Cd(1)-N(12/13)	91.00(8)	91.90(8)
S(11)-O(12)	1.455(2)	1.450(2)	N(3)-Cd(1)-N(12/13)	139.67(7)	140.52(8)
S(11)-N(11)	1.592(2)	1.593(2)	N(2)-Cd(1)-N(12/13)	112.81(8)	145.28(7)
S(11)-C(15)	1.755(3)	1.774(3)	N(22)-Cd(1)-N(11)	97.31(8)	125.32(7)
N(11)-C(11)	1.367(3)	1.369(3)	N(1)-Cd(1)-N(11)	137.08(8)	105.91(8)
N(14)-C(18)	1.372(4)	1.376(4)	N(3)-Cd(1)-N(11)	86.17(7)	85.47(8)
S(21)-O(21)	1.447(2)	1.445(2)	N(2)-Cd(1)-N(11)	94.58(7)	159.00(8)
S(21)-O(22)	1.454(2)	1.450(2)	N(12/13)-Cd(1)-N(11)	54.37(7)	55.40(7)
S(21)-N(21)	1.588(2)	1.596(2)	N(3)-Cd(1)-N(21)	78.51(7)	96.87(9)
S(21)-C(25)	1.768(2)	1.770(3)	N(1)-Cd(1)-N(21)	73.62(7)	145.75(8)
N(21)-C(21)	1.360(3)	1.368(3)	N(13)-C(11)-N(12)	124.6(2)	125.1(2)
N(24)-C(28)	1.364(3)	1.378(4)	N(23)-C(21)-N(22)	123.8(2)	125.1(2)
			N(21)-Cd(1)-N(13)	129.04(7)	87.28(8)
			N(21)-Cd(1)-N(2)	109.36(7)	86.09(8)
			N(21)-Cd(1)-N(11)	146.52(7)	101.67(8)

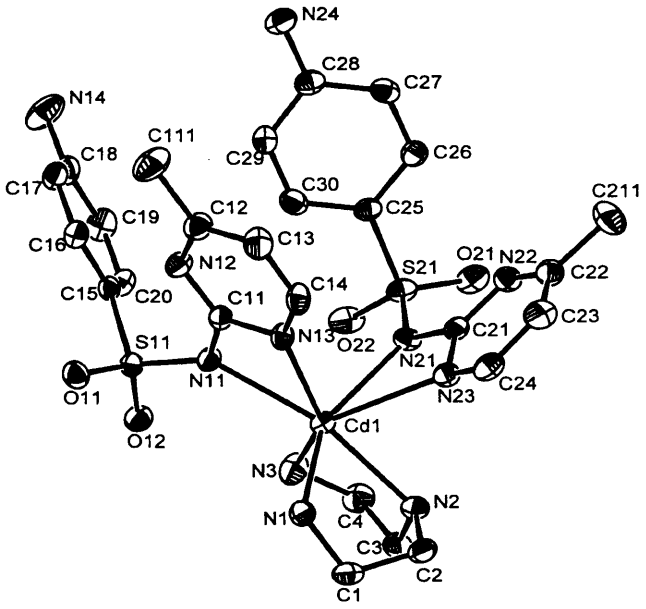

Figure 4.47
X-ray structure of [Cd(smr)$_2$(dien)].H_2O (17) showing crystallographic atom numbering scheme used. Thermal ellipsoids are drawn at 50% probability level. The hydrogen atoms and water molecule are omitted for clarity.

The geometry of the complex is highly distorted pentagonal pyramid[94] and lies between monocapped trigonal prism and monocapped octahedron. Inspecting Figure 4.48, it is observed that for a monocapped trigonal prism when N(11) is the capped N, then the close distance between N(1) and N(22) causes the deviation from the ideality. However, if we describe the coordination sphere as monocapped octahedron with N(21) as the capping N, then it is the longer distance between N(1) and N(3) which causes the deviation from ideality.

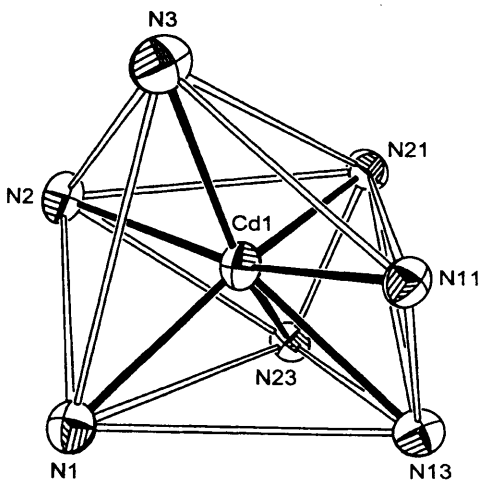

Figure 4.48
Monocapped octahedron structure of the complex [Cd(smr)$_2$(dien)].H_2O (17) containing *only the bonded nitrogen atom*

The sulfonyl ($-SO_2-$) and amino ($-NH_2$) groups of the drug molecules and amino groups of diethylenetriamine molecules appear to be hydrogen bonded with each other and also hydrogen bonded to the lattice DMF in (**16**) and water in (**17**) of the complexes. The N(14)–H(14B)...O(11), N(14)–H(14A)...O(11), N(24)–H(24A)...O(1) and N(2)–H(2A) ...N(21) hydrogen bonds shows very short donor-acceptor distances and nearly linear donor-acceptor angles, which indicate that these interactions are very strong. The packing diagram of the complexes (**16**) and (**17**) are shown in Figures 4.49 and 4.50 respectively, where the hydrogen bonds are shown by open bonds in (**16**) and dashed lines in (**17**).

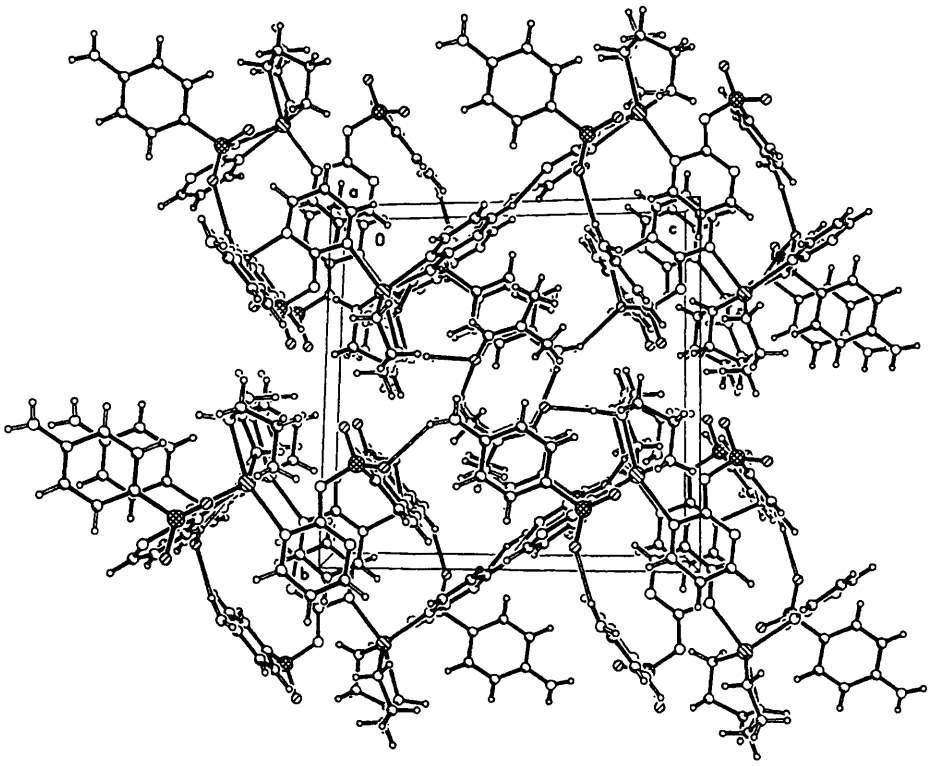

Figure 4.49
*Packing diagram of the complex [Cd(sdz)$_2$(dien)].DMF (**16**) showing the hydrogen bonds with open bonds*

The several hydrogen bonds present in the complex Cd(sdz)$_2$(dien)].DMF (**16**) are listed in Table 4.51 and are shown in the packing diagram (Figure 4.50). The hydrogen bonds are strong with short donor-acceptor distances and linearity of the bond angles.

Table 4.51: The hydrogen bonds for $Cd(sdz)_2(dien)].DMF$ (16) (distances and angles given in (Å) and (°) respectively)

Donor-H	Donor...Acceptor	H...Acceptor	Donor-H.....Acceptor
N2 -H2	N2 ....O1 (0)	H2 ...O1 (0)	N2 -H2 ...O1 (0)
1.095(.003)	2.971(.005)	1.879(.004)	175.06(0.14)
N3 -H3B	N3 ....O12 (0)	H3B ...O12 (0)	N3 -H3B ...O12 (0)
0.920(.024)	3.014(.023)	2.151(.011)	155.84(0.23)
N14 -H14A	N14 ....O1 (1)	H14A...O1 (1)	N14 -H14A...O1 (1)
0.936(.025)	3.057(.035)	2.141(.021)	165.75(0.44)
N14 -H14B	N14 ....O22 (2)	H14B...O22 (2)	N14 -H14B...O22 (2)
0.893(.003)	3.076(.005)	2.281(.003)	147.96(0.21)
N1 -H1A	N1 ....O12 (3)	H1A ...O12 (3)	N1 -H1A ...O12 (3)
0.920(.020)	3.119(.030)	2.225(.019)	163.91(0.32)
N24 -H24B	N24 ....O22 (3)	H24B...O22 (3)	N24 -H24B...O22 (3)
0.923(.024)	3.144(.027)	2.412(.015)	136.17(0.29)
N24 -H24B	N24 ....N23 (3)	H24B...N23 (3)	N24 -H24B...N23 (3)
0.923(.024)	3.179(.029)	2.379(.019)	144.77(0.23)
N24 -H24A	N24 ....O11 (4)	H24A...O11 (4)	N24 -H24A...O11 (4)
0.891(.004)	2.988(.005)	2.104(.003)	171.55(0.23)

Equivalent positions:
(0) x, y, z; (1) –x–1, –y+1, –z+1; (2) x–1,+y,+z+1; (3) x+1,+y,+z; (4) –x+1, –y, –z

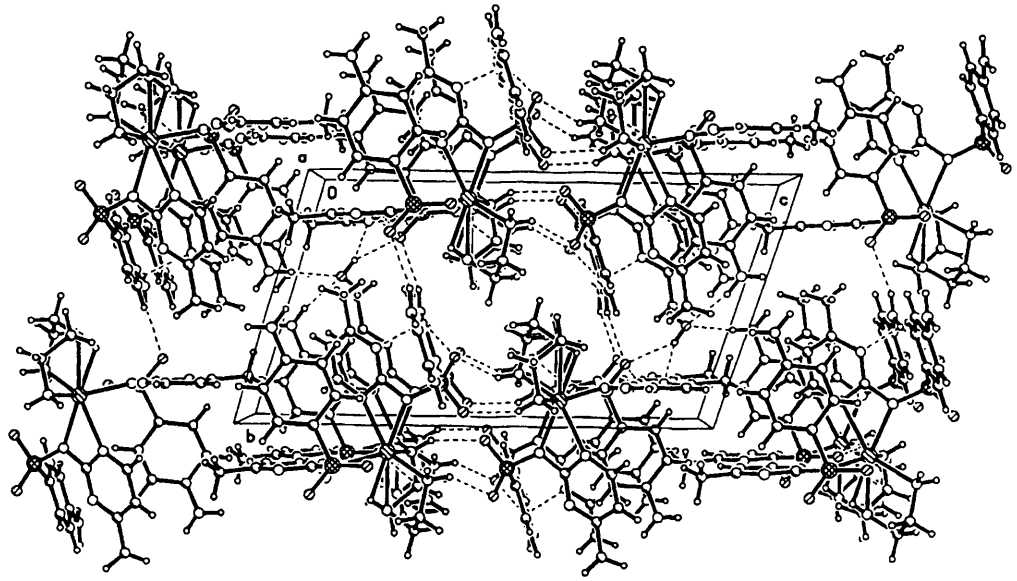

Figure 4.50
Packing diagram of the complex $[Cd(smr)_2(dien)].H_2O$ (17) showing the hydrogen bonds by dashed lines

The other hydrogen bonds present in the complex $Cd(smr)_2(dien)].H_2O$ (**16**) are listed in Table 4.51 and are shown in the packing diagram (Figure 4.51). These are strong with short donor-acceptor distances and linearity of the bond angles.

Table 4.52: Possible hydrogen bonds in $[Cd(smr)_2(dien)].H_2O$ (17) (distances and angles given in Å and deg respectively)

Donor-H	Donor...Acceptor	H...Acceptor	Donor-H.....Acceptor
N2 -H2	N2 ....N21 (0)	H2 ...N21 (0)	N2 -H2 ...N21 (0)
0.880(1)	3.256(4)	2.399(2)	164.66(4)
N24 -H24B	N24 ....O1 (1)	H24B...O1 (1)	N24 -H24B...O1 (1)
0.935(3)	3.142(3)	2.210(3)	174.48(6)
N14 -H14B	N14 ....O11 (2)	H14B...O11 (2)	N14 -H14B...O11 (2)
0.933(4)	3.230(5)	2.360(3)	154.91(6)
N24 -H24A	N24 ....O1 (3)	H24A...O1 (3)	N24 -H24A...O1 (3)
0.928(2)	3.145(3)	2.247(3)	162.75(5)
N1 -H1C	N1 ....O22 (4)	H1C ...O22 (4)	N1 -H1C ...O22 (4)
0.920(3)	3.045(5)	2.331(8)	134.21(5)
O1 -H1E	O1 ....N22 (5)	H1E ...N22 (5)	O1 -H1E ...N22 (5)
0.926(3)	3.043(4)	2.154(4)	160.49(5)
N1 -H1D	N1 ....O12 (6)	H1D ...O12 (6)	N1 -H1D ...O12 (6)
0.920(8)	3.019(8)	2.197(4)	148.46(3)
N3 -H3C	N3 ....O11 (6)	H3C ...O11 (6)	N3 -H3C ...O11 (6)
0.920(3)	3.319(4)	2.501(4)	148.32(4)

Equivalent positions:
(0) x,y,z; (1) x,+y-1,+z; (2) x+1,+y,+z; (3) -x+1,-y,-z; (4) x-1,+y,+z; (5) -x+1,-y+1,-z; (6) -x,-y,-z+1

4.9.2 Description and discussion of the complex (18), (19), (20) and (21)

Single crystals suitable for X-ray determination were obtained for the complexes $[Cd(sdz)_2(bpy)]$ (**18**), $[Cd(sdz)_2(phen)]$ (**19**), $[Cd(sdz)_2(dmbpy)]$.DMF (**20**) and $[Cd(smr)_2(phen)]$ (**21**). The bond lengths and angles are listed in Table 4.53.

Table 4.53: Selected bond lengths [Å] and angles [°] in the complexes (18) – (21)

Bonds	(18) Å	(19) Å	(20) Å	(21) Å
Cd(1)-N(11)	2.283(3)	2.275(2)	2.253(2)	2.194(2)
Cd(1)-N(12)	2.501(3)	2.517(2)	2.504(2)	2.793(2)
Cd(1–N(1)	2.313(3)	2.315(2)	2.313(2)	2.303(2)
S(11)-O(11)	1.442(3)	1.443(2)	1.444(2)	1.446(2)
S(11)-O(12)	1.443(3)	1.448(2)	1.450(2)	1.448(2)
S(11)-N(11)	1.607(3)	1.603(2)	1.606(2)	1.616(2)
S(11)-C(15)	1.759(4)	1.763(3)	1.757(3)	1.760(3)
N(11)-C(11)	1.371(5)	1.379(3)	1.371(3)	1.377(3)
N(14)-C(18)	1.358(5)	1.374(3)	1.362(4)	1.367(4)
Angle	(°)	(°)	(°)	(°)
N(11)-Cd(1)-N(12)	55.79(10)	55.69(7)	56.11(7)	52.25(9)
N(1)-Cd(1)-N(12)	88.18(11)	86.44(8)	91.24(8)	91.24(8)
N(11′)-Cd(1)-N(11)	103.49(15)	105.45(11)	116.96(11)	108.74(11)
N(11′)-Cd(1)-N(1)	110.47(11)	113.05(8)	102.86(8)	116.98(9)
N(11)-Cd(1)-N(1)	131.04(12)	125.92(8)	128.99(8)	119.31(9)
N(1)-Cd(1)-N(1′)	71.29(17)	72.28(12)	70.91(11)	72.35(13)
N(11′)-Cd(1)-N(12)	92.14(11)	91.10(8)	95.55(7)	93.00(1)
N(1′)-Cd(1)-N(12)	136.12(12)	142.01(8)	134.16(8)	148.65(9)
N(12′)-Cd(1)-N(12)	129.83(14)	126.57(10)	127.68(10)	122.54(9)
N(13)-C(11)-N(12)	125.4(4)	125.7(2)	125.6(2)	126.5(2)

Symmetry transformations used to generate equivalent atoms: (′) $-x, y, -z+½$

The geometry of the complexes [(**18**), (**19**) and (**20**)] is trigonal prismatic with the Cd atom lying on a two-fold axis which are very similar to that found in the cadmium complex $[Cd(L)(NCS)_2]$[75,95] (where L is bis-(1-pyridin-2-yl-ethylidene)-propane-1,3-diamine) which is also similar to the zinc complex $[Zn(py)_3(ch)]$[96] (where py = pyridine-2-carboxaldimino and ch = cyclohexane). In the complexes both the sulfa drug molecules are bonded to the Cd atom through the sulfonamidic nitrogen [N(11)] and the pyrimido nitrogen [N(12)/N(13)] atoms and the secondary ligands are coordinated through the nitrogen N(1) atoms.

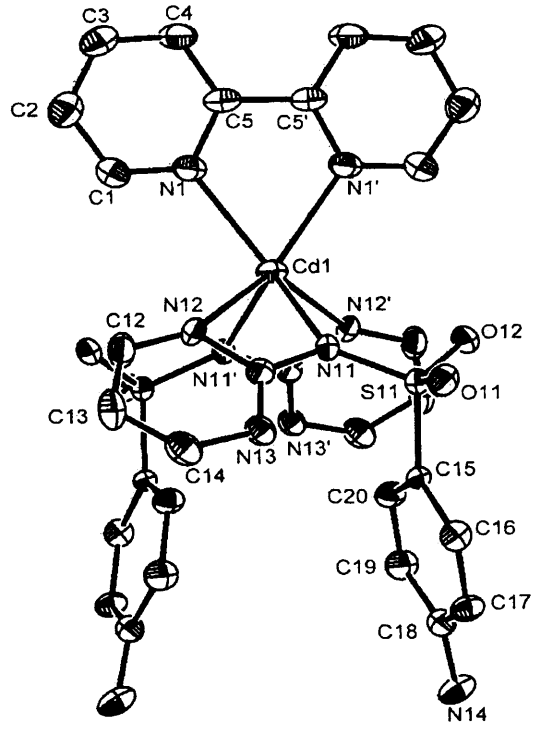

Figure 4.51
*X-ray structure of the complex [Cd(sdz)$_2$(bpy)] (**18**) showing crystallographic atom numbering scheme used. Thermal ellipsoids are drawn at 50% probability level. The ring hydrogen atoms are omitted for clarity.*

The Cd–N(1) bond distances of 2.313(3)Å in (**18**), 2.315(2)Å in (**19**), 2.313(2)Å in (**20**) and 2.303(2)Å in (**21**) are very similar with each other and are comparable with the corresponding distances of the values of 2.314(9) and 2.32(1)Å in the complex $[Cd_2(pda)(bpy)_2Cl_2]_n$[76], 2.297(3) and 2.309(2)Å in the complex $[Cd(bpy)_2(OAc)](ClO_4)\cdot nH_2O$[77], 2.325(3) and 2.352(2)Å in the complex $[Cd_2(bpy)_2(OAc)_4(H_2O)_2]$[77], 2.322(9)Å in the complex $[Cd(bpy)\{N(CN)_2\}_2]$[78] and 2.322(3) and 2.342(2)Å in the complex $[Cd(phen)\{N(CN)_2\}_2]$[78] and shorter than the corresponding values of 2.383(4) and 2.381(4)Å in the complex $[Cd(sac)_2(bpy)]$[79], 2.391(6) and 2.352(5)Å in the complex [Cd(bipy)(tsgluO)][80], 2.340(8) and 2.385(8)Å in the complex [Cd(L)(phen)][81] where L is 2-(2-mercaptophenyl)-iminophenoxy] and 2.371(4)Å in the complex [Cd(L)(phen)][82] where L is 2-[(2-methoxyphenyl)iminomethyl]-pyrrolato.

The Cd–N distances involving sulfonamidic nitrogen atoms, 2.283(3), 2.275(2), 2.253(2) and 2.194(2), are shorter than the corresponding bonds with values of 2.495(2)Å in the complex $[Cd(sdz)_2(dien)]$.DMF (**16**) and 2.434(2)Å in the complex $[Cd(sdz)_2(dien)]$.DMF (**17**) and are very similar to that of 2.240(2)Å in the complex $[Cd(sdz)_2].2H_2O$.[74]

The N(14)–H(14A)···O(12) and N(14)–H(14B)···N(13) hydrogen bonds in $[Cd(sdz)_2(bpy)]$ complex have short donor-acceptor distances and nearly linear donor-acceptor angles, indicating the interactions are very strong.

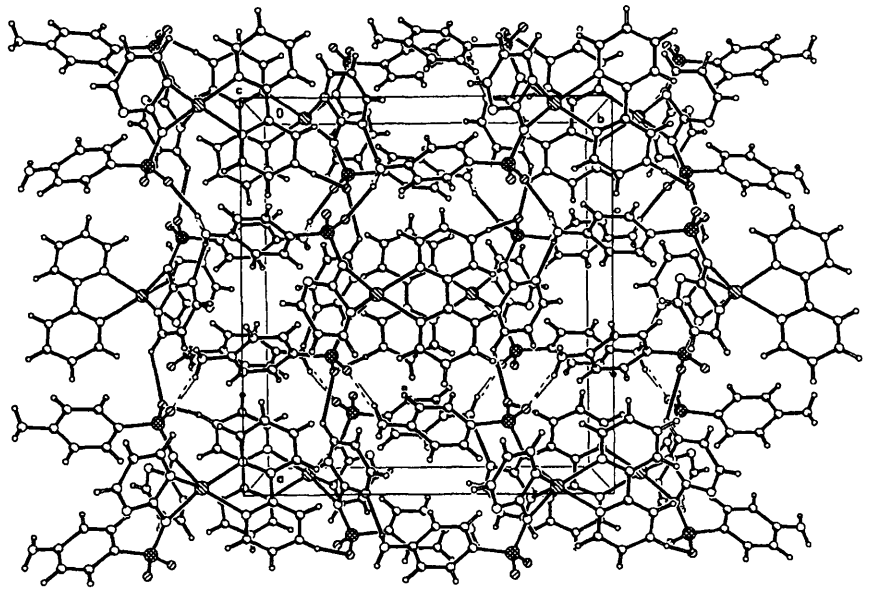

Figure 4.52
Packing diagram of the complex $[Cd(sdz)_2(bpy)]$ (18) showing the hydrogen bonds by dashed lines

Table 4.54: Possible hydrogen bonds and short interactions in $[Cd(sdz)_2(bpy)]$ (18) (distances and angles given in Å and deg respectively)

Donor-H	Donor...Acceptor	H...Acceptor	Donor-H.....Acceptor
N14 -H14A	N14 ....O12 (1)	H14A...O12 (1)	N14 -H14A...O12 (1)
0.891(1)	2.925(1)	2.068(6)	161.09(4)
N14 -H14B	N14 ....N13 (2)	H14B...N13 (2)	N14 -H14B...N13 (2)
0.930(4)	3.034(1)	2.203(7)	148.26(2)
C12 -H12	C12 ....O11 (3)	H12 ...O11 (3)	C12 -H12 ...O11 (3)
0.950(1)	3.238(2)	2.528(7)	131.59(1)
C3 -H3	C3 ....O11 (4)	H3 ...O11 (4)	C3 -H3 ...O11 (4)
0.950(6)	3.218(5)	2.379(2)	147.09(3)

Equivalent positions:
(1) $-x+½, +y+½, +z$; (2) $x, -y+1, +z-½$; (3) $x-½, -y+½, -z+1$; (4) $-x, -y, -z+1$

The crystal structure of $[Cd(sdz)_2(phen)]$ (**19**) is shown in Figure 4.54 together with the crystallographic atom numbering scheme used.

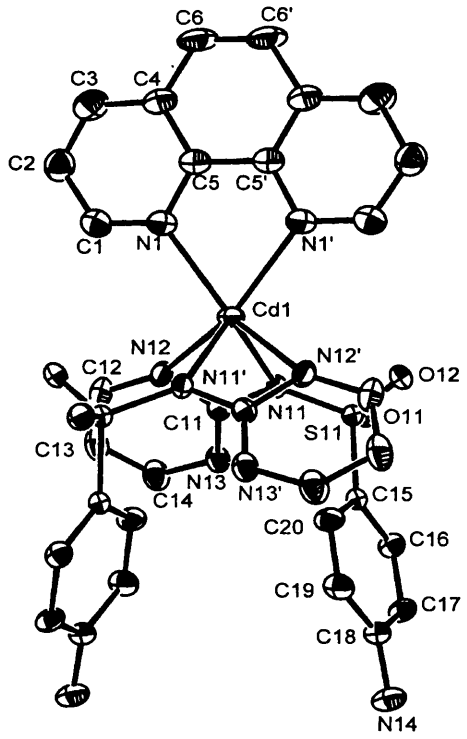

Figure 4.54
*X-ray structure of the complex $[Cd(sdz)_2(phen)]$ (**19**) showing crystallographic atom numbering scheme used. Thermal ellipsoids are drawn at 50% probability level. The hydrogen atoms are omitted for clarity.*

In addition, it is found that the complex prefers the distribution of the ligands and sulfa drug molecules in a way that the secondary ligand molecules remain on one side and two sulfa drug molecules remain on the other sides of the complexes.

The N(14)–H(14A)···O(11), N(14)–H(14B)···O(12) and N(14)–H(14A)···N(13) hydrogen bonds in $[Cd(sdz)_2(phen)]$ (**19**) complex show strong interactions because of the short donor-acceptor distances and linear angles.

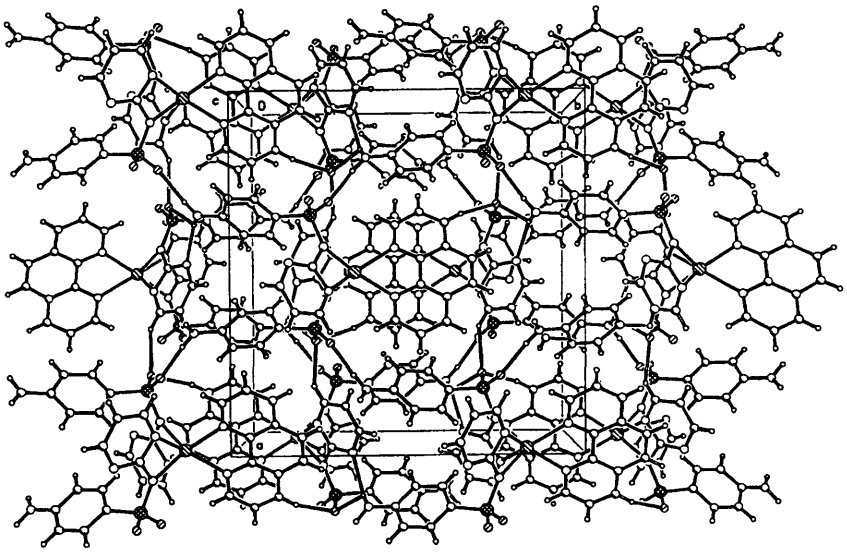

Figure 4.55
*Packing diagram of the complex [Cd(sdz)$_2$(phen)] (**19**) showing the hydrogen bonds by dashed lines*

Table 4.55: Possible hydrogen bonds and short interactions in [Cd(sdz)$_2$(phen)] (19) (distances and angles given in Å and deg respectively)

Donor-H	Donor...Acceptor	H...Acceptor	Donor-H.....Acceptor
N14 -H14A 0.946(4)	N14 ....N13 (1) 3.215(7)	H14A...N13 (1) 2.353(7)	N14 -H14A...N13 (1) 151.32(3)
N14 -H14A 0.946(4)	N14 ....O11 (1) 3.066(2)	H14A...O11 (1) 2.418(3)	N14 -H14A...O11 (1) 125.54(2)
N14 -H14B 0.947(2)	N14 ....O12 (2) 2.984(6)	H14B...O12 (2) 2.041(2)	N14 -H14B...O12 (2) 174.20(3)

Equivalent positions:
(1) x, –y+1,+z–½; (2) –x+½,+y+½,+z; (3) x–½, –y+½, –z+1; (4) –x, –y, –z+1

The crystal structure of the complex [Cd(sdz)$_2$(dmbpy)].DMF (**20**) is shown in Figure 4.56 together with the crystallographic atom numbering scheme used.

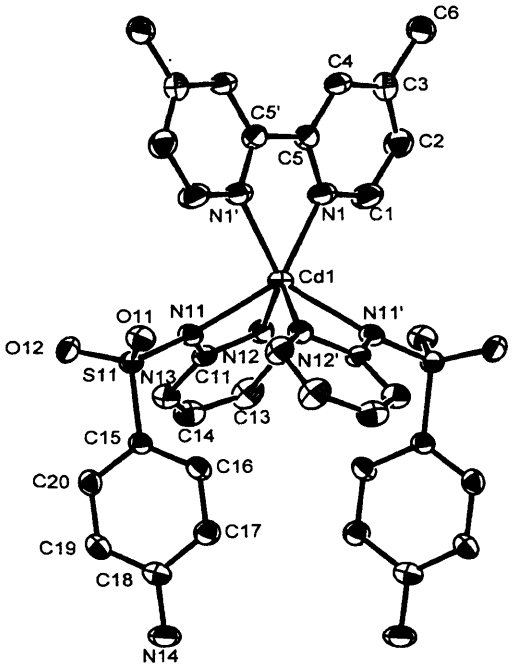

Figure 4.56

*X-ray structure of the complex [Cd(sdz)$_2$(dmbpy)].2DMF (**20**) showing crystallographic atom numbering scheme used. Thermal ellipsoids are drawn at 50% probability level. The hydrogen atoms and DMF molecules are omitted for clarity.*

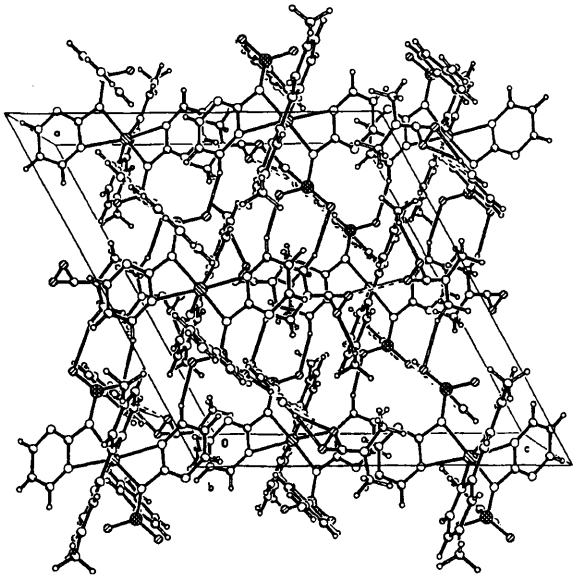

Figure 4.57
*Packing diagram of the complex [Cd(sdz)$_2$(dmbpy)].2DMF (**20**) showing the hydrogen bonds by dashed lines*

The N(14)–H(14B)···O(11), N(14)–H(14A)···O(12) and N(14)–H(14B)···O(1) hydrogen bonds in [Cd(sdz)$_2$(dmbpy)].2DMF (**20**) have very short donor-acceptor distances and nearly linear donor-acceptor angles showing the interactions are very strong.

Table 4.56: Possible hydrogen bonds and short contracts in $[Cd(sdz)_2(dmbpy)].2DMF$ (20) (distances and angles given in Å and deg respectively)

Donor-H	Donor...Acceptor	H...Acceptor	Donor-H.....Acceptor
N14 -H14A	N14 ....O12 (1)	H14A...O12 (1)	N14 -H14A...O12 (1)
0.894(.078)	2.948(.088)	2.061(.049)	171.66(0.26)
N14 -H14B	N14 ....O1'_(2)	H14B...O1'_(2)	N14 -H14B...O1'_(2)
0.886(.093)	3.044(.350)	2.161(.336)	175.19(0.63)
N14 -H14B	N14 ....O1_A(2)	H14B...O1_A(2)	N14 -H14B...O1_A(2)
0.886(.093)	2.859(.210)	2.026(.178)	156.13(0.38)
C1 -H1	C1 ....O11 (3)	H1 ...O11 (3)	C1 -H1 ...O11 (3)
0.950(.023)	3.283(.047)	2.494(.027)	140.53(0.21)
C12 -H12	C12 ....O11 (4)	H12 ...O11 (4)	C12 -H12 ...O11 (4)
0.950(.089)	3.392(.088)	2.476(.043)	161.93(0.26)

Equivalent positions:
(1) $-x+½,+y+½,-z+½$; (2) x, $-y+1,+z+½$; (3) $-x$, $+y$, $-z+½$; (4) $x-½,-y+½,+z-½$

The six coordinate cadmium complex is trigonal prismatic since the bpy molecule lies on the one part of the molecule and the two larger sulfadiazine molecules lie on the other part. It is found that the N–Cd–N chelate angles within the complex are virtually identical.

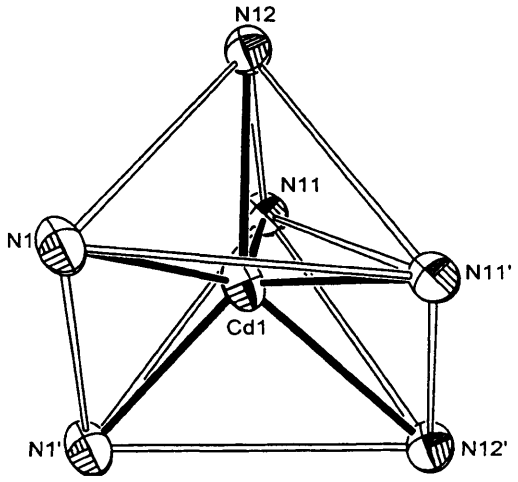

Figure 4.53
Trigonal prismatic structure of the complex $[Cd(sdz)_2(dmbpy)].2DMF$ (20) containing only nitrogen atoms

The crystal structure of $[Cd(smr)_2(phen)]$ (**21**) is shown in Figure 4.58 together with the crystallographic atom numbering scheme used. The complex shows a bicapped tetrahedral arrangement around the cadmium centre which is similar in the zinc complex[97] and hafnium complex.[98]

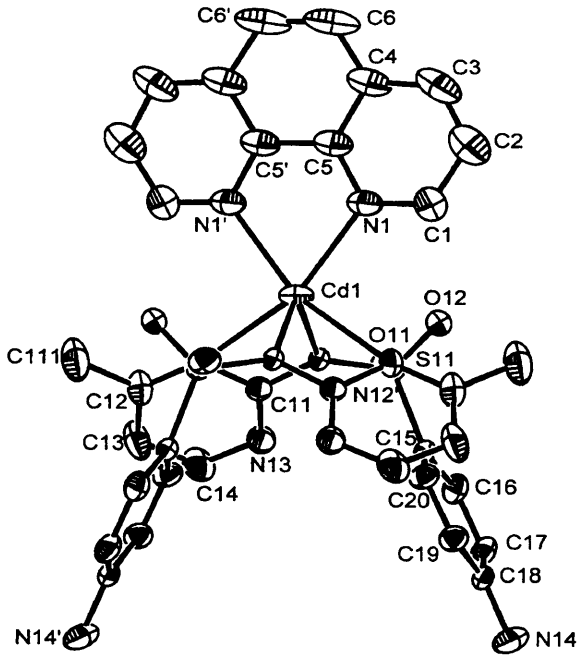

Figure 4.58
*X-ray structure of [Cd(smr)$_2$(phen)] (**21**) showing crystallographic atom numbering scheme used. Thermal ellipsoids are drawn at 50% probability level. The hydrogen atoms are omitted for clarity.*

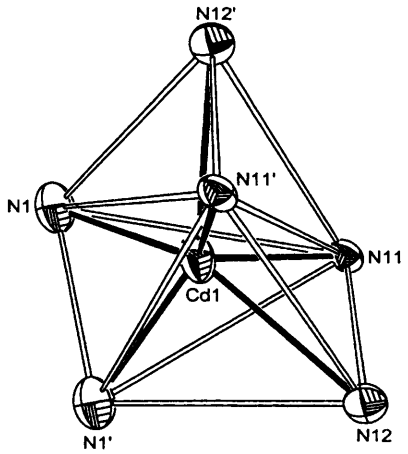

Figure 4.59
*The bicapped tetrahedral structure for the complex [Cd(smr)$_2$(phen)] (**21**) containing only the bonded nitrogen atoms*

The N(14)–H(14A)···O(11) and N(14)–H(14B)···N(13) hydrogen bonds in [Cd(smr)$_2$(phen)] show strong interactions having very short donor-acceptor distances and nearly linear donor-acceptor angles which are shown in the packing diagram (Figure 4.60). The other hydrogen bonds and short contacts of the complex [Cd(smr)$_2$(phen)] (**21**) are listed in Table 4.57.

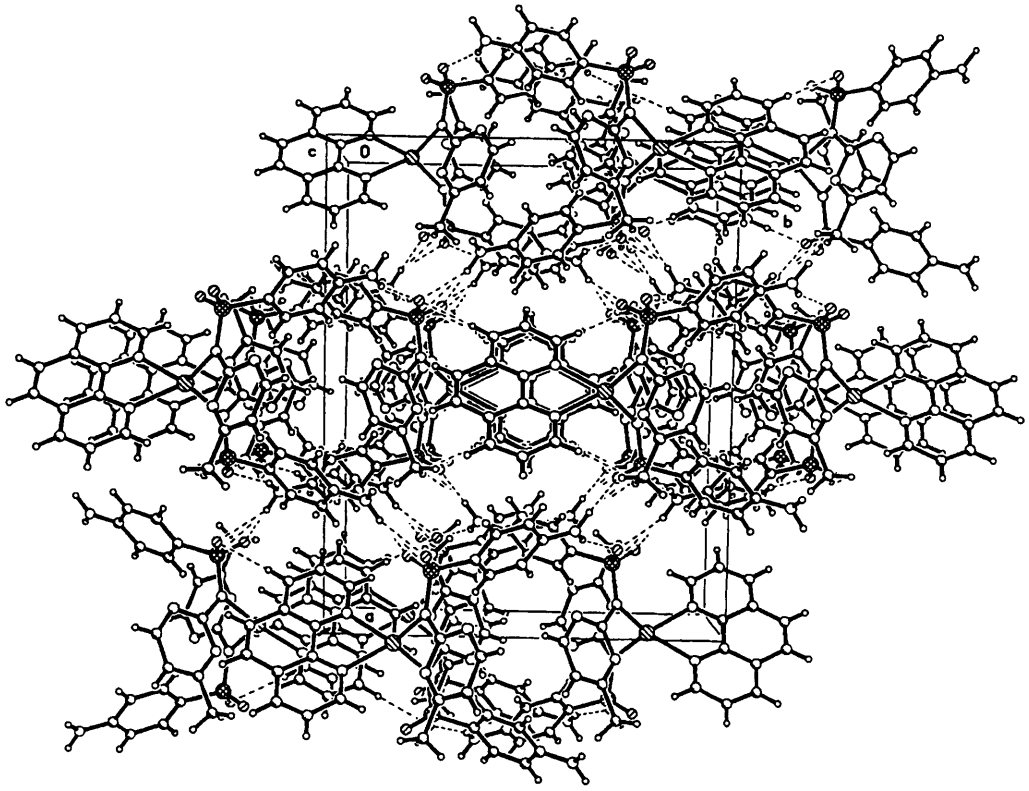

Figure 4.60
*Packing diagram of the complex [Cd(smr)$_2$(phen)] (**21**) showing the hydrogen bonds by dashed lines*

Table 4.57: Possible hydrogen bonds and short interactions in [Cd(smr)$_2$(phen)] (21) (distances and angles given in Å and deg respectively)

Donor-H	Donor...Acceptor	H...Acceptor	Donor-H.....Acceptor
N14 -H14A	N14 ....O11 (1)	H14A...O11 (1)	N14 -H14A...O11 (1)
0.950(9)	2.994(1)	2.083(9)	160.24(3)
N14 -H14B	N14 ....N13 (2)	H14B...N13 (2)	N14 -H14B...N13 (2)
0.949(7)	3.125(1)	2.381(7)	135.02(4)
N14 -H14B	N14 ....O11 (2)	H14B...O11 (2)	N14 -H14B...O11 (2)
0.949(7)	3.173(2)	2.375(7)	141.55(2)
C16 -H16	C16 ....N12 (3)	H16 ...N12 (3)	C16 -H16 ...N12 (3)
0.950(9)	3.503(1)	2.556(6)	174.33(3)
C3 -H3	C3 ....O11 (4)	H3 ...O11 (4)	C3 -H3 ...O11 (4)
0.950(7)	3.213(5)	2.375(2)	146.87(3)

Equivalent positions:
(1) -x+½,+y+½,-z+½; (2) x,-y+1,+z+½; (3) -x,+y,-z+½; (4) x,-y,+z+½

4.9.3 Crystal structure of the polymeric cadmium complexes $\{[Cd(smz)_2(H_2O)].DMF\}_n$ (22) and $\{[Cd(smz)_2(H_2O)].2H_2O\}_n$ (23)

The complexes consist of a polymeric crystal structures held together in the crystals by very strong hydrogen bonds and Van der Waals' interactions.

Table 4.58: Selected bond lengths [Å] and angles [°] in (22) and (23)

Bond	(22)[a]	(23)[b]	Angle	(22)[a]	(23)[b]
Cd(1)-N(11)	2.307(3)	2.320(3)	N(11)-Cd(1)-O(1)	86.38(11)	86.63(12)
Cd(1)-N(12)	2.407(3)	2.411(4)	N(11)-Cd(1)-N(21)	177.50(11)	171.99(12)
Cd(1)-N(21)	2.355(3)	2.337(3)	O(1)-Cd(1)-N(21)	95.61(11)	95.82(12)
Cd(1)-N(22)	2.356(3)	2.322(3)	N(11)-Cd(1)-N(22)	124.65(11)	114.80(13)
Cd(1)-O(1)	2.325(3)	2.336(3)	O(1)-Cd(1)-N(22)	90.14(11)	98.54(12)
Cd(1)-N(14)#1	2.400(3)	2.372(4)	N(21)-Cd(1)-N(22)	56.97(10)	57.33(13)
S(11)-O(11)	1.444(3)	1.448(3)	N(11)-Cd(1)-N(14)#1	91.24(11)	98.47(13)
S(11)-O(12)	1.454(3)	1.457(3)	O(1)-Cd(1)-N(14)#1	106.31(11)	95.57(13)
S(11)-N(11)	1.583(3)	1.586(4)	N(21)-Cd(1)-N(14)#1	86.75(11)	88.89(13)
S(11)-C(15)	1.770(4)	1.761(4)	N(22)-Cd(1)-N(14)#1	141.81(11)	144.40(13)
N(11)-C(11)	1.390(5)	1.382(6)	N(11)-Cd(1)-N(12)	57.01(10)	56.65(12)
N(14)-C(18)	1.425(5)	1.411(6)	O(1)-Cd(1)-N(12)	140.23(10)	143.27(12)
S(21)-O(21)	1.445(3)	1.452(3)	N(21)-Cd(1)-N(12)	121.48(11)	120.38(12)
S(21)-O(22)	1.459(3)	1.454(3)	N(22)-Cd(1)-N(12)	98.16(10)	96.29(12)
S(21)-N(21)	1.596(3)	1.597(4)	N(14)#1-Cd(1)-N(12)	90.79(10)	91.48(13)
S(21)-C(25)	1.760(4)	1.750(4)	N(13)-C(11)-N(12)	126.3(3)	126.6(4)
N(21)-C(21)	1.385(5)	1.372(6)	N(23)-C(21)-N(22)	125.8(3)	125.9(4)
N(24)-C(28)	1.383(5)	1.369(6)	C(18)-N(14)-Cd(1)#2	112.2(2)	113.9(3)

Symmetry transformations used to generate equivalent atoms:
([a]) #1 and ([b]) #2 -x+1,y+½,-z+½; ([a]) #2 and ([b]) #1 -x+1,y-½,-z+½

The cadmium ions lie on the centre of symmetry in the complexes and exhibit highly distorted octahedral geometry, being coordinated to the sulfonamidic [N(11)/N(21)] and pyrimido N[(12)/(22)] nitrogen atoms of two bidentate sulfamethazine ligands generating four-membered rings. The nitrogen atom N(14) from the terminal amino group of a third sulfamethazine, which is bonded to the adjacent Cd(II) ion, and the O(1) atom of water molecule complete the coordination sphere. Although both ligands are bound to cadmium, only one sulfamethazine presents two equivalent Cd–N bond distances [Cd(1)–N(21) and Cd(1)–N(22) are 2.355(3) and 2.356(3)Å respectively in the complex (**22**) and 2.337(3) and 2.322(3)Å respectively in the complex (**23**)]. The other Cd-N bond distances

Cd(1)–N(11) and Cd(1)–N(12) are 2.307(3) and 2.407(3)Å respectively in (**22**) and 2.320(3) and 2.411(3)Å respectively in (**22**).

The terminal N(24)–C(28) bond distance [1.383(5)Å in (**22**) and 1.369(6)Å in (**23**)] is shorter than the N(14)–C(18) bond distance [1.425(5)Å in (**22**) and 1.411(6)Å in (**23**)] which is comparable with the corresponding value of 1.413(9)Å in the polymeric complex $\{[Cd(smz)_2(H_2O)].2H_2O\}_n$[1] and 1.428(4)Å in the previous polymeric cobalt complex $\{[Co(smz)_2(H_2O)].DMF\}_n$ (**3**) and is consistent with the coordination of the terminal amino group [N(14)] to the adjacent Cd(II) ion. The packing of the complex unit is governed by a long chain formed by the bridging sulfamethazine ligand which is bound to Cd(1) via N(11)/N(12) and Cd(1)#1 via $-NH_2$ of the N(14)–Cd distances of 2.400(2)Å in (**22**) and 2.372(4)Å in (**23**) are comparable of the bond distance of 2.379(7)Å in the complex $[Cd(smz)_2(H_2O)].2H_2O$.[1] That is, one of the sulfamethazine molecules attached to the cadmium ion acts as bridging ligand with the adjacent cadmium ion of the second molecule to form the polymer. The bond lengths and angles of the phenyl rings conform to those found in the free sulfamethazine molecule.[9,10] Stacking interactions are present in the crystal structure involving phenyl and heterocyclic rings.

The asymmetric unit of the complex (**22**) is shown in Figure 4.61 together with the crystallographic atom numbering used and polymeric form is shown in Figure 4.62.

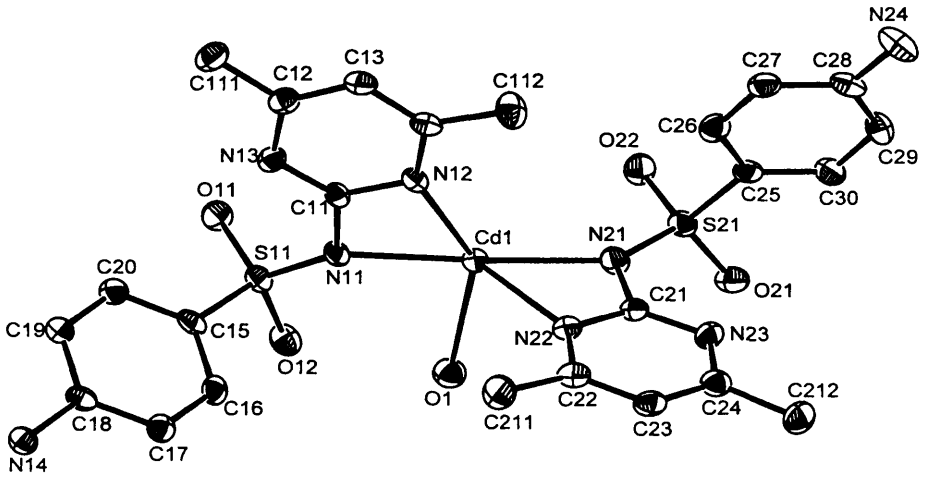

Figure 4.61
X-ray structure of $[Cd(smz)_2(H_2O)].DMF$ (22) showing crystallographic atom numbering scheme used. Thermal ellipsoids are drawn at 50% probability level. The hydrogen atoms and DMF molecule are omitted for clarity.

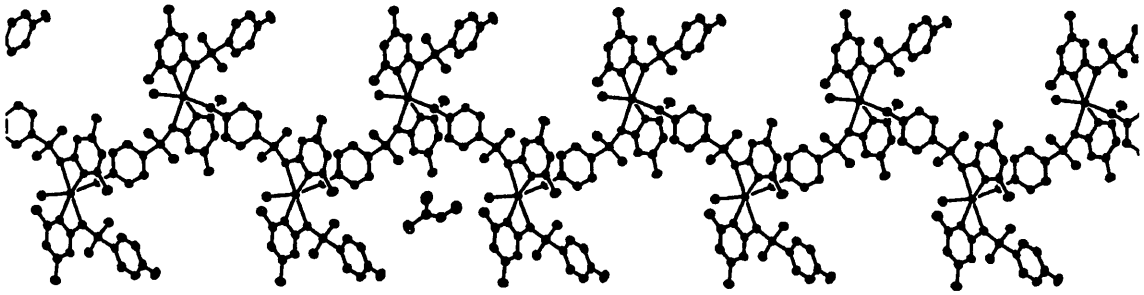

Figure 4.62

Structure of polymeric form of [Cd(smz)$_2$(H$_2$O)].DMF (22) where cobalt ion is bonded to the terminal N(14) atom of the adjacent cobalt ion.

In complex (**22**), there exist several hydrogen bonds between the electronegative elements and hydrogen atoms. The N(14)–H(14B)···O(11), N(14)–H(14A)···O(12) and N(14)–H(14B)···N(13) hydrogen bonds in the complex show very short donor-acceptor distances and nearly linear donor-acceptor angles indicating strong interactions. In the packing diagram the hydrogen bonds are shown by dashed lines (Figure 4.63).

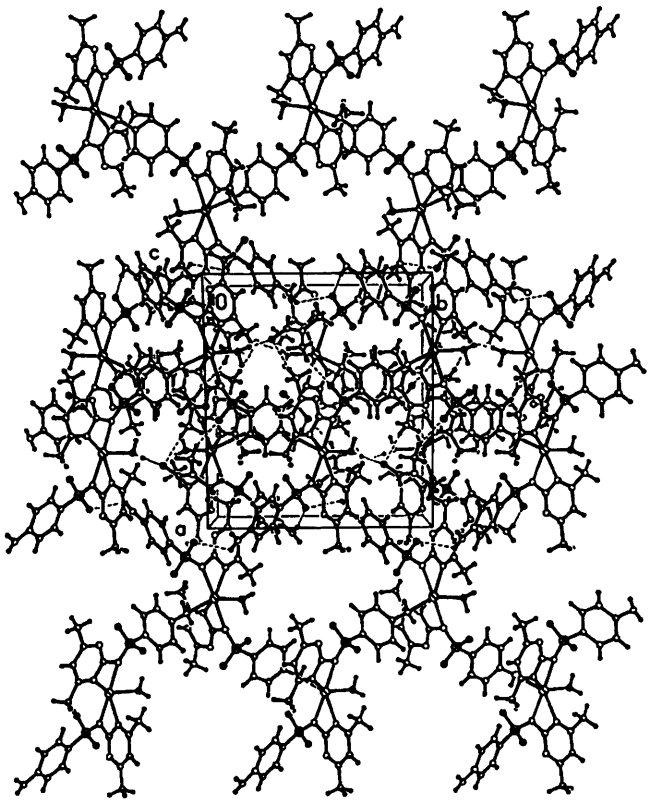

Figure 4.63

Packing diagram of the complex [Cd(smz)$_2$(H$_2$O)].DMF (22) showing the hydrogen bonds with open bonds

Table 4.59: The hydrogen bonds in $[Cd(smz)_2(H_2O)].DMF$ (22) (distances and angles given in Å and deg respectively)

Donor-H	Donor...Acceptor	H...Acceptor	Donor-H.....Acceptor
O1 -H1A 0.821(4)	O1 ...O2 (0) 2.733(5)	H1A ...O2 (0) 1.931(4)	O1 -H1A ...O2 (0) 165.58(4)
O1 -H1B 0.890(4)	O1 ...O12 (0) 2.767(4)	H1B ...O12 (0) 1.892(4)	O1 -H1B ...O12 (0) 167.28(4)
N14 -H14A 0.926(3)	N14 ...O11 (1) 2.978(4)	H14A ...O11 (1) 2.095(3)	N14 -H14A ...O11 (1) 159.18(3)
N14 -H14B 0.863(4)	N14 ...O22 (2) 2.933(4)	H14B ...O22 (2) 2.076(4)	N14 -H14B ...O22 (2) 172.49(3)
N24 -H24B 0.972(7)	N24 ...O21 (3) 3.011(5)	H24B ...O21 (3) 2.059(7)	N24 -H24B ...O21 (3) 165.95(5)

Equivalent positions:
(0) x,y,z; (1) x,-y+½,+z-½; (2) -x+1,+y-½,-z+½; (3) x,-y+½+1,+z-½

The asymmetric unit of the complex (**23**) is shown in Figure 4.64 together with the crystallographic atom numbering used and the polymeric form is shown in Figure 4.65.

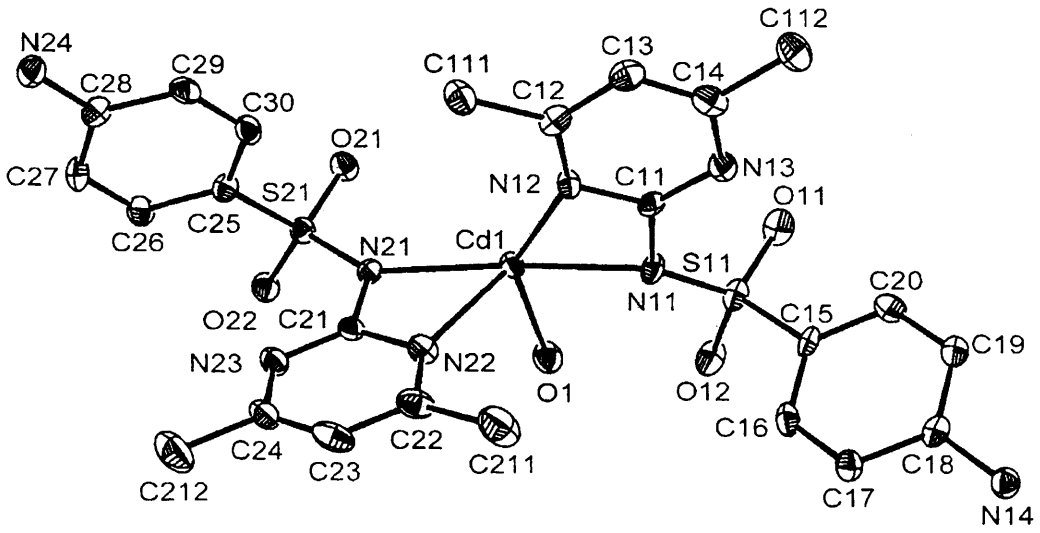

Figure 4.64
X-ray structure of $[Cd(smz)_2(H_2O)].2H_2O$ (23) showing crystallographic atom numbering scheme used. Thermal ellipsoids are drawn at 50% probability level. The hydrogen atoms and lattice water molecules are omitted for clarity.

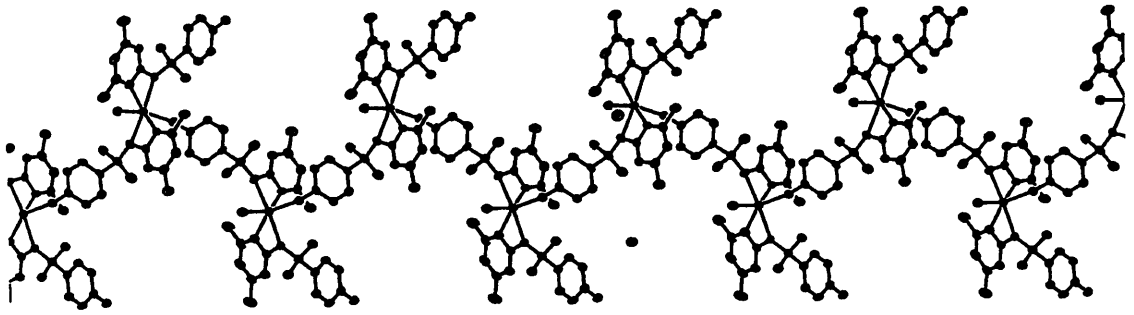

Figure 4.65
Polymeric structure of $[Cd(smz)_2(H_2O)].2H_2O$ (23) in the polymeric form where cobalt ion is bonded to the terminal N(14) atom of sulfamethazine attached to the adjacent cobalt ion.

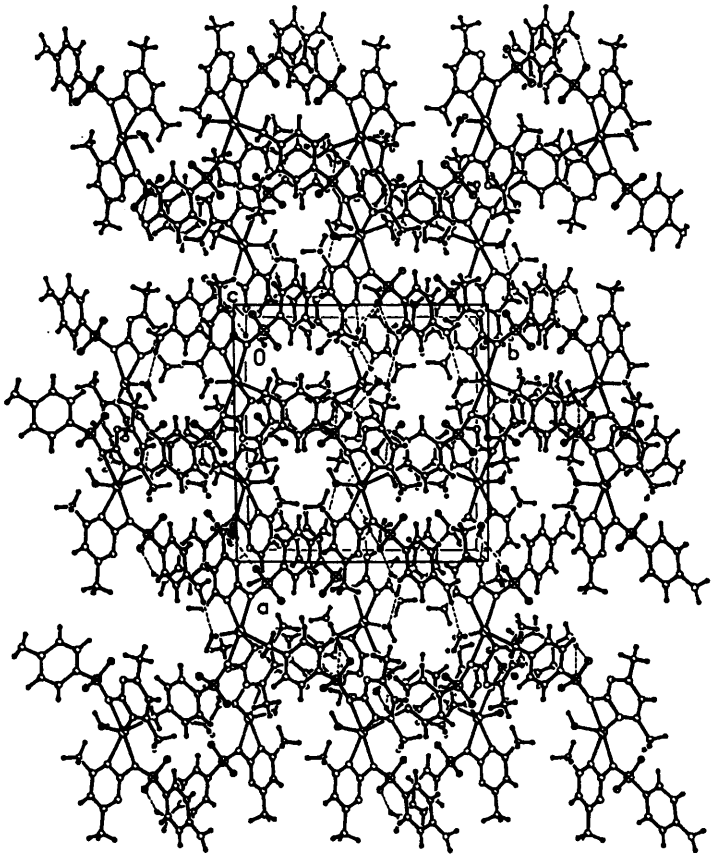

Figure 4.66
Packing diagram of the complex $[Cd(smz)_2(H_2O)].2H_2O$ (23) showing the hydrogen bonds with open bonds

In the complex the cadmium species has a distorted octahedral stereochemistry with the equatorial plane defined by two sulfonamidic nitrogen atoms [N(11) and N(21)] in *trans* position, two pyrimido nitrogen atoms [N(12) and N(22)] in *cis* position, one terminal

amino atom [N(24)] and one oxygen atom from the lattice water completing the coordination sphere. The N(14)–H(14B)···O(1), N(14)–H(14A)···O(12) and N(24)–H(24A)···O(11) hydrogen bonds and short interactions in $\{[Cd(smz)_2.H_2O].2H_2O\}_n$ are very strong with almost linear bond angles and short distances. The hydrogen bonds and short contacts are shown in packing diagram (Figure 4.66).

Table 4.60: The hydrogen bonds in $[Cd(smz)_2(H_2O)].2H_2O$ (23) (distances and angles given in Å and deg respectively)

Donor-H	Donor...Acceptor	H...Acceptor	Donor-H.....Acceptor
O1 -H1B 0.949(5)	O1 ...O22 (0) 2.750(5)	H1B ...O22 (0) 1.832(5)	O1 -H1B ...O22 (0) 161.81(4)
N14 -H14A 0.947(4)	N14 ...O12 (1) 3.076(5)	H14A ...O12 (1) 2.210(4)	N14 -H14A ...O12 (1) 151.62(3)
N14 -H14B 0.949(3)	N14 ...O1 (2) 3.098(5)	H14B ...O1 (2) 2.151(2)	N14 -H14B ...O1 (2) 175.05(2)
N24 -H24A 0.948(3)	N24 ...O11 (3) 2.946(5)	H24A ...O11 (3) 2.038(3)	N24 -H24A ...O11 (3) 159.70(2)
N24 -H24B 0.947(3)	N24 ...O21 (4) 2.963(5)	H24B ...O21 (4) 2.024(3)	N24 -H24B ...O21 (4) 171.20(2)
O1 -H1A 0.948(2)	O1 ...O3 (5) 2.699(5)	H1A ...O3 (5) 1.754(2)	O1 -H1A ...O3 (5) 174.28(2)
O2 -H2A 0.948(4)	O2 ...O12 (6) 3.062(4)	H2A ...O12 (6) 2.118(4)	O2 -H2A ...O12 (6) 173.35(3)
O2 -H2B 0.949(6)	O2 ...N13 (7) 3.131(5)	H2B ...N13 (7) 2.200(6)	O2 -H2B ...N13 (7) 166.69(5)
O3 -H3A 0.948(4)	O3 ...O21 (8) 2.890(5)	H3A ...O21 (8) 2.019(4)	O3 -H3A ...O21 (8) 151.91(3)
O3 -H3B 0.949(6)	O3 ...O2 (8) 2.774(5)	H3B ...O2 (8) 1.835(5)	O3 -H3B ...O2 (8) 169.45(5)

Equivalent positions:
(0) x, y, z; (1) x,-y-½,+z+½; (2) -x+2,+y-½,-z+½; (3) -x+1,+y+½,-z+½; (4) x,-y+½,+z+½; (5) x,+y,+z-1; (6) -x+1,-y,-z; (7) x-1,+y,+z; (8) -x+1,-y,-z+1

4.9.4 Crystal structure of the complex [Cd(smz)$_2$(en)].2DMF (24)

The crystal structure of the complex [Cd(smz)$_2$(en)].2DMF (**24**) is shown in Figure 4.67 together with the crystallographic atom numbering scheme used. The bond lengths and angles are given in Table 4.61 and the hydrogen bond dimensions are listed in Table 4.62.

The geometry of the complex is distorted octahedral with the Cd atom lying on a two-fold axis. Both the sulfamethazinato ligands are bonded to Cd by a sulfonamidic nitrogen [N(11)] atom and a pyrimido nitrogen [N(12)] atom and two nitrogen atoms from the ethylenediamine molecules complete the coordination sphere on the cadmium ion.

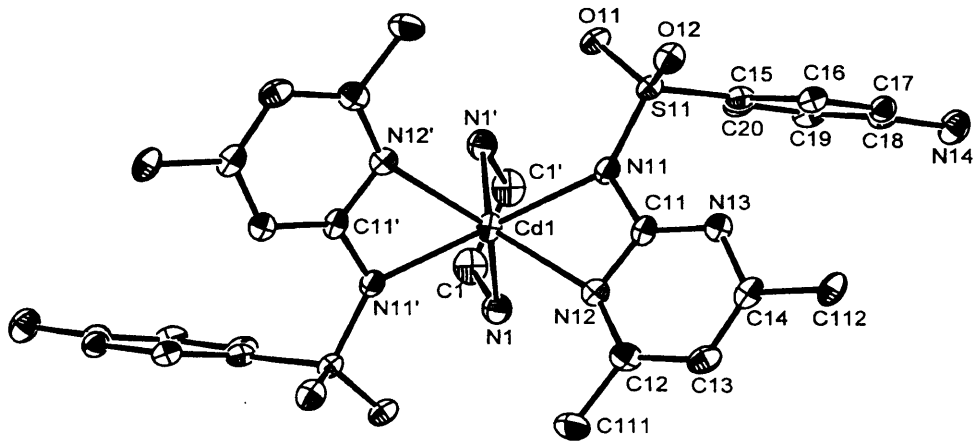

Figure 4.67
*X-ray structure of [Cd(smz)$_2$(en)].2DMF (**24**) showing crystallographic atom numbering scheme used. Thermal ellipsoids are drawn at 50% probability level. Hydrogen atoms and DMF molecules are omitted for clarity.*

The ethylenediamine molecule is chelated to the Cd atom symmetrically in the octahedral structure. The Cd–N(1)(en) distance of 2.321(4)Å is comparable with the values of 2.39(2) and 2.26(2)Å in the complex [Cd(en)][Ni(CN)$_4$].2C$_6$H$_6$[83] and 2.317(3)Å in [Cd(en)(NO$_3$)$_2$(4,4′-bpy)]$_n$[84] and the Cd–N(11) distance of 2.311(3)Å is shorter than Cd–N(12) distance of 2.471(4)Å which are comparable with the corresponding distance of 2.307(3)Å in the complex {[Cd(smz)$_2$(H$_2$O)].DMF}$_n$ (**22**), 2.337(3) and 2.322(3)Å in the complex {[Cd(smz)$_2$(H$_2$O)].2H$_2$O}$_n$ (**23**) and 2.426(6) and 2.326(6)Å in the complex [Cd(smz)$_2$(H$_2$O)].2H$_2$O.[1] The Cd–N(1) bonds are similar in length to the Cd–N(11) bonds and the difference between these two types of Cd–N bonds, [Δ = {d[Cd–N(1)] – d[Cd–N(11)]} (Å)], –0.010(4)Å suggesting that the Cd–N(1) bonds have similar strengths as the Cd–N(11) bonds in the complex.

Table 4.61: Selected bond lengths [Å] and angles [deg] in [Cd(smz)$_2$(en)].2DMF (24)

Bond	(Å)	Bond	(Å)
Cd(1)-N(11)	2.311(3)	Cd(1)-N(1)	2.321(4)
Cd(1)-N(12)	2.471(4)	S(11)-O(12)	1.448(3)
S(11)-O(11)	1.449(3)	S(11)-N(11)	1.608(3)
S(11)-C(15)	1.763(4)	N(11)-C(11)	1.368(5)
N(14)-C(18)	1.382(6)		
Angle	**(°)**	**Angle**	**(°)**
N(11)-Cd(1)-N(11′)	144.99(18)	N(11)-Cd(1)-N(1)	117.47(12)
N(11′)-Cd(1)-N(1)	90.46(12)	N(1)-Cd(1)-N(1′)	77.44(19)
N(11)-Cd(1)-N(12′)	104.23(12)	N(1)-Cd(1)-N(12′)	137.34(12)
N(11)-Cd(1)-N(12)	56.00(11)	N(1)-Cd(1)-N(12)	94.44(12)
N(1′)-Cd(1)-N(12)	137.34(12)	N(12′)-Cd(1)-N(12)	117.22(16)
O(12)-S(11)-O(11)	116.46(18)	O(12)-S(11)-N(11)	112.00(19)
O(11)-S(11)-N(11)	104.99(17)	O(12)-S(11)-C(15)	107.42(18)
O(11)-S(11)-C(15)	107.32(19)	N(11)-S(11)-C(15)	108.33(18)
C(11)-N(11)-S(11)	121.3(3)	N(13)-C(11)-N(12)	125.7(4)

Symmetry transformations used to generate equivalent atoms: (′) $-x, -y, z$

The N(14)–H(14B)···O(11), N(14)–H(14A)···O(12), N(1)–H(1A)···O(1) and N(1)–H(1B)···O(11) are very strong with almost linear bond angles and short distances. The several hydrogen bonds are shown in the packing diagram (Figure 4.68).

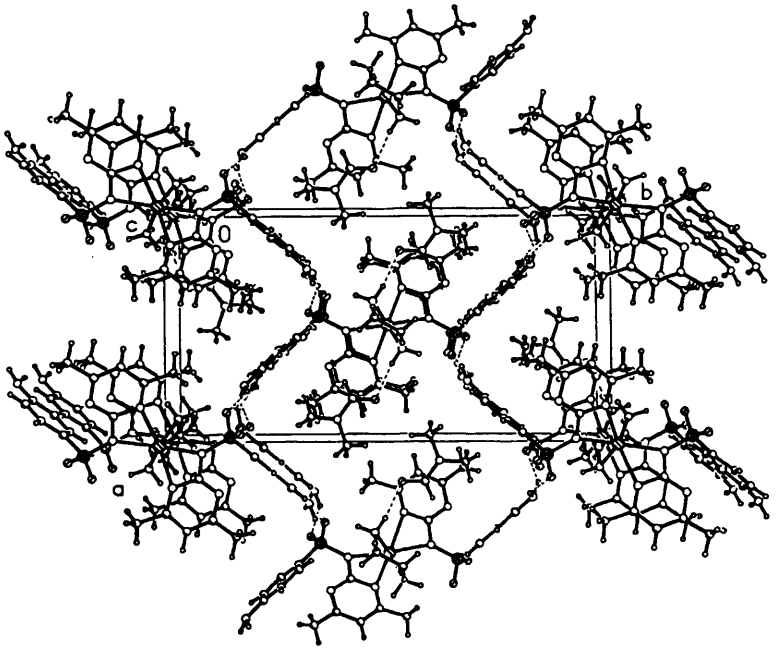

Figure 4.68
Packing diagram of the complex [Cd(smz)$_2$(en)].2DMF (22) showing the hydrogen bonds with open bonds

Table 4.62: The hydrogen bonds in [Cd(smz)$_2$(en)].2DMF (24) (distances and angles given in Å and deg respectively)

Donor-H	Donor...Acceptor	H...Acceptor	Donor-H.....Acceptor
N14 -H14A 0.950(9)	N14 ....O12 (1) 3.111(7)	H14A...O12 (1) 2.265(8)	N14 -H14A...O12 (1) 148.07(2)
N14 -H14B 0.949(3)	N14 ....O11 (2) 3.134(4)	H14B...O11 (2) 2.324(5)	N14 -H14B...O11 (2) 142.97(2)
N1 -H1A 0.920(6)	N1 ....O1 (3) 2.958(9)	H1A ...O1 (3) 2.062(7)	N1 -H1A ...O1 (3) 164.15(9)
N1 -H1B 0.920(2)	N1 ....O11 (3) 3.088(1)	H1B ...O11 (3) 2.286(5)	N1 -H1B ...O11 (3) 145.48(2)

Equivalent positions:
(1) $x-½, -y-½, -z+1$; (2) $x-½, -y-½, -z$; (3) $-x, -y, +z$

4.10 Mercury complexes of triple sulfa drugs (TSD)

The diversity of the coordination numbers for the mercury complexes can be found in the literature. In monoorganomercury(II) compounds, the primary bonds leave the Hg atom with enough residual acidity for it to be able to reach a coordination number of six when the donor atoms forming the secondary bonds are small. There are only a small number of Hg complexes with coordination number two.[85] On the other hand, Hg(II), has an extremely high affinity for thiol-containing compounds, and forms 1:2 metal:ligand linear complexes with them.[86]

The tetrahedral geometry was postulated in the mercury(II) complexes of the type HgX_2L_2 (where L = 1,3-imidazole-2-thione, 1-methyl-1,3-imidazole-2-thione; X = Cl^-, Br^-) on the basis of IR and NMR data.[87] In the Hg(II) complex with 2-(α-hydroxybenzyl)thiamine, the metal coordination unit consists of two distorted tetrahedra sharing two vertexes, and the high basicity of the N of the pyrimidine ring allows the coordination with the metal.[88] An example of octahedral local geometry is the complex of Hg(II) with the bidentate ligand lactobionic acid (L): $[HgL_2].2H_2O$.[89] With respect to Hg(II)-sulfa drug complexes, both geometries (linear arrangement[1] and tetrahedral[3]) were founded by X-ray crystal structure.

In this section, we will discuss the mercury complexes of sulfa drugs with two (sulfamerazine complex), four (sulfadiazine and sulfamethazine) and six (sulfamerazine with 2,2′-bipyridine) coordination geometry.

4.10.1 Crystal structure of the complexes (25), (26), (27) and (28)

Single crystals suitable for X-ray determination were obtained for the complexes and characterised by independent analytical and spectroscopic data. We also determined the modes of coordination and molecular geometry and compared these with other related species. The crystal data and refinement details for the complexes are listed in Table 4.63.

The crystal structures of the complexes $[Hg(sdz)_2(DMF)_2]$ (**25**), $[Hg(smr)_2]$ (**26**), $[Hg(smr)_2(bpy)]$ (**27**) and $[Hg(smz)_2(DMF)_2]$ (**28**) are shown in Figures 4.69, 4.71, 4.73 and 4.75 respectively together with the crystallographic atom numbering scheme used. The selected bond lengths and angles are collected together in Table 4.64.

Table 4.63 Crystal data and details of data collection and structure refinement for the complexes $[Hg(sdz)_2(DMF)_2]$ (25), $[Hg(smr)_2]$ (26), $[Hg(smr)_2(bpy)]$ (27) and $[Hg(smz)_2(DMF)_2]$ (28)

	$[Hg(sdz)_2(DMF)_2]$ (**25**)	$[Hg(smr)_2]$ (**26**)	$[Hg(smr)_2(bpy)]$ (**27**)	$[Hg(smz)_2(DMF)_2]$ (**28**)
Empirical Formula	$C_{26}H_{32}HgN_{10}O_6S_2$	$C_{22}H_{22}HgN_8O_4S_2$	$C_{32}H_{30}HgN_{10}O_4S_2$	$C_{30}H_{40}HgN_{10}O_6S_2$
Formula Weight	845.33	727.19	883.37	901.43
Crystal System	Monoclinic	Monoclinic	Monoclinic	Monoclinic
Space Group	*C*2/*c*	*C* 2/*c*	*C* 2/*c*	$P2_1/c$
a(Å)	20.0760(5)	12.8834(5)	18.7483(8)	12.4196(2)
b(Å)	8.3210(3)	14.5693(5)	15.0824(7)	8.8066(2)
c(Å)	19.8380(6)	12.7683(6)	12.1143(6)	17.0090(3)
β(°)	108.659(2)	97.5505(14)	100.202(2)	107.9718(14)
V/Å^{-3}	3139.8(2)	2375.86(17)	3139.8 (2)	1769.58(6)
Z	4	4	4	2
T/K	150	150	150	150
Crystal Size/mm	0.12 × 0.10 × 0.08	0.15 × 0.12 × 0.08	0.18 × 0.15 × 0.12	0.16 × 0.12 × 0.10
Shape	Block	Block	Block	Block
Colour	White	White	White	White
θ-range for data collection	3.01 – 27.46	3.19 – 27.46	3.20 – 27.51	2.93 – 27.47
Reflection Collected	14863	16902	14955	19422
Unique Reflections	3570	2713	3874	4020
R_{int}	0.0761	0.0866	0.0722	0.0842
Index ranges	−26<=h<=25 −10<=k<=10 −25<=l<=25	−16<=h<=16 −18<=k<=18 −16<=l<=16	−24<=h<=19 −19<=k<=19 −14<=l<=15	−16<=h<=15 −11<=k<=11 −22<=l<=21
Data/parameters	3570/214	2713/177	3874/231	4020/235
Final *R* indices [$I>2\sigma(I)$]	0.0373/0.0629	0.0386/0.0842	0.0360/0.0644	0.0357/0.0703
R indices (all data)	0.0523/0.0679	0.0465/0.0872	0.0508/0.0674	0.0624/0.0804
Largest diff. peak and hole Å^{-3}	1.248 and −0.895	1.125 and −2.001	1.142 and −0.710	0.509 and −0.983

Table 4.64: Selected bond lengths [Å] and angles [°] in the complexes $[Hg(sdz)_2(DMF)_2]$ (25), $[Hg(smr)_2]$ (26), $[Hg(smr)_2(bpy)]$ (27) and $[Hg(smz)_2(DMF)_2]$ (28)

Bond	(25) [Å][a]	(26)[Å][a]	(27) [Å][a]	(28) [Å][b]
Hg–N(11)	2.047(3)	2.017(4)	2.216(3)	2.048(4)
Hg–N(12)			2.881(3)	
Hg–O(1)	2.713(3)			2.727(4)
Hg–N(1)			2.322(3)	
S(11)-O(11)	1.443(3)	1.433(4)	1.434(3)	1.441(3)
S(11)-O(12)	1.444(3)	1.444(2)	1.457(3)	1.445(3)
S(11)-N(11)	1.630(4)	1.648(4)	1.612(3)	1.636(4)
S(11)-C(15)	1.759(4)	1.749(5)	1.764(3)	1.754(4)
N(11)-C(11)	1.386(6)	1.397(6)	1.389(5)	1.400(6)
N(14)-C(18)	1.384(6)	1.369(7)	1.373(5)	1.372(6)
Angle	(°)	(°)	(°)	(°)
N(11)–Hg–N(11′)	179.4(2)	171.5(2)	107.55(15)	180.0
N(12)–Hg–N(12)			132.13(11)	
O(1)–Hg–O(1′)	162.7(2)			180.0
N(1)–Hg–N(1′)			69.98(16)	
N(11)–Hg–O(1′)	88.0(1)			94.8(2)
O(1)–Hg–N(11′)	92.1(2)			85.2(2)
N(11′)-Hg(1)-N(1)			123.41(11)	
N(11)-Hg(1)-N(1)			114.68(12)	
N(12′)-Hg(1)-N(1)			86.04(11)	
N(12)-Hg(1)-N(11)			51.12(12)	
N(12′)-Hg(1)-N(11)			98.52(16)	
N(13)-C(11)-N(12)	127.1(4)	128.0(5)	126.3(3)	127.9(4)

Symmetry transformations used to generate equivalent atoms: ([a]) $-x, y, -z+½$
Symmetry transformations used to generate equivalent atoms: ([b]) $-x, -y+1, -z$

The geometry of the complexes $[Hg(sdz)_2(DMF)_2]$ (**25**) and $[Hg(smz)_2(DMF)_2]$ (**28**) are square planar with the Hg atom lying on the two-fold axis showing the Hg(II) atom is four coordinated with two oxygen [O(1)] atoms from two DMF molecules and two nitrogen [N(11)] atoms from the sulfa drug molecules. The DMF molecules are coordinated to the Hg atom from the *trans* position in the structure. The complex $[Hg(smr_2]$ (**26**) is linear with two molecules of sulfamerazine coordinated through the sulfonamidic nitrogen atoms and the complex $[Hg(smr)_2(bpy)]$ (**27**) is six coordinate with trigonal prismatic structure.

The oxygen atom of the DMF molecule makes longer bonds with mercury atoms in the complexes (**25**) and (**28**) and the Hg–O(1) distances of 2.713(3)Å for (**25**) and 2.727(4)Å for (**28**) are comparable with the corresponding bonds of the values of Hg–O(1) = 2.769(7)Å in the complex $[Hg(sdz)_2(DMSO)_2]$.[3] The Hg–N(11) bond distances of

2.047(3)Å for (**25**), 2.017(4)Å for (**26**) and 2.084(4)Å for (**28**) are also comparable with the values of 2.071(4)Å in the complex $[Hg(smpz)_2]$[1], 2.087(4)Å in $[Hg(sdz)_2(DMSO)_2]$[3], 2.041(6) and 2.031(6)Å in $[Hg(mq)_2]$[90] and 2.14(2)Å in $[Hg(bpy)_2(NO_2psgly\text{-}N,O)]0.5H_2O$[91] where smpz,, sdzH, mq and NO_2psgly are sulfamethoxypiridazine, sulfadiazine, 4-mehtyl-2(1*H*)-quinoline and *N*-2-nitrophenylsulfonylglycine respectively but the Hg–N(11) distance of 2.216(3)Å for (**27**) is slightly longer than the others.

The C(18)-N(14) bond distances of 1.384(6)Å in (**25**), 1.369(7)Å in (**26**), 1.373(5)Å in (**27**) and 1.372(6)Å in (**28**) are in good agreement with the corresponding bond in the pure ligands suggesting the terminal amino group is not coordinated with the Hg atoms in the complexes and are also comparable with the corresponding bond found in the mercury-sulfadiazinato complex $[Hg(sdz)_2(DMSO)_2]$[3] and in the previous complexes.

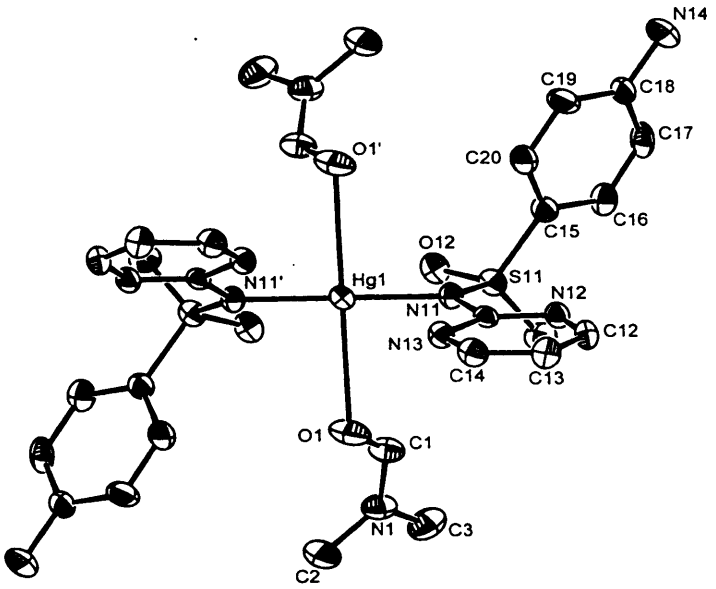

Figure 4.69
*X-ray structure of $[Hg(sdz)_2(DMF)_2]$ (**25**) showing crystallographic atom numbering scheme used. Thermal ellipsoids are drawn at 50% probability level. The hydrogen atoms are omitted for clarity.*

The square planar geometry around Hg atom in the complexes (**25**) and (**28**) is fairly regular showing only minor variations from ideal geometry of the mutually *cis* 90° and *trans* 180° angles. This is evident from the values of *trans* angles N(11')–Hg(1)–N(11) and O(1')–Hg(1)–O(1) are 179.4(2)° for (**25**) and 162.7(2)° for (**25**) and 180.0° for (**28**) respectively and the *cis* angles vary from 88.0(1) and 92.1(2)° in the complex (**25**) and 85.2(2) and 94.8(2)° in the complex (**28**).

The packing of the complex units is governed by long chains formed by weak hydrogen bonds between the amino ($-NH_2$) group of one complex unit and the sulfonyl oxygen and the pyrimido nitrogen atoms of the next unit, N(14)–H(14A)···O(12) (other complex unit) = 2.346(2)Å with an angle of 157.75(3)° and N(14)–H(14B)···N(13) (other complex unit) = 2.452(1)Å with an angle of 136.74(3)° and the packing diagram of the complex $[Hg(sdz)_2(DMF)_2]$ (**25**) is shown in Figure 4.70.

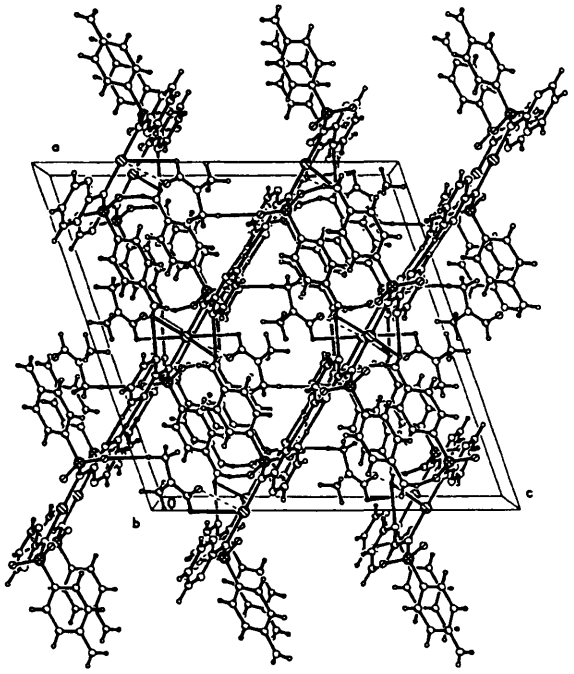

Figure 4.70
Packing diagram of the complex (25) showing the hydrogen bonds by dashed lines

Table 4.65: Possible hydrogen bonds and short interactions in $[Hg(sdz)_2(dmf)_2]$ (25) (distances and angles given in Å and deg respectively)

Donor-H	Donor...Acceptor	H...Acceptor	Donor-H.....Acceptor
N14 -H14A	N14 ....O12 (1)	H14A...O12 (1)	N14 -H14A...O12 (1)
0.950(8)	3.244(4)	2.346(2)	157.75(3)
N14 -H14B	N14 ....N13 (2)	H14B...N13 (2)	N14 -H14B...N13 (2)
0.949(5)	3.210(2)	2.452(1)	136.74(3)
C13 -H13	C13 ....O11 (3)	H13 ...O11 (3)	C13 -H13 ...O11 (3)
0.950(2)	3.148(1)	2.429(1)	132.31(1)
C2 -H2B	C2 ....O11 (4)	H2B ...O11 (4)	C2 -H2B ...O11 (4)
0.980(2)	3.476(1)	2.499(1)	174.74(1)

Equivalent positions:

(1) $-x-\frac{1}{2},+y+\frac{1}{2},-z+\frac{1}{2}$; (2) $x-\frac{1}{2},+y-\frac{1}{2},+z$; (3) $x,+y+1,+z$; (4) $-x,-y,-z$

The hydrogen bonds in the complex $[Hg(sdz)_2(DMF)_2]$ (**25**) are associated with very short donor-acceptor distances and nearly linear donor-acceptor angles, which indicate that these have weak interactions.

The complex (**26**) lies on a two-fold axis in which the sulfamerazinato ligands are bonded to Hg-atom through the sulfonamidic nitrogen [N(11)] atom with an angle N(11)–Hg–N(11′) of 171.5(2)° indicating the linearity of the complex.

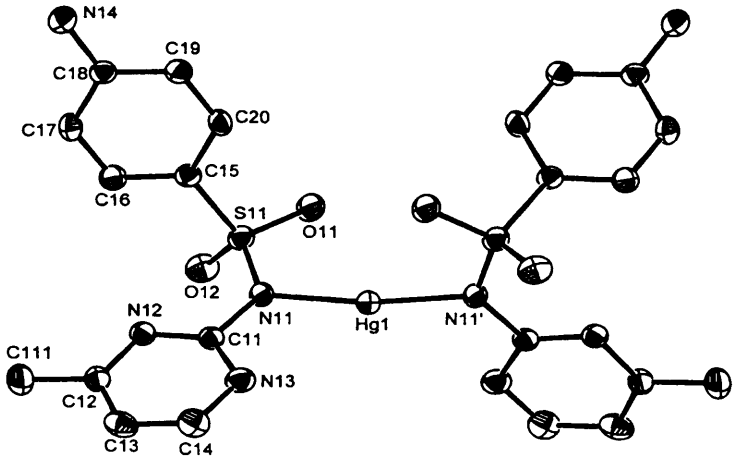

Figure 4.71
X-ray structure of $[Hg(smr)_2]$ (26) showing crystallographic atom numbering scheme used. Thermal ellipsoids are drawn at 50% probability level. The hydrogen atoms are omitted for clarity

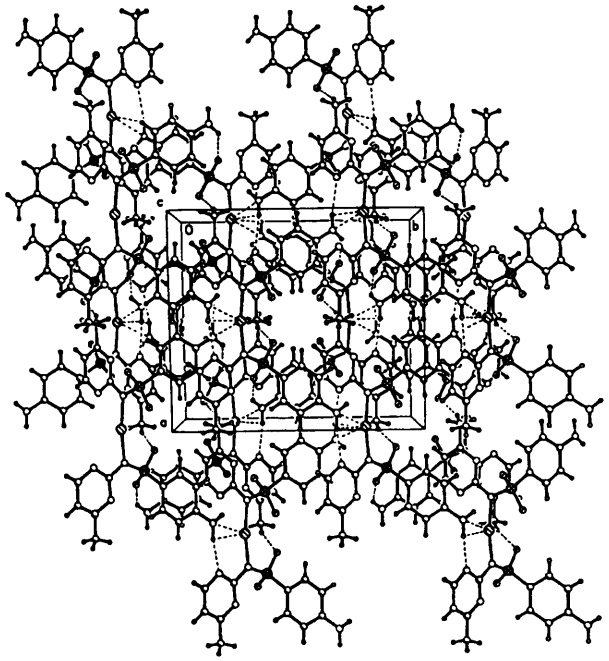

Figure 4.72
Packing diagram of the complex $[Hg(smr)_2]$ (26) showing hydrogen bonds by dashed lines

In the packing diagram of the complex (**26**) the amino group, sulfonyl oxygen and pyrimido nitrogen atoms are hydrogen bonded which is shown in Figure 4.72 by dashed lines.

Table 4.66: Possible hydrogen bonds and short interactions in $[Hg(smr)_2]$ (26) (distances and angles given in Å and deg respectively)

Donor-H	Donor...Acceptor	H...Acceptor	Donor-H.....Acceptor
N14 -H14A	N14 ...N13 (1)	H14A ...N13 (1)	N14 -H14A...N13 (1)
0.931(3)	3.323(7)	2.583(4)	136.78(2)
N14 -H14B	N14 ...O12 (2)	H14B ...O12 (2)	N14 -H14B...O12 (2)
0.937(6)	3.173(7)	2.399(7)	139.93(5)
C111 -H11C	C111 ...O11 (3)	H11C ...O11 (3)	C111 -H11C...O11 (3)
0.960(6)	3.377(7)	2.455(4)	161.06(4)

Equivalent positions: (1) x+½, +y-½, +z; (2) x, -y, +z+½; (3) x+½, -y+½, +z+½

The Hg atom in the complex (**27**) is six coordinate bonding through the two sulfonamidic and pyrimido nitrogen atoms and two nitrogen atoms from the bpy molecules complete the coordination sphere.

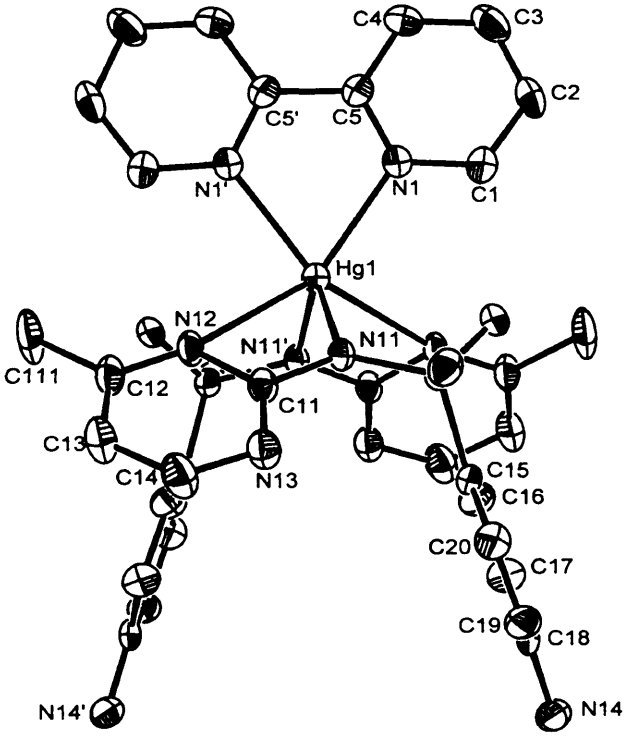

Figure 4.73
X-ray structure of $[Hg(smr)_2(bpy)]$ (27) showing crystallographic atom numbering scheme used. Thermal ellipsoids are drawn at 50% probability level. The hydrogen atoms are omitted for clarity.

The Hg–N_{bpy} bond distance of 2.323(3)Å is longer than the corresponding bond lengths of 2.140(3) and 2.124(3)Å in [Hg(1,3-dimethyluracil-C5)(bpy)](ClO_4)[92] and 2.130Å in [Hg(sac)(bpy)].[93]

The geometry of the complex (**27**) is trigonal prismatic (Figure 4.74) like the previous cadmium complexes (**18**, **19** and **20**) with the Hg atom lying on a two-fold axis. The geometry of the complex is trigonal prismatic since the bpy molecule lies on the one part and the two larger sulfamerazine molecules lie on the other part. The sulfamerazinato ligands are bonded to Hg through sulfonamidic nitrogen [N(11)] atom and the pyrimido nitrogen [N(12)] atom of the sulfamerazine molecules and the N(1) atom of the bpy ligand.

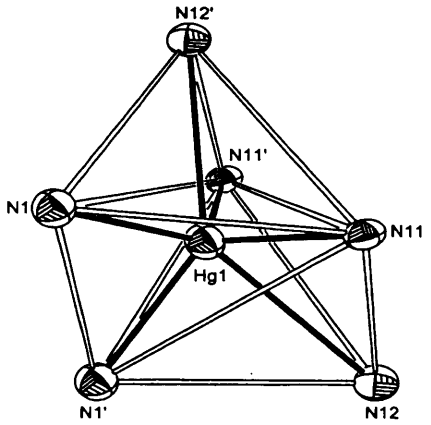

Figure 4.74
Trigonal prismatic structure of the complex [Hg(smr)$_2$(bpy)] (27) containing only the bonded nitrogen atoms

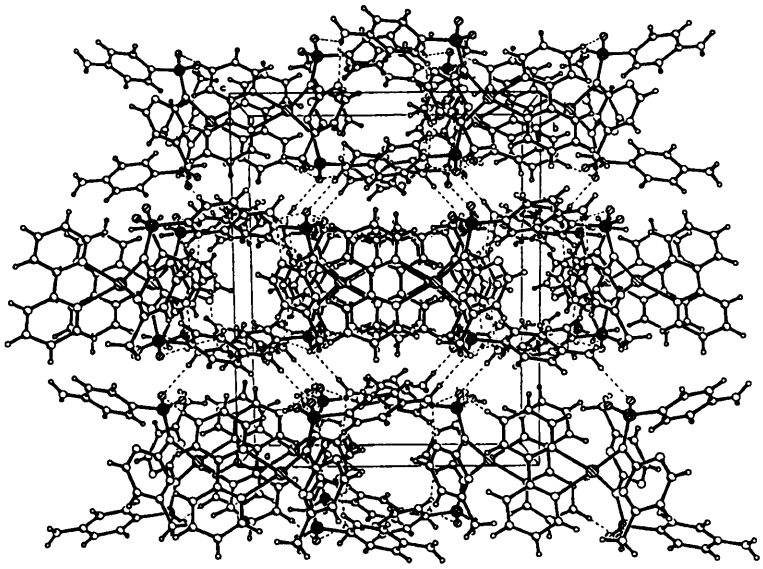

Figure 4.75
Packing diagram of the complex [Hg(sdz)$_2$(bpy)$_2$] (27) where hydrogen bonds are shown by dashed lines

The N(14)–H(14A)···O(11) hydrogen bond in (**27**) is associated with very short donor-acceptor distances and nearly linear donor-acceptor angles indicating strong interactions. The bipyridine molecule is chelated to the Hg atom symmetrically in the complex.

Table 4.67: Possible hydrogen bonds and short interactions in [Hg(smr)$_2$(bpy)] (27) (distances and angles given in Å and deg respectively)

Donor-H	Donor...Acceptor	H...Acceptor	Donor-H.....Acceptor
N14 -H14A	N14 ....O11 (1)	H14A...O11 (1)	N14 -H14A...O11 (1)
0.950(9)	2.994(1)	2.083(9)	160.24(3)
N14 -H14B	N14 ....N13 (2)	H14B...N13 (2)	N14 -H14B...N13 (2)
0.949(7)	3.125(2)	2.381(7)	135.02(4)
N14 -H14B	N14 ....O11 (2)	H14B...O11 (2)	N14 -H14B...O11 (2)
0.949(7)	3.173(2)	2.375(7)	141.55(2)
C3 -H3	C3 ....O11 (4)	H3 ...O11 (4)	C3 -H3 ...O11 (4)
0.950(7)	3.213(5)	2.375(2)	146.87(3)

Equivalent positions:

(1) $-x+½, +y+½, -z+½$; (2) $x, -y+1, +z+½$; (3) $x, -y, +z+½$

In the complex (**28**) the Hg atom is four coordinate with two oxygen atoms from DMF molecules and two nitrogen atoms from sulfamethazine molecules.

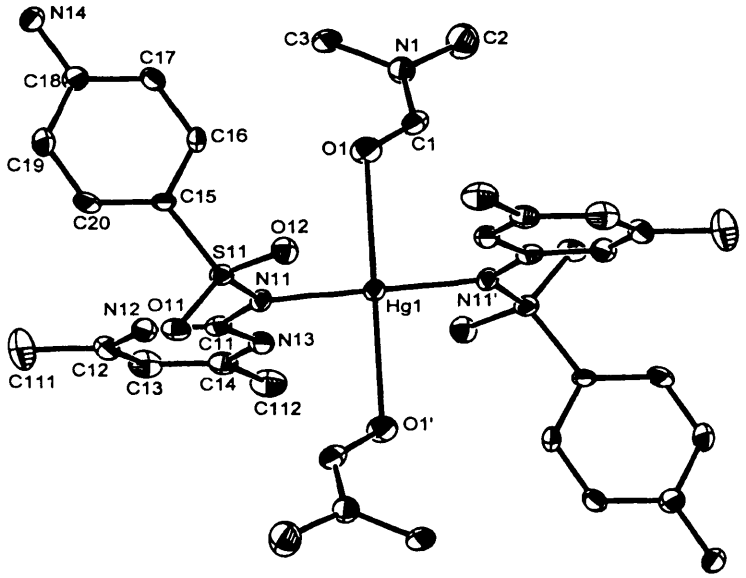

Figure 4.76
X-ray structure of [Hg(smz)$_2$(DMF)$_2$] (28) showing crystallographic atom numbering scheme used. Thermal ellipsoids are drawn at 50% probability level. Hydrogen atoms are omitted for clarity.

The sulfonyl oxygen and pyrimido nitrogen atoms are hydrogen bonded in the complex, are shown by dashed lines in the packing diagram (Figure 4.77).

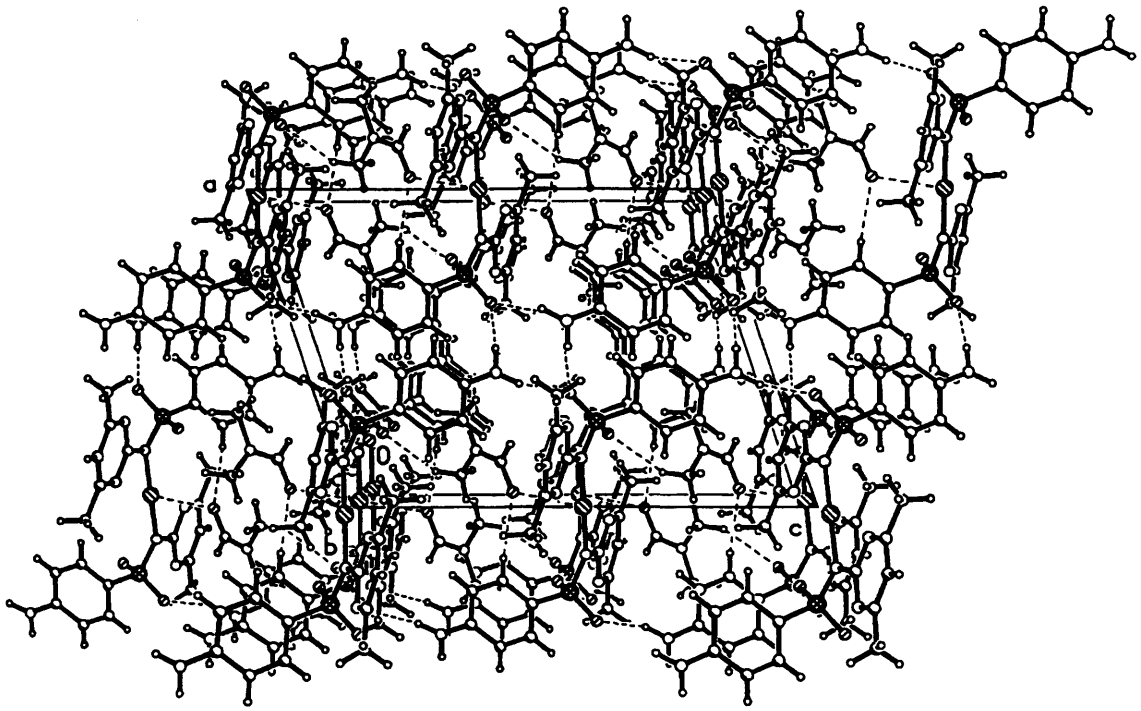

Figure 4.77
Packing diagram of the complex [Hg(sdz)$_2$(DMF)$_2$] (28) showing the hydrogen by dashed lines

Table 4.68: The hydrogen bonds and short interactions in [Hg(smz)$_2$(DMF)$_2$] (28) (distances and angles given in Å and deg respectively)

Donor-H	Donor...Acceptor	H...Acceptor	Donor-H.....Acceptor
C16 -H16	C16 ....O1 (0)	H16 ...O1 (0)	C16 -H16 ...O1 (0)
0.950(9)	3.388(1)	2.482(8)	159.53(8)
N14 -H14A	N14 ....O11 (1)	H14A...O11 (1)	N14 -H14A...O11 (1)
0.948(8)	3.031(1)	2.104(8)	165.47(3)
N14 -H14B	N14 ....O11 (2)	H14B...O11 (2)	N14 -H14B...O11 (2)
0.949(8)	3.038(7)	2.223(4)	143.46(6)

Equivalent positions:

(0) x, y, z; (1) $-x+1,+y-½,-z+½$; (2) $x,-y+½,+z+½$

4.11 Summary

We synthesized the following new metal (Co, Ni, Cu, Zn, Cd and Hg) complexes of triple sulfa drugs (TSD) with secondary ligands such as water, ammonia, pyridine (py), dimethylformamide (DMF), dimethylsulfoxide (DMSO), ethylenediamine (en), 2,2′-bipyridine (bpy), 4,4′-dimethyl-2,2′-bipyridine (dmbpy), 1,10-phenanthroline (phen), diethylenetriamine (dien) and *N,N′*(3-aminopropyl)-bis-ethylenediamine (apen) and characterised them by elemental analysis, spectroscopic and X-ray crystallographic methods.

Cobalt complex

1. $\{[Co(smz)_2(H_2O)].DMF\}_n$ (**3**)

Nickel complexes

2. $[Ni(en)_3][(sdz)_2.H_2O]$ (**4**)
3. $[Ni(smr)_2(py)_2].4py$ (**5**)

Copper complexes

4. $[Cu(en)_2(sdz)_2]$ (**6**)
5. $[Cu(dien)(sdz)_2]$ (**7**)
6. $[Cu(en)_2(H_2O)_2][(smr)_2]$ (**8**)
7. $[Cu(en)_2(H_2O)_2][(smr)_2].H_2O$ (**9**)
8. $[Cu_2(smr)_4].2DMF$ (**10**)
9. $[Cu_2(smr)_4].2DMSO$ (**11**)
10. $[Cu(smz)_2(apen)].3H_2O.CH_3OH$ (**12**)
11. $\{[Cu(smz)_2(NH_3)].2H_2O\}_n$ (**13**)

Zinc complexes

12. $[Zn(smz)_2(NH_3)_2]$ (**14**)
13. $[Zn(smz)_2(py)_2].2py$ (**15**)

Cadmium complexes

14. $[Cd(dien)(sdz)_2].DMF$ (**16**)
15. $[Cd(dien)(smr)_2].DMF$ (**17**)
16. $[Cd(sdz)_2(bpy)]$ (**18**)
17. $[Cd(sdz)_2(phen)]$ (**19**)
18. $[Cd(sdz)_2(dmbpy)].2DMF$ (**20**)
19. $[Cd(smr)_2(phen)]$ (**21**)
20. $\{[Cd(smz)_2(H_2O)].DMF\}_n$ (**22**)
21. $\{[Cd(smz)_2(H_2O)].2H_2O\}_n$ (**23**)
22. $[Cd(smz)_2(en)].2DMF$ (**24**)

Mercury complexes

23. $[Hg(sdz)_2(DMF)_2]$ (**25**)
24. $[Hg(smr)_2]$ (**26**)
25. $[Hg(smr)_2(bpy)]$ (**27**)
26. $[Hg(smz)_2(DMF)_2]$ (**28**)

We also synthesised the metal complexes of sulfathiazole (Chapter 5) with ethylenediamine and sulfadimethoxine (Chapter 6) with ammonia as secondary ligands.

Metal complexes of sulfathiazole

1. $[CoCl_4][(H_2stz)_2].CH_3COOH$ (**30**); 2. $[Cu(en)_2(H_2O)_2][stz)_2].2H_2O$ (**31**)

Zinc complex of sulfadimethoxine

1. $[Zn(sdm)_2(NH_3)_2].2H_2O$ (**33**)

4.11.1 Type of coordination around the metal centres

The metal atoms in the complexes studied display different coordination numbers. The most common coordination number found is six with the metal having octahedral, $\{[Co(smz)_2(H_2O)].DMF\}_n$ (**3**), $[Ni(en)_3][(sdz)_2.H_2O]$ (**4**), $[Ni(smr)_2(py)_2].4py$ (**5**), $[Cu(dien)(sdz)_2]$ (**7**), $[Cu(en)_2(H_2O)_2][(smr)_2]$ (**8**), $[Cu(en)_2(H_2O)_2][(smr)_2].H_2O$ (**9**) $[Cu(smz)_2(apen)].3H_2O.CH_3OH$ (**12**), $\{[Cu(smz)_2(NH_3)].2H_2O\}_n$ (**13**), $[Zn(smz)_2(NH_3)_2]$ (**14**), $[Zn(smz)_2(py)_2].2py$ (**15**), $\{[Cd(smz)_2(H_2O)].DMF\}_n$ (**22**), $\{[Cd(smz)_2(H_2O)]H_2O\}_n$ (**23**), $[Cd(smz)_2(en)].2DMF$ (**24**) and $[Cu(en)_2(H_2O)_2][stz)_2].2H_2O$ (**31**); trigonal prismatic, $[Cd(sdz)_2(bpy)]$ (**18**), $[Cd(sdz)_2(phen)]$ (**19**), $[Cd(sdz)_2(dmbpy)].2DMF$ (**20**), $[Hg(smr)_2(bpy)]$ (**27**) and $[Zn(sdm)_2(NH_3)_2].2H_2O$ (**33**); and bicapped tetrahedral geometry, $[Cd(smr)_2(phen)]$ (**21**). The two copper complexes $[Cu_2(smr)_4].2DMF$ (**10**) and $[Cu_2(smr)_4].2DMSO$ (**11**) are five coordinate with one metal-metal bond. The complexes $[Cu(en)_2(sdz)_2]$ (**6**), $[Hg(sdz)_2(DMF)_2]$ (**25**), $[Hg(smz)_2(DMF)_2]$ (**28**), $[CoCl_4][(smz)_2]$-CH_3COOH (**30**) show a coordination number of four (square planar) and the only mercury complex of sulfamerazine $[Hg(smr)_2]$ (**26**) shows a coordination number of two with linear arrangement. The complexes $[Cd(dien)(sdz)_2].DMF$ (**16**) and $[Cd(dien)(smr)_2].DMF$ (**17**) have seven coordination number with distorted pentagonal bipyramidal geometry. The geometries are often associated with distortions from ideal geometries both in bond lengths and in angles. These aspects have already been discussed and explained when describing each individual structure in the previous chapters. However it needs to be emphasised here that the distortions are in most cases due to electronic effects, steric factors and also, in most cases, due to the intra- and/or inter-molecular hydrogen bonding effects.

4.11.2 Status of TSD anion as ligand

It has been mentioned earlier (Chapter 2) that TSD ions have six possible donor sites for potential binding with a metal ion. These six sites are the sulfonamidic nitrogen, two pyrimido nitrogen, two sulfonyl oxygen and amino nitrogen atoms. Since the neutral TSD molecules contain a hydrogen atom on the sulfonamidic nitrogen atom, after deprotonation

the negative charge is located (entirely or at least most of it) on the nitrogen atom of the TSD anion. Therefore, the N atom with a negative charge should be the most preferred site for bonding with a metal ion. In fact, this mode of coordination of the TSD anion has been found as the most common in the complexes where most of the sulfa drug molecules are directly bonded with the metals. Thus N-coordinated complexes are listed in Table 4.68. In one unusual case, the sulfamethazinato ion is bonded to the metal centre, not through the sulfonamidic nitrogen atom, but through the sulfonyl oxygen atom (**12**).

Table 4.68: Comparison of the M–N(11) and M–N(12) bond lengths

Complexes	Bonds	
	M–N(11)	M–N(12)
$\{[Co(smz)_2(H_2O)].DMF\}_n$ (**3**)	2.142(2)	2.187(2)
$[Ni(smr)_2(py)_2].4py$ (**5**)	2.139(2)	2.100(2)
$[Cu_2(smr)_4].2DMF$ (**10**)	2.057(3)	1.992(3)
$[Cu_2(smr)_4].2DMSO$ (**11**)	2.040(5)	1.998(5)
$\{[Cu(smz)_2(NH_3)].2H_2O\}_n$ (**13**)	2.044(3)	2.035(3)
$[Zn(smz)_2(NH_3)_2]$ (**14**)	2.040(3)	2.844(3)
$[Zn(smz)_2(py)_2].2py$ (**15**)	2.223(3)	2.323(3)
[Cd(dien)(sdz)$_2$].DMF (**16**)	2.495(2)	2.403(2)
[Cd(dien)(smr)$_2$].DMF (**17**)	2.434(2)	2.416(2)
[Cd(sdz)$_2$(bpy)] (**18**)	2.283(3)	2.501(3)
[Cd(sdz)$_2$(phen)] (**19**)	2.275(2)	2.517(2)
[Cd(sdz)$_2$(dmbpy)].2DMF (**20**)	2.253(2)	2.504(2)
[Cd(smr)$_2$(phen)] (**21**)	2.193(2)	2.793(2)
$\{[Cd(smz)_2(H_2O)].DMF\}_n$ (**22**)	2.307(3)	2.407(3)
$\{[Cd(smz)_2(H_2O)].H_2O\}_n$ (**23**)	2.337(3)	2.322(3)
[Cd(smz)$_2$(en)].2DMF (**24**)	2.311(3)	2.471(4)
[Hg(sdz)$_2$(DMF)$_2$] (**25**)	2.047(3)	
[Hg(smr)$_2$] (**26**)	2.017(4)	
[Hg(smr)$_2$(bpy)] (**27**)	2.216(3)	2.881(3)
[Hg(smz)$_2$(DMF)$_2$] (**28**)	2.048(4)	

In some cases, the nickel and copper complexes [(**4**), (**6**), (**7**), (**8**), (**9**), (**30**) and (**31**) complexes], the sulfa drug molecules are not coordinated with the metal ions because a stronger ligand such as ethylenediamine and/or diethylenetriamine are attached to the metal centres, and they remain outside the coordination sphere and are attached to the cationic species through very strong hydrogen bonds. In complex (**30**), the cobalt atom is surrounded by four chloride ions forming the negatively charged anion and the two molecules of positively charged sulfathiazole cations remain outside the coordination spheres. These complexes are typical examples for the formation of "cation-anion" pairs.

Thus our studies clearly indicate that (i) the sulfa drug anions are not directly coordinated with the metals in some cases, and (ii) when it is coordinated to a metal, it commonly involves the sulfonamidic and pyrimido nitrogen atoms. Involvement of the sulfonyl oxygen atom is also possible and in fact, it is observed in one case of the copper complex of sulfamethazine (**12**), and in the polymeric complexes of sulfamethazine, the terminal amino group takes part in the coordination to the metal centres.

Another aspect that was stated earlier but should also be pointed out here is that the sulfa drug anions may act as a monodentate, bidentate or tridentate chelating as well as bridging ligands, as observed in polymeric complex of sulfadiazine $[Zn(sdz)_2]$[1] and $[Cd(sdz)_2].2H_2O$[2] and in the complex of sulfamethazine $[Cd(smz)_2(H_2O)].2H_2O$.[3] In our present complexes, however, the ligands are also monodentate, bidentate or tridentate in some cases.

The question that may arise in this context is: why do the sulfa drug molecules show different coordination modes in different complexes. The explanation is not simple, but it would obviously depend on the competition between different possible coordinating species in the reaction media as well as their relative basicities. Ligands such as H_2O, NH_3, pyridine, etc., are well known Lewis bases, and can bind with metal ions due to the ease with which these species can donate their electrons to the metal ions, which act as Lewis acids. Since in our complexes sulfa drug molecules are found to coordinate with the metal centres along with H_2O, pyridine, ethylenediamine, bipyridine, phenanthroline, we believe that sulfa drug molecules are also relatively strong ligands and can compete with the above mentioned secondary ligands for bonding with the metal ions. The relative basicities at the sulfonyl oxygen atoms of the sulfa drug molecules would be much less compared with that of the sulfonamidic and pyrimido nitrogen atoms. So coordination involving sulfonyl oxygen atoms is rather rare, and such modes of coordination would be guided not by the electron donating capacity alone, but by other factors such as hydrogen bonding and/or steric reasons.

4.11.3 Role of hydrogen bonds in the formation of crystal architecture

Hydrogen bonds between a proton and corresponding donor and acceptor atoms are probably the most important non-covalent interactions in organic and metal complexes.

Their roles in determining molecular geometry, conformations, and crystal architecture and the overall stability have long been emphasised and recognised.

In the complexes studied in this work, both intra- and inter-molecular/ionic hydrogen bonds and short van der Waals' interactions have been noted and listed in selected Tables for the individual complexes. These hydrogen bonds are of the O–H···O/N type and in the case of diamine/triamine complexes of the N–H···O type. They play important roles in the distribution of ligands around the metal centres and their relative orientations. The sulfa drug anions that remain outside the coordination sphere are held in the crystal due to the extensive hydrogen bonding network. This determines the overall packing arrangement in the unit cell. The truth of this statement lies in the fact that for ALL the complex species containing water molecules either coordinated and/or in the lattice, hydrogen bonds are always present and their dimensions indicate that they are fairly strong hydrogen bonds based on normal criteria [O(–H)···O/N = 3.1, H···O/N = 2.0 Å]. The complexes that do not contain any water molecules do not have such strong hydrogen bonds, but these complexes also contain weaker interactions of the type C–H···O and van der Waals' interactions, and these are the forces that hold individual molecules together in the crystal.

4.11.4 Conclusion

The work in this thesis is not complete as far as the global aim is concerned, but nonetheless, it embraces the structural studies of the metal complexes of sulfa drugs. The metal complexes of sulfa drugs, which have been studied, are Co, Ni, Cu, Zn, Cd and Hg with sulfadiazine, sulfamerazine, sulfamethazine, sulfathiazole and sulfadimethoxine. It has been shown that when sulfa drugs are bonded to the metal atom, it is usually through the sulfonamidic and pyrimido nitrogen atoms. In most of the complexes the bonds through the sulfonamidic nitrogen atom is shorter than that of the pyrimido nitrogen atom.

4.11.5 Further works

As the sulfa drugs are active antibacterial compounds and some metal complexes are still used as topical medicine for burn treatment, the compounds, which we have synthesized in the laboratory, may also have some biological activity and antibacterial activity. In addition there may be more complexes of sulfa drugs with metal ions and secondary ligands. Their biological activity may be investigated in future.

References

1. A. Garcia-Raso, J.J. Fiol, S. Rigo, A. Lopez-Lopez, E. Molins, E. Espinosa, E. Borras, G. Alzuet, Joaquin Borras and A. Castineiras; *Polyhedron*; 2000, **19**, 991

2. J. Casanova, G. Aluzet, S. Ferrer, J. Borras, S. Garcia-Granda and E. Perez-Carreno; *J. Inorg. Biochem.*, 1993, **51**, 689

3. A. García-Raso, J. J. Fiol, G. Martorell, A. López-Zafra and M. Quirós; *Polyhedron*, 1997, **16,** 613

4. J. R. Pilbrow; "*Transition Ion Electron Paramagnetic Resonance*", Oxford Science Publications, 1990, 20

5. H. S. Shin, G. S. Ihn, H. S. Kim and C. H. Koo; *J. Korean Chem. Soc.*, 1974, **18**, 329

6. M. K. kokila, Puttaraja, M. V. Kulkarni and S. Thampi; *Acta Cryst.*, 1995, **C51**, 333

7. K. R. Acharya; K.N. Kuchela and G. Kartha; *J. Cryst. Spectros. Res.*, 1982, **12**, 369

8. M. R. Caira and R. Mohamed; *Acta Cryst.*, 1992, **B48**, 492

9. A. K. Basak, S. K. Mazumdar and S. Chaudhuri; *Acta Crsyt.*, 1983, **C39**, 492

10. R. K. Tiwari, M. Haridas and T. P. Sing; *Acta Cryst.*, 1984, **C40**, 655

11. A. Camerman; *Canadian J. Chem.*, 1970, **48**, 179

12. M. R. Truter; *J. Chem. Soc.*, 1962, 3400

13. A. M. O'Connel and E. N. Maslen; *Acta Cryst.*, 1967, **22**, 134

14. V. V. Joshi, R. K. Tiwari, T. C. Patel and T. P. Singh; *Indian J. Physics*, 1983, **57A**, 79

15. G. D. Munno, T. Poerio , M. Julve, F. Lloret and G. Viau; *New J. Chem.*, 1998, **3**, 299

16. C. –Z. Xie, B.-F. Zhang, X. –Q. Wang, G. –Q. Shen and D.-Z. Shen; *Acta Cryst.*, 2004, **E60**, m1703

17. M. U. Haque, C. N. Caughlan and K. Emerson; *Inorg. Chem.*, 1970, **9**, 2421

18. R. E. Cramer and J. T. Hunke; *Inorg. Chem.*, 1978, **17**, 365

19. C. L. Raston, A. H. White and A. C. Willis; *Aust. J. Chem.*, 1978, **31**, 415

20. J. D. Korp, I. Bernal, R. A. Palmer and J. C. Robinson; *Acta Cryst.*, 1980, **B36**, 560

21. J. G. H. D. Preez, H. E. Rohwer, B. J. van Brecht and M. R. Caira; *J. Chem. Soc., Dalton Trans.*,1984, 975

22. R. E. Cramer, W. van Doone and J. T. Hunke; *Inorg. Chem.*, 1976, **15**, 529

23. T. Mizuta, H. Yoneda and Y. Kushi; *Inorg. Chim. Acta*, 1987, **132**, 11

24. G. V. Romanenco, V. L. Varand, N. V. Podberezskaya, D. Y. Naumov, S. A. Gromilov and S. V. Larionov; *J. Struct. Chem.*, 2001, **42**, 1036

25. J. Ellermeier, C. Nather and Wolfgang Bensch; *Acta Cryst.*, 1999, **C55**, 501

26. H. –L. Liu, H. –Y. Mao, C. Xu, H. –Y. Zhang, H. –W. Hou, Q. –A. Wu, Y. Zhu, B. –X. Ye and L. –J. Yuan; *Polyhedron*, 2004, **23**, 1799

27. C. Xu, H. –Y. Mao, H. –Y. Zhang, Q. –A. Wu, H. –L. Liu, H. –W. Hou, Y. Zhu and G. Li; *J. Mol. Struct.*, 2003, **658**, 59

28. W. Lei, Q. Hao, L. Lu, Z. Yang and X. Wang; *J. Chem. Cryst.*, 2004, **34**, 387

29. S. Ooi, and Q. Fernando; *Inorg. Chem.*, 1976, **6**, 1558

30. S. X. Liu, C. C. Lin, Z. Xu, Y. P. Yu and X. Z. You; *China J. Org. Chem.*, 1987, **5**, 369

31. L. Escriche, J. A. Muñoz, J. Rosell, R. Kivekäs, R. Sillanpää, and J. Casabó; *Inorg. Chem.*, 1998, **37**, 4807

32. J. Lokaj, K. Gyerova, A. Sopkova, J. Sivy, V. Kettman and V. Vrabel; *Acta Cryst.*, 1991, **C47**, 2447

33. J. R. Anacona, N. Ramos, G. D. D. Delgado and E. M. Roque; *J. Coord. Chem.*, 2002, **55**, 901

34. L. A. Kovbasyuk, I. O. Frisky, V. N. Kokozay and T. S. Iskenderov; *Polyhedron*, 1997, **16**, 1723

35. H. –K. Fun, Q. –L. Hao, J. Wu, X. –J. Yang, L. Lu, X. Wang, S. Chantrapromma, I. A. Razak and A. Usman; *Acta Cryst.*, 2002, **C58**, m87

36. C. Kazak, V. T. Yilmaz and T. K. Yazicilar; *Acta Cryst.*, 2004, **E60**, m593

37. F. S. Stephens; *J. Chem. Soc.*, 1969, (**A**), 2233

38. B. –H. Ye, L. –N. Ji, F. Xue and T. C. W. Mak; *Polyhedron*, 1998, **17**, 2687

39. M. J. Begley, P. Hubberstey and J. Stroud; *Polyhedron*, 1997, **16**, 805

40. S. –J. Liu and C. –C. Su; *Polyhedron*, 1996, **15**, 1141

41. F. S. Stephens; *J. Chem. Soc.*, A, 1969, 833

42. J. Cernák, J. Chomic and W. Massa; *Acta Cryst.*, 2002, **C58**, m490

43. L. Gutierrez, G. Alzuet, J. Borras, A. Castineiras; A. Rodriguez-Fortea and E. Ruiz; *Inorg. Chem.*, 2001, **40**, 3089

44. Z. –D. Liu, M. –Y. Tan and H. –L. Zhu; *Acta Cryst.*, 2004, **E60**, m1081

45. D. Sonnenfroh and R. W. Kerilick; *Inorg. Chem.*, 1980, **19**, 1259

46. J. Casanova, G. Alzuet, J. LaTorre and J. Borras; *Inorg. Chem.*, 1997, **36**, 2052

47. J. C. Pedregosa, J. Casanova, G. Alzuet, J. Borrás, S. García-Granda, M. R. Diaz and A. Gutierrez-Rodriguez; *Inorg. Chim. Acta.*, 1995, **232**, 117

48. A. Nanthakumar, J. Miura, S. Diltz, C. –K. Lee, G. Aguirre, F. Ortega, J.W. Ziller and P. J. Walsh; *Inorg. Chem.*, 1999, **38**, 3010

49. J. Casanova, G. Alzuet, J. Borra´s, J. LaTorre, M. Sanau´, and S. Garcia-Granda; *J. Inorg. Biochem.*, 1995, **60**, 219

50. A. Pezeshk, and V. Pezeshk; *J. Inorg. Biochem.*, 1990, **38**, 185

51. V. M. Rao, D. N. Sathaynarayana and H. Manohar; *J. Chem. Soc., Dalton Trans.*, 1983, 2167

52. P. de Meester, S. R. Fletcher and A. C. Skapski; *J. Chem. Soc., Dalton Trans.*, 1975, 2575

53. Y. A. Simonov, V. I. Ivanov, T. I. Malinovskii and L. I. Landa; *Izv. Akad. Nauk. Mold. SSR, Ser. Fiz-Tekh. Mat. Nauk.*, 1976, **3**, 33

54. G. A. Barclay and C. H. L. Kennard; *J. Chem. Soc.*, 1961, 5244

55. F. Hanic, D. Stempelova and K. Hanikova; *Acta Cryst.*, 1964, **17**, 633

56. Y. A. Simonov, V. I. Ivanov, A. V. Ablov, L. N. Milkova and T. I. Malinovskii; *Zh. Strukt. Khim.*, 1976, **17**, 516

57. C. –H. Kwak, J. Jeong and J. Kim; *Inorg. Chem. Comm.*, 2001, **4**, 264

58. T. –Y. Lee, T. –J. Lee, C. –Y. Hong, M. –Y. Hsieh, D. –T. Wu and C. S. Chung; *Acta Cryst.*, 1986, **C42**, 1316 and the references therein.

59. T. G. M. Fawcett, S. M. Rudich, B. H. Toby, R. A. Lanlancette, J. A. Potenza and H. J. Schugar; *Inorg. Chem.*, 1980, **19**, 940

60. C.J. Brown, D.S. Cook and L. Sengier; *Acta Cryst.*, 1987, **C43**, 2332

61. N.C. Baenziger; *Acta Cryst.*, 1983, **C39**, 1620

62. R. –X. Yuan, R. –G. Xiong, Z. –F. Chen, P. Zhang, H. –X. Ju, Z. Dai, Z. –J. Guo, H. 2K. Fun and X. –Z. You; *J. Chem. Soc. Dalton Trans.*, 2001, 774

63. M. A. Torzilli, S. Colquhoun, D. Doucet and R. H. Beer; *Polyhedron*, 2002, **21**, 697

64. K. A. Fraser and M. M. Harding; *Acta Cryst.*, 1967, **22**, 75

65. E. Szłyk, A. Wojtczak, A. Surdykowski and M. Gozdzikiewicz; *Inorg. Chim. Acta*, 2005, **358**, 467

66. M. Bochmann, G. C. Bwembya, A. K. Powell and X. Song; *Polyhedron*, 1995, **14**, 3495

67. P. J. Toscano, P. T. DiMauro, S. Geremia, L. Randaccio and E. Zangrando; *Inorg. Chim. Acta*, 1994, **217**, 195

68. W. L. Steifen and G.J. Palenik; *Acta Cryst.*, 1976, **B32**, 298

69. M. Mazzanti, S. Gambarotta, C. Floriani, A. Chiesi-Villa and C. Guastini; *Inorg. Chem.*, 1986, **25**, 2308

70. P. G. Jones, I. Dix, A. J. Kirbyc and C. Beckmann; *Acta Cryst.*, 2003, **E59**, m171

71. A. Mondal, G. Mostafa, A. Ghosh, I. R. Laskar and N. R. Chaudhuri; *J. Chem. Soc., Dalton Trans.*, 1999, 9

72. H. Kurihara, S. Nishikiori and T. Iwamoto; *Chem. Lett.*, 1997, 61

73. C. A. Johns and K. M. A. Malik; *Polyhedron*, 2002, **21**, 395

74. L. Menabue and M. Saladini; *J. Inorg. Biochem.*, 1993, **49**, 201

75. S. Banerjee, A. Ghosh, B. Wu, P. –G. Lassahan and C. Janiak; *Polyhedron*, 2005, **24**, 593

76. Y. –F. Zhou, R. –H. Wang, B. –L. Wu, R. Cao and M. –C. Hong; *J. Mol. Struct.*, 2004, **697**, 73

77. B. –H. Ye, X. –M. Chen, F. Xue, L. –N. Ji and T. C. W. Mak; *Inorg. Chim. Acta*, 2000, **299**, 1

78. J. –H. Luo, M. –C. Hong, R. Cao, Y. –C. Liang, Y. –J. Zhao, R. –H. Wang and J. –B. Weng; *Polyhedron*, 2002, **21**, 893

79. C. A. Johns, G. M. G. Hossain, K. M. A. Malik, S. Z. Haider and U. K. R. Romman; *Polyhedron*, 2001, **20**, 721

80. A. B. Corradi, G. Lusvardi, L. Menabue, M. Saladini and P. Sgarabotto; *Polyhedron*, 1999, **18**, 1975

81. E. Labisbal, J. Romero, J. A. Garcia-Vasquez, C. Gomez, A. Sousa, R. Pritchard and C. A. McAuliffe; *Polyhedron*, 1994, **13**, 1735

82. J. A. Castro, J. Romero, J. A. Garcia-Vazquez, A. Sousa, E. E. Castellano and J. Zukerman-Schpector; *Polyhedron*, 1993, **12**, 31

83. T. Miyoshi, T. Iwamoto and Y. Sasaki; *Inorg. Chim. Acta*, 1972, **6**, 59

84. L. Li, B. Chen, Y. Song, G. Li, H. Hou, Y. Fan and L. Mi; *Inorg. Chim. Acta*, 2003, **344**, 95

85. J. S. Casas, M. S. García-Tasende and J. Sordo; *Coord. Chem. Rev.*, 1999, **193-195**, 283

86. K. K. Divine, F. Ayala-Fierro, D. S. Barber and D. E. Carter; *J. Toxicol. Environ. Health,* 1999, **A57**, 489

87. Z. Popovic, D. Matkovic-Calogovic, Z. Soldin, G. Pavlovic, N. Davidovic and D. Vikic-Topic; *Inorg. Chim. Acta*, 1999, **294**, 35

88. N-H. Hu, T. Norifusa and K. Aoki; *Polyhedron*, 1999, **18**, 2987

89. B. Gyurcsik and L. Nagy; *Coord. Chem. Rev.*, 2000, **203**, 81

90. D. M. L. Goodgame, S. P. W. Hill and D. J. Williams; *Polyhedron*, 1992, **11**, 1507

91. M. Saladini, L. Menabue, E. Ferrari and D. Iacopino; *J. Chem. Soc., Dalton Trans.*, 2001, 1513

92. F. Zamora, M. Sabat and B. Lippert; *Inorg. Chim. Acta*, 1998, **282**, 237

93. A. Hergold-Brundic, B. kamenar and G. Jovanovski; *Acta Cryst.*, 1989, **C45**, 556

94. J. –L. Tian, M. –J. Xie, S. –P. Yan, D. –Z. Liao, Z. –H. Jiang and P. Cheng; *Acta Cryst.*, 2004, **E60**, m1689 and the references therein.

95. S. Gao, J. –W. Liu, L. –H. Huo and H. Zhao; *Acta Cryst.*, 2004, **E60**, m1728

96. W.O. Gillum, J.C. Huffman, W.E. Streib, R. A. D. Wentworth; J. Chem. Soc., Chem. Commun., 1969, 843

97. G. Rajsekhar, C. P. Rao, K. Nättinen and K. Rissanen; *Inorg. Chem. Comm.*, 2003, **6**, 1156

98. M. D. Fryzuk, A. Carter, S. J. Rettig; *Organometallics*; 1992, **11**, 469

Chapter 5

SYNTHESIS AND STRUCTURAL STUDIES OF METAL COMPLEXES OF SULFATHIAZOLE WITH SECONDARY LIGANDS

COMPLEXES OF SULFATHIAZOLE

5.1 Introduction

Sulfathiazole (Figure 5.1) shows an extensive polymorphism, in fact highest among all the sulfa drugs.[1,2] It also has a remarkable solvate forming ability with interesting structural and conformational properties. Some 100 plus solvate containing sulfathiazoles are known and a lot of them have been studied crystallographically.[3] On the basis of these results, it has been suggested that different crystal structures in these systems can be explained in the presence of similar hydrogen bonding association but different supramolecular assemblies.

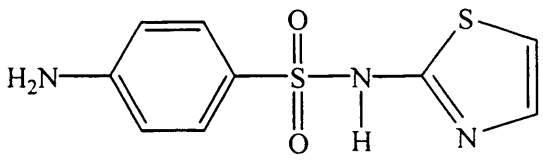

Figure 5.1: Structure of sulfathiazole

Shirotani *et al.*[4] described three solvates of sulfathiazole. Kruger *et al.* reported the crystal structures of polymorphs II[5], I[6] and III.[6] Hughes *et al.*[7] and Chan *et al.*[8] reported the polymorph V of sulfathiazole.

Caira *et al.*[9] reported the crystal structure of the 1:1 complex of sulfathiazole and cyclodextrin and these molecules are hydrogen bonded with each other making a layer and these layers are linked by hydrogen bonding with water molecules.

The deprotonated sulfonamidic nitrogen atom co-ordinates with a suitable metal(II) ion (Figure 5.2).

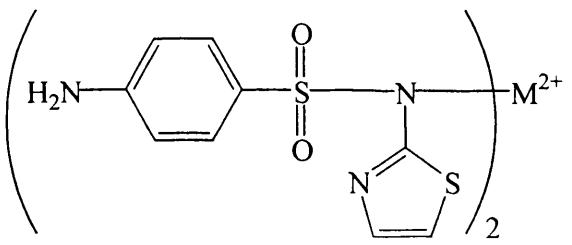

Figure 5.2

In addition to this, the other potential donor sites are sulfonyl oxygen atoms, amino and thiazolato nitrogen and sulfur atoms. But in this chapter we will discuss the complexes where the sulfathiazole acts as a counter ion.

Casanova *et al.*[10–13] reported some copper complexes of sulfathiazole with different secondary ligands such as the Cu(II) complex of dichlorodisulfathiazole ethanol $[Cu(stz)_2Cl_2].EtOH$[10] in which the Cu(II) ion is five coordinate with two nitrogen atoms from the amino ($-NH_2$) group of the two sulfathiazole molecules, two chloride ions and one oxygen atom from the ethanol molecule. The coordination polyhedron is intermediate between square pyramid and trigonal bipyramid and is very similar to the complex of dichlorodisulfathiazole methanol $[Cu(stz)_2Cl_2].MeOH$.[11] Both the complexes are triclinic with a space group of $P\bar{1}$ and are isostructural with the same arrangement of ligands about the metal centre.

The copper complex of chlorodisulfathiazole tris-(pyridine) $[Cu(stz)(py)_3Cl_2]$[12] is orthorhombic with the space group of *Pbca* and is a distorted square pyramid consisting of mononuclear units linked via hydrogen bonds to form the tridimensional pyramid.

The dimeric copper complex of sulfathiazole $[Cu_2(stz)_4]$ is orthorhombic with the space group of $P2_1cn$ in which the copper atom is four coordinate and the chromophore is CuN_4. There exists a metallic Cu–Cu bond in the complex.

Henderson *et al.*[14] described the platinum and palladium complexes of sulfathiazole. Again Casanova *et al.*[15] reported the copper complex of sulfathiazole with 1,2-dimethylimidazole ligand. Alzuet *et al.*[16] synthesised the copper complex of sulfathiazole with dimethyl sulfoxide and more recently Anacona *et al.*[17] reported the copper complex of sulfathiazole where sulfathiazole acts as a counter ion.

5.2 Experimental

5.2.1 Preparation of sulfathiazole nitrate $[(C_9H_{10}N_3O_2S_2][NO_3].H_2O$ (29)

Solid sulfathiazole (0.255g; 1 mmol) was dissolved in 1M HNO_3 (50 mL) and stirred for 30 minutes, filtered off and the clear solution was left at room temperature for crystallization. Pale yellow block crystals of sulfathiazole nitrate were obtained by slow evaporation of the solution. *Anal.* Found: C, 32.11, H, 3.57; N, 16.65%. Calc. for

$C_9H_{12}N_4O_6S_2$: C, 32.16; H, 3.55; N, 16.63%. IR: (KBr disc): cm^{-1}, 3510(b), 3410(s), 3375(m), 1621(s), 1535(vs), 1329(vs), 1269(vs), 1143(m), 933(m), 689(w), 627(vw).

5.2.2 Preparation of cobalt complex of sulfathiazole $[CoCl_4][(stz)_2].CH_3COOH$ (30)

Solid sulfathiazole (0.565g, 2 mmol) was dissolved in hot methanol and methanolic solution of $CoCl_2.6H_2O$ (0.238g, 1 mmol) was added with constant stirring. The purple precipitate was filtered off and dried over silica gel. It was dissolved in water in presence of acetic acid. After three days green crystals were obtained. *Anal.* Found: C, 31.03, H, 3.10; N, 10.86%. Calc. for $C_{20}H_{24}Cl_4CoN_6O_6S_4$: C, 31.10; H, 3.15; N, 10.75%. IR: (KBr disc): cm^{-1}, 3513(b), 3426(s), 3383(m), 1625(s), 1537(vs), 1331(vs), 1267(vs), 1141(m), 933(m), 689(w), 625(vw).

5.2.3 Preparation of the complex $[Cu(en)_2(H_2O)_2][(stz)_2].2H_2O$ (31)

Sodium salt of sulfathiazole (Nastz) (2 mmol) was dissolved in hot methanol and to this methanolic solution of $CuCl_2.2H_2O$ (1 mmol) was added with constant stirring. The pale blue precipitate was filtered off and dried over silica gel. It was again dissolved in 1:10 ethylenediamine:water solution and stirred for 30 min. The solution was filtered off and the filtrate was kept for crystallisation. After seven days purple crystals were obtained, filtered and dried over silica gel. The compound is soluble in water, DMF and DMSO. Anal. Found: C, 35.54, H, 5.23; N, 18.31%. Calc. for $C_{22}H_{40}CuN_{10}O_8S_4$: C, 35.48; H, 5.27; N, 18.35%. IR: (KBr disc): cm^{-1}, 3512(b), 3436(s), 3390(m), 1623(s), 1537(vs), 1328(vs), 1270(vs), 1141(m), 931(m), 687(w), 625(vw).

5.3 Results and discussion for the complexes (29), (30) and (31)

5.3.1 IR Spectra

The bands at 3510, 3513 and 3512 cm^{-1} are assigned to O–H of water molecules in (**29**) and (**30**) and acetic acid in (**31**) respectively. The bands at 3410 and 3375 cm^{-1} for (**29**), 3426 and 3383 cm^{-1} for (**31**) are assigned to *as*(N–H) and *sy*(N–H) vibrations of the $-NH_2$ group which are shifted with respect to those of the free sulfathiazole (3349 and 3319 cm^{-1}). The bands due to *as*(SO_2) at 1328 – 1331 cm^{-1} and *sy*(SO_2) at 1141 – 1137 cm^{-1} remain unchanged. There is no change of the bands at 1537, 933 and 625 – 687 cm^{-1} assigned to the characteristic thiazole ring, (S–N) and (C–S) vibrations respectively.

5.3.2 Crystal structures of the complexes (29), (30) and (31)

The crystal data and refinement details for (**29**), (**30**) and (**31**) are summarized in Table 5.1. The compounds (**29**) and (**30**) are new complexes and have been characterised by X-ray diffraction methods and the complex (**31**) was published recently.[17]

Table 5.1: Crystal data and details of data collection and structure refinement for the complexes (29), (30) and (31)

	(29)	(30)	(31)
Empirical Formula	$C_9H_{12}N_4O_6S_2$	$C_{20}H_{24}Cl_4CoN_6O_6S_4$	$C_{22}H_{40}CuN_{10}O_8S_4$
Formula Weight	336.35	773.42	764.42
Crystal System	Monoclinic	Triclinic	Triclinic
Space Group	$P\,2_1/c$	$P\bar{1}$	$P\bar{1}$
a(Å)	12.1917(2)	8.07940(10)	7.3770(2)
b(Å)	7.6348(2)	10.98430(10)	8.2760(2)
c(Å)	15.3895(2)	18.1087(2)	13.5565(4)
α(°)	90	83.3332(4)	78.4912(8)
β(°)	107.4660(10)	83.5157(4)	86.0748(8)
γ(°)	90	72.5918(6)	82.0850(10)
V/Å^3	1366.43(5)	1517.91(3)	802.57(4)
Z	4	2	1
T/K	150	150	150
Crystal Size/mm	0.18×0.15×0.12	0.25×0.22×0.20	0.18×0.15×0.10
Shape	Block	Block	Block
Color	White	Green	Purple
θ-range for data collection	3.01 – 27.49	2.97 – 27.38	3.07 – 27.43
Reflection Collected	17799	24140	14729
Unique Reflections	3117	6716	3642
R_{int}	0.0813	0.0271	0.0743
Index ranges	−15<=h<=15 −9<=k<=9 −19<=l<=18	−10<=h<=10 −14<=k<=14 −23<=l<=23	−9<=h<=9 −10<=k<=10 −17<=l<=17
Data/parameters	3117/214	6716/411	3642/229
Final R indices [I>2σ(I)]	0.0377/0.1003	0.0270/0.0800	0.0382/0.0891
R indices (all data)	0.0456/0.1055	0.0287/0.0810	0.0491/0.0947
Largest diff. peak and hole e.Å^{-3}	0.465 and −0.605	0.588 and −0.497	0.588 and −0.748

5.3.2.1 Structure of the complex $[(C_9H_{10}N_3O_2S_2][NO_3].H_2O$ (29)

An ORTEP drawing of the sulfathiazole nitrate is shown in Figure 5.3 together with the crystallographic atom numbering scheme used. The sulfathiazole molecule is hydrogen bonded with nitrate ion which is also hydrogen bonded with a water molecule present in the complex. The sulfathiazole molecule is positively charged gaining one proton on its terminal amino group. The O(1) atom of the nitrate ion is hydrogen bonded with the

H(13A) atom of the amino group of sulfathiazole and O(2) is hydrogen bonded with H(4A) atom of the water molecule.

The planes of the phenyl and thiazole rings are inclined in a *Gauche* conformation about S(12)–N(11) bond with a torsion angle of 87.63(6)°. The crystal structure is stabilized by network hydrogen bonds and van der Waals' interactions.

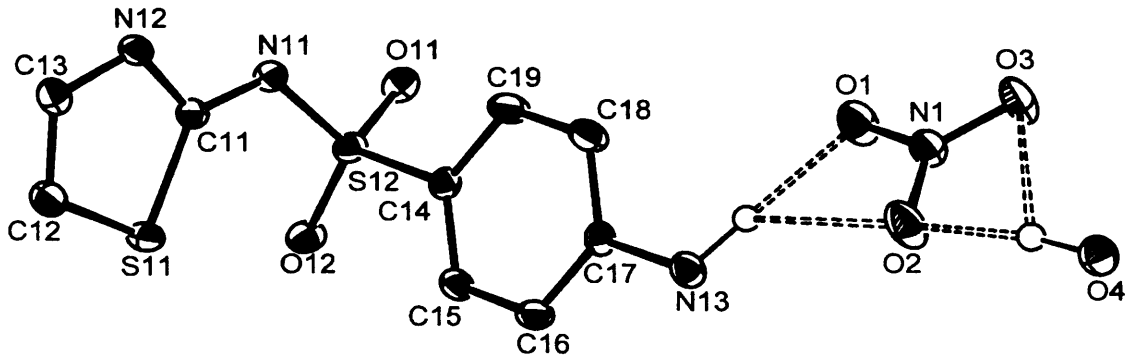

Figure 5.3
*X-ray structure of the complex sulfathiazole nitrate [($C_9H_{10}N_3O_2S_2$][NO_3].H_2O (**29**) showing crystallographic atom numbering scheme used. Thermal ellipsoids are drawn at 50% probability level. The hydrogen atoms are omitted for clarity. Intermolecular hydrogen bonds are indicated by dashed lines.*

The bond angles in the benzene ring differ slightly from the theoretical value of 120°. The C(17)–N(13) bond distance of 1.462(2)Å is slightly longer than the corresponding bond in sulfathiazole III[6] and in good agreement with the distance proposed by Camerman[18] for the length of C(sp^2)–N(sp^2) single bond of 1.470(5)Å.

The S(12)–C(14) bond distance of 1.774(2)Å is slightly longer than the theoretical S–C(sp^2) value (1.75Å) calculated from the atomic radii and electronegativities given by Truter[19] and with the experimental data obtained for sulfonamides.[20–23]

The S(12)–O distances of 1.444(2) and 1.457(2)Å are slightly longer than the corresponding bonds with values of 1.42(1) and 1.43(1)Å in sulfaguanidine monohydrate,[24] 1.41(2) and 1.42(2)Å in sulfadiazine,[25] 1.424(4) and 1.435(3)Å and 1.414(4) and 1.431(3)Å in sulfamerazine[26] and 1.431(2) and 1.435(2)Å and 1.426(8) and 1.430(6)Å in sulfamethazine.[27,28] This is due to the presence of the negative nitrate ion in the complex.

Table 5.2: Selected bond lengths [Å] and angles [°] in $[(C_9H_{10}N_3O_2S_2][NO_3].H_2O$ (29)

Bond	(Å)	Bond	(Å)
S(11)–C(13)	1.732(2)	S(11)–C(11)	1.736(2)
S(12)–O(12)	1.444(2)	S(12)–O(11)	1.457(2)
S(12)–N(11)	1.582(2)	S(12)–C(14)	1.774(2)
N(11)–C(11)	1.344(2)	N(12)–C(11)	1.335(2)
N(12)–C(12)	1.384(2)	N(13)–C(17)	1.462(2)
C(12)–C(13)	1.335(3)	C(14)–C(15)	1.381(2)
C(14)–C(19)	1.398(2)	C(15)–C(16)	1.392(2)
C(16)–C(17)	1.382(2)	C(17)–C(18)	1.382(2)
C(18)–C(19)	1.384(3)		
Angle	**(°)**	**Angle**	**(°)**
C(13)–S(11)–C(11)	90.84(8)	O(12)–S(12)–O(11)	117.06(8)
O(12)–S(12)–N(11)	114.68(8)	O(11)–S(12)–N(11)	104.67(8)
O(12)–S(12)–C(14)	106.87(8)	O(11)–S(12)–C(14)	106.67(8)
N(11)–S(12)–C(14)	106.17(8)	C(11)–N(11)–S(12)	120.76(13)
C(11)–N(12)–C(12)	115.14(15)	N(12)–C(11)–N(11)	119.41(15)
N(12)–C(11)–S(11)	109.85(12)	N(11)–C(11)–S(11)	130.74(14)
C(13)–C(12)–N(12)	112.90(17)	C(12)–C(13)–S(11)	111.26(14)
C(15)–C(14)–C(19)	121.33(15)	C(15)–C(14)–S(12)	120.22(13)
C(19)–C(14)–S(12)	118.45(13)	C(14)–C(15)–C(16)	119.52(15)
C(17)–C(16)–C(15)	118.86(15)	C(18)–C(17)–C(16)	121.95(16)
C(18)–C(17)–N(13)	118.90(15)	C(16)–C(17)–N(13)	119.15(15)
C(17)–C(18)–C(19)	119.43(16)	C(18)–C(19)–C(14)	118.90(16)

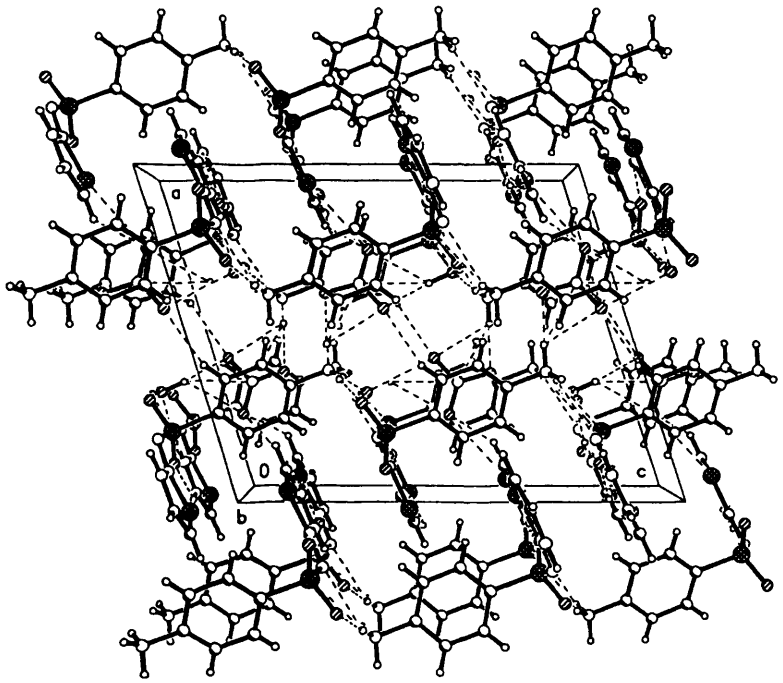

Figure 5.4
Packing diagram of the complex (29) where the hydrogen bonds are shown by dashed lines

In this compound the sulfathiazole acquires a positive charge on its amino ($-NH_2$) group forming a $[-NH_3]^+$ cation that is balanced by the negative nitrate ion. In the nitrate ion the bond distances of O(1)–N(1) = 1.261(2)Å, O(2)–N(1) = 1.263(2)Å and O(3)–N(1) = 1.236(2)Å and the O–N–O angles of O(1)–N(1)–O(2 = 119.04(15)°, O(3)–N(1)–O(2) = 120.16(15)° and O(3)–N(1)–O(1) = 120.80(15)° are in agreement with the planar configuration. The H–O–H angle of 103(2)° is very similar to the theoretical value of the tetrahedral configuration of a water molecule.

Table 6.3: The hydrogen bonds in $[(C_9H_{10}N_3O_2S_2][NO_3].H_2O$ (29) (distances and angles given in [Å] and [°] respectively)

Donor-H	Donor...Acceptor	H...Acceptor	Donor-H.....Acceptor
N13 -H13A 0.948(5)	N13 ....O1 (0) 2.765(5)	H13A...O1 (0) 1.818(5)	N13 -H13A...O1 (0) 177.47(6)
N13 -H13A 0.948(5)	N13 ....N1 (0) 3.308(4)	H13A...N1 (0) 2.467(3)	N13 -H13A...N1 (0) 147.92(4)
O4 -H4A 0.945(7)	O4 ....O2 (0) 2.803(1)	H4A ...O2 (0) 1.867(1)	O4 -H4A ...O2 (0) 170.21(5)
N12 -H12A 0.945(5)	N12 ....O4 (1) 2.905(4)	H12A...O4 (1) 2.002(5)	N12 -H12A...O4 (1) 159.27(2)
O4 -H4B 0.945(2)	O4 ....O11 (1) 2.881(3)	H4B ...O11 (1) 1.966(6)	O4 -H4B ...O11 (1) 162.12(1)
N13 -H13C 0.883(3)	N13 ....O11 (2) 2.907(2)	H13C...O11 (2) 2.026(3)	N13 -H13C...O11 (2) 175.68(2)
N13 -H13B 0.949(2)	N13 ....O4 (3) 2.857(2)	H13B...O4 (3) 1.910(2)	N13 -H13B...O4 (3) 174.89(1)

Equivalent positions:
(0) x, y, z; (1) –x+1, +y+½, –z+½; (2) x, –y+½, +z–½; (3) –x+1, –y, –z

5.3.2.2 Structure of the complex $[CoCl_4][(stz)_2].CH_3COOH$ (30)

The crystal structure of the complex $[CoCl_4][(H_2stz)_2].CH_3COOH$ (**30**) is shown in Figure 5.6. It is found that there is no direct bonding of sulfathiazole with the cobalt atom and the solid state structure consists of $[CoCl_4]^{2-}$ anions and the protonated sulfathiazole $[stzH_2]^+$ cation in the ratio of 1:2. In addition there is, in the crystal lattice, one molecule of acetic acid per metal centre. All these species are held together in the crystal by an extensive hydrogen bonding network which is shown in packing diagram (Figure 5.9).

The structural determination shows that the sulfathiazole molecule (**A**) is protonated in the complex (**30**) and becomes a cation like (**B**).

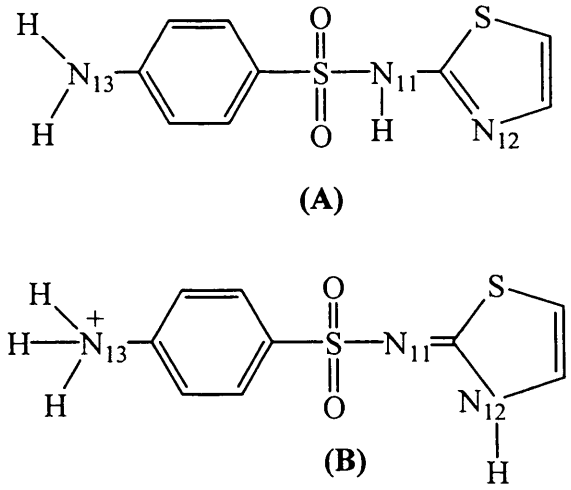

*Figure 5.5: Neutral molecule (**A**) is protonated to form a positive cation (**B**)*

Moreover, the hydrogen atom shifted from N(11) to N(12) and has brought some changes in bond lengths and angles in the neutral molecules.

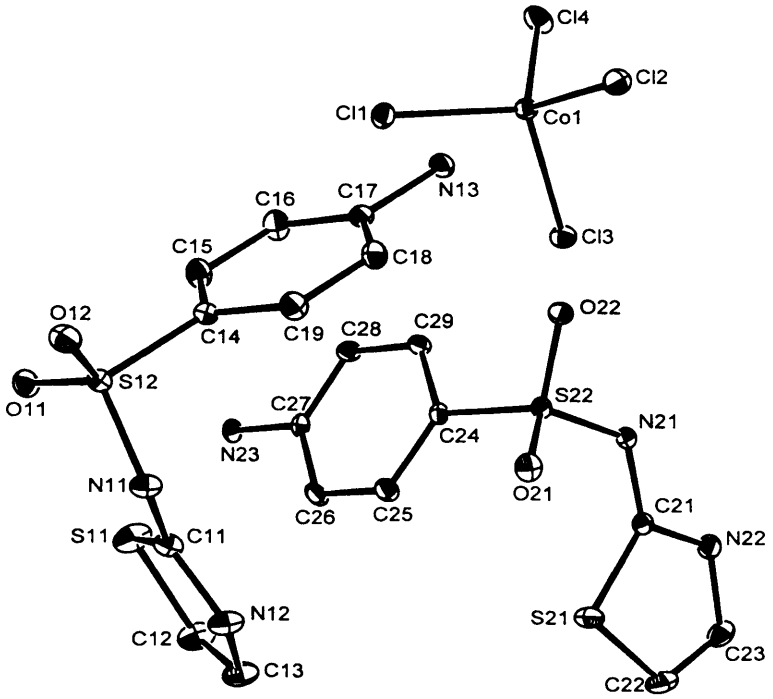

Figure 5.6
*X-ray structure of the complex $[CoCl_4][(stzH_2)_2].CH_3OH$ (**30**) showing crystallographic atom numbering scheme used. Thermal ellipsoids are drawn at 50% probability level. Hydrogen atoms and acetic acid molecule are omitted for clarity.*

The cobalt atom in the $[CoCl_4]^{2-}$ anion is four coordinate with tetrahedral geometry with four chloride ligands. The bond distances in $[CoCl_4]^{2-}$ anion are Co–Cl(1) = 2.276(1)Å, Co–Cl(2) = 2.290(1)Å, Co–Cl(3) = 2.278(1)Å and Co–Cl(4) = 2.266(1)Å which are comparable to the corresponding bonds in 1,3-diammonium tetrachlorocobaltate $[CoCl_4][C_3H_{12}N_2]$[29] with the values of Co–Cl(1) = 2.273(2)Å, Co–Cl(2) = 2.282(2)Å, Co–Cl(3) = 2.278(3)Å and Co–Cl(4) = 2.258(2)Å, in bis(4-dimethylaminopyridinium) tetrachlorocobaltate [4DMAP]-$[CoCl_4]$[30] with the values of Co–Cl(1) = 2.2754(11)Å, Co–Cl(2) = 2.2683(11)Å, Co–Cl(3) = 2.2813(11)Å and Co–Cl(4) = 2.2668(11)Å and in bis-[1,3-(diammonium-methyl)benzene] tetrachlorocobaltate [DAMB]$[CoCl_4]$[30] with the values of Co–Cl(1) = 2.2664(7)Å, Co–Cl(2) = 2.2768(7)Å, Co–Cl(3) = 2.2666(7)Å and Co–Cl(4) = 2.2557(7)Å.

Table 5.4: Selected bond lengths [Å] and angles [°] in the complex (30)

Bond	(Å)	Bond	(Å)
Co(1)–Cl(1)	2.276(5)	Co(1)–Cl(2)	2.290(5)
Co(1)–Cl(3)	2.278(5)	Co(1)–Cl(4)	2.266(5)
S(11)–C(11)	1.731(2)	S(11)–C(13)	1.733(2)
S(12)–O(11)	1.440(1)	S(12)–O(12)	1.449(2)
S(12)–N(11)	1.596(2)	S(12)–C(14)	1.771(2)
N(11)–C(11)	1.336(2)	N(12)–C(11)	1.337(2)
N(12)–C(12)	1.380(2)	N(13)–C(17)	1.471(2)
S(21)–C(23)	1.731(2)	S(21)–C(21)	1.731(2)
S(22)–O(21)	1.437(2)	S(22)–O(22)	1.451(2)
S(22)–N(21)	1.602(2)	S(22)–C(24)	1.771(2)
Angle	**(°)**	**Angle**	**(°)**
Cl(4)–Co(1)–Cl(1)	113.05(2)	Cl(4)–Co(1)–Cl(3)	106.89(2)
Cl(1)–Co(1)–Cl(3)	109.39(2)	Cl(4)–Co(1)–Cl(2)	115.65(2)
Cl(1)–Co(1)–Cl(2)	103.75(2)	Cl(3)–Co(1)–Cl(2)	107.93(2)
C(11)–S(11)–C(13)	90.84(9)	O(11)–S(12)–O(12)	117.37(8)
O(11)–S(12)–N(11)	113.33(8)	O(12)–S(12)–N(11)	104.70(8)
O(11)–S(12)–C(14)	107.74(8)	O(12)–S(12)–C(14)	107.90(8)
C(23)–S(21)–C(21)	91.22(9)	O(21)–S(22)–O(22)	117.78(8)
O(21)–S(22)–N(21)	112.99(8)	O(22)–S(22)–N(21)	103.66(7)
O(21)–S(22)–C(24)	107.29(8)	O(22)–S(22)–C(24)	107.47(8)
N(22)–C(21)–S(21)	109.66(12)		

The acidic hydrogen atom in the acetic acid molecule is distributed to both of the oxygen atoms in the ratio of 40% and 60%. These two hydrogen atoms are in equatorial position with each other.

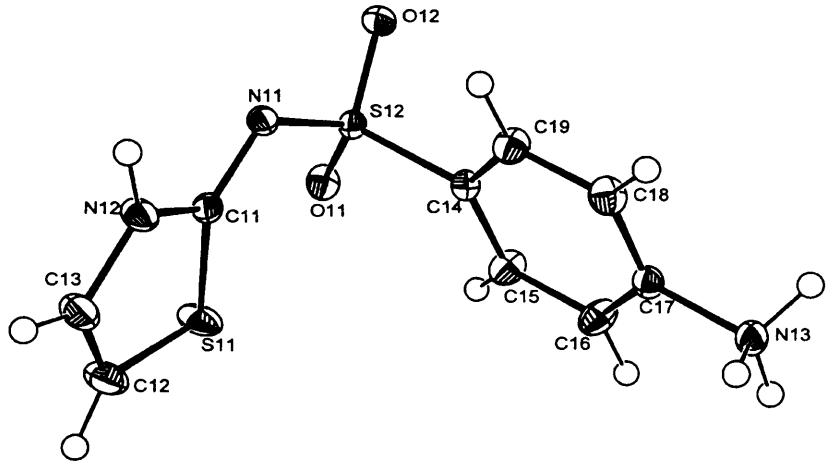

Figure 5.7
*X-ray structure of sulfathiazole cation (**30A**) in the complex (**30**) showing crystallographic atom numbering scheme used. Thermal ellipsoids are drawn at 50% probability level.*

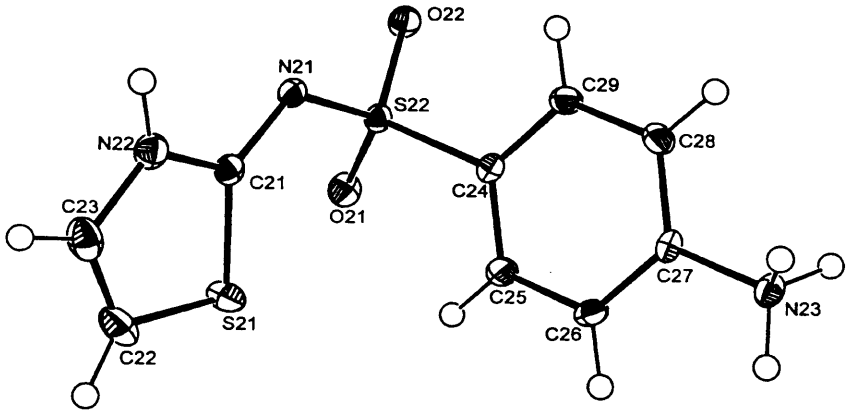

Figure 5.8
*X-ray structure of sulfathiazole cation (**30B**) in the complex (**30**) showing crystallographic atom numbering scheme used. Thermal ellipsoids are drawn at 50% probability level.*

The two sulfathiazole cations in the complex (**30**) have a different conformation. The torsion angles C11–N11–S11–C14 for molecule (**30A**) is 76.00(10)° whereas that for the molecule (**30B**) it is 80.90(10)°. The dihedral angles between the planes of the phenyl ring and thiazole ring is 88.30(6)° for (**30A**) and 79.65(5)° for (**30B**). The dihedral angles of the previous one is larger than the later one because the previous is very close to the acetic acid molecule present in the complex.

Several hydrogen bonds and van der Waals' interactions exist in the crystal to hold them together. These are shown in the packing diagram (Figure 5.9) by dashed lines.

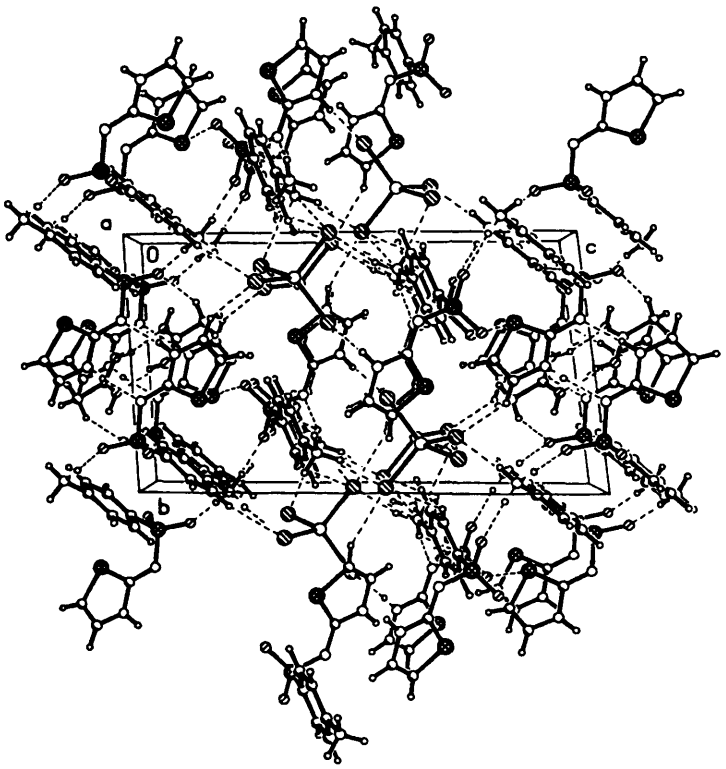

Figure 5.9
*Packing diagram of the complex (**30**) where the hydrogen bonds are shown by dashed lines*

Table 6.5: Possible hydrogen bonds (distances and angles given in [Å] and [°] respectively) for $[CoCl_4][(H_2stz)_2].CH_3COOH$ (30)

Donor-H	Donor...Acceptor	H...Acceptor	Donor-H.....Acceptor
N13 -H13B	N13 ....O22 (0)	H13B...O22 (0)	N13 -H13B...O22 (0)
0.946(1)	2.766(1)	1.843(6)	164.57(3)
N13 -H13C	N13 ....Cl1 (0)	H13C...Cl1 (0)	N13 -H13C...Cl1 (0)
0.946(7)	3.194(1)	2.254(8)	171.82(4)
N12 -H12A	N12 ....N11 (1)	H12A...N11 (1)	N12 -H12A...N11 (1)
0.947(7)	2.847(1)	1.920(5)	165.46(4)
O1 -H1	O1 ....O2 (2)	H1 ...O2 (2)	O1 -H1 ...O2 (2)
0.953(2)	2.623(2)	1.755(1)	149.74(6)
N13 -H13A	N13 ....O12 (3)	H13A...O12 (3)	N13 -H13A...O12 (3)
0.945(2)	2.792(2)	1.847(2)	178.67(4)
N23 -H23C	N23 ....N21 (4)	H23C...N21 (4)	N23 -H23C...N21 (4)
0.949(2)	3.024(2)	2.087(2)	169.12(2)
N23 -H23A	N23 ....Cl2 (4)	H23A...Cl2 (4)	N23 -H23A...Cl2 (4)
0.949(1)	3.226(3)	2.309(3)	162.34(3)

Equivalent positions:
(0) x, y, z; (1) -x+2,-y-1,-z; (2) -x+1,-y-1,-z; (3) -x+1,-y,-z; (4) x+1,+y,+z

5.3.2.3 Structure of $[Cu(en)_2(H_2O)_2][(stz)_2].2H_2O$ (31)

The crystal structure of the complex $[Cu(en)_2(H_2O)_2][(stz)_2].2H_2O$ (**31**) is shown in Figure 5.10 together with the crystallographic atom numbering scheme used. Selected bond lengths and angles and the hydrogen bond dimensions are given in Tables 5.6 and 5.7.

Complex (**31**) is the formation of a "cation-anion pair" involving the $[Cu(en)_2(H_2O)_2]^{2+}$ cation and the $[stz]^-$ anion which are held together in the crystal by very strong intermolecular hydrogen bonds and van der Waals' interactions.

The structure has a Jahn-Teller distorted octahedral geometry around the Cu(II) with four equatorially *N*-coordinated ethylenediamine molecules forming the base and two axial O-atoms from two molecules of water.

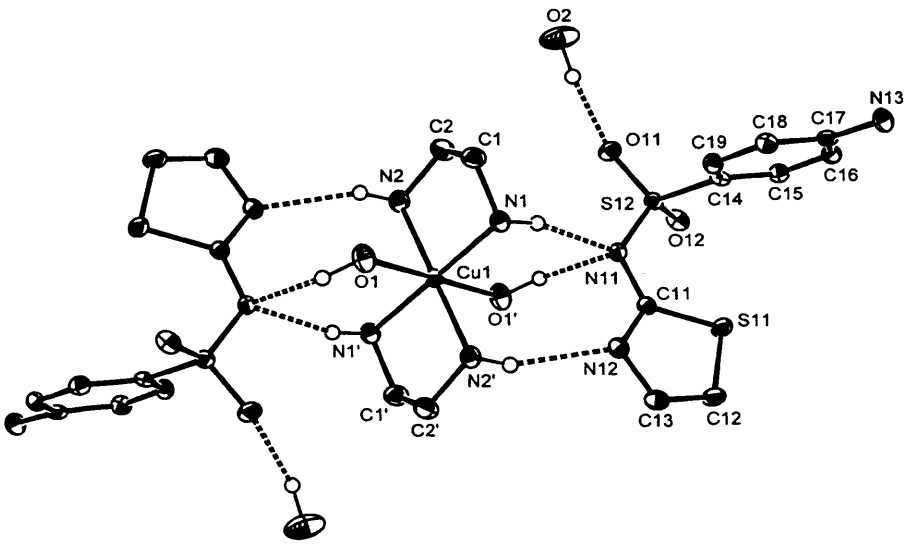

Figure 5.10
X-ray structure of the complex $[Cu(en)_2(H_2O)_2][(stz)_2].2H_2O$ (31) showing crystallographic atom numbering scheme used. Thermal ellipsoids are drawn at 50% probability level. The hydrogen atoms are omitted for clarity.

The elements of the structure are joined to each other in the crystal packing by means of extended systems of hydrogen bonds where the protons belonging to the water molecules or NH_2 groups of ethylenediamine molecules act as donors.

The cation contains two ethylenediamine molecules that coordinate the Cu atom in the equatorial plane in chelate mode and two water molecules occupying the apical positions of the elongated octahedral structure.

The Cu–N bond distances of 2.029(2) and 2.030(2)Å involving ethylenediamine molecules are similar to the values of 2.042(3) and 2.033(3)Å found in the same complex reported by Anacona *et al.*[17] and are also comparable with the corresponding bonds in the previous complexes (**6**), (**8**) and (**9**) and 1.997(3) and 2.001(3)Å in bis(en)copper(II) tetrachloronickelate $[Cu(en)_2][Ni(CN)_4]$,[31] 2.007(3) – 2.024(3)Å in diaquabis(en)copper(II) *N*-carboxyglycinate $[Cu(en)_2(H_2O)_2][OOCCH_2NHCOO].H_2O$[32] and 1.996(2) and 2.022(2)Å in diaquabis(en)copper(II) ethylenediaminebicarboxylate $[Cu(en)_2(H_2O)_2][OOCNHCH_2CH_2NHCOO].2H_2O$.[32]

The Cu-O bond distances of 2.466(2)Å are elongated due to the Jahn-Teller effect. These bonds are comparable with the corresponding bonds in the previous complexes (**8**) and (**9**) and shorter than the corresponding bonds with the values of 2.591(3)Å and 2.741(3)Å in the complex $[Cu(en)_2(H_2O)_2][OOCCH_2NHCOO].H_2O$[32] and 2.556(2)Å in the complex $[Cu(en)_2(H_2O)_2][OOCNH_2CH_2NHCOO].2H_2O$.[32]

Table 5.6: Selected bond lengths [Å] and angles [°] in complex (31)

Bond	(Å)	Bond	(Å)
Cu(1)–N(1)	2.029(2)	Cu(1)–N(2)	2.030(2)
Cu(1)–O(1)	2.466(2)	S(11)–C(12)	1.724(2)
S(12)–O(11)	1.455(2)	S(12)–O(12)	1.456(2)
S(12)–N(11)	1.580(2)	S(12)–C(14)	1.762(2)
N(11)–C(11)	1.368(3)	N(13)–C(17)	1.382(3)
Angle	**(°)**	**Angle**	**(°)**
N(1)–Cu(1)–N(1')	180.00(1)	N(1)–Cu(1)–N(2)	84.24(8)
N(1') –Cu(1) –N(2)	95.76(8)	N(2')–Cu(1)–N(2)	180.00(1)
C(12)–S(11)–C(11)	89.58(11)	O(11)–S(12)–O(12)	114.74(10)
O(11)–S(12)–N(11)	105.23(10)	O(12)–S(12)–N(11)	113.88(10)
O(11)–S(12)–C(14)	108.38(10)	O(12)–S(12)–C(14)	106.06(10)

Symmetry transformations used to generate equivalent atoms: (') $-x+1, -y+1, -z+2$

The N–Cu–N *trans* angles are 180° and the *cis* angles have values ranging from 84.87(12) to 95.13(12)° which shows the regular octahedral arrangement in the complex.

In the sulfathiazole anions, the C(11)–N(11) bond distance of 1.368(3)Å is increased from that of the free ligand due to the formation of hydrogen bonds with the cationic species in the complex.

Table 6.7: Possible hydrogen bonds (distances and angles given in Å and deg respectively) for $[Cu(en)_2(H_2O)_2][(stz)_2].2H_2O$ (31)

Donor-H	Donor...Acceptor	H...Acceptor	Donor-H.....Acceptor
N1 -H1B 0.920(1)	N1 ....N11 (0) 3.096(2)	H1B ...N11 (0) 2.198(2)	N1 -H1B ...N11 (0) 164.95(2)
O2 -H2E 0.946(2)	O2 ....O11 (0) 2.779(3)	H2E ...O11 (0) 1.957(3)	O2 -H2E ...O11 (0) 144.12(7)
N13 -H13A 0.947(5)	N13 ....O2 (1) 3.305(2)	H13A...O2 (1) 2.488(2)	N13 -H13A...O2 (1) 144.58(3)
N13 -H13A 0.947(5)	N13 ....O11 (1) 3.241(1)	H13A...O11 (1) 2.424(1)	N13 -H13A...O11 (1) 144.31(2)
N1 -H1A 0.920(4)	N1 ....N13 (2) 3.222(1)	H1A ...N13 (2) 2.456(1)	N1 -H1A ...N13 (2) 140.78(2)
N13 -H13B 0.947(2)	N13 ....N12 (2) 3.118(3)	H13B...N12 (2) 2.175(2)	N13 -H13B...N12 (2) 173.56(3)
O1 -H1F 0.948(4)	O1 ....O2 (3) 2.756(4)	H1F ...O2 (3) 1.831(4)	O1 -H1F ...O2 (3) 164.49(4)
O1 -H1E 0.947(7)	O1 ....N11 (4) 2.928(7)	H1E ...N11 (4) 2.070(9)	O1 -H1E ...N11 (4) 149.95(5)
N2 -H2B 0.920(1)	N2 ....N12 (4) 3.150(1)	H2B ...N12 (4) 2.308(6)	N2 -H2B ...N12 (4) 152.14(2)
N2 -H2A 0.920(1)	N2 ....O11 (5) 3.160(4)	H2A ...O11 (5) 2.390(2)	N2 -H2A ...O11 (5) 141.29(2)
O2 -H2F 0.948(3)	O2 ....O12 (6) 2.777(3)	H2F ...O12 (6) 1.876(3)	O2 -H2F ...O12 (6) 157.87(9)

Equivalent positions:
(0) x,y,z; (1) -x+1,-y,-z+1; (2) -x+1,-y+1,-z+1; (3) x,+y+1,+z; (4) -x+1,-y+1,-z+2; (5) -x+1,-y,-z+2; (6) x-1,+y,+z

The ethylenediamine molecules in the cation $[Cu(en)_2(H_2O)_2]^{2+}$ are hydrogen bonded with $[stz]^-$ anions through N(1)–H(1B)...N(11) and N(2)–H(2B)...N(12) and the water molecule through O(1)–H(1E)---N(11). The lattice water molecule is also hydrogen bonded with the sulfonyl oxygen atom of sulfathiazole through O(2)–H(2E)---O(11). These hydrogen bonds are shown by dashed lines in the packing diagram (Figure 5.11).

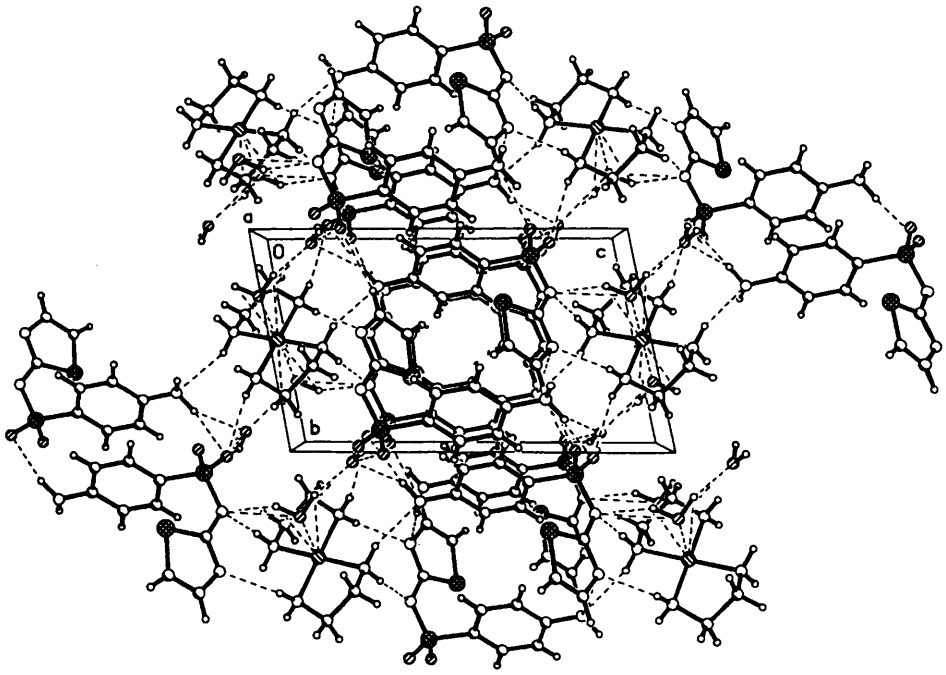

Figure 5.11
Packing diagram of the complex (31) where the hydrogen bonds are shown by dashed lines

5.4 Summary

The complexes (**30**) and (**31**) consist of discrete molecules of $[CoCl_4]^{2-}$ anion and $[Cu(en)_2(H_2O)]^{2+}$ cation with $[H_2stz]^+$ cation and $[stz]^-$ anion respectively, held together by hydrogen bonds and van der Waals' interactions. The $[CoCl_4]^{2-}$ anion has a four coordinate tetrahedral geometry and the $[Cu(en)_2(H_2O)_2]^{2+}$ cation has a six coordinate octahedral geometry.

The octahedral geometry in (**31**) is distorted slightly with the *cis* and *trans* angle lying, respectively, in the ranges 84.24(8)°-95.76(8)° and 180.00°. The tetrahedral geometry around the Co(II) atom in (**30**) shows variance from the ideal angles, with values in the range of 103.75(2)°–115.65(2)°.

References

1. M. Kuhnert-Brandstaetter; *Thermomicroscopy in the Analysis of Pharmaceuticals,* Pergamon Press, Oxford, 1974

2. S. Yang and J. K. Guillory; *J. Pharm. Sci.*, 1972, **61**, 26

3. A. L. Bingham, D. S. Hughes, M. B. Hursthouse, R. W. Lancaster, S. Tavener and T. L. Threlfall; *Chem. Commun.*, 2001, **7**, 603

4. K. -I. Shirotani, E. Suzuki and K. Sekiguchi; *Chem. Pharm. Bull.*, 1983, **31**, 2085

5. G.J. Kruger and G. Gafner; *Acta Cryst.*, 1971, **B27**, 326

6. G.J. Kruger and G. Gafner; *Acta Cryst.*, 1972, **B28**, 272

7. D. S. Hughes, M. B. Hursthouse, T. Threlfall and S. Tavener; *Acta Cryst.*, 1999, **C55**, 1831

8. F. C. Chan, J. Anwar, R. Cernik, P. Barnes and R. M. Wilson; *J. Appl. Cryst.*, 1999, **32**, 436

9. M. R. Caira, V. J. Griffith, L. R. Nassimbeni, R. Luigi and B. V. Oudtshoom; *J. Inclus. Phen. Mole. Recog. Chem.*, 1994, **17**, 187

10. J. Casanova, G. Aluzet, J. Borras, J. Timoneda, S. Garcia-Granda and I. Candano-Gonzalez; *J. Inorg. Biochem.*, 1994, **56**, 65

11. J. Casanova, G. Aluzet, S. Ferrer, J. Borras, S. Garcia-Granda and E. Perez-Carreno; *J. Inorg. Biochem.*, 1993, **51**, 689

12. J. Casanova, G. Aluzet, J. Borras, J. Latorre, M. Sanau and S. Garcia-Granda; *J. Inorg. Biochem.*, 1995, **60**, 219

13. J. Casanova, G. Aluzet, J. Latorre, M. Sanau and J. Borras; *Inorg. Chem.*, 1997, **36**, 2052

14. W. Henderson, L.J. McCaffrey, M.B. Dinger and B.K. Nicholson; *Polyhedron*, 1998, **17**, 3137

15. J. Casanova, G. Aluzet, J. Borras and O. Carugo; *J. Chem. Soc. Dalton Trans.*, 1996, 2239

16. G. ALzuet, J. A. Real, R. Santiago-Garcia and S. Garcia-Granda; *Inorg. Chem.*, 2001, **40**, 2420

17. J.R. Anacona, N. Ramos, G.D.D. Delgado and E. M. Roque; *J. Coord. Chem.*, 2002, **55**, 901

18. A. Camerman; *Canad. J. Chem.*, 1970, **48**, 179

19. M. R. Truter; *J. Chem. Soc.*, 1962, 3400

20. B. H. O'Conner B.H and E. N. Maslen; *Acta Cryst.*, 1965, **18**, 363

21. B. H. O'Conner and E. N. Maslen; *Acta Cryst.*, 1967, **22**, 134

22. M. Alkaume and J. Decap; *Acta Cryst.*, 1965, **18**, 731

23. M. Alkaume and J. Decap; *Acta Cryst.*, 1965, **19**, 394

24. C. H. Koo, H. S. Kim, W. C. Shin and C. H. Choe; *J. Korean Chem. Soc.*, 1974, **18**, 97

25. H. S. Shin, G. S. Ihn, H. S. Kim and C. H. Koo; *J. Korean Chem. Soc.*, 1974, **18**, 329

26. M. R. Caira and R. Mohamed; *Acta Cryst.*, 1992, **B48**, 492

27. A. K. Basak, S. K. Mazumdar and S. Chaudhuri; *Acta Crsyt.*, 1983, **C39**, 492

28. R. K. Tiwari, M. Haridas and T. P. Singh; *Acta Crsyt.*, 1984, **C40**, 655

29. G. Ning, L. Yong_hua, Z. Guang-Fu and X. Shi-Quan; *Acta Crsyt.*, 1992, **C48**, 542

32. S. Haddad, A. Vij and R. D. Willett; *J. Chem.Crsyt.*, 2003, **33**, 245

31. J. Lokaj, K. Gyerova, A. Sopkova, J. Sivy, V. Kettman and V. Vrabel; *Acta Cryst.*, 1991, **C47**, 2447

32. L. A. Kovbasyuk, I. O. Fritsky, V. N. Kokozay and T. S. Iskenderov; *Polyhedron*, 1997, **16**, 1723 and the references therein.

Chapter 6

SYNTHESIS AND STRUCTURAL STUDIES OF ZINC COMPLEX OF SULFADIMETHOXINE WITH AMMONIA

COMPLEX OF SULFADIMETHOXINE

6.1 Introduction

The crystal structure of sulfadimethoxine (Figure 6.1) has been reported in the literature[1,2] and a few of its metal complexes have been published earlier.[3,4]

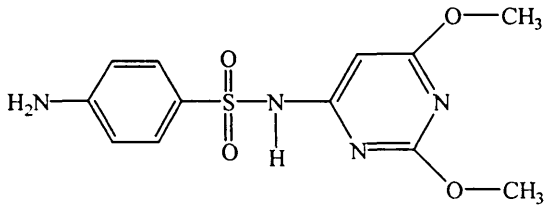

Figure 6.1: Structure of sulfadimethoxine

Removal of the acidic hydrogen from the sulfadimethoxine molecule produces a negative centre on the sulfonamidic nitrogen atom, which can then coordinate with a suitable metal(II) ion (Figure 7.2).

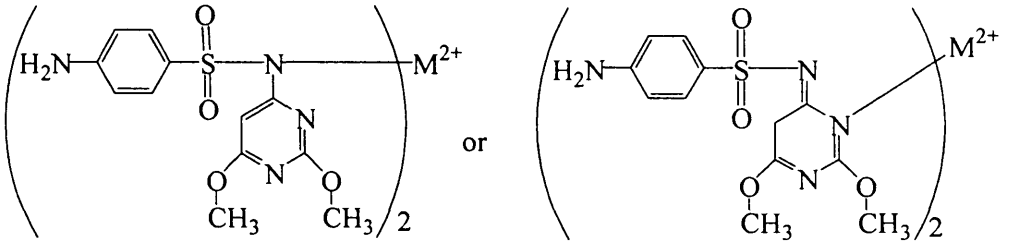

Figure 6.2

But in our complex, the short bond is through the pyrimido nitrogen atom. In addition, the amino nitrogen and sulfonyl oxygen atoms may coordinate with the metal ion.

6.2 Experimental

Solid sulfadimethoxine (0.520g; 2 mmol) was dissolved in methanol (50 mL) and to this solution $(CH_3COO)_2Zn.2H_2O$ (0.220g, 1 mmol) was added. This was stirred for six hours, a white precipitate was formed, filtered and dried over silica gel in a dessicator. This was dissolved in a solution of ammonia and water mixture (1:1) and stirred for 30 min., filtered

and the filtrate was kept for crystallisation. After a week, two types of crystals were obtained, one was block and the other was needle like crystals. The block type crystal was the ligand molecule sulfadimethoxine (**32**) and the needle like crystal was the zinc complex $[Zn(sdm)_2(NH_3)_2].2H_2O$ (**33**). IR for (**32**): (KBr disc), cm^{-1}, 3456(s), 3125(s), 2956(sh), 1625(vs), 1598, 1570, 1507(vs), 1465(sh), 1408, 1351, 1306(m), 1259(vs), 1190(sh), 1155(vs), 1125(s), 1093(s), 1005(s), 968(vs), 881(vw), 834, 805, 589, 535(vs). ^{1}H NMR (DMSO-d_6): δ 11.18s [1H, N(11),] 6.11 [2H, NH_2], 5.97 [1H, C(14)], 6.63d [2H, C(17)/C(19), J = 8.6], 7.60d [2H, C(16)/C(20), J = 8.6], 3.79s [C(111)] and 3.78s [C(112)], ^{13}C NMR (DMSO-d_6): δ 160.1 [C(11)], 164.3 [C(12)], 171.6 [C(13)], 84.2 [C(14)], 124.1 [C(15)], 129.3 [C(16)/C(20)], 112.4 [C(17)/C(19)], 153.3 [C(18)], 54.4 [C(111)] and 53.6 [C(112)]. IR for (**33**): (KBr disc), cm^{-1}, 3461(s), 1629(vs), 1599, 1582, 1501(vs), 1460(sh), 1404, 1373, 1224(vs), 1152(vs), 1122(s), 1096(s), 1014(s), 876(vw), 830, 805, 702(vs), 574, 554(vs). ^{1}H NMR (DMSO-d_6): δ 5.78 [2H, NH_2], 5.71 [1H, C(14)], 6.57d [2H, C(17)/C(19), J = 10.6], 7.45d [2H, C(16)/C(20), J = 8.6], 3.71s [C(111)] and 3.54 [C(112)], ^{13}C NMR (DMSO-d_6): δ 163.6 [C(11)], 166.4 [C(12)], 171.6 [C(13)], 84.6 [C(14)], 128.3 [C(15)], 128.9 [C(16)/C(20)], 112.3 [C(17)/C(19)], 151.4 [C(18)], 53.8 [C(111)] and 53.3 [C(112)].

6.3 Results and discussion for the compounds (32) and (33)

6.3.1 IR Spectra

The absorption bands at 3461 cm^{-1} suggest the presence of water molecules and NH_2 groups in the complex. This peak is very broad and split because of the involvement of water molecules and NH_2 group in hydrogen bonding to various extents.

The peak at 3125 cm^{-1} for N–H of the sulfonamidic group is not present in the IR spectra of the complex, and this confirms the deprotonation of the $-SO_2NH-$ moiety. The characteristic ν(C–C) (ring) and ν(C–N) absorptions in the IR spectra appear at 1570 cm^{-1} and 1351 cm^{-1} respectively in the sulfadimethoxine molecule. These peaks are observed at 1582 cm^{-1} and 1373 cm^{-1}, respectively, in the complex.

The scissoring vibrations for the $-NH_2$ group appear at 1629 and the peaks at 1570–1598 cm^{-1} are due to the phenyl rings. The peaks at 1306 and 1259 cm^{-1} are assigned to $as(SO_2)$, and that at 1125 cm^{-1} to $sy(SO_2)$. The (CC) absorption band overlaps with the $as(SO_2)$

peak at 1259 cm^{-1}. The band at 968 cm^{-1} in the sulfadimethoxine assigned to (S–N) is changed to the higher frequency 1005 cm^{-1} as a consequence of coordination to zinc ion.

6.3.2 ^{1}H NMR and ^{13}C NMR spectra

^{1}H and ^{13}C NMR spectra for the compounds (**32**) and (**33**) were obtained from a solution of DMSO-d_6. The ^{1}H spectra of the complex (**33**) are consistent with the X-ray structure obtained. It consists of two doublets for the para substituted phenyl ring and two singlets for the methyl substituents as methoxy groups at two different positions and one singlet for hydrogen on the pyrimidine ring and a broad singlet for the amino group on the phenyl ring. All integrals are consistent with this assignment. Small shifts in resonances are observed for complex compared to the parent ligand.

Table 6.1: ^{1}H NMR and ^{13}C NMR shift assignment of sulfadimethoxine (32) and its zinc complex (33) in DMSO-d_6[a]

Assignment	^{1}H (**32**)	^{1}H(**33**)	^{13}C(**32**)	^{13}C(**33**)	Δδ (H)[b]	Δδ (C)[b]
N(11)-H	11.18					
C(11)			160.1	163.6		+3.5
C(12)			164.4	166.4		+2.0
C(13)			171.0	171.6		+0.6
C(14)–H	5.97	5.71	84.2	84.6	–0.26	+0.4
C(15)			124.1	128.3		+4.2
C(16)–H/C(20)–H	7.60	7.45	129.4	128.9	–0.15	–0.5
C(17)–H/C(19)–H	6.63	6.57	112.4	112.3	–0.06	–0.1
C(18)			153.3	151.4		–1.9
C111	3.79	3.54	54.4	53.8	–0.25	–0.6
C112	3.78	3.71	53.6	53.3	–0.07	–0.3
NH_2	6.11	5.78			–0.33	

[a] Relative to TMS with DMSO-d_6 peak as reference (^{1}H, 2.60 ppm, ^{13}C, 43.5 ppm)
[b] $\Delta\delta = \delta_{(complex)} - \delta_{(sulfadimethoxine)}$

The N(11)–H peak has disappeared upon complexation with zinc(II) ion and a shift was observed for the C(11) resonance of sulfadimethoxine and from this observation it is probable that the zinc(II) ion is bonded to N(11) atom as also suggested by the X-ray structure. Another shift was observed for the C(12) atom confirming the bonding of N(12) with the zinc ion. In addition the amino protons, in the complex, are shifted down field from the "free" ligand value upon coordination.

The ^{13}C spectra (d^6–DMSO) of the complex are relatively simple to interpret and are similar to that observed for the free ligand, with ten peaks for sulfadimethoxine.

7.3.3 Crystal structures of sulfadimethoxine (32) and its zinc complex (33)

The crystals were characterised by X-ray analysis and compared with other related species.

Table 6.2: Crystal data and details of data collection and structure refinement for sulfadimethoxine (32) and its zinc complex $[Zn(sdm)_2(NH_3)_2].2H_2O$ (33)

	(32)	(33)
Empirical Formula	$C_{12}H_{14}N_4O_4S$	$C_{24}H_{36}N_{10}ZnO_{12}S_2$
Formula Weight	310.33	786.12
Crystal System	Triclinic	Orthorhombic
Space Group	$P\bar{1}$	*Pbcn*
a(Å)	7.9123(2)	12.288(3)
b(Å)	9.2293(2)	21.078(2)
c(Å)	10.3055(3)	13.328(4)
α(°)	93.8300(9)	90
β(°)	94.4410(10)	90
γ(°)	113.6202(13)	90
V/Å^3	683.49(3)	3452.1(14)
Z	2	4
T/K	150	150
Crystal Size/mm	0.10 × 0.10 × 0.08	0.15 × 0.12 × 0.12
Shape	Block	Needlelike
Colour	White	White
θ-range for data collection	2.97 to 27.48	3.98 to 26.04
Reflection Collected	12647	6266
Unique Reflections	3122	3370
Goodness-of-fit on F^2	1.063	1.036
R_{int}	0.0729	0.0496
Index ranges	$-10<=h<=10$ $-11<=k<=11$ $-13<=l<=13$	$-15<=h<=15$ $-25<=k<=26$ $-16<=l<=16$
Data/parameters in the refinement	3122/192	3370/245
Final *R* indices I>2σ(I)	0.0385/0.0938	0.0591/0.1449
R indices (all data)	0.0460/0.0987	0.0934/0.1652
Largest diff. peak and hole e.Å^{-3}	0.382 and −0.527	1.085 and −0.627

6.3.3.1 Structure of the sulfadimethoxine molecule (32)

The structure of sulfadimethoxine (**32**) is shown in Figure 6.3 together with the crystallographic atom numbering scheme used. The planes of the phenyl and pyrimidine rings are inclined to *Gauche* conformation about S(11)−N(11) bond with a torsion angle of 91.29(9)°. The crystal structure is stabilized by the network hydrogen bonding and van der Waals' interactions. The dihedral angle between the planes of phenyl and pyrimidine rings is 76.10(5)° which is smaller than the value of 77.6(8)° proposed by Patel *et al.*[2]

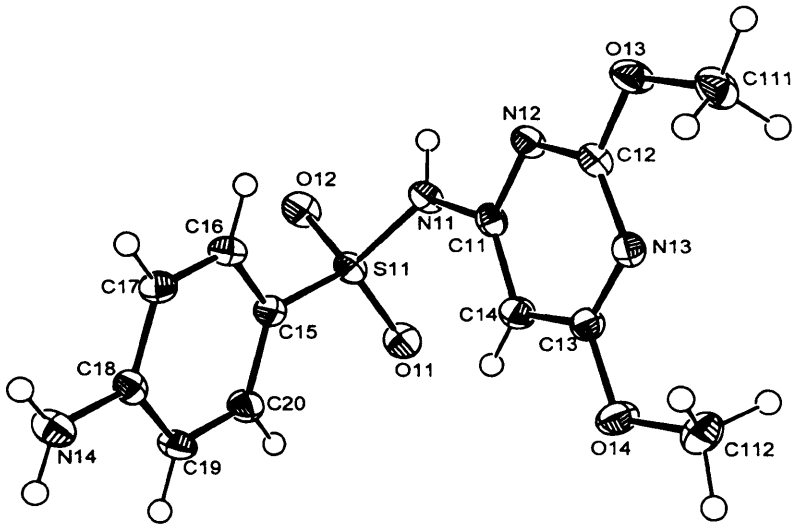

Figure 6.3
X-ray structure of sulfadimethoxine (32) showing crystallographic atom numbering scheme used. Thermal ellipsoids are drawn at 50% probability level.

The sulfadimethoxine forms a dimer through the hydrogen bonding N(11)–H(11)...O(12) which is shown in Figure 6.4. The bond length and angle are 1.988(8)Å and 158.68(2)° respectively confirming the strong hydrogen bonding.

Table 6.3: Selected bond lengths [Å] and angles [deg] in sulfadimethoxine (32)

Bond	(Å)	Bond	(Å)
S(11)-O(11)	1.429(2)	S(11)-O(12)	1.442(2)
S(11)-N(11)	1.647(2)	S(11)-C(15)	1.743(2)
O(13)-C(12)	1.337(2)	O(14)-C(13)	1.342(2)
N(11)-C(11)	1.399(2)	N(12)-C(12)	1.334(2)
N(12)-C(11)	1.343(2)	N(13)-C(12)	1.328(2)
N(13)-C(13)	1.328(2)	N(14)-C(18)	1.367(2)
C(11)-C(14)	1.383(2)	C(13)-C(14)	1.390(2)
C(15)-C(16)	1.395(2)	C(15)-C(20)	1.397(2)
C(16)-C(17)	1.379(2)	C(17)-C(18)	1.407(2)
C(18)-C(19)	1.401(2)	C(19)-C(20)	1.380(2)
Angle	**(°)**	**Angle**	**(°)**
O(11)-S(11)-O(12)	117.73(7)	O(11)-S(11)-N(11)	109.47(7)
O(12)-S(11)-N(11)	102.69(7)	O(11)-S(11)-C(15)	108.58(7)
O(12)-S(11)-C(15)	110.94(7)	N(11)-S(11)-C(15)	106.81(7)
C(11)-N(11)-S(11)	125.15(10)	C(12)-N(12)-C(11)	114.84(13)
C(12)-N(13)-C(13)	114.88(13)	N(12)-C(11)-C(14)	123.48(14)
N(12)-C(11)-N(11)	112.87(13)	C(14)-C(11)-N(11)	123.64(14)
N(13)-C(12)-N(12)	127.87(14)	N(13)-C(12)-O(13)	118.88(14)
N(12)-C(12)-O(13)	113.23(13)	N(13)-C(13)-O(14)	118.75(14)
N(13)-C(13)-C(14)	124.13(14)	O(14)-C(13)-C(14)	117.11(14)

The bond angles in the benzene ring differ slightly from the theoretical value of 120°. The C(18)–N(14) bond distance of 1.367(2)Å is very similar to the corresponding bond in sulfamerazine with the values 1.367(2)Å (**2**), 1.357(7) and 1.354(72)Å[7] and shorter than the bond lengths proposed by Camerman[8] for the length of C(sp^2)–N(sp^2) single bond 1.470(5)Å.

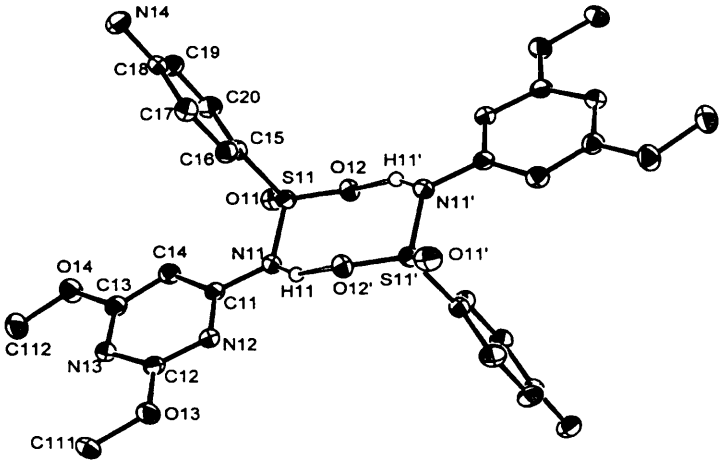

Figure 6.4
Dimeric form of the structure of sulfadimethoxine (32) through the N(11)–H(11)···O(12) *hydrogen bond. Thermal ellipsoids are drawn at 50% probability level. The hydrogen atoms are omitted for clarity*

The S(11)–C(15) bond distance of 1.743(2)Å is also comparable with the theoretical S–C(sp^2) value (1.75Å) calculated from the atomic radii and electronegativities given by Truter[11] and with the experimental data obtained for sulfonamides.[10–13]

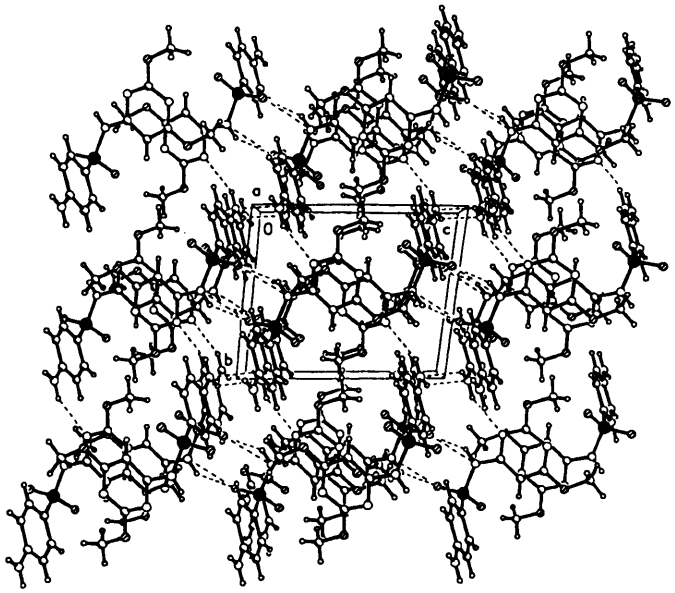

Figure 6.5
Packing diagram of sulfadimethoxine (32) where the hydrogen bonds are shown by dashed lines

The S(11)–O distances, 1.429(2)Å and 1.443(2)Å, are slightly longer than the corresponding bonds in the following structures: sulfaguanidine monohydrate [1.42(1) and 1.43(1)Å][14], sulfadiazine [1.41(2) and 1.42(2)Å][15], sulfamerazine [1.424(4) and 1.435(3)Å, and 1.414(4) and 1.431(3)Å][7] and are in good agreement with the corresponding bonds with values of 1.431(2) and 1.435(2)Å[16] and 1.426(8) and 1.430(6)Å[17] in sulfamethazine.

The several hydrogen bonds are shown in the packing diagram by dashed lines which is shown in Figure 6.5.

Table 6.4: Possible hydrogen bonds in sulfadimethoxine (32) (distances and angles given in Å and deg respectively)

Donor-H	Donor...Acceptor	H...Acceptor	Donor-H.....Acceptor
N11 -H11	N11 ....O12 (1)	H11 ...O12 (1)	N11 -H11 ...O12 (1)
0.946(3)	2.890(8)	1.988(8)	158.68(2)
N14 -H14A	N14 ....N12 (2)	H14A...N12 (2)	N14 -H14A...N12 (2)
0.948(3)	3.182(5)	2.244(3)	170.44(2)

Equivalent positions:
(1) -x,-y+1,-z; (2) x+1,+y+1,+z

6.3.3.2 Structure of the complex $[Zn(sdm)_2(NH_3)_2].2H_2O$ (33)

The structure of the zinc complex $[Zn(sdm)_2(NH_3)_2].2H_2O$ (**33**) is shown in Figure 6.6 together with the crystallographic atom numbering scheme used. The bond lengths and angles are given in Table 6.5 and the possible hydrogen bonds are summarized in Table 6.6. The Zn(II) ion lies on the two fold axis and is coordinated to two sulfonamidic and two pyrimidino nitrogen atoms from two sulfadimethoxine anions and two other nitrogen atoms from the coordinated ammonia ligands. This structure shows that Zn(II) has a six coordinate bicapped tetrahedral geometry like the previous cadmium complex (**21**) in which two nitrogen [N(1)] atoms from ammonia and two from pyrimido [N(12)] atoms form the tetrahedron and two sulfonamidic nitrogen [N(11)] atoms complete the coordination sphere around the zinc ion. The core geometry is shown in Figure 6.8.

The N(11) atom has a longer interaction with the bond distance of 2.834(3)Å than the N(12) atom with the Zn–N(12) bond distance of 2.015(3)Å which is comparable with the corresponding bonds in $[Zn(smz)_2(NH_3)_2]$ (**14**) with the values of 2.045(3) and 2.036(3)Å and in $[Zn(sdz)_2(NH_3)_2]$[18] 2.166(4) and 2.078(4)Å but shorter than the values of 2.122(3)Å

and 2.324(3)Å in $[Zn(smz)_2(py)_2].2py$ (**15**). The Zn–N(1) (ammonia) distance of 2.032(4)Å is also comparable with the values of 2.019(5) and 2.045(5)Å in $[Zn(smz)_2(NH_3)_2]$ (**14**) and 2.036(4) and 2.050(4)Å in $[Zn(sdz)_2(NH_3)_2]$.[18]

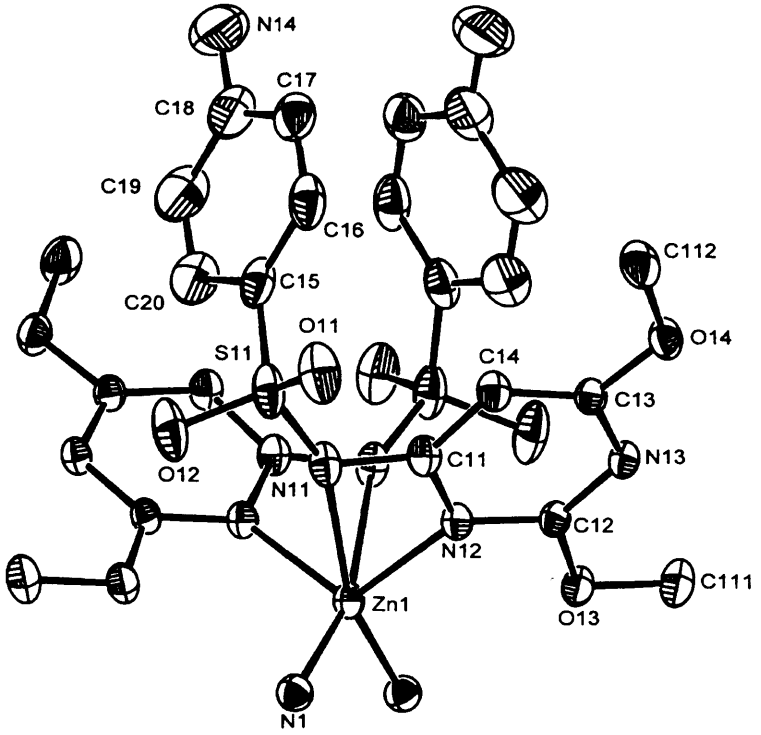

Figure 6.6
*X-ray structure of the complex $[Zn(sdm)_2(NH_3)_2].2H_2O$ (**33**) showing crystallographic atom numbering scheme used. Thermal ellipsoids are drawn at 35% probability level. The hydrogen atoms and water molecules are omitted for clarity.*

Table 6.5: Selected bond lengths [Å] and angles [deg] in $[Zn(sdm)_2(NH_3)_2].2H_2O$ (33)

Bond	(Å)	Bond	(Å)
Zn(1)-N(11)	2.834(3)	Zn(1)-N(12)	2.015(3)
Zn(1)-N(1)	2.032(4)	S(11)-O(12)	1.449(4)
S(11)-O(11)	1.453(4)	S(11)-N(11)	1.599(4)
S(11)-C(15)	1.742(6)	N(11)-C(11)	1.350(5)
N(14)-C(18)	1.360(9)		
Angle	**(°)**	**Angle**	**(°)**
N(12')-Zn(1)-N(12)	112.9(2)	N(12')-Zn(1)-N(1)	113.8(2)
N(12)-Zn(1)-N(1)	107.8(2)	N(11)-Zn(1)-N(11')	96.2(2)
N(12)-Zn(1)-N(1')	113.8(2)	N(1)-Zn(1)-N(1')	100.2(2)
O(12)-S(11)-O(11)	114.7(2)	O(12)-S(11)-N(11)	104.4(2)
O(11)-S(11)-N(11)	113.6(2)	O(12)-S(11)-C(15)	107.6(3)
O(11)-S(11)-C(15)	107.7(3)	N(11)-S(11)-C(15)	108.6(2)
C(11)-N(11)-S(11)	121.4(3)	N(13)-C(13)-C(14)	124.6(4)

Symmetry transformations used to generate equivalent atoms: (') $-x, y, -z+{}^3/_2$

The Zn–N(1) bonds are very similar to the Zn–N(12) bonds and the difference between these two types of Zn–N bonds, ∇ = d[Zn–N(1)] – d[Zn–N(12)] (Å), +0.017 suggests that the Zn–N(1) bond has similar strength as the Zn–N(12) bond in the complex.

The planes of the phenyl and pyrimidine rings are inclined to *Gauche* conformation about S(11)–N(11) bond with a torsion angle of 71.11(5)° which is larger than that of the free ligand which has a value of 58.16(2)°. The dihedral angle between the planes of phenyl and pyrimidine rings in the complex is 83.28(15)° which is larger than the value of 76.10(5)° of the free ligand due to the coordination of the sulfadimethoxine with the zinc atom.

The lattice water molecules and coordinated ammonia form several hydrogen bonds with sulfonyl oxygen atoms, pyrimido nitrogen and amino nitrogen atoms in the complexes and these are shown in the packing diagram (Figure 6.7).

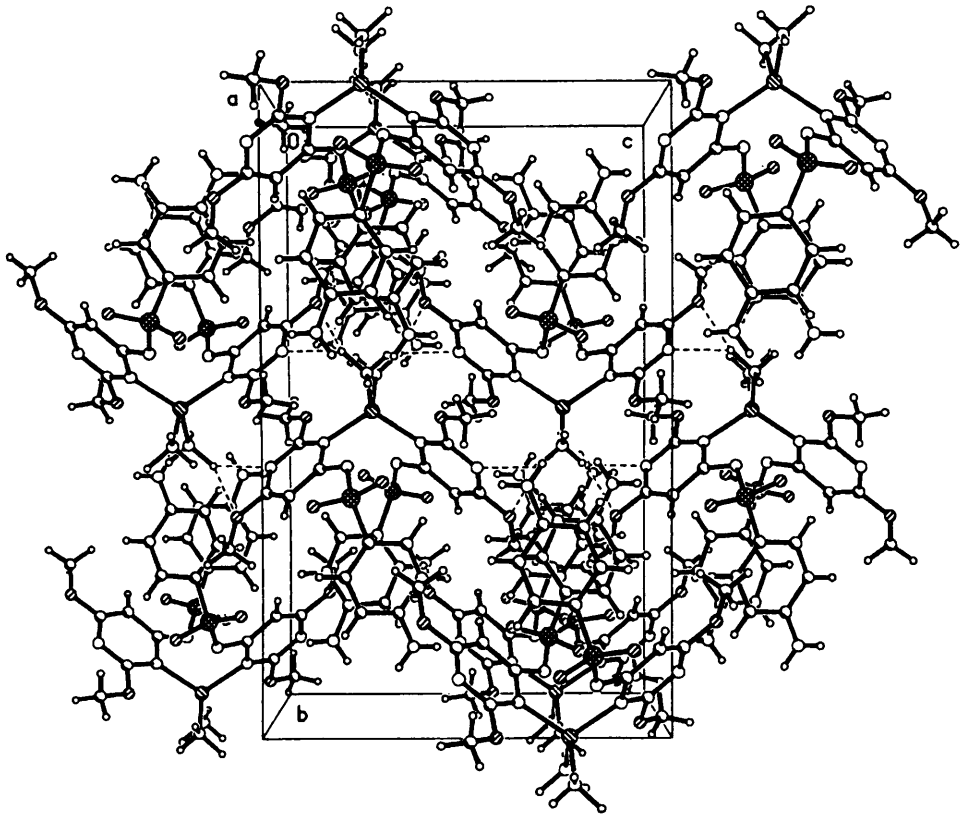

Figure 6.7
*Packing diagram of the complex (**33**) where the hydrogen bonds are shown by dashed lines*

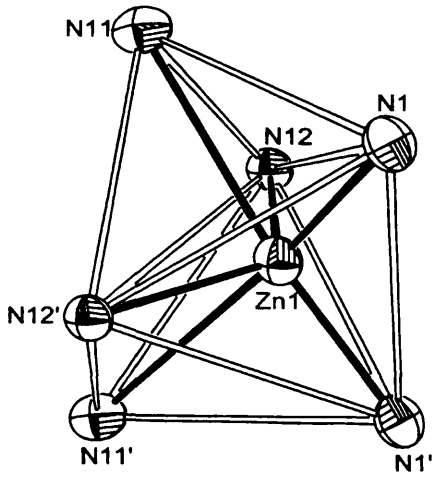

Figure 6.8
The bicapped tetrahedral structure of the complex $[Zn(sdm)_2(NH_3)_2].2H_2O$ (33) containing only bonded nitrogen atoms with the zinc ion

Table 6.6: The possible hydrogen bonds in $[Zn(sdm)_2(NH_3)_2].2H_2O$ (33) (distances and angles given in Å and deg respectively)

Donor-H	Donor...Acceptor	H...Acceptor	Donor-H.....Acceptor
N1 -H1C	N1 ....O1 (0)	H1C ...O1 (0)	N1 -H1C ...O1 (0)
0.949(5)	3.007(2)	2.112(7)	156.46(2)
O1 -H1E	O1 ....O3 (0)	H1E ...O3 (0)	O1 -H1E ...O3 (0)
0.836(7)	2.574(2)	1.776(1)	159.13(4)
O2 -H2A	O2 ....O3 (0)	H2A ...O3 (0)	O2 -H2A ...O3 (0)
1.086(3)	2.689(6)	1.801(5)	135.94(7)
O2 -H2B	O2 ....O11 (0)	H2B ...O11 (0)	O2 -H2B ...O11 (0)
1.144(9)	2.732(1)	1.618(8)	162.75(7)
N14 -H14A	N14 ....O2 (1)	H14A...O2 (1)	N14 -H14A...O2 (1)
0.880(5)	3.047(8)	2.172(5)	172.47(3)
N14 -H14B	N14 ....O1 (2)	H14B...O1 (2)	N14 -H14B...O1 (2)
0.880(1)	2.842(6)	1.999(6)	159.85(5)
N1 -H1A	N1 ....N13 (3)	H1A ...N13 (3)	N1 -H1A ...N13 (3)
0.949(6)	3.096(2)	2.189(3)	159.57(3)
O1 -H1D	O1 ....N14 (4)	H1D ...N14 (4)	O1 -H1D ...N14 (4)
0.913(4)	2.842(6)	2.016(4)	149.67(5)
O3 -H3D	O3 ....O3 (5)	H3D ...O3 (5)	O3 -H3D ...O3 (5)
1.153(7)	2.305(1)	1.153(8)	179.98(6)

Equivalent positions:
(0) x, y, z; (1) -x+½, -y-½, +z-½; (2) -x+½, +y-½, +z; (3) -x, -y, -z+2; (4) -x+½, +y+½, +z; (5) -x+1, -y, -z+2.

References

1. P. Narula; M. Haridas; T. P. Singh; *Indian J. Phys*; 1987, **61A**, 132
2. U. H. Patel, B. H. Patel, and B. N. Patel, *Cryst. Res. Tech.*; 2001, **36**, 1445
3. Y. A. Simonov, M. D. Mazus, I. A. Popa, V. N. Shafranskii and T. I. Malonovskii, *Zh. Strukt. Khim*; 1990, **31**, 77
4. M. H. Torre, G. Facchin, E. Kremer, E. Castellano, O. E. Piro and E. J. Baran; *J. Inorg. Biochem.*, 2003, **94**, 200.
5. G. M. Sheldrick; *Acta Cryst.*, 1990, **A46**, 467
6. G. M. Sheldrick; SHELXL-97*; Program for Crystal structure refinement*, University of Göttingen, Germany, 1996
7. M. R. Caira, R. Mohamed; *Acta Cryst.*, 1992, **B48**, 492.
8. A. Camerman; *Canad. J. Chem.*, 1970, **48**, 179
9. M. R. Truter; *J. Chem. Soc.*, 1962, 3400
10. B. H. O'Conner and E. N. Maslen; *Acta Cryst.*, 1965, **18**, 363
11. B.H. O'Conner and E. N. Maslen; *Acta Cryst.*, 1967, **22**, 134
12. M. Alkaume and J. Decap; *Acta Cryst.*, 1965A, **18**, 731
13. M. Alkaume and J. Decap; *Acta Cryst.*, 1965B, **19**, 394
14. C. H. Koo, H. S.Kim, W. C. Shin and C. H. Choe; *J. Kor. Chem. Soc.*, 1974, **18**, 97
15. H. S. Shin, G. S Ihn, H. S. Kim and C. H. Koo; *J. Korean Chem. Soc.*, 1974, **18**, 329
16. A. K. Basak, S.K. Mazumdar and S. Chaudhuri; *Acta Crsyt.*, 1983, **C39**, 492
17. R.K. Tiwari, M. Haridas and T. P. Singh; *Acta Crsyt.*, 1984, **C40**, 655
18. N. C. Baenziger, S. L. Modak and C. L. Fox Jr., *Acta Cryst.*, 1983, **C39**, 1620